IAEA-TECDOC-1844

IAEA TECDOC SERIES

IAEA-TECDOC-1844

Analyses Supporting Conversion of Research Reactors from High Enriched Uranium Fuel to Low Enriched Uranium Fuel

The Case of the Miniature Neutron Source Reactors

IAEA
International Atomic Energy Agency

ANALYSES SUPPORTING CONVERSION OF RESEARCH REACTORS FROM HIGH ENRICHED URANIUM FUEL TO LOW ENRICHED URANIUM FUEL

The following States are Members of the International Atomic Energy Agency:

AFGHANISTAN
ALBANIA
ALGERIA
ANGOLA
ANTIGUA AND BARBUDA
ARGENTINA
ARMENIA
AUSTRALIA
AUSTRIA
AZERBAIJAN
BAHAMAS
BAHRAIN
BANGLADESH
BARBADOS
BELARUS
BELGIUM
BELIZE
BENIN
BOLIVIA, PLURINATIONAL STATE OF
BOSNIA AND HERZEGOVINA
BOTSWANA
BRAZIL
BRUNEI DARUSSALAM
BULGARIA
BURKINA FASO
BURUNDI
CAMBODIA
CAMEROON
CANADA
CENTRAL AFRICAN REPUBLIC
CHAD
CHILE
CHINA
COLOMBIA
CONGO
COSTA RICA
CÔTE D'IVOIRE
CROATIA
CUBA
CYPRUS
CZECH REPUBLIC
DEMOCRATIC REPUBLIC OF THE CONGO
DENMARK
DJIBOUTI
DOMINICA
DOMINICAN REPUBLIC
ECUADOR
EGYPT
EL SALVADOR
ERITREA
ESTONIA
ETHIOPIA
FIJI
FINLAND
FRANCE
GABON
GEORGIA
GERMANY
GHANA
GREECE
GUATEMALA
GUYANA
HAITI
HOLY SEE
HONDURAS
HUNGARY
ICELAND
INDIA
INDONESIA
IRAN, ISLAMIC REPUBLIC OF
IRAQ
IRELAND
ISRAEL
ITALY
JAMAICA
JAPAN
JORDAN
KAZAKHSTAN
KENYA
KOREA, REPUBLIC OF
KUWAIT
KYRGYZSTAN
LAO PEOPLE'S DEMOCRATIC REPUBLIC
LATVIA
LEBANON
LESOTHO
LIBERIA
LIBYA
LIECHTENSTEIN
LITHUANIA
LUXEMBOURG
MADAGASCAR
MALAWI
MALAYSIA
MALI
MALTA
MARSHALL ISLANDS
MAURITANIA
MAURITIUS
MEXICO
MONACO
MONGOLIA
MONTENEGRO
MOROCCO
MOZAMBIQUE
MYANMAR
NAMIBIA
NEPAL
NETHERLANDS
NEW ZEALAND
NICARAGUA
NIGER
NIGERIA
NORWAY
OMAN
PAKISTAN
PALAU
PANAMA
PAPUA NEW GUINEA
PARAGUAY
PERU
PHILIPPINES
POLAND
PORTUGAL
QATAR
REPUBLIC OF MOLDOVA
ROMANIA
RUSSIAN FEDERATION
RWANDA
SAINT VINCENT AND THE GRENADINES
SAN MARINO
SAUDI ARABIA
SENEGAL
SERBIA
SEYCHELLES
SIERRA LEONE
SINGAPORE
SLOVAKIA
SLOVENIA
SOUTH AFRICA
SPAIN
SRI LANKA
SUDAN
SWAZILAND
SWEDEN
SWITZERLAND
SYRIAN ARAB REPUBLIC
TAJIKISTAN
THAILAND
THE FORMER YUGOSLAV REPUBLIC OF MACEDONIA
TOGO
TRINIDAD AND TOBAGO
TUNISIA
TURKEY
TURKMENISTAN
UGANDA
UKRAINE
UNITED ARAB EMIRATES
UNITED KINGDOM OF GREAT BRITAIN AND NORTHERN IRELAND
UNITED REPUBLIC OF TANZANIA
UNITED STATES OF AMERICA
URUGUAY
UZBEKISTAN
VANUATU
VENEZUELA, BOLIVARIAN REPUBLIC OF
VIET NAM
YEMEN
ZAMBIA
ZIMBABWE

The Agency's Statute was approved on 23 October 1956 by the Conference on the Statute of the IAEA held at United Nations Headquarters, New York; it entered into force on 29 July 1957. The Headquarters of the Agency are situated in Vienna. Its principal objective is "to accelerate and enlarge the contribution of atomic energy to peace, health and prosperity throughout the world".

IAEA-TECDOC-1844

ANALYSES SUPPORTING CONVERSION OF RESEARCH REACTORS FROM HIGH ENRICHED URANIUM FUEL TO LOW ENRICHED URANIUM FUEL

THE CASE OF THE MINIATURE NEUTRON SOURCE REACTORS

INTERNATIONAL ATOMIC ENERGY AGENCY
VIENNA, 2018

Marketing and Sales Unit, Publishing Section
International Atomic Energy Agency
Vienna International Centre
PO Box 100
1400 Vienna, Austria
fax: +43 1 2600 29302
tel.: +43 1 2600 22417
email: sales.publications@iaea.org
http://www.iaea.org/books

For further information on this publication, please contact:

Research Reactor Section
International Atomic Energy Agency
Vienna International Centre
PO Box 100
1400 Vienna, Austria
Email: Official.Mail@iaea.org

Printed by the IAEA in Austria
May 2018

IAEA Library Cataloguing in Publication Data

Names: International Atomic Energy Agency.
Title: Analyses supporting conversion of research reactors from high enriched uranium fuel to low enriched uranium fuel : the case of the miniature neutron source reactors / International Atomic Energy Agency.
Description: Vienna : International Atomic Energy Agency, 2018. | Series: IAEA TECDOC series, ISSN 1011–4289 ; no. 1844 | Includes bibliographical references.
Identifiers: IAEAL 18-01154 | ISBN 978–92–0–101818–2 (paperback : alk. paper)
Subjects: LCSH: Nuclear fuels. | Nuclear reactors. | Nuclear engineering. | Uranium as fuel.

FOREWORD

Research reactors are ubiquitous around the world, with 245 currently operating in 55 countries. At the core of science, research and experimentation, research reactors are used to conduct neutron activation analysis, education and training, radioisotope production, fuel testing, and basic and applied research. Research reactors vary broadly in design, although a few, such as TRIGA, Slowpoke and miniature neutron source reactors (MNSRs), were manufactured and exported to various countries.

Historically, many of these research reactors utilized high enriched uranium (HEU) fuel in order to increase the neutron flux for their complex experimental testing. However, since the late 1970s, efforts to convert research reactors from HEU to low enriched uranium (LEU) fuel have been taking place around the world. Given the varied design of research reactors, each conversion requires specific analyses to ensure the technical capabilities and safety of the reactor are maintained.

MNSRs are small 30 kW research reactors, located in Ghana, the Islamic Republic of Iran, Nigeria, Pakistan and the Syrian Arab Republic. These reactors were exported from China in the 1980s and 1990s and are primarily used for neutron activation analysis, research, and education and training. The reactors located in these countries are the commercial version of the prototype MNSR, located in Beijing, China. As these reactors were designed to operate using small cores of HEU, the IAEA was requested to organize a coordinated research project to evaluate the technical aspects that would support conversion to LEU fuel. This publication focuses on the design, safety and performance analyses of these Chinese designed MNSRs.

The IAEA wishes to thank all project participants for their contribution to this publication, in particular J.E. Matos (United States), who supervised most of the technical work of the coordinated research project. The IAEA officers responsible for this publication were P. Adelfang, I. Goldman, R. Sollychin, J. Dix, C. Ames and M. Voronov of the Division of Nuclear Fuel Cycle and Waste Technology.

CONTENTS

1. INTRODUCTION 1
1.1. BACKGROUND 1
1.2. PURPOSE 1
1.3. SCOPE 1
1.4. STRUCTURE 2
2. DESIGN, PERFORMANCE, AND SAFETY ANALYSES FOR GENERIC MNSR HEU AND LEU CORES 3
2.1. INTRODUCTION 3
2.2. GENERIC HEU CORE MODEL 3
2.3. ESTABLISHMENT OF THE 345 PIN GENERIC HEU CORE CONFIGURATION 8
2.4. CHARACTERISTICS OF THE GENERIC HEU CORE 9
2.5. ADAPTATION OF GENERIC HEU CORE MODEL TO HEU REACTOR GHARR-1 IN GHANA 12
2.6. ADAPTATION OF GENERIC HEU CORE MODEL TO HEU REACTOR NIRR-1 IN NIGERIA 13
2.7. CHARACTERISTICS OF THE BASE GENERIC LEU CORE MODEL 15
2.8. ADAPTATION OF THE GENERIC LEU CORE MODEL TO GENERIC 'WORKING CORES' 19
2.9. REVIEW OF ^{235}U LOADING AND DESIGN UNCERTAINTIES 21
2.10. ANALYSES FOR LEU CONVERSION 22
2.10.1. Why 12.5% enrichment instead of 19.75% enrichment? 22
2.10.2. Neutron flux performance 24
2.10.3. Core lifetime performance 24
2.10.4. Shutdown margin 26
2.10.5. Plutonium production 26
2.10.6. Steady state thermal-hydraulic safety margins 28
2.10.6.1. Results using the PLTEMP version 4.1 code 28
2.10.6.2. Results using the RELAP5 version 3.3 code 37
2.10.7. Temperature reactivity coefficients and kinetics parameters 45
2.10.8. Safety analyses 46
2.10.8.1. Selection of initiating events 46
2.10.8.2. Insertion of excess reactivity of 3.77 mk (commissioning test) 46
2.10.8.3. Inadvertent reactivity insertions 54
2.10.8.4. Handling of the top beryllium reflector 54
2.10.8.5. Inadvertent reactivity increase due to rabbit tubes filled with water 55
2.10.8.6. Loss of pool water shielding 55
2.10.8.7. DBA and the maximum credible accident 58
2.10.8.8. BDBA and maximum hypothetical accident 71
2.10.8.9. HEU core removal and LEU core installation reactivity insertion accident scenarios 74
REFERENCES TO SECTION 2 81
3. CONVERSION ANALYSIS OF CHINA'S MNSRS 84
3.1. INTRODUCTION 84
3.2. MNSR DESCRIPTION 84

3.2.1. Critical assembly for MNSR IAE 84
3.2.1.1. *Reactor core* 85
3.2.1.2. *Side beryllium reflector* 85
3.2.1.3. *Bottom beryllium reflector* 85
3.2.1.4. *Top beryllium reflector* 86
3.2.1.5. *Irradiation sites* 86
3.2.1.6. *Five ionization chamber tubes* 86
3.2.2. Critical assembly for MNSR-SZ 88
3.2.2.1. *Critical assembly* 88
3.2.2.2. *Reactor core* 89
3.2.2.3. *Side beryllium reflector* 89
3.2.2.4. *Bottom beryllium reflector* 89
3.2.2.5. *Top beryllium reflector* 90
3.2.2.6. *Irradiation sites* 90
3.2.2.7. *Four reactivity regulator tubes* 90
3.2.2.8. *Fission chamber tubes* 90
3.3. CALCULATED RESULTS FOR THE HEU CORE 92
3.3.1. MNSR IAE 92
3.3.2. MNSR-SZ 94
3.4. LEU CORE CALCULATION RESULTS 95
3.4.1. Overview 95
3.4.2. MNSR-IAE 95
3.4.3. MNSR-SZ 98
3.5. RADIOLOGICAL CONSEQUENCE ANALYSIS 101
3.5.1. DBA 101
3.5.1.1. *Accident scenario* 101
3.5.1.2. *Calculation assumptions* 101
3.5.1.3. *Release* 101
3.5.2. BDBA 102
3.5.2.1. *Accident scenario* 102
3.5.2.2. *Calculation assumptions* 102
3.5.2.3. *Release* 103
3.5.3. Calculation results 103
3.6. CONCLUSION 104
4. ANALYSIS FOR CORE CONVERSION OF GHANA RESEARCH REACTOR-1 FROM HEU TO LEU FUEL 105
4.1. INTRODUCTION 105
4.1.1. Reactor facility changes 106
4.1.2. Operation license and procedural changes 106
4.1.3. Characteristics of reference GHARR-1 LEU core 106
4.2. CORE CONVERSION ANALYSES 108
4.2.1. Neutronics analyses 108
4.2.1.1. *Method of analysis* 108
4.2.1.2. *Results and discussion* 108

4.2.1.3. *Core lifetime analysis* 118
4.2.2. Thermal-hydraulic analyses 119
4.2.2.1. *Method of analysis* 121
4.2.2.2. *Transients analysis* 125
4.3. RADIOLOGICAL CONSEQUENCES ANALYSES 129
4.3.1. DBA 129
4.3.1.1. *Scenario* 129
4.3.1.2. *Fission inventory and source term determination* 129
4.3.1.3. *Assumptions for dose calculations* 131
4.3.1.4. *Calculated results* 131
4.3.2. BDBA 132
4.4. CONCLUSION 134
REFERENCES TO SECTION 4 135
5. ANALYSIS REPORT FOR CONVERSION OF THE NIGERIAN MNSR NIRR-1 TO LEU FUEL: 2006–2012 137
5.1. INTRODUCTION 137
5.2. NEUTRONICS STUDIES 139
5.2.1. MCNP HEU model 139
5.2.2. LEU feasibility search 140
5.2.3. Impact of conversion on utilization 144
5.2.4. Neutronics analysis of two additional control rods for improved MNSR safety 145
5.3. THERMAL-HYDRAULICS STUDIES 146
5.3.1. Steady state temperature and heat flux parameters using PLTEMP code 147
5.3.2. Transient analysis using PARET code 148
5.4. RADIOLOGICAL CONSEQUENCES ANALYSES 151
5.4.1. DBA 151
5.4.1.1. *Scenario* 151
5.4.1.2. *Fission inventory and source term determination* 151
5.4.1.3. *Assumptions for dose calculations* 152
5.4.1.4. *Calculated results* 153
5.4.2. BDBA 155
5.5. SUMMARY AND CONCLUSION 156
REFERENCES TO SECTION 5 157
6. THERMAL-HYDRAULIC AND TRANSIENT ANALYSIS OF THE EXISTING HEU CORE AND PROPOSED LEU CORES FOR THE IRAN ENTC MNSR USING PARET/ANL CODE 158
6.1. SCOPE 158
6.2. METHODOLOGY 158
6.3. RESULTS AND DISCUSSION 162
6.3.1. HEU core 162
6.3.2. LEU cores 166

REFERENCES TO SECTION 6 171
7. ANALYSIS OF CORE CONVERSION FROM HEU TO LEU FUEL FOR PAKISTAN RESEARCH REACTOR-2 (PARR-2) 172
7.1. INTRODUCTION 172
7.2. NEUTRONIC ANALYSIS 175
7.2.1. Methodology 176
7.2.2. Results and discussion 177
7.3. THERMAL-HYDRAULIC ANALYSIS 184
7.3.1. Methodology 184
7.3.2. Results and discussion 185
7.3.2.1. HEU core 185
7.3.2.2. LEU core 185
7.4. RADIOLOGICAL CONSEQUENCE ANALYSIS 195
7.4.1. DBA 195
7.4.1.1. Accident scenario 195
7.4.1.2. Assumptions 195
7.4.1.3. Dose calculations 195
7.4.2. BDBA 199
7.4.2.1. Accident scenario 199
7.4.2.2. Assumptions 199
7.4.2.3. Dose calculations 200
7.4.2.4. Decay heat calculations 201
7.5. CONCLUSION 201
REFERENCES TO SECTION 7 203
8. FEASIBILITY STUDY FOR CONVERTING THE SYRIAN MNSR CORE FROM HEU TO LEU FUEL 204
8.1. INTRODUCTION 204
8.2. THE NEUTRONIC ANALYSIS 206
8.2.1. Results and discussion 209
8.3. THERMAL-HYDRAULIC ANALYSIS 209
8.4. CONCLUSION AND FUTURE ANALYSES 213
REFERENCES TO SECTION 8 215
APPENDIX I 217
APPENDIX II 221
APPENDIX III 231
APPENDIX IV 239
ACRONYMS AND ABBREVIATIONS 243
CONTRIBUTORS TO DRAFTING AND REVIEW 245

1. INTRODUCTION

1.1. BACKGROUND

Miniature neutron source reactors (MNSRs) have been designed and manufactured by the China Institute of Atomic Energy since the mid-1980s. A total of nine MNSRs have been built: four in China and one each in Pakistan (1989), Islamic Republic of Iran (1994), Ghana (1995), Syrian Arab Republic (1996), and Nigeria (2004). MNSRs are used mainly for neutron activation analysis, training and education. The cores contain less than 1 kg of high enriched uranium (HEU) fuel, enriched to approximately 90% ^{235}U. Two MNSRs, located in Shanghai and Shandong in China, have been shut down.

Since 1978, various national and international activities have been undertaken to convert research and test reactors from the use of HEU fuel to the use of low enriched uranium (LEU) fuel. These activities support the objective of reducing and eventually eliminating the use of HEU fuel in civil nuclear applications.

Based on the interest of Member States, the IAEA initiated a coordinated research project (CRP) in 2006 with the overall objective of assisting institutions in Member States with HEU-fuelled MNSRs to convert to LEU fuel, with minimal reduction to the capacity utilization rate of the reactors. The first research coordination meeting of the CRP was held in December 2006 in Vienna. Recommendations, actions and a project work plan were adopted. The final meeting was held in March 2012, also in Vienna, where participants in the CRP made presentations on their contributions to this report.

This report documents the numerous analyses that were conducted to evaluate both generic and reactor-specific HEU and LEU MNSR cores to support LEU fuel conversion studies. The analyses of the generic HEU core can be easily adopted by each individual commercial MNSR to model their own HEU MNSR core and easily modified to establish a generic LEU core for use in analysing conversion to an LEU core.

1.2. PURPOSE

The main objective of this report is to document the numerous analyses that were conducted to evaluate both generic and reactor-specific HEU and LEU MNSR cores to support LEU fuel conversion. The analyses of the generic HEU core can be adopted by each individual commercial reactor to model their own HEU MNSR core and easily modified to establish a generic LEU core to serve as a base model for LEU fuel conversion studies. As the reactors prepare to undergo conversion, these analyses and evaluations will provide a basis for the technical information required in their Safety Analysis Report.

1.3. SCOPE

This report contains design, performance and safety analyses of generic and reactor-specific HEU and LEU MNSR cores located in China, Ghana, the Islamic Republic of Iran, Nigeria, Pakistan, and the Syrian Arab Republic. Information concerning the design and performance of each reactor is used to analyse the effects of a conversion from an HEU to an LEU core, particularly relating to the neutron flux, core lifetime and required level of fuel enrichment. Neutronic, thermal-hydraulic, and radiological consequence analyses for each reactor are discussed in depth.

1.4. STRUCTURE

This report is broken into eight major sections, including this introductory section, and four appendices. Each section was authored separately, with this publication serving as a compendium of all results.

Section 2, provided by Argonne National Laboratory (USA), provides information on the design, performance and safety analyses for models of generic HEU and LEU cores, as well as analyses for LEU conversion.

Section 3, provided by the China Institute of Atomic Energy (China), discusses the conversion analyses for China’s two operational MNSRs, MNSR-IAE and MNSR-SZ. This includes analyses of the HEU core and LEU core for both reactors as well as a radiological consequence analysis.

Section 4, provided by the National Nuclear Research Institute (Ghana), discusses the core conversion analyses (neutronic and thermal-hydraulic) and radiological consequences analyses for the conversion of the GHARR-1 MNSR to operate with an LEU core.

Section 5, provided by the Centre for Energy Research and Training (Nigeria), describes the neutronic and thermal-hydraulic studies and radiological consequence analyses for the conversion of the NIRR-1 MNSR to operate with an LEU core.

Section 6, provided by the Nuclear Science and Technology Research Institute (Islamic Republic of Iran), provides the thermal-hydraulic and transient analysis of the existing HEU core and proposed LEU cores for the ENTC MNSR.

Section 7, provided by the Pakistan Institute of Nuclear Science and Technology (Pakistan), describes the neutronic analysis, thermal-hydraulic analysis, and radiological consequence analysis associated with the core conversion from HEU to LEU fuel for the PARR-2 MNSR.

Section 8, provided by Atomic Energy Commission (Syrian Arab Republic), discusses the neutronic and thermal-hydraulic analyses regarding the feasibility of converting the Syrian MNSR core from HEU to LEU fuel.

Appendix I provides detailed information on the geometries of various core components for the generic HEU and LEU core models. Appendix II provides material compositions used in the MCNP models for the generic HEU and LEU MNSR core models. Appendix III evaluates the initiating events that could be used as a basis for the safety analyses, highlighting those that would need to be re-analysed as a result of converting the core from HEU to LEU. Appendix IV provides a description of the steps required to remove the existing HEU core and install a fresh LEU core, the change in reactivity of the core, and the net excess reactivity after each step. All appendices were provided by Argonne National Laboratory (USA).

2. DESIGN, PERFORMANCE, AND SAFETY ANALYSES FOR GENERIC MNSR HEU AND LEU CORES

2.1. INTRODUCTION

This report provides information on establishment of the Argonne National Laboratory (ANL) models of generic HEU and LEU cores for an MNSR and on the results of analyses for conversion of MNSRs to LEU fuel.

The generic HEU core model was established from existing HEU models for the NIRR-1 reactor [2.1] in Nigeria and the GHARR-1 reactor [2.2] in Ghana. The main purposes for this generic HEU core are twofold: (1) it can be easily adopted by each individual commercial reactor operator to model their own HEU MNSR; and (2) it can also be easily modified to establish a generic LEU core that will serve as the base model for an LEU conversion study of individual commercial MNSRs. Since the generic HEU core model preserves all common features in many HEU-fuelled MNSRs, this approach could make the LEU conversion study by various commercial MNSR operators more consistent and efficient. While this section contains detailed information and calculations on the NIRR-1 and GHARR-1 cores, the information is intended to serve as a demonstration of the generic HEU and LEU core models and how they are adaptable for each individual MNSR.

Based on discussions at the China Institute of Atomic Energy (CIAE), it was assumed that CIAE began with a generic model of the HEU core with 345 pins for the contractual discussions. Initial adjustments were then made to accommodate individual reactors based on critical experiments at CIAE before shipping the reactor components to the customer site. Final adjustments were made at the reactor site. These adjustments were needed to accommodate as-built materials, actual conditions at the site, or to make adjustments requested by customers (who may for example choose to build in a higher excess reactivity to prolong the life of the core).

In this study, a base generic HEU model was first defined and then augmented to form as-built, working cores for the GHARR-1 and NIRR-1 reactors. A generic LEU model was then defined using the specifications that were agreed to at the second research coordination meeting (RCM) in Vienna in May 2008 [2.3]. An enrichment of 12.5% was chosen so that the HEU and LEU cores have approximately the same number of fuel pins, similar water to fissile material ratios, and hence, roughly the same negative reactivity feedback and power coefficients. The reactivity worth of different possible positive and negative reactivity adjustments were then computed to provide information on the choices. The LEU cores are likely to be built to accommodate both as-built parameters and customer choices.

2.2. GENERIC HEU CORE MODEL

The Monte Carlo N-Particle (MCNP) [2.4] model includes the reactor core, grid plates, tubes for instrumentation and irradiation, the reactor container, pool, and pool liner. Table 2.1 and Figs 2.1–2.4 show the materials and various views of the modelled reactor components. These figures provide the terminology that will be used to describe each component, and are intended to resemble figures in Chapter 5 of the GHARR-1 SAR [2.2]. Each colour in the figure represents one of the materials used in the MCNP model. The legend is provided in Table 2.1 for each material.

Detailed information on the geometries of various core components is provided in Appendix I. Material compositions used in the MCNP models are provided in Appendix II.

The control rod is fully withdrawn from the core, and there are no beryllium shim plates in the top shim tray. The bottom of the outer irradiation tubes and the adjuster rod guide tubes are assumed to be at the same axial level as the bottom of the active fuel zone in the generic reference core.

TABLE 2.1. MATERIALS IN THE MCNP MODEL OF THE REFERENCE GENERIC MNSR HEU CORE

Material	Legend	Locations
Cadmium	yellow	Central control rod, cadmium adjuster rods
Stainless steel	pink	Control rod cladding, stainless steel adjuster rod, control rod drive mechanism, reactor pool liner
Water	light blue	Coolant and moderator
Aluminium alloy LT-21	orange	Reactor vessel, lower core support, slant tube, shim tray, irradiation channel tubes, fission chambers, radial support structure, reactivity adjustor tubes, control rod guide tube, grid plates
UAl alloy	light green	HEU fuel meat
Beryllium	purple	Radial reflector and bottom reflector
Al-303-1	grey	Dummy rods, tie rods, fuel pin cladding

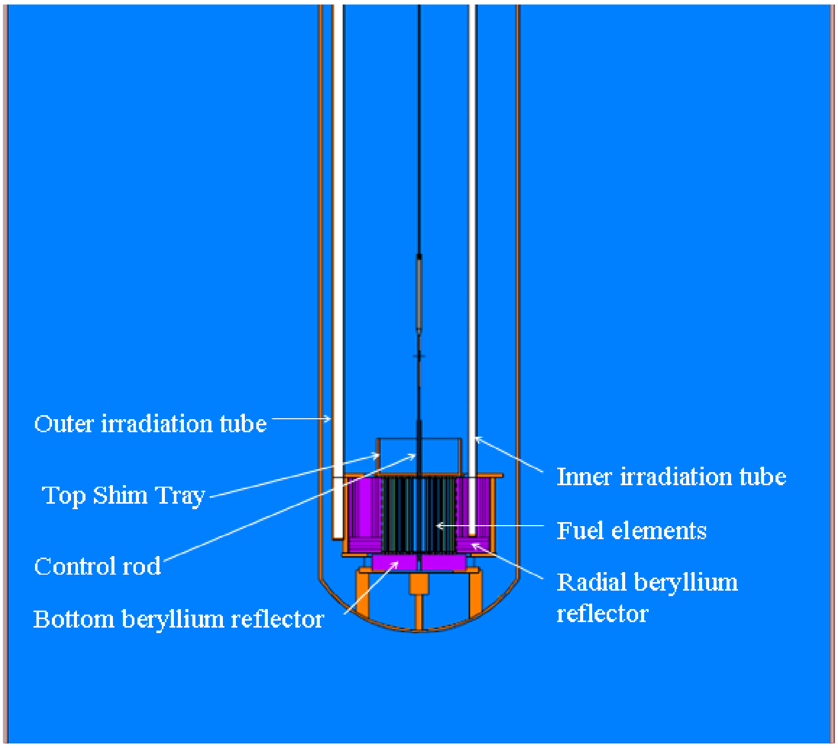

FIG. 2.1. Side view of the modelled generic MNSR HEU core (Courtesy of Argonne National Laboratory, USA).

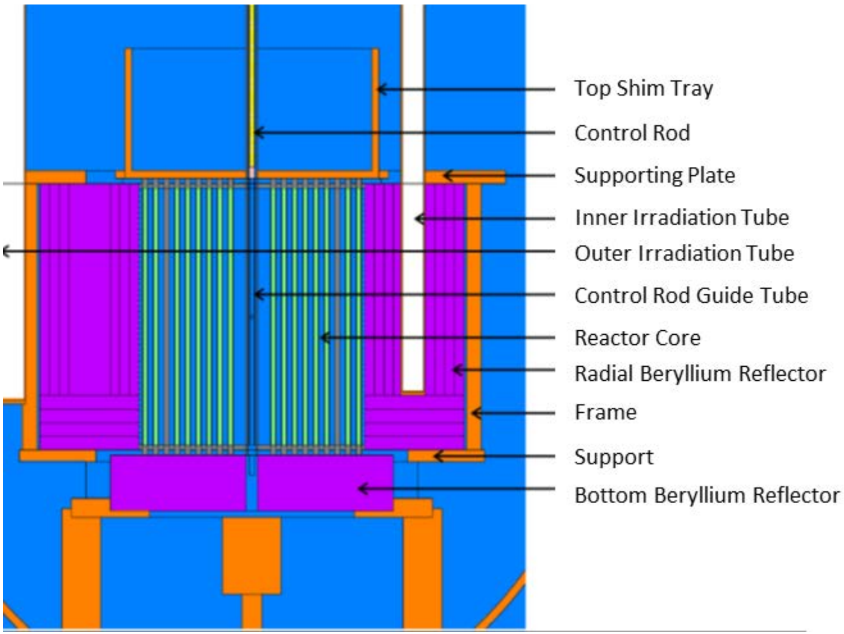

FIG. 2.2. Closer side view of the modelled generic MNSR HEU core (Courtesy of Argonne National Laboratory, USA).

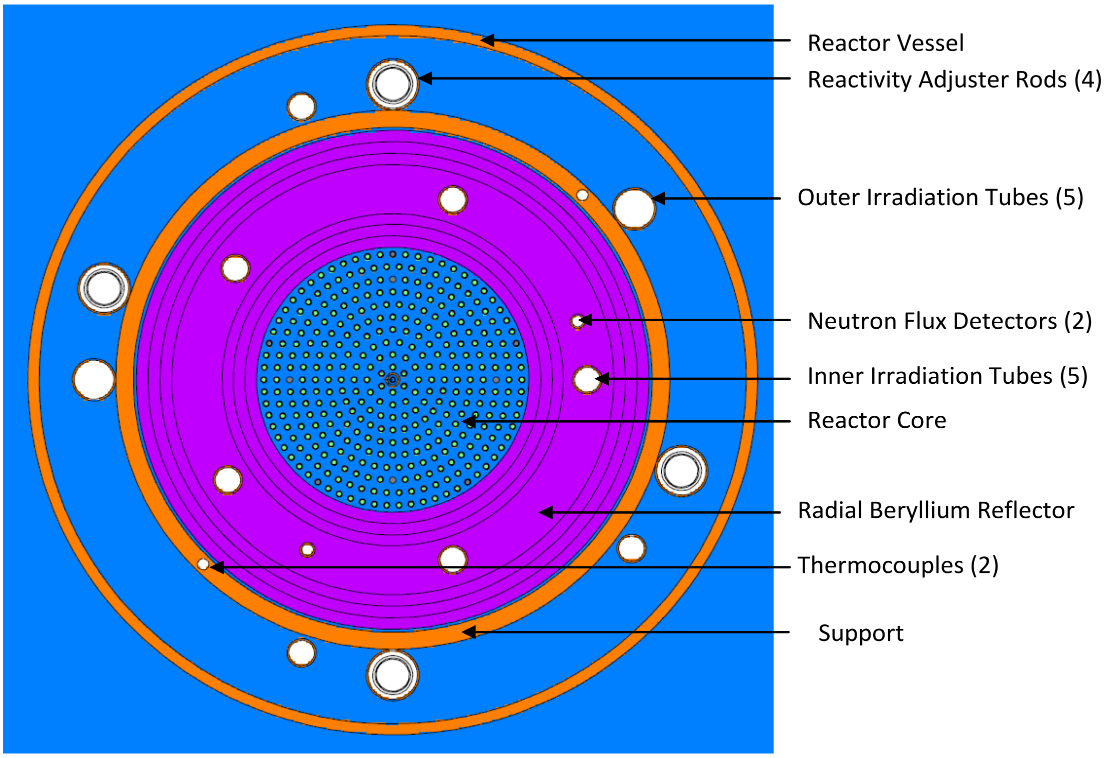

FIG. 2.3. Top view of the modelled generic MNSR HEU core (Courtesy of Argonne National Laboratory, USA).

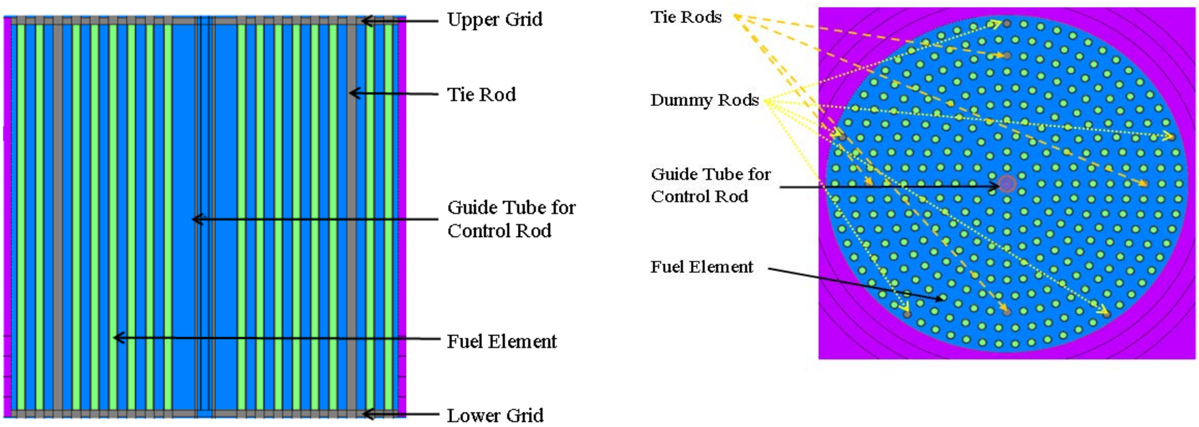

FIG. 2.4. Fuel cage of the generic MNSR HEU core (Courtesy of Argonne National Laboratory, USA).

Four reactivity adjuster rods are located in aluminium guide tubes just outside the core support and frame. Their location in the MCNP model is shown in Table 2.2. According to CIAE, adjuster rods are composed of stainless steel with an outer diameter (OD) of 36 mm, inner diameter (ID) of 26 mm and height of 350 mm, with a measured reactivity worth about 0.4 mk. However, the reactivity worths of adjuster rods calculated using these materials and dimensions in the MCNP models of the GHARR-1 and NIRR-1 HEU cores do not agree well with measured reactivity worths because insufficient information is available on the actual design of the adjuster rods.

Information on the as-built designs of the adjuster rods used in the GHARR-1 and NIRR-1 reactors is not available from the reactor operators or from the CIAE. As a result, designs based on the estimated design parameters of the adjuster rods used in the In-Hospital Neutron Irradiation reactor at CIAE (see Fig. 2.5) were utilized to match the reactivity worths measured in the GHARR-1 and NIRR-1 HEU cores [2.6]. Table 2.3 compares the design specifications of the generic and In-Hospital Neutron Irradiator adjuster rods. The specific designs used in the models and analyses of the HEU cores of GHARR-1 and NIRR-1 are discussed in following sections. These same adjuster rod designs were then utilized in the conversion analyses for the LEU cores.

TABLE 2.2. LOCATION OF THE FOUR REACTIVITY ADJUSTER RODS IN THE GENERIC MODEL

Rod	x (cm)	y (cm)
Central control rod	0.0	0.0
Reactivity adjuster rod 1	0.0000	25.75
Reactivity adjuster rod 2	–24.48971	7.95719
Reactivity adjuster rod 3	0.0000	–25.75
Reactivity adjuster rod 4	24.48971	–7.95719

TABLE 2.3. ESTIMATED REACTIVITY ADJUSTER DESIGN PARAMETERS USED IN MNSR MODELS

Parameter	Generic value (mm)	In-Hospital Neutron Irradiator specifications (mm)
Total length	373	530[1]
Diameter of central Al rod	18	23
Outer diameter of Cd sleeve	20	25
Thickness of Cd sleeve	1	1
Thickness of cladding	2	2
Material of cladding	SS-304	Al
Outer diameter of cladding	34	29
Inner diameter of guide tube	42	n.a.
Outer diameter of guide tube	45	n.a.

[1] This consists of a Be lower length of 250 mm, an Al middle length of 30 mm and a Cd upper length of 250 mm.

FIG. 2.5. Adjuster rod used in the In-Hospital Neutron Irradiator (Reproduced from Ref. [2.5] with permission courtesy of Argonne National Laboratory, USA).

2.3. ESTABLISHMENT OF THE 345 PIN GENERIC HEU CORE CONFIGURATION

A commercial MNSR has 350 grid plate locations in ten rows into which fuel pins, along with four tie rods for support and a central guide tube for the control rod, may be inserted. The number of fuel pins in seven of the eight HEU commercial MNSRs is shown in Table 2.4.

TABLE 2.4. NUMBER OF FUEL PINS IN HEU COMMERCIAL MNSRs

Reactor	Year of first criticality	Number of fuel pins in core	Number of dummy pins
MNSR-SZ, China	1988	345	5
MNSR-SD, China[1]	1989	344	6
MNSR-SH, China[2]	1991	n.a.	n.a.
GHARR-1, Ghana	1995	344	6
ENTC MNSR, Iran	1994	343	7
NIRR-1, Nigeria	2004	347	3
PARR-2, Pakistan	1989	344	6
SRR-1, Syria	1996	347	3

n.a.: not available.
[1] Shut down in 2010.
[2] Shut down in 2008.

The average number of fuel pins in the seven cores shown is 345±2. On this basis, a generic HEU core model with 345 fuel pins and five dummy pins was constructed. In this study, the locations of the five dummy pins were selected in order to keep them as far as possible from the five inner and five outer irradiation sites, to minimize their adverse effect on the flux in the tubes. The three dummy pins in the NIRR-1 reactor and the six dummy pins in the GHARR-1 reactor are located in different positions than shown in Fig. 2.4. Nevertheless, it has been shown that the location of the dummy pins in the outermost ring has only a small effect the overall core excess reactivity.

2.4. CHARACTERISTICS OF THE GENERIC HEU CORE

The generic HEU core assumed a fuel loading of 2.872 g ^{235}U per pin (equivalent to a UAl alloy fuel meat density of 3.456 g/cm^3 with 27.7 wt% U, or a uranium density of 0.957 g/cm^3). Al-303-1 was used in the fuel cladding, four tie rods and five dummy fuel rods. No top shim tray was modelled. The four adjuster rod guide tubes are air filled in place of an adjuster rod. No cadmium foils were inserted in the rabbit tubes. HEU fuel impurities were derived from the 2005 NIRR-1 Final SAR [2.1]. The major characteristics of the generic HEU core are shown in Table 2.5.

Since US and Russian HEU with 90—93% enrichments contain approximately 1 wt% ^{234}U, it is very likely that Chinese origin HEU (90%) also contains about 1 wt% ^{234}U. No ^{236}U is included because ^{236}U does not occur naturally. It is found in HEU (90%) if recycled uranium is re-enriched or if HEU (90%) was obtained by blending a higher enrichment with recycled uranium. For reference purposes, a concentration of 0.5 wt% ^{236}U is worth about 0.32 mk.

TABLE 2.5. CHARACTERISTICS OF THE GENERIC HEU CORE

Excess reactivity	7.74 ± 0.06 mk
Fuel pins in core	345
^{235}U enrichment, wt%	90.0
^{235}U/pin, grams	2.872
^{234}U content, wt%	1.0
^{236}U content, wt%	0.0
Top shim tray	None
Adjuster rod guide tubes	Air filled aluminium tubes
Adjuster rods	None
Cd in rabbit tubes	None

In an actual MNSR, adjustments to the excess reactivity are needed to compensate for differences between the reactor design data and the manufacturer’s as-built materials and geometry data. Some of the most important of these differences are in the as-built ^{235}U and ^{234}U loadings and the as-built impurity levels in the fuel meat. Several parameters are available to make these adjustments, depending on the results of the low power experiments that are done at the CIAE before the reactor is shipped to the customer’s site. Possible reactivity adjustments for the generic HEU core are shown in Table 2.6. The calculated reactivity adjustments are shown in Table 2.7.

TABLE 2.6. POSSIBLE REACTIVITY ADJUSTMENTS FOR GENERIC HEU CORE

Positive reactivity adjustments	Negative reactivity adjustments
— Add up to two fuel pins to core — Flood adjuster rod guide tubes with water	— Remove up to two fuel pins from core — Add top aluminium shim tray — Insert two to four adjuster rods composed of stainless steel or stainless steel with a cadmium sleeve (see Table 2.3) — Insert cadmium in rabbit tubes

TABLE 2.7. CALCULATED VALUES FOR POSSIBLE REACTIVITYADJUSTMENTS OF GENERIC HEU MNSR CORE

Starting excess reactivity of generic HEU MNSR (345 pins)	+7.74 ± 0.06 mk
Add top aluminium shim tray	–1.61 ± 0.08 mk
Subtract one fuel pin (344 pins)	–0.80 ± 0.08 mk
Subtract two fuel pins (343 pins)	–1.50 ± 0.08 mk
Add one fuel pin (346 pins)	+0.73 ± 0.08 mk
Add two fuel pins (347 pins)	+1.73 ± 0.08 mk
Flood 4 adjuster rod guide tubes with water	+0.94 ± 0.08 mk

The reactivity change as a function of water temperature in the core, tank, and pool needs to be considered when the reactor is installed. The water temperature will affect the excess reactivity at criticality and at operating power levels, depending on where the reactor is located and the season of the year. Calculated reactivity changes as a function of water temperature and its corresponding density are shown in Table 2.8 and plotted in Fig. 2.6. The reactivity change due to water temperature changes in the ranges between 20—60°C are probably the most interesting. The reactivity temperature effect due to the beryllium reflector is also estimated and its reactivity coefficient is about –0.01 mk/°C.

TABLE 2.8. CALCULATED EFFECTS OF CHANGING WATER TEMPERATURE AND DENSITY IN GENERIC HEU MNSR CORE

Water temperature (°C)	Excess reactivity (mk)	Uncertainty (mk)	Temperature increment (°C)	Change in reactivity (mk)
20	7.82	±0.08	N/A	N/A
30	7.17	±0.08	30—20	–0.66
40	6.08	±0.08	40—30	–1.09
50	4.62	±0.08	50—40	–1.46
60	2.83	±0.08	60—50	–1.79
70	0.77	±0.08	70—60	–2.06
80	–1.51	±0.08	80—70	–2.28

Calculated k_{eff} values versus temperature were 1.00789±0.00006 at 20°C; 1.00720±0.00006 at 30°C; 1.00466±0.00006 at 50°C; 1.00282±0.00006 at 60°C; and 0.99352±0.00007 at 100°C.

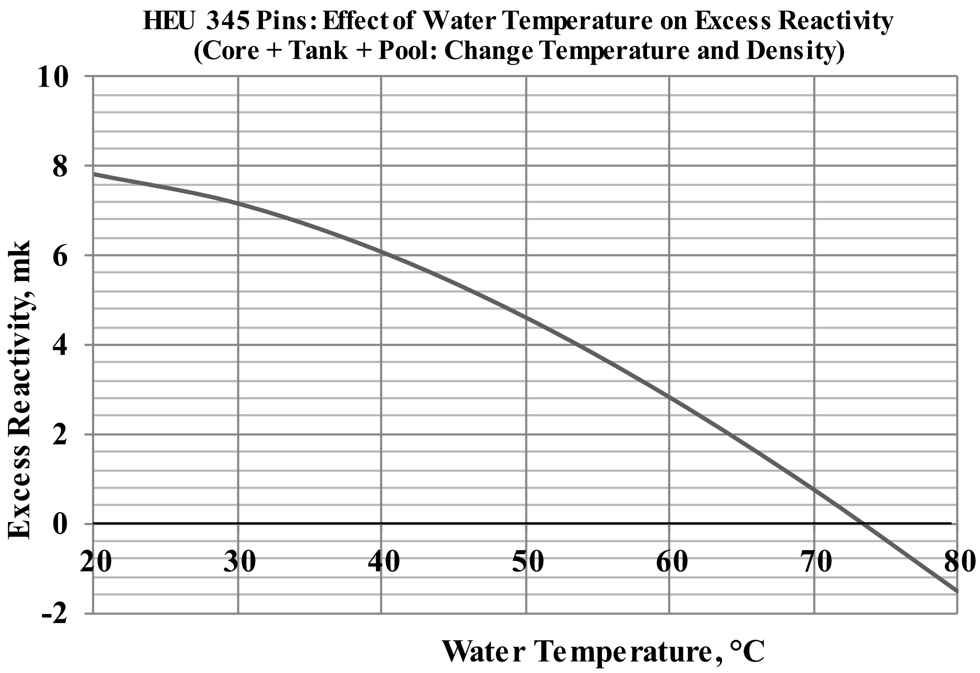

FIG. 2.6. Effect of water temperature on excess reactivity for generic HEU MNSR core for conditions shown in Table 2.5 (Courtesy of Argonne National Laboratory, USA).

2.5. ADAPTATION OF GENERIC HEU CORE MODEL TO HEU REACTOR GHARR-1 IN GHANA

Individual MNSRs are configured slightly different from the generic HEU MNSR in order to make adjustments to the excess reactivity based on the low power experiments that are done at CIAE before the reactor is shipped to the customer's site. Table 2.9 below shows excess reactivities for modifications of the generic reactor that approximate the as-built configuration of the GHARR-1 MNSR in Ghana. GHARR-1 has 344 fuel pins, 1 pin less than the generic HEU core, with slightly different lattice positions in the outermost ring than the generic HEU core. GHARR-1 measured excess reactivity was 3.97 mk, and the top aluminium shim tray was added. The difference between calculation and measurement is (3.76 – 3.97) = –0.21 mk for a water temperature of 20°C. This difference becomes (3.05 – 3.97) = 0.92 mk if the water temperature is 30°C. The four adjuster rods are inserted 48% from the top of the core to match the measured excess reactivity. The measured reactivity worth of four adjuster rods was –1.6 mk. Flooding the four adjuster rod guide tubes (adjuster rods in) with water would increase reactivity by 0.82 ± 0.08 mk.

TABLE 2.9. HEU GHARR-1 EXCESS REACTIVITY

Starting excess reactivity of generic HEU MNSR (345 pins)	+7.74 ± 0.06 mk
Add top aluminium shim tray	–1.61 ± 0.08 mk
Subtract one pin (for a total of 344 pins)	–0.76 ± 0.08 mk
Insert fully 4 stainless steel clad adjuster rods with Cd sleeves in air-filled guide tubes (Cd sleeve inner diameter=18 mm, 1 mm thick)	–1.61 ± 0.08 mk
Total (Based on all water temperature of 20°C and 4 adjuster rods 100% inserted)	+3.76 ± 0.08 mk
Total (Based on all water temperature of 30°C and 4 adjuster rods 100% inserted)	+3.05 ± 0.08 mk
Total (Based on all water temperature of 30°C and 4 adjuster rods 48% inserted)	+4.02 ± 0.08 mk

The reactivity worth of the adjuster rods measured during the commissioning tests of the GHARR-1 reactor was about –0.4 mk per rod. However, the calculated reactivity worth of four SS-304 stainless steel adjuster rods in air-filled guide tubes was only around 0.57 mk. In order to match the measured reactivity worth of -0.4 mk per adjuster rod in air-filled guide tubes for the GHARR-1 HEU core, the adjuster rod design shown in Table 2.10 and Fig. 2.7 was adopted. The overall length is 373 mm as measured at GHARR-1 in August 2010. The ID of the 1 mm thick cadmium sleeve was adjusted to 18 mm in order to obtain the measured reactivity worth of the rods.

TABLE 2.10. REACTIVITY ADJUSTER ROD DESIGN PARAMETERS USED IN GHARR-1 MNSR HEU MODEL

Parameter	GHARR-1 value (mm)
Length of adjuster rod	373
Diameter of central Al rod	18
Outer diameter of Cd sleeve	20
Thickness of Cd sleeve	1
Thickness of cladding	2
Material of cladding	SS-304
Outer diameter of cladding	34
Inner/outer diameter of guide tube	42/45

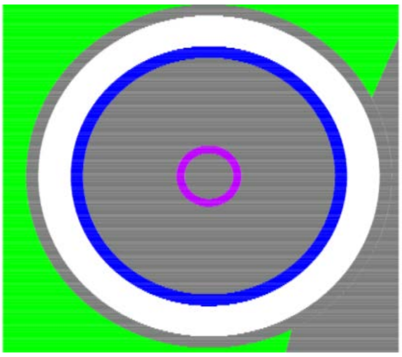

FIG. 2.7. Radial design of adjuster rod design used in GHARR-1 model; Purple=Cd, grey=Al, blue=stainless steel, white=air, green=water (Courtesy of Argonne National Laboratory, USA).

2.6. ADAPTATION OF GENERIC HEU CORE MODEL TO HEU REACTOR NIRR-1 IN NIGERIA

Similar to Section 2.5, Table 2.11 shows excess reactivities for modifications of the generic reactor that approximate the as-built configuration of the NIRR-1 MNSR in Nigeria. NIRR-1 has 347 fuel pins (two pins more than the generic HEU core) with slightly different lattice positions in the outermost ring than the generic HEU core. In addition, the adjuster rod guide tubes are flooded with water. The top aluminium shim tray was added. With these modifications to the generic HEU core, the NIRR-1 core had a calculated excess reactivity of 6.16 ± 0.08 mk, compared with the measured value of 4.97 mk. Cadmium foils were inserted in the rabbit tubes to reduce the excess reactivity to 3.77 mk for start-up.

TABLE 2.11. HEU NIRR-1 REACTOR IN NIGERIA

Starting excess reactivity of generic HEU MNSR (345 pins)	+7.74 ± 0.06 mk
Add top aluminium shim tray	–1.61 ± 0.08 mk
Add two pins (for a total of 347 pins)	+1.73 ± 0.08 mk
Flood four adjuster rod guide tubes with water	+0.94 ± 0.08 mk
Insert fully 4 stainless steel clad adjuster rods with Cd sleeves in water filled guide tubes (Cd sleeve inner diameter=34 mm, 1 mm thick)	–2.64 ± 0.08 mk
Total (Based on water temperature of 20°C and 4 adjuster rods 100% inserted)	+6.16 ± 0.08 mk
Total (Based on water temperature of 25°C and 4 adjuster rods 100% inserted)	+5.80 ± 0.08 mk

(1) The clean NIRR-1 core measured excess reactivity is 4.97 mk [2.1]. The bias between calculation and measurement is (6.16 – 4.97) = 1.19 mk at a water temperature of 20°C. This difference becomes (5.80 – 4.97) = 0.83 mk when the water temperature is 25°C.
(2) Cadmium foils were inserted in the rabbit tubes to reduce the excess reactivity to 3.77 mk for start-up.
(3) The reactivity worth of each of the four adjuster rods was measured to be –0.63 mk, –0.64 mk, –0.69 mk, and –0.67 mk. The total measured reactivity worth is –2.63 mk. The calculated net worth for the four adjuster rods with flooded guide tubes is –2.64 ± 0.08 mk.
(4) Clean NIRR-1 core excess reactivity would be 5.62 ± 0.08 mk if the four adjustor rod guide tubes were air-filled instead of flooded with water.

The reactivity worth of the four adjuster rods measured during the commissioning tests of the NIRR-1 reactor was –2.63 mk. To match this measured reactivity worth, the adjuster rod design shown in Table 2.12 and Fig. 2.8 was adopted. The ID of the 1 mm thick cadmium sleeve was adjusted to 34 mm to obtain the measured reactivity worth.

TABLE 2.12. REACTIVITY ADJUSTER ROD DESIGN PARAMETERS USED IN NIRR-1 MNSR HEU MODEL

Parameter	NIRR-1 value (mm)
Length of adjuster rod	373
Diameter of central Al rod	34
Outer diameter of Cd sleeve	36
Thickness of Cd sleeve	1
Thickness of cladding	2
Material of cladding	SS-304
Outer diameter of cladding	40
Inner/outer diameter of guide tube	42/45

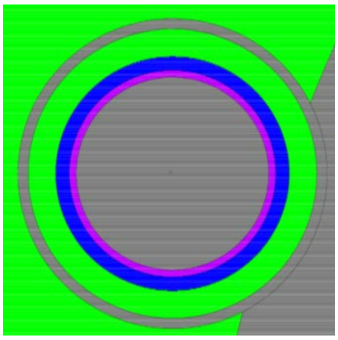

FIG. 2.8. Radial design of adjuster rod design used in NIRR-1 model; purple=Cd, grey=Al, blue=stainless steel, green=water (Courtesy of Argonne National Laboratory, USA).

2.7. CHARACTERISTICS OF THE BASE GENERIC LEU CORE MODEL

The generic LEU core base model was established from the generic HEU core base model. All structures and materials of the HEU core were kept the same, except for the fuel cage, the central control rod, and the central control rod guide tube. A control rod design with a larger outer diameter for the cadmium absorber and a guide tube composed of Zircaloy-4 were also implemented for the LEU core, as shown in Table 2.13, so that the LEU core would have about the same shutdown margin as the HEU core. Uranium isotopes used in the fuel meat of the HEU and LEU fuel pins of the generic MNSR models are compared in Table 2.14 (see Appendix II; Section II.1 for HEU; Section II.9 for LEU).

The number of fuel pins (345) and the core layout were initially kept the same as in the HEU core. The excess reactivity without the top shim tray was calculated to be 4.42 mk. Installing the top shim tray (worth –1.21 mk) would reduce the excess reactivity to 3.21 mk. For reasons described below, three additional LEU fuel pins were added to the core to increase the excess reactivity. Comparison of key core parameters between the HEU and LEU base models are shown in Table 2.15.

TABLE 2.13. CONTROL ROD AND GUIDE TUBE DESIGN PARAMETERS IN GENERIC MNSR MODELS

Parameter	HEU (mm)	LEU (mm)
Outer diameter of cadmium	3.9	4.5
Thickness of stainless steel cladding	0.5	0.5
Thickness of water gap	2.0	1.7
Thickness of guide tube	1.5	1.5
Material of guide tube	LT-21	Zircaloy-4
Outer diameter of guide tube	11.9	11.9

TABLE 2.14. COMPARISON OF URANIUM ISOTOPICS IN GENERIC HEU AND LEU FUEL PINS

Uranium isotopes	HEU (wt%)	LEU (wt%)
^{235}U	90.0	12.5
^{238}U	9.0	87.05
^{234}U	1.0	0.2 (max.)
^{236}U	0.0	0.25 (max.)
Total	100.0	100.0

TABLE 2.15. COMPARISON OF KEY PARAMETERS FOR BASE GENERIC HEU AND LEU CORE MODELS

Key parameters	HEU	LEU
Excess reactivity	7.74 ± 0.06 mk	6.34 ± 0.06 mk
Fuel meat	UAl alloy	UO_2
^{235}U total core loading, g	990.9	1354.3
^{235}U per pin, g	2.872	3.892
^{235}U enrichment, wt %	90.0	12.5
^{234}U content, wt%	1.0	0.2
^{236}U content, wt%	0.0	0.25
Density of fuel meat, g/cm^3	3.456	10.6
Wt% U in fuel meat	27.7	88.1
Fuel meat diameter, mm	4.3	4.3
Active fuel meat length, mm	230	230
Cladding outer diameter, mm	5.5	5.5
Cladding thickness, mm	0.6	0.6
Thickness of He gap, mm	None	0.05
Cladding material	Al-303-1	Zircaloy-4
Number of fuel rods	345	348
Fuel rod pitch	Variable[1]	Variable[1]
Material for grid plates	LT-21	Zirc-4
Material for top shim tray	LT-21	LT-21
Fuel element layout in grids	Same	Same
Number of dummy elements	5	2
Material for dummy elements	Al-303-1	Zircaloy-4
Number of tie rods	4	4
Material for tie rods	Al-303-1	Zircaloy-4
No. of adjuster guide tubes	4	4
Adjuster rod guide tubes	Air-filled Al tubes	Air-filled Al tubes
Top shim tray	None	None
Adjuster rods (Al rod, Cd sleeve, stainless steel cladding)	None	None

[1] Circle diameter and rod pitch for the ten fuel rings are provided in Table I.1 of Appendix I.

In a working LEU MNSR, adjustments to the excess reactivity are likely to be needed to compensate for differences between the reactor design data and the manufacturer's as-built materials and geometry data. Some of the most important of these differences are in the as-built ^{235}U, ^{234}U and ^{236}U loadings, and the as-built impurity levels in the fuel meat. Several parameters similar to those for an HEU MNSR as shown in Table 2.6 are available to make these adjustments, depending on the results of the zero-power experiments that are planned at the CIAE before the reactor is shipped to the customer's site, and choices made by the customer. The calculated possible reactivity adjustments for the generic LEU MNSR core are shown in Table 2.16. For calculation of the reactivity coefficients and performance of the safety analyses for the generic LEU MNSR core, the top shim tray was used and the reactivity adjuster rods were inserted in order to reduce the excess reactivity to about 4 mk.

TABLE 2.16. CALCULATED VALUES FOR POSSIBLE REACTIVITY ADJUSTMENTS OF GENERIC LEU MNSR CORE

Starting excess reactivity of generic LEU MNSR (348 pins)	+6.34 ± 0.06 mk
Add top aluminium shim tray	–1.36 ± 0.08 mk
Subtract one fuel pin (347 pins)	–0.77 ± 0.08 mk
Subtract two fuel pins (346 pins)	–1.26 ± 0.08 mk
Subtract three fuel pins (345 pins)	–1.95 ± 0.08 mk
Add one fuel pin (349 pins)	+0.57 ±0.08 mk
Add two fuel pins (350 pins)	+1.30 ± 0.08 mk
Add four Cd adjuster rods (as in GHARR1 HEU core) fully inserted in air-filled guide tubes	–1.66 ± 0.08 mk
Flood four adjuster rod guide tubes with water (as in NIRR-1 HEU core)	+0.87 ± 0.08 mk
Add four Cd adjuster rods (as in NIRR-1 HEU core) fully inserted in water-flooded guide tubes	–2.49 ± 0.08 mk

Table 2.17 and Fig. 2.9 show the reactivity change as a function of water temperature in the core, tank, and pool for consideration when the LEU core is installed. The corresponding data for the HEU core is included in Fig. 2.9 in order to have a direct comparison of the effects of changes in water temperature in the two cores.

TABLE 2.17. CALCULATED EFFECTS OF CHANGING WATER TEMPERATURE AND DENSITY IN GENERIC LEU MNSR CORE

Water temperature (°C)	Excess reactivity (mk)	Uncertainty (mk)	Temperature increment (°C)	Change in reactivity (mk)
20	4.56 ± 0.08	4.00 ± 0.08	—	—
30	3.91 ± 0.08	3.35 ± 0.08	30—20	–0.55
40	2.97 ± 0.08	2.41 ± 0.08	40—30	–0.94
50	1.76 ± 0.08	1.20 ± 0.08	50—40	–1.30
60	0.26 ± 0.08	–0.30 ± 0.08	60—50	–1.64

Calculated k_{eff} values versus temperature were 1.00467±0.00006 at 20°C; 1.00414±0.00006 at 25°C; 1.00193±0.00006 at 50°C; 1.00011±0.00006 at 60°C; and 0.99152±0.00006 at 100°C.

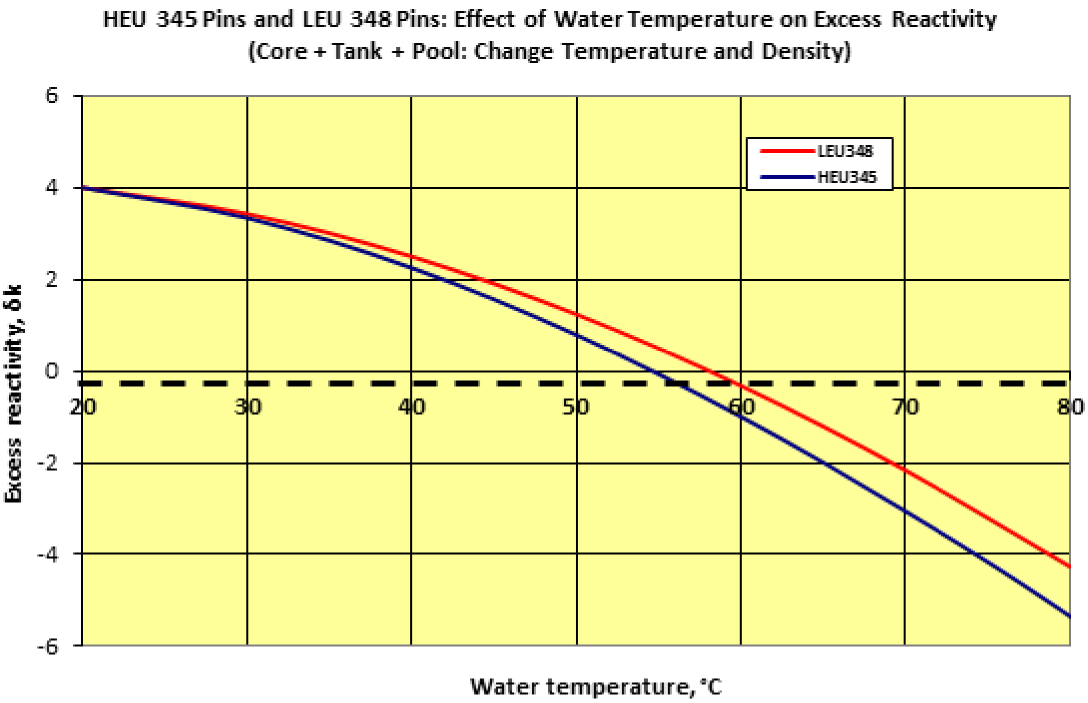

FIG. 2.9. Effect of water temperature on excess reactivity for generic LEU and HEU MNSR cores (Courtesy of Argonne National Laboratory, USA).

2.8. ADAPTATION OF THE GENERIC LEU CORE MODEL TO GENERIC ‘WORKING CORES’

Adaptation of the generic LEU core model with 348 pins to a ‘working core’ for LEU conversion is straightforward, but depends on the design of the reactivity adjuster rods and whether the adjuster rod guide tubes are filled with air (as in the GHARR-1) or flooded with water (as in the NIRR-1). Two example adaptations are shown below.

Both cases begin with the base LEU core with 348 pins and a starting excess reactivity of 6.34 mk. Adding the top aluminium shim tray which has a reactivity worth of –1.36 mk reduced the net excess reactivity to 4.98 mk.

For working core 1, four cadmium adjuster rods with the design described in Section 2.5, Table 2.10, for the GHARR-1 HEU core are inserted 48% from the top of the active fuel zone into air-filled guide tubes, as shown in Fig. 2.10. These adjuster rods have a reactivity worth of –0.96 mk and reduce the net excess reactivity to 4.02±0.08 mk. The data above are based on a water temperature of 20°C for the pool, tank, and core. If the water temperature in these regions were 30°C, the core excess reactivity will decrease to 3.50±0.08 mk. The four adjuster rods need to be inserted 12% from the top of the active fuel zone in order to bring the excess reactivity back to 4.02±0.08 mk. This data is shown in Table 2.18.

TABLE 2.18. GENERIC LEU WORKING CORE 1

Starting excess reactivity of generic LEU MNSR (348 pins)	+6.34 mk	±0.06 mk
Add top aluminium shim tray	–1.36 mk	±0.08 mk
Add four Cd adjuster rods (as in GHARR-1 HEU core) 48% inserted into air-filled guide tubes	–0.96 mk	±0.08 mk
Total (Based on all water temperature of 20°C and 4 adjuster rods 48% inserted)	+4.02 mk	±0.08 mk
Total (Based on all water temperature of 30°C and 4 adjuster rods 48% inserted)	+3.50 mk	±0.08 mk
Total (Based on all water temperature of 30°C and 4 adjuster rods 12% inserted)	+4.02 mk	±0.08 mk

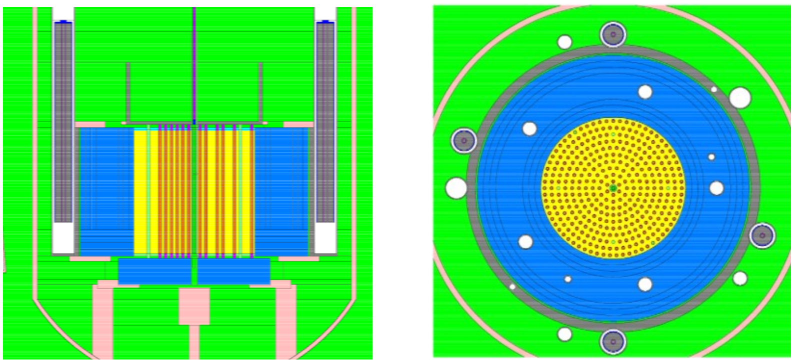

FIG. 2.10. Vertical (left) and horizontal (right) cross-section of generic LEU MNSR working core 1 (Courtesy of Argonne National Laboratory, USA).

For working core 2, four adjuster rods with the design described in Section 2.6, Table 2.12, for the NIRR-1 HEU core are inserted 65% from the top of the active fuel zone into guide tubes that are flooded with water. These adjuster rods have a net reactivity worth of –1.83 mk and reduce the net excess reactivity to 3.98 ± 0.08 mk. The above data are all based on a water temperature of 20°C for the pool, tank, and core. If the water temperature in these regions is 25°C, the core excess reactivity will be reduced to 3.66 ± 0.08 mk. The four adjuster rods need to be inserted 55% from the top of the active fuel zone in order to bring the excess reactivity to 4.02 ± 0.08 mk. This data is summarized in Table 2.19.

TABLE 2.19. GENERIC LEU WORKING CORE 2

Starting excess reactivity of generic LEU MNSR (348 pins)	+6.34 mk	±0.06 mk
Add top aluminium shim tray	−1.36 mk	±0.08 mk
Flood 4 adjuster rod guide tubes with water	+0.83 mk	±0.08 mk
Add four Cd adjuster rods (as in NIRR1 HEU core) 65% inserted into the water flooded guide tubes	−1.83 mk	±0.08 mk
Total (Based on all water temperature of 20°C and 4 adjuster rods 65% inserted)	+3.98 mk	±0.08 mk
Total (Based on all water temperature of 25°C and 4 adjuster rods 65% inserted)	+3.66 mk	±0.08 mk
Total (Based on all water temperature of 25°C and 4 adjuster rods 55% inserted)	+4.02 mk	±0.08 mk

2.9. REVIEW OF ^{235}U LOADING AND DESIGN UNCERTAINTIES

Uncertainties in the LEU fuel loading have not yet been specified. Some of these uncertainties and those in the adjuster rod design and content of the guide tubes for individual MNSRs are shown in Table 2.20.

TABLE 2.20. UNCERTAINTIES IN LEU FUEL LOADING AND DESIGN PARAMETERS

Parameter	Value
^{235}U enrichment (wt%)	12.5
^{235}U loading per pin (g)	3.89
^{234}U content (wt%)	0.2
^{236}U content (wt%)	0.25
Fuel pin cladding diameter (mm)	5.5
Fuel pellet diameter (mm)	4.3
Thickness of He gap (mm)	0.05
Zr impurities	Maximum values are specified
Adjuster rod design	Varies by reactor
Guide tubes air filled or flooded with water	Varies by reactor

Measurements to be made in the zero power experiments will account for the accumulated effects of the uncertainties in the fuel pin loading. The adjustment parameters described in this report are intended to provide insights into the choices that are available to construct an acceptable LEU core for LEU conversion for each reactor. Adjuster rod design and content of the guide tubes will need to be accounted for on an individual reactor basis.

2.10. ANALYSES FOR LEU CONVERSION

2.10.1. Why 12.5% enrichment instead of 19.75% enrichment?

Early studies by Argonne National Laboratory (ANL) [2.6] in the CRP addressed two ways in which MNSRs could be converted to LEU fuel. It was realized from the beginning that the ^{235}U content of UO_2 fuel with 19.75% enriched uranium and the same number of fuel pins as in the HEU core is too large to meet the maximum excess reactivity requirement of 4 mk for MNSRs. The design choices considered were to maintain the number of fuel rods in the current HEU-fuelled MNSRs and reduce the enrichment of the uranium below 19.75%, or to reduce the number of fuel rods in the core using 19.75% enriched uranium to achieve an excess reactivity of 4 mk.

The reactor physics parameters most likely to be affected by these choices are reactivity changes with temperature during start-up (power coefficient) and during reactor transients. An important design goal for LEU conversion cores has been to have reactivity temperature coefficients that are comparable between the HEU and LEU cores [2.7]. In this way, it is likely that the power coefficient for the LEU core will remain negative for the entire operating temperature range of the reactor, and that reactor transients in the HEU and LEU cores will result in comparable changes in physics parameters.

Table 2.21 compares reactivity changes due to changing water temperature only, water density only, and fuel temperature only for four cases: HEU (90%) UAl alloy fuel and 347 fuelled pins; LEU (12.5%) UO_2 fuel and 347 pins; LEU (19.75%) UO_2 fuel with 206 fuelled pins and no dummy pins; and LEU (19.75%) UO_2 fuel with 242 fuelled pins and 108 zircaloy dummy pins. Reactivity changes for all reactivity change components are negative and comparable in the HEU (90%) and LEU (12.5%) cases with 347 fuel pins.

TABLE 2.21. TEMPERATURE REACTIVITY CHANGES FOR HEU AND 3 LEU MNSR DESIGNS (ALL DATA IN %δk/k)

Temperature interval	HEU (90%) UAl alloy 347 pins	LEU (12.5%) UO_2 347 pins	LEU (19.75%) UO_2 206 pins, no dummies	LEU (19.75%) UO_2 242 pins, 108 dummies
		Water temperature		
20—30°C	–0.0299	–0.0169	+0.0419	+0.0399
20—50°C	–0.1658	–0.1007	+0.0419	+0.0100
20—100°C	–0.5253	–0.3298	+0.0150	–0.0649
		Water density (void coefficient)		
20—30°C	–0.0968	–0.0928	–0.0659	–0.0959
20—50°C	–0.3713	–0.3802	–0.3001	–0.3385
20—100°C	–1.4405	–1.5074	–1.2553	–1.3719
		Fuel temperature (Doppler)		
20—30°C	–0.0009	–0.0077	–0.0054	–0.0037
20—50°C	–0.0028	–0.0232	–0.0162	–0.0112
20—100°C	–0.0075	–0.0619	–0.0433	–0.0299
		Total reactivity change		
20—30°C	–0.1276	–0.1174	–0.0294	–0.0597
20—50°C	–0.5399	–0.5054	–0.2745	–0.3397
20—100°C	–1.9733	–1.8991	–1.2836	–1.4667

Reducing the number of LEU fuel pins to 206 results in a substantial increase in the ratio of water to fissile in the core and leads to small calculated positive reactivity changes when the water temperature only is increased. Reactivity changes for water density only and fuel temperature only are negative, but smaller in magnitude than in the HEU or LEU (12.5%) cores with 347 pins. The dummy pins were inserted into the last case as shown in the final column of Table 2.21 in order to decrease the ratio of water to fissile in the core. All of the coefficients become more negative, but the magnitude is still substantially smaller than in the case of the LEU (12.5%) fuel.

These absolute reactivity coefficients are somewhat difficult to calculate, but the relative trends are correct. On this basis, it was decided to use an LEU core with the same number of pins as the current HEU core and reduce the enrichment of the uranium to 12.5%. The next section evaluates the neutron flux performance for the HEU and LEU (12.5%) cases.

2.10.2. Neutron flux performance

The detailed MCNP models described previously for the HEU and LEU cores were used to calculate thermal, epithermal, and fast neutron fluxes in the inner and outer irradiation positions, and also the fission chamber and the slant tube. These calculations were made to compare the relative performance of the cores. The results in Table 2.22 show a reduction of 7–10% in the thermal neutron flux in the irradiation channels of the LEU core in comparison to the HEU core. Consequently, the power level of the LEU core would need to be increased by approximately 10% from the current value of 30 kW in order to match the nominal flux level for MNSRs using HEU fuel.

TABLE 2.22. COMPARISON OF NEUTRON FLUX DATA AT INNER IRRADIATION CHANNELS, OUTER IRRADIATION CHANNELS, FISSION CHAMBERS AND SLANT TUBE IN NIRR-1

Neutron energy	Thermal flux ($\times 10^{11}$ cm^{-2}s^{-1})		Epithermal flux ($\times 10^{11}$ cm^{-2}s^{-1})		Fast flux ($\times 10^{11}$ cm^{-2}s^{-1})	
Location	Inner	Outer	Inner	Outer	Inner	Outer
HEU 90.2%	11.6 ± 0.01	6.60 ± 0.01	12.9 ± 0.01	1.85 ± 0.01	2.69 ± 0.01	0.36 ± 0.003
UO_2 12.5%	10.4 ± 0.01	6.19 ± 0.01	12.6 ± 0.01	1.80 ± 0.01	2.59 ± 0.01	0.35 ± 0.003
Location	Fission chamber	Slant tube	Fission chamber	Slant tube	Fission chamber	Slant tube
HEU 90.2%	11.9 ± 0.01	0.255 ± 0.002	13.3 ± 0.01	0.036 ± 0.0005	2.60 ± 0.01	0.018 ± 0.0004
UO_2 12.5%	10.6 ± 0.01	0.241 ± 0.002	12.8 ± 0.01	0.033 ± 0.0005	2.47 ± 0.01	0.017 ± 0.0004

2.10.3. Core lifetime performance

Core lifetimes were estimated for the generic HEU core with 345 pins (HEU345) at a power level of 30 kW and the LEU core with 348 pins (LEU348) at a power level of 34 kW using a simple reactivity rundown model with the REBUS3 diffusion theory burnup code [2.8].

A much more detailed and realistic simulation of the MNSR operational scheme exists in which top beryllium shim additions were added cycle-by-cycle to maintain core excess reactivity between 4.0 mk at the beginning of the cycle, and 2.3 mk at the end of cycle for every cycle until the total beryllium shim height reached 10.95 cm [2.9]. In the simple reactivity rundown model, it was assumed that the top beryllium shim tray was filled to the maximum of 10.95 cm for the fresh core and the reactivity was rundown to 2.3 mk. The two methods are demonstrated in Ref. [2.9] to give very similar results for estimated core lifetimes.

For the HEU345 core at a power level of 30 kW, the REBUS3 excess reactivity rundown curve was adjusted for a bias of –0.47 mk between the MCNP5 model and the REBUS3 model, and the equilibrium xenon worth of 3.81 mk. For the LEU348 core at a power level of 34 kW, the REBUS3 excess reactivity rundown curve was adjusted for the bias of 2.45 mk between the MCNP5 model and the REBUS3 model, and the equilibrium xenon worth of 3.18 mk. The end of core life was reached when the excess reactivity of the generic LEU348 core decreased to 2.3 mk in both models.

The results shown in Fig. 2.11 indicate that the generic LEU348 core operated at power level of 34 kW would have a lifetime of about 903 full power equivalent days (FPED) based on reactivity, while for the generic HEU345 core operated at a power level of 30 kW would have a lifetime of about 810 FPED. That is, the lifetime of the LEU core is predicted to be approximately 11% longer than that of the HEU core.

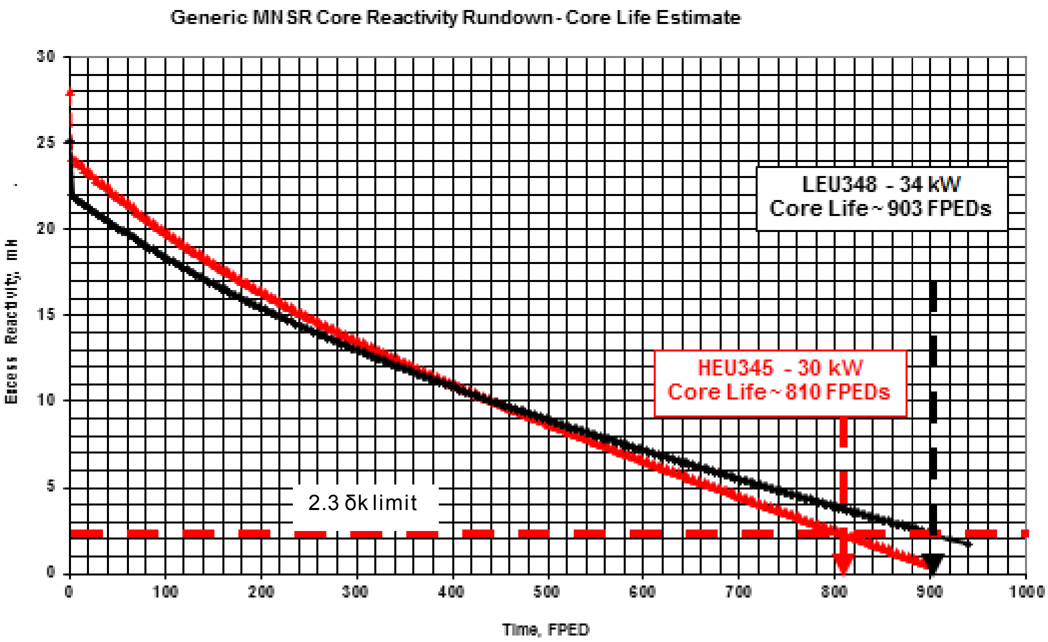

FIG. 2.11. MNSR generic HEU345 and LEU348 core lifetime estimates based on REBUS3 model using simple reactivity rundown calculations for fresh core loaded with 10.95 cm top Be shims and operated at powers of 30 kW for the HEU345 core and 34 kW for the LEU348 core (Courtesy of Argonne National Laboratory, USA).

In terms of practical reactor operation, assuming that the HEU345 core is operated at 30 kw for two hours per day, four days per week, and 48 weeks per year, the estimated core life of 810 FPEDs is equivalent to 50.6 years ($810 / (2 \times 4 \times 48 / 24) = 50.6$). Assuming that the MNSR generic LEU348 core is operated at 34 kw for two hours per day, four days per week, and 48 weeks per year, the estimated core life of 903 FPEDs is equivalent to 56.4 years ($903 / (2 \times 4 \times 48 / 24) = 56.4$).

For reference purposes, calculated integral and differential reactivity worths of the top beryllium shim plates are shown in Fig. 2.12 (from Ref. [2.9]) for both HEU and LEU cores. The top beryllium shim plates' worth is slightly more in the HEU core than in the LEU core. After adding around 10–12 cm of beryllium shim plates, the worth diminishes for any further addition.

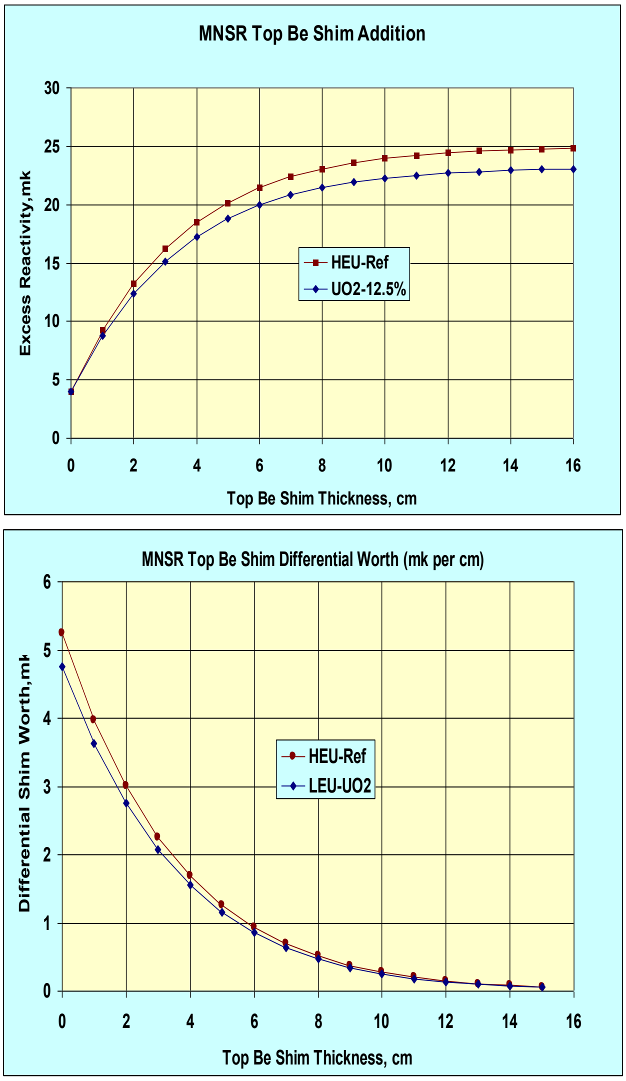

FIG. 2.12. Excess reactivity increases due to top Be shim addition (top) and differential worth of top Be shim plates (mk/cm) (bottom). Comparison between the HEU core and the LEU core with UO_2 12.5% fuel (Reproduced from Ref. [2.9] with permission courtesy of Argonne National Laboratory, USA).

2.10.4. Shutdown margin

As described in Section 2.7, a control rod design with a larger outer diameter for the cadmium absorber and a guide tube composed of Zircaloy-4 were implemented for the LEU core so that the LEU core would have about the same shutdown margin as the HEU core. Both cores have a maximum excess reactivity of 4 mk. The maximum excess reactivity was calculated to be 6.95 mk in the HEU core and 6.74 mk with the new control rod design in the LEU core. Thus, the minimum shutdown margins are –2.95 mk in the HEU core and –2.74 mk in the LEU core.

2.10.5. Plutonium production

The depletion of ^{235}U and the production of ^{239}Pu were analysed for the generic MNSR cores using both REBUS3 [2.8] and ORIGEN2 [2.10] codes. The mass inventories of ^{239}Pu and ^{235}U obtained in ORIGEN2 calculations are shown in Table 2.23 for the HEU345 and LEU348 cores. The data is plotted in Fig. 2.13.

With ORIGEN2, the HEU345 fuel at the end of 810 FPED reached an average burnup of 3.05 wt%, almost identical with the 3.09 wt% burnup obtained using the REBUS3 code. Both codes predict that about 0.16 grams of ^{239}Pu would build up over the HEU345 core lifetime of 810 FPED.

The LEU348 fuel at the end of 910 FPED reached an average burnup of 2.85 wt%, almost identical with the 2.81 wt% burnup obtained using the REBUS3 code. Both codes predict that about 4.15 grams of ^{239}Pu would build up over the LEU348 core lifetime of 910 FPED.

TABLE 2.23. ORIGEN2 CALCULATED MASS INVENTORIES OF ^{239}PU AND ^{235}U FOR 810 FPED IRRADIATION IN THE HEU345 CORE AND 910 FPED IRRADIATION IN THE LEU348 CORE

HEU345, 30 kW FPEDs	HEU345, 30 kW ^{239}Pu (g)	HEU345, 30 kW ^{235}U (g)	LEU348, 34 kW FPEDs	LEU348, 34 kW ^{239}Pu (g)	LEU348, 34 kW ^{235}U (g)
0	0.000	0.000	0	0.000	0.000
75	0.014	988.1	90	0.407	1350.2
150	0.029	985.3	180	0.828	1346.4
225	0.045	982.5	270	1.247	1342.5
300	0.059	979.7	360	1.663	1338.7
375	0.074	976.9	450	2.076	1334.9
450	0.089	974.1	540	2.486	1331.1
525	0.104	971.3	630	2.895	1327.3
600	0.119	968.5	720	3.300	1323.5
675	0.133	965.7	810	3.703	1319.7
810	0.159	960.7	910	4.148	1315.4
ORIGEN2 ^{235}U burnup (wt%)		3.05%			2.85%
REBUS3 ^{235}U burnup (wt%)		3.09%			2.81%

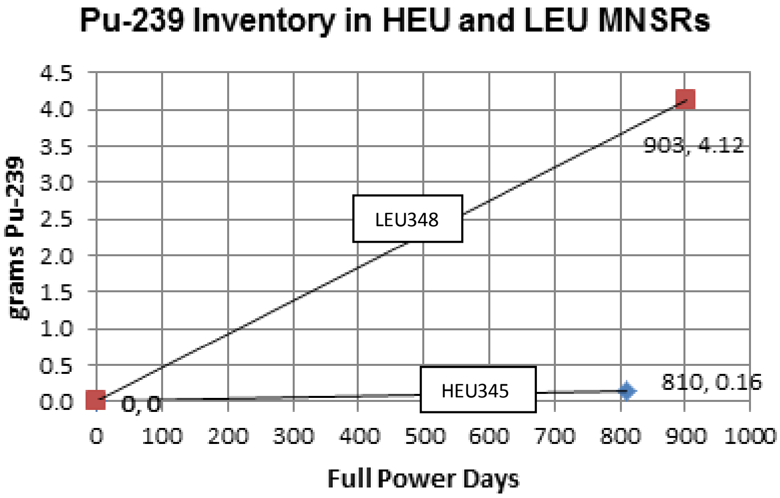

FIG. 2.13. Comparison of ^{239}Pu production from ORIGEN2 for the HEU345 and LEU348 cores (Courtesy of Argonne National Laboratory, USA).

2.10.6. Steady state thermal-hydraulic safety margins

2.10.6.1. Results using the PLTEMP version 4.1 code

The power level at which ONB occurs was calculated for the HEU and LEU cores of the generic MNSR using a one pin model (Fig. 2.14) in the PLTEMP/ANL V4.1 code [2.11] and in the RELAP5 V3.3 code [2.12]. Analyses were first done in both PLTEMP/ANL and RELAP5 using the Churchill–Chu heat transfer correlation without hot channel factors (HCF) to show that both codes give nearly the same results. R2 is the mean radius of the fuel meat, and the value for each radius is given in Table 2.24.

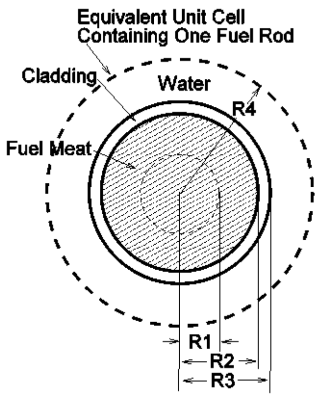

FIG. 2.14. PLTEMP/ANL model of the generic HEU core fuel pin (not to scale) (Courtesy of Argonne National Laboratory, USA).

TABLE 2.24. UNIT CELL DIMENSIONS OF HEU FUEL ROD

	Radius (mm)
R1	1.075
R2	2.15
R3	2.75
R4	6.2167

Calculations were also done with PLTEMP/ANL using HCFs to estimate the effects of uncertainties in various reactor parameters, including power, flow, and manufacturing tolerances. These uncertainties were also simulated in RELAP5 code and the results compared with those from PLTEMP/ANL.

In addition, a heat transfer correlation developed by the CIAE for HEU MNSRs [2.13] was incorporated into PLTEMP/ANL and calculations were done for ONB, both with and without HCFs. Finally, calculations were done using the RELAP5 code, including the simulated HCFs, with power levels beyond ONB to determine the power level at which OSV and power oscillations occur.

The reactor design data used in the safety margin calculations are given in Table 2.25 [2.14]. The power distributions in the HEU and LEU cores of the generic MNSR were calculated using the MCNP5 code [2.4]. The axial power profiles of the peak and average power fuel pins in the HEU and LEU cores are shown in Table 2.26 and plotted in Fig. 2.15. The axial power profiles given in Table 2.26 are normalized to the actual power produced by the pin at the nominal power of the reactor. The grid locations of the peak power pins in the HEU and LEU cores are shown in Fig. 2.16.

TABLE 2.25. THERMAL-HYDRAULIC ANALYSIS OF THE GENERIC MNSR USING PLTEMP/ANL CODE

Thermal-hydraulic data	HEU	LEU
Reactor power	30	34
Number of fuel pins in reactor	345	348
Peak pin power (W)	99.66	113.19
Average pin power (W)	86.96	97.70
Peak pin/average pin power ratio	1.1461 ± 0.3% (3σ)	1.1586 ± 0.3% (3σ)
Location of peak pin in core*	Row 2	Row 2
Fuel meat	UAl alloy	UO_2
Uranium enrichment	90.2 %	12.5 %
U wt% in fuel meat	27.5	88.1
Cladding material	Al alloy	Zircaloy-4
Gas in meat cladding gap	—	He
Meat radius (mm)	2.15	2.15
Gas gap thickness (mm)	—	0.05
Cladding thickness (mm)	0.6	0.6
Fuelled length (m)	0.230	0.230
Unheated length below the fuelled length (m)	0.009	0.009
Unheated length above the fuelled length (m)	0.009	0.009
Total height of a fuel pin (m)	0.248	0.248
Height above the pins through which whole core mixed coolant flows (m)	~0.016	~0.016
Inner diameter of annular beryllium around all fuel pins (m)	0.231	0.231
Fuel meat thermal conductivity (W/m°C)	140	5.78
Cladding thermal conductivity (W/m°C)	180	14.74
Gap gas thermal conductivity (W/m°C)	—	0.1767
Gap thermal resistance (m^2°C/W)	—	~0.000283
Hydraulic diameter for hot pin (m) [2.2]	0.0231	0.0231
Flow area for hot pin (m^2)*	9.978×10^{-5}	9.978×10^{-5}

* Based on a row-by-row calculation of flow area per fuel rod.

TABLE 2.25. THERMAL-HYDRAULIC ANALYSIS OF THE GENERIC MNSR USING PLTEMP/ANL CODE (cont.)

Thermal-hydraulic data	HEU	LEU
Depth of water above core top (m)	4.7	4.7
Pressure at core top (MPa)	0.1468	0.1468
Calibration of hydraulic loss based on a test at 15 kW:		
Core inlet temperature (°C)	24.5	24.5
Coolant temperature rise (°C)	13	13
Calibrated loss coefficient	67.3	68.6
Calculated core flow rate (kg/s)	0.277	0.277
Steady state at nominal reactor power with core inlet temperature adjusted for an exit temperature of 70°C:		
Adjusted inlet temperature (°C)	53.78	52.28
Core flow rate (kg/s)	0.441	0.47
Coolant outlet temperature (°C)	70.0	70.0
Max. cladding surface temperature (°C)	86.4	87.8
Max. fuel centre line temperature (°C)	86.7	100.5

* The innermost row of six fuel pins around the central control rod is counted as the first row.
** Based on a row-by-row calculation of flow area per fuel rod.

TABLE 2.26. AXIAL POWER PROFILES OF PEAK AND AVERAGE POWER PINS IN GENERIC HEU AND LEU CORES

Axial segment	HEU generic core, 30 kW, 345 fuel pins				LEU generic core, 34 kW, 348 fuel pins			
	HEU peak pin		HEU average pin		LEU peak pin		LEU average pin	
Position (cm)	Power (kW)	Sigma	Power (kW)	Sigma	Power (kW)	Sigma	Power (kW)	Sigma
-10.35	10.03	0.28%	8.59	0.02%	11.55	0.30%	9.66	0.02%
-8.05	10.11	0.28%	8.56	0.02%	11.39	0.30%	9.62	0.02%
-5.75	10.84	0.27%	9.20	0.02%	12.21	0.29%	10.34	0.02%
-3.45	11.24	0.27%	9.64	0.02%	12.95	0.28%	10.85	0.02%
-1.15	11.20	0.27%	9.76	0.02%	12.90	0.28%	10.98	0.02%
1.15	10.77	0.27%	9.55	0.02%	12.29	0.29%	10.73	0.02%
3.45	10.15	0.28%	9.00	0.02%	11.46	0.30%	10.10	0.02%
5.75	9.18	0.30%	8.15	0.02%	10.33	0.31%	9.15	0.02%
8.05	7.99	0.31%	7.18	0.02%	8.99	0.34%	8.06	0.02%
10.35	8.14	0.31%	7.33	0.02%	9.11	0.33%	8.22	0.02%
Peak pin total	99.66	0.10%	86.95	0.01%	113.19	0.10%	97.70	0.01%

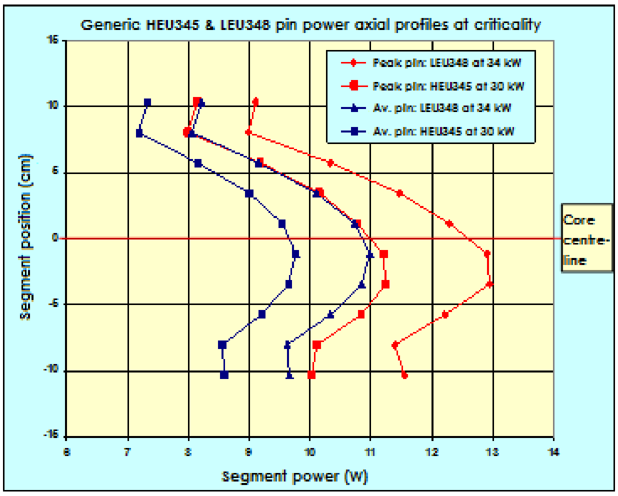

FIG. 2.15. Axial power profiles of peak and average power pins in generic MNSR HEU and LEU cores (Courtesy of Argonne National Laboratory, USA).

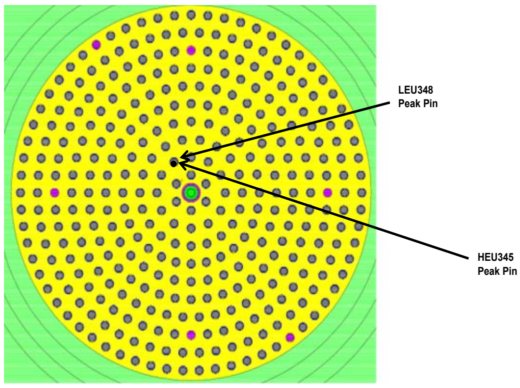

FIG. 2.16. Location of peak power pin in the generic MNSR HEU and LEU cores (Courtesy of Argonne National Laboratory, USA).

Table 2.27 shows predicted values at ONB without HCFs in the HEU and LEU cores.

TABLE 2.27. THERMAL-HYDRAULIC RESULTS AT ONB FOR THE HEU AND LEU CORES WITHOUT HCFs USING THE CHURCHILL–CHU AND CIAE HEAT TRANSFER CORRELATIONS IN THE PLTEMP/ANL CODE

	Churchill–Chu correlation		CIAE correlation	
	HEU	LEU	HEU	LEU
Reactor power at ONBR=1 on peak pin without HCFs	65.2	67.8	78.6	80.6
Core flow rate (kg/s)	0.586	0.588	0.657	0.627
Coolant outlet temperature (°C)	80.6	79.7	83.7	82.9
Max. cladding surface temperature (°C)	112.9	112.9	113.1	113.2
Max. fuel centre line temperature (°C)	113.5	149.2	113.8	154.8

HCFs in natural circulation with fuel pins: Six HCFs are used in the PLTEMP/ANL V4.1 code to calculate research reactor safety margins.

System wide or global HCFs:

- FFLOW: factor to account for the uncertainty in total reactor flow;
- FPOWER: factor to account for the uncertainty in total reactor power; and
- FNUSLT: factor to account for the uncertainty in Nusselt number correlation.

Local HCFs:

- FBULK: factor for local bulk coolant temperature rise;
- FFILM: factor for local temperature rise across the coolant film; and
- FFLUX: factor for local heat flux from cladding surface.

The six HCFs used by PLTEMP/ANL for these calculations were obtained from typical fuel fabrication tolerances and other uncertainties, using the formulas described in detail in Ref. [2.15]. Typical tolerances were used due to the unavailability of the actual tolerances specific to the Chinese fuel fabrication process for these reactors. Table 2.28 shows the values of fuel fabrication tolerances and other uncertainties that were used. Tables 2.29 and 2.30 show the values of HCFs calculated for the HEU and LEU cores of a generic MNSR.

TABLE 2.28. UNCERTAINTIES INCLUDED IN THE SIX HCFs

Uncertainty type	Fractional value		Effect on HCF (× implies an uncertainty affects an HCF)					
	HEU	LEU	FPOWER	FFLOW	FNUSLT	FBULK	FFILM	FFLUX
Neutronics calculation of local power density in a pin	0.10	0.10				×	×	×
^{235}U loading per pin	0.03	0.03				×	×	×
Local fuel meat radius	0.003	0.003					×	×
U enrichment in a pellet	n.a.	0.016					×	×
UO_2 pellet density	n.a.	0.044						
Fuel pin radius	0.003	0.003				×	×	×
Fuel pin pitch	0.003	0.003				×	×	
Flow redistribution among channels	0.064	0.064				×		
Uncertainty (3σ) in calculated reactor power level (global)	0.003	0.003	×					
Uncertainty in channel flow (global)	0.0385	0.0385		×				
Heat transfer coefficient uncertainty due to uncertainty in Nusselt number correlation (global)	0.13	0.13			×			

n.a.: not applicable.

The PLTEMP/ANL code obtains, for an input nominal reactor power, a thermal-hydraulic solution using the three global HCFs FFLOW, FPOWER and FNUSLT for a hot pin. The random HCFs FBULK, FFILM and FFLUX are not used in this solution. Having obtained the above solution, the random HCFs FBULK, FFILM and FFLUX are applied to the temperatures obtained. The ONB ratio is computed using the temperatures with all six HCFs applied.

The hydraulic resistance of the coolant flow circuit in the PLTEMP/ANL model was obtained by calibrating the model to reproduce an experimentally measured coolant temperature rise of 13°C (from 24.5°C to 37.5°C) at a reactor power of 15 kW [2.16, 2.17]. The results of this calibration for both reactor cores are also given in Table 2.25. Using the calibrated model, the coolant inlet temperature was raised and adjusted to get an outlet temperature of 70°C in steady state at the nominal reactor power. Table 2.25 also shows the adjusted inlet temperature and some operating parameters found by this calculation.

Using the adjusted coolant inlet temperature in the calibrated model, the allowed reactor power without HCF was calculated to compare results using the PLTEMP/ANL code and the RELAP5 code [2.12]. In this calculation, the maximum allowed reactor operating power corresponding to the onset of boiling (ONB ratio = 1.0) was calculated for the HEU and LEU cores of each reactor without applying the HCFs. However, the radial power peaking factor of the peak fuel pin was included in this calculation. The maximum allowed reactor operating power was found to be 65.2 kW and 67.8 kW for the generic MNSR HEU and LEU cores using the Churchill–Chu heat transfer correlation, as shown in Table 2.27.

TABLE 2.29. DERIVED UNCERTAINTIES FOR HEU AND LEU CORES OF A GENERIC MNSR

	HEU	LEU
Fractional uncertainty in local ^{235}U homogeneity	0.03[1]	0.0472[2]
Fractional uncertainty in local AD**2 of a channel	0.0247	0.0247
Fractional uncertainty in channel hydraulic diameter	0.0087	0.0087

[1] This is a typical value for uncertainty in ^{235}U loading used in manufacturing specifications.
[2] This value of 4.7% may be compared with the corresponding value of 3% reported in the Final SAR of the Shearon Harris Nuclear Power Plant [2.18], which is a relatively recent commercial PWR that began producing power on 2 May 1987.

TABLE 2.30. DERIVED HCFs FOR THE HEU AND LEU FUEL PINS IN NATURAL CIRCULATION

HCF	FBULK	FFILM	FFLUX	FPOWER	FFLOW	FNUSLT
HEU	1.0814	1.1150	1.1146	1.1477[1]	1.0385	1.1300
LEU	1.0814	1.1150	1.1146	1.1621[1]	1.0385	1.1300

[1] FPOWER=1.003×(Peak pin to average power ratio). The maximum power is reported as true power, and therefore the power measurement uncertainty is not included in this HCF.

The power (true nominal) corresponding to an ONB ratio of 1.0 with all HCFs using the Churchill–Chu heat transfer correlation and the CIAE heat transfer correlation are given in Table 2.31. Using all six HCFs, the true power corresponding to the onset of boiling is found to be 51.2 kW and 53.0 kW respectively for the generic MNSR HEU and LEU cores using the Churchill–Chu heat transfer correlation, and 61.1 kW and 63.1 kW using the CIAE heat transfer correlation. The CIAE correlation gives larger heat transfer coefficients compared to the Churchill–Chu correlation, resulting in higher powers for ONB.

These are true power values in the sense that there is no allowance for error in the power measuring instrument. The maximum cladding surface temperature (equal to the ONB temperature) is 112.7°C for the HEU and LEU cores using the Churchill–Chu correlation and 112.9°C using the CIAE correlation.

TABLE 2.31. THERMAL-HYDRAULIC ANALYSIS OF THE GENERIC MNSR WITH HCFs USING THE CHURCHILL–CHU AND THE CIAE HEAT TRANSFER CORRELATIONS IN THE PLTEMP/ANL CODE

Thermal-hydraulic data:	Churchill–Chu correlation		CIAE correlation	
	HEU	LEU	HEU	LEU
	HCFs:			
(1) Global HCF: FPOWER	1.150	1.162	1.150	1.162
(2) Global HCF: FFLOW	1.039	1.039	1.039	1.039
(3) Global HCF: FNUSLT	1.130	1.130	1.130	1.130
(4) Local HCF: FBULK	1.081	1.081	1.081	1.081
(5) Local HCF: FFILM	1.109	1.115	1.109	1.115
(6) Local HCF: FFLUX	1.109	1.115	1.109	1.115
Steady state at reactor power raised for an ONB ratio minimum of 1.0:				
Inlet temperature (°C)	53.78	52.28	53.78	52.28
Reactor power at min. ONB ratio=1 with all six HCFs	51.2	53.0	61.1	63.1
Location of min. ONB ratio	Node 10	Node 10	Node 10	Node 10
ONB temperature at location of min. ONB ratio	112.7	112.7	112.9	112.9
Flow rate in hot channel (kg/s)	0.00157	0.00157	0.00168	0.00167
Coolant velocity in hot channel (m/s)	0.0160	0.0160	0.0168	0.0170
Channel outlet temperature (°C)	81.7	81.2	85.0	84.7
Max. cladding surface temperature (°C)	112.7	112.7	112.9	112.9
Max. fuel centre line temperature (°C)	113.9	145.2	114.3	149.9

2.10.6.2. Results using the RELAP5 version 3.3 code

Analysis of the generic MNSR with LEU fuel was performed using the RELAP5 Version 3.3 code [2.12] to determine safety margins during normal steady state operation for comparison with the PLTEMP/ANL results shown above. Steady state conditions were used to limit operating conditions. The temperature in the upper part of the reactor vessel was held constant while cases were run at higher power levels to determine the power levels for ONB and OSV. The reactor behaviour beyond OSV was also investigated.

The RELAP5 core treatment includes a peak channel for the highest power pin and its coolant, and an average channel for the remaining 347 pins and their coolant. The RELAP5 model also includes an inlet plenum, an outlet plenum, a downcomer region between the beryllium moderator annulus and the vessel wall, an orifice coefficient between the outlet plenum and the upper part of the vessel, an orifice coefficient between the inlet plenum and the downcomer region, and source and sink volumes to represent the coolant in the upper part of the vessel. The calculation accounted for thermal conduction from the average core channel to the downcomer region, through the beryllium annulus. Therefore, the core inlet temperature was somewhat higher than the coolant temperature in the upper part of the vessel, however the core temperature rise was lower than it would be without thermal conduction through the beryllium.

The limiting operating conditions used for a typical MNSR are listed in Table 2.32. These conditions led to a temperature of 50.96°C at the top of the downcomer.

TABLE 2.32. LIMITING OPERATING CONDITIONS FOR LEU GENERIC MNSR

Condition	Value
Reactor power (kW)	34
Coolant outlet temperature (°C)	70
Depth of water above the top of the core (m)	4.7

(a) Flow rate calibration

The flow rate was calibrated by adjusting the orifice coefficients for the external orifices below the inlet plenum and above the outlet plenum to fit measured temperatures in the NIRR-1 MNSR reactor in Nigeria. A comparison of measured and calculated inlet and outlet temperatures in Fig. 2.17 shows that use of an orifice coefficient of 1.35 for nominal cases gives excellent results. For cases to be discussed later that include uncertainties simulating HCFs, an orifice coefficient of 1.70 was used.

Cases were run for higher power levels, holding the temperature at the top of the downcomer at 50.96°C. Even though steady state operation was simulated, the cases were run as transients. All temperatures started at 50.96°C, the power started at one watt, and all coolant flow rates started at zero. The power was then raised to its specified value in one second, and the transient was run for 1000 s. Calculated temperatures and flows settled to steady state conditions well before 1000 s of the transient, except at high power levels.

(b) Results without uncertainties

Comparison of ONB results using PLTEMP/ANL and RELAP5 for the generic LEU MNSR operating at 34 kW without uncertainties using the Churchill-Chu heat transfer correlation is shown in Table 2.33. The reactor power level at which ONB is predicted to occur in the hot channel is 68.7 kW, using RELAP5 Version 3.3. This is in excellent agreement with the power level of 67.8 kW calculated using PLTEMP/ANL Version 4.1.

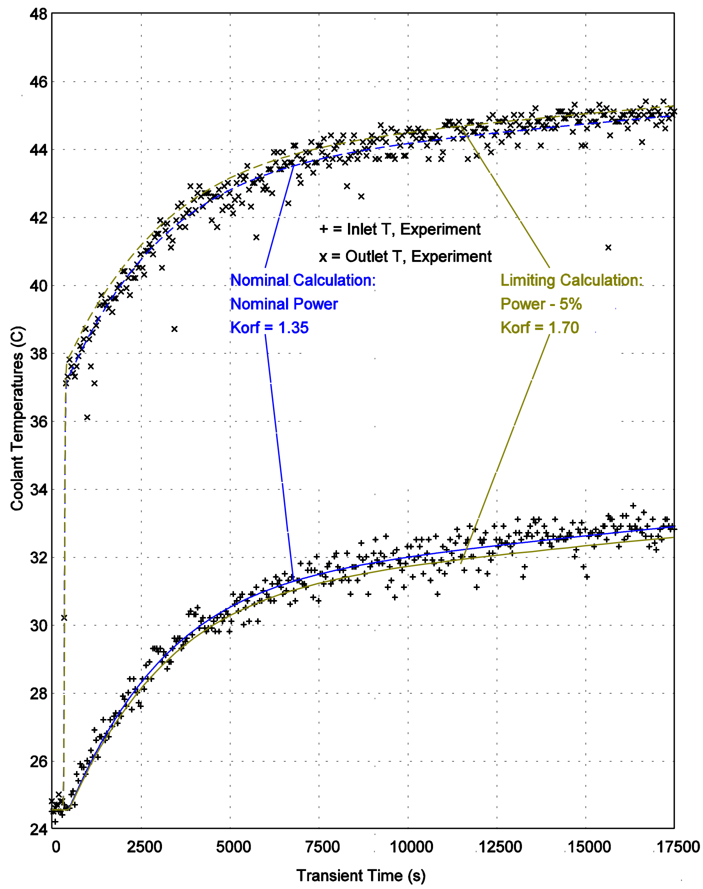

FIG. 2.17. Calibration of external orifice coefficients using NIRR-1 MNSR reactor data (Courtesy of Argonne National Laboratory, USA).

TABLE 2.33. COMPARISON OF ONB RESULTS USING PLTEMP/ANL AND RELAP5 FOR THE GENERIC LEU MNSR OPERATING AT 34 kW WITHOUT UNCERTAINTIES USING THE CHURCHILL-CHU HEAT TRANSFER CORRELATION

Parameter	PLTEMP/ANL	RELAP5
Core flow (kg/s)	0.47	0.43
Peak clad temperature for average channel (°C)	87.8	87.0
Peak fuel T for average channel (°C)	100.5	101.7
Power at ONB (kW)	67.8	68.7

(c) Results with uncertainties

Modifications were made to the RELAP5 input model to account for uncertainties in coolant flow, pin power and the film heat transfer coefficient. Uncertainties in the coolant flow are almost entirely due to uncertainties in pressure decrease in the external orifices: about 99% of the pressure decrease in the system is in the external orifices. The orifice coefficient of 1.70 was used for the external orifices to simulate uncertainties in the natural circulation flow rate. As seen in Fig. 2.17, 2.70 is the highest orifice coefficient that would provide a reasonable fit to the measured temperature data, even if one assumes a 5% error in the measured power during the test.

Considering local power peaking, the MCNP results give a total power-to-pin ratio in the peak channel that is a factor of 1.1586 times the average channel value. This value was multiplied by a factor of 1.003 to account for the uncertainty in the MCNP results and then multiplied by an additional factor of 1.115 to account for local power density uncertainties. The resulting value of 1.296 was used for the ratio of the total power or pin in the peak channel to that of the average channel. To account for film heat transfer coefficient uncertainties a ‘fouling factor’ of 0.885 was used in the peak channel; i.e. the nominal film heat transfer coefficient was multiplied by 0.885.

RELAP5 results for ONB for the LEU generic MNSR with and without uncertainties starting from a nominal power level of 34 kW using the Churchill–Chu heat transfer correlation are shown in Table 2.34. The power levels at which ONB occurs was calculated to be 68.6 kW without uncertainties, and 56.4 kW with uncertainties.

TABLE 2.34. RELAP5 RESULTS FOR LEU GENERIC MNSR POWER WITH A NOMINAL POWER OF 34 kW WITH AND WITHOUT UNCERTAINTIES USING THE CHURCHILL-CHU HEAT TRANSFER CORRELATION

Parameter	No uncertainties	With uncertainties
Inlet temperature (°C)	51.2	51.2
Outlet temperature (°C)	70.0	71.5
Peak channel outlet temperature (°C)	69.9	71.4
Average channel outlet temperature (°C)	70.0	71.5
Total coolant flow rate (kg/s)	0.431	0.399
Peak channel flow rate (kg/s)	0.00147	0.00152
Max. clad temperature, peak channel (°C)	88.4 (node 10)	93.4 (node 10)
Max clad temperature, average channel (°C)	87.0 (node 10)	88.3 (node 10)
Max. fuel temperature, peak channel (°C)	106.8 (node 5)	114.8 (node 5)
Max. fuel temperature, average channel (°C)	101.7 (node 6)	102.6 (node 6)
Saturation temperature, peak channel (°C)	110.7 (node 10)	110.7 (node 10)
Power for ONB in peak channel (kW)	68.6	56.4

In Table 2.35, the power level at which ONB occurs was calculated to be 56.4 kW using the RELAP5 code and 53.0 kW using the PLTEMP/ANL code. Both codes predict ONB power levels including uncertainties that are far above the maximum operating power level of 34 kW in the LEU core. The maximum temperature range of 111—113°C at the surface of the zircaloy cladding is far below its melting temperature of 1850°C. The maximum temperature range of 145—147°C at the fuel centre line is far below the melting temperature of 2865°C for UO_2 fuel.

TABLE 2.35. RELAP5 AND PLTEMP ONB RESULTS FOR THE LEU GENERIC MNSR WITH UNCERTAINTIES

Parameter	RELAP5	PLTEMP
Power at ONB (kW)	56.4	53.0
Peak channel coolant flow rate (kg/s)	0.00183	0.00157
Peak channel coolant outlet temperature (°C)	79.1	81.2
Max. clad surface temperature (°C)	110.9 (node 10)	112.7 (node 10)
Max. fuel centre line temperature (°C)	146.8	145.2

(d) Results beyond ONB

Three sets of results are shown for power levels beyond the power, at which ONB occurs, to illustrate the effects of the model choices of inlet and outlet temperatures and the effect of including uncertainty (hot channel) factors.

In the first case, calculations were done using a nominal inlet temperature of 30°C, one average channel, and no HCFs. The results are shown in Figs 2.18 and 2.19 [2.19].

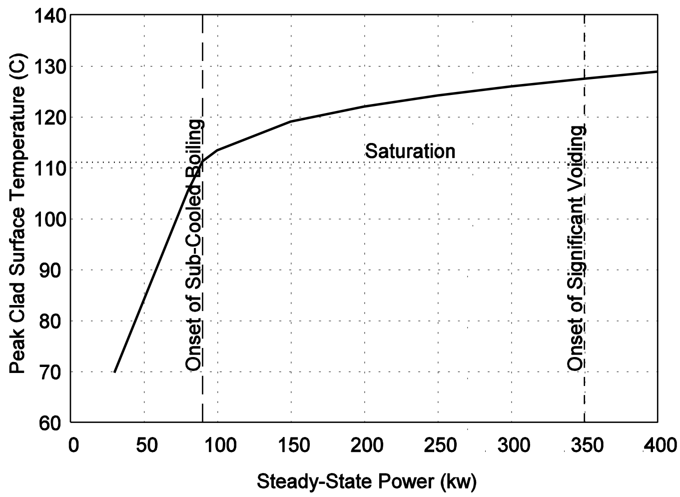

FIG. 2.18. Case one: peak clad surface temperature of the LEU core using a nominal inlet temperature of 30°C, one average channel and no HCFs (Courtesy of Argonne National Laboratory, USA).

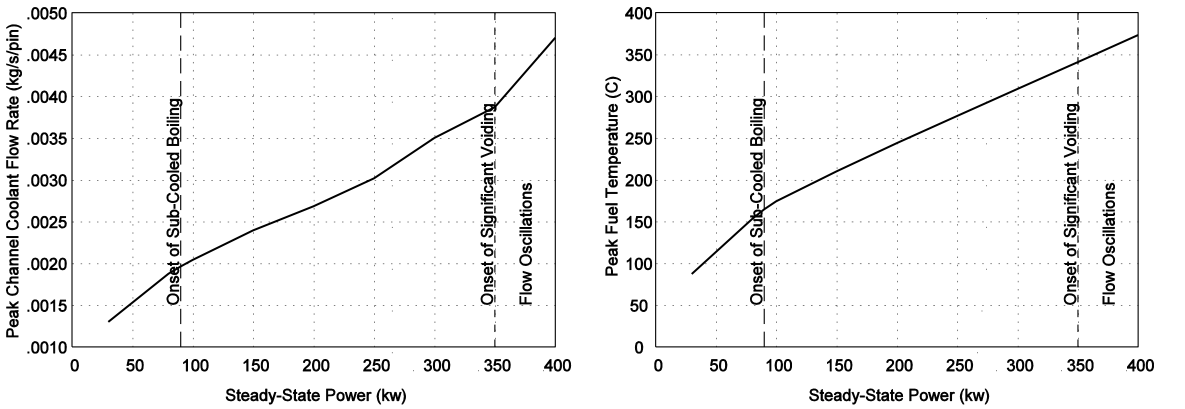

FIG. 2.19. Case one: coolant flow rates and fuel temperatures of the LEU core using a nominal inlet temperature of 30°C, one average channel and no HCFs (Courtesy of Argonne National Laboratory, USA).

In this first case, the onset of subcooled boiling occurs at a power level of 90 kW and OSV occurs at a power level of about 350 kW. At 300 kW and above, flow oscillations occur in RELAP5-3D, so there is not a single steady state for each power level. In this range, the flow rates shown in Fig. 2.19 are approximate averages of the oscillating values.

In the second case, calculations were done using a coolant outlet temperature of 70°C for 34 kW and a coolant inlet temperature of 51°C. Both peak and average channels were modelled, but no HCFs were included. The operating limits and conditions for MNSRs specify a maximum coolant outlet temperature of 70°C. Calculations were done to determine the inlet temperature of 51°C that corresponds to an outlet temperature of 70°C during steady state operation.

The results for the second case are shown in Fig. 2.20. The saturation temperature at the axial node where ONB first occurs was calculated to be 110.7°C. ONB occurred at a power level of 62 kW, and OSV occurred at a power level of 164 kW. Temperature and flow oscillations occur in RELAP5 V3.3 at power levels above OSV.

The third case is the same as the second case, except that uncertainties (HCFs) were included in the calculations. The coolant outlet temperature was 70°C for 34 kW, the coolant inlet temperature was 51°C, and both peak and average channels were modelled. The results are shown in Fig. 2.21. As noted previously, ONB was calculated to occur at a power level of 56.4 kW.

At power levels above ONB, the reactor operates in the subcooled boiling regime until OSV occurs at a power level of approximately 145 kW. The location where bubbles begin to detach from the heated wall is the location of OSV. As power was increased above the level at which OSV occurs, oscillations in coolant flow rates, coolant void fraction, and pin temperatures occurred, and no true steady state was calculated. At these high power levels, the oscillations settled into a somewhat regular pattern well before 1000 s. The critical heat flux would be reached at a power level above that at which OSV is predicted to occur.

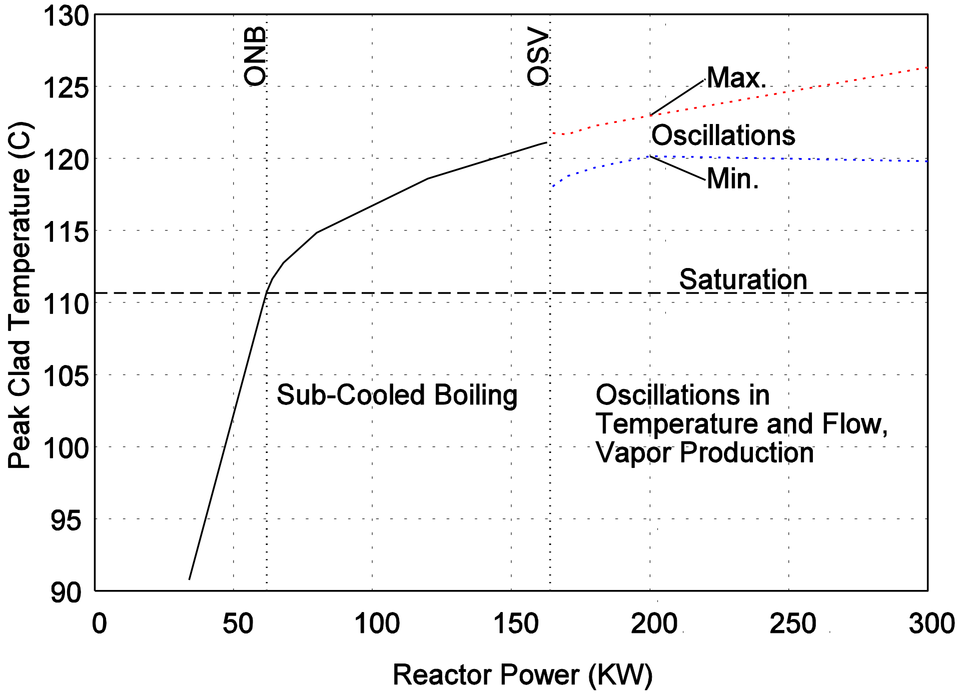

FIG. 2.20. Case two: peak clad temperatures for increasing reactor power levels for the LEU core calculated for a coolant outlet temperature of 70°C and no HCFs (Courtesy of Argonne National Laboratory, USA).

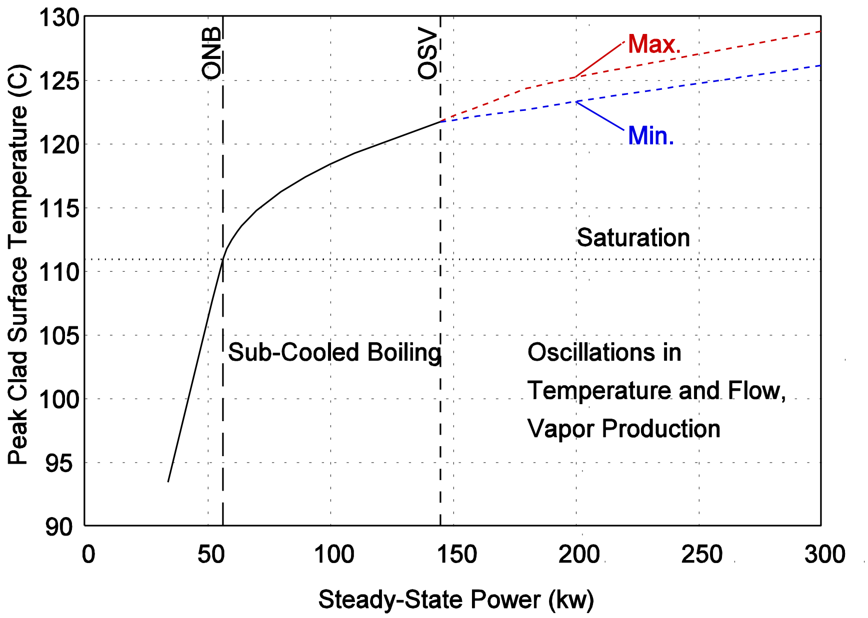

FIG. 2.21. Case three: peak clad temperatures for increasing reactor power levels for the LEU core calculated for a coolant outlet temperature of 70°C, including uncertainties (HCFs) (Courtesy of Argonne National Laboratory, USA).

TABLE 2.36. COMPARISON OF STEADY STATE THERMAL-HYDRAULIC SAFETY MARGINS FOR THREE INPUT CASES

Case	Coolant temperature (°C)		Uncertainties included	Power level at ONB (kW)	Power level at OSV (kW)
	Inlet	Outlet			
1	30	50	No	90	350
2	51	70	No	62	164
3	51	70	Yes	56.4	145

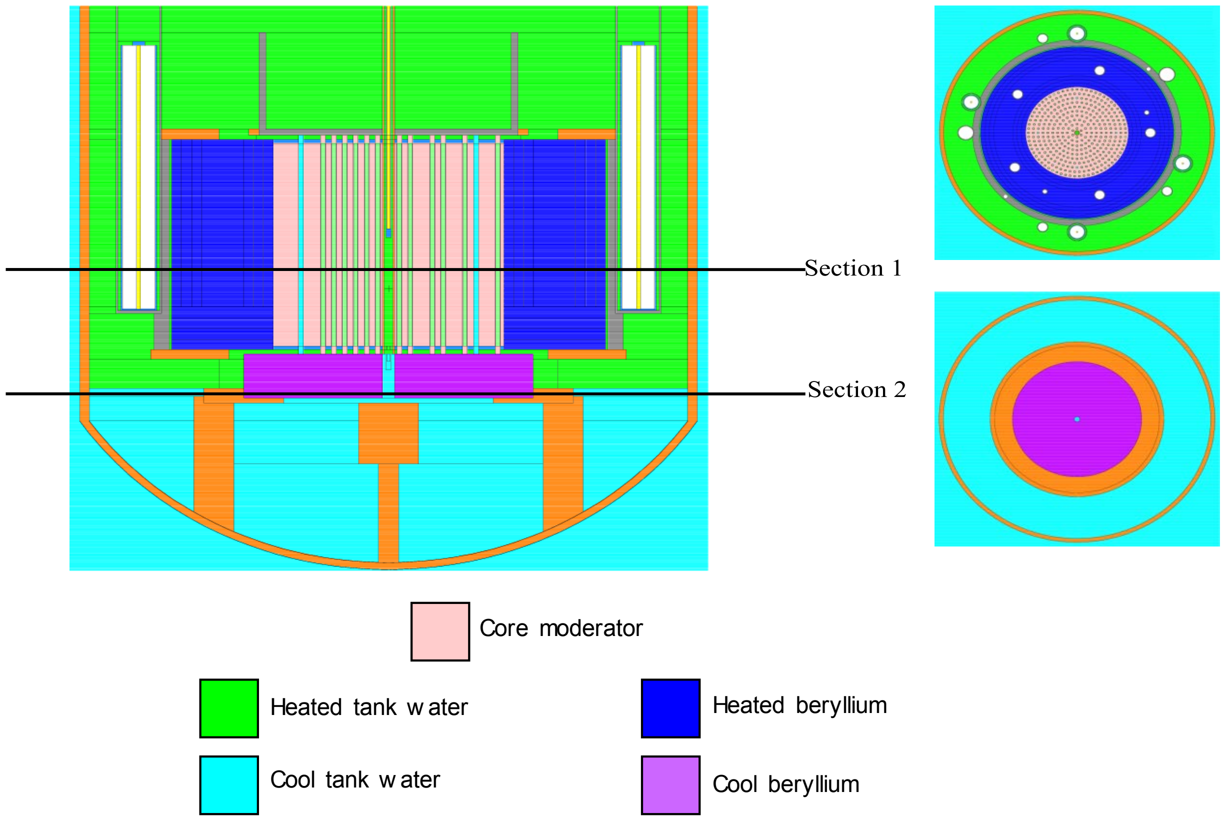

FIG. 2.22. MCNP geometry and regions used to calculate temperature reactivity coefficients. Section 1 (top right): heated region near the core; Section 2 (bottom right): cool region below the core (Courtesy of Argonne National Laboratory, USA).

Case 3 is recommended for the steady state safety margins because this case includes the maximum coolant outlet temperature allowed in the operating limits and conditions, and incorporates uncertainties.

In summary, these results indicate that at normal operating power levels there is a large margin to ONB, and a very large margin to OSV. The critical heat flux would be reached at a power level higher than that at which OSV is predicted to occur.

2.10.7. Temperature reactivity coefficients and kinetics parameters

Extensive calculations using the MCNP-4C code [2.20] were performed to obtain power shapes and reactivity feedback coefficients for the HEU and LEU cores. Figure 2.22 shows the geometry used for these calculations. Tables 2.37—2.40 show the kinetic parameters and reactivity feedback coefficients obtained from these calculations [2.19].

TABLE 2.37. KINETIC PARAMETERS FOR THE GENERIC MNSR CORES

Parameter	HEU	LEU (12.5%)
Prompt neutron lifetime (μs)	57.9 ± 4.8	47.0 ± 0.7
β_{eff} (%)	0.857 ± 0.0086[1]	0.845 ± 0.008[2]

[1]Rod out
[2]Rod inserted 15 cm

TABLE 2.38. CORE MODERATOR REACTIVITY CHANGES

Temperature (°C)	Density (kg/m^3)	Reactivity changes for moderator temperature and density, Δρ (mk) HEU	LEU (12.5%)
19.85	998.34	0.0	0.0
30	995.67	–0.1657 ± 0.009	–0.1467 ± 0.007
50	988.07	–0.6324 ± 0.008	–0.5775 ± 0.007
60	983.24	–0.9183 ± 0.008	–0.8272 ± 0.007
100	958.58	–2.2859 ± 0.009	–2.1787 ± 0.007

TABLE 2.39. FUEL REACTIVITY FEEDBACK COEFFICIENTS

	HEU	LEU (12.5%)
Doppler coefficient, mk/°C	–0.00029 ± 0.00010[1]	–0.00092[2]

[1]Rod out
[2]Rod inserted 15 cm

TABLE 2.40. POSITIVE REACTIVITY FEEDBACK COEFFICIENTS FOR HEATED TANK WATER AND RADIAL BERYLLIUM REFLECTOR

	HEU	LEU (12.5%)
Heated tank water outside core (mk/°C)	+0.00591 ± 0.00023	+0.00647
Radial Be reflector (mk/°C)	+0.00223 ± 0.00028	+0.00270

In addition to the negative reactivity feedbacks due to increasing the temperatures of the core water and fuel, small positive reactivity feedback effects were calculated for the heated tank water outside the core and for the radial beryllium reflector. The water and beryllium reflector below the core do not heat up much during a rod withdrawal transient and were neglected in the feedback calculations.

2.10.8. Safety analyses

2.10.8.1. Selection of initiating events

This section addresses the selection of initiating events that could be used as a basis for the safety analyses that require recalculation for conversion of MNSRs from HEU to LEU fuel.

The IAEA Safety Standards NS-R-4 [2.21] provides a list of initiating events that need to be considered for the safety analysis of a research reactor. For the purpose of MNSR core conversion from HEU to LEU, these initiating events need to be reviewed and the ones which are applicable for core conversion need to be addressed.

The 19 initiating events shown in Table 2.41 are taken from Chapter 16, Safety Analyses, of two operating MNSRs [2.1, 2.2] using HEU fuel that were supplied under IAEA Project and Supply Agreements.

Analyses for reactor conversions from HEU to LEU fuel need to address only those events that would change due to changing the reactor fuel. All of the initiating events in Table 2.41 were reviewed to determine which events need to be reanalysed for conversion. Detailed results are shown in Appendix III. Of the 19 initiating events that were assessed, only the 8 events shown in the “Yes” column in Table 2.41 need to be re-analysed in the LEU conversion analysis.

2.10.8.2. Insertion of excess reactivity of 3.77 mk (commissioning test)

The maximum allowed excess reactivity in MNSRs is 4 mk (0.4% $\Delta k/k$). Insertion of this maximum allowed reactivity by withdrawal of the control rod is an important part of the commissioning process for each MNSR and is a key measurement in defining the reactor safety basis.

Experimental data [2.22] from operation at constant power and from a 3.77 mk rod withdrawal during commissioning of the NIRR-1 reactor was provided by the Center for Energy Research and Training at Ahmadu Bello University, Nigeria, for use in these analyses. This measured data was used to validate a RELAP5-3D model of an MNSR.

The validated model was then used to analyse a 3.77 mk rod withdrawal transient in an LEU core with UO_2 fuel. In addition, a hypothetical withdrawal of 6 mk was evaluated to determine the potential behaviour of the LEU core and provide an indication of the margin of safety.

TABLE 2.41. POSTULATED INITIATING EVENTS EVALUATED IN A TYPICAL MNSR SAR

Reanalysis needed		Initiating event
Yes	No	
√		1. Insertion of excess reactivity of 3.77 mk (commissioning test)
√		2. Inadvertent reactivity insertion
	√	3. Loss of electrical power
	√	4. Control system failure
	√	5. Loss of reactor coolant accident
√		6. Loss of pool water shielding
	√	7. Flooding accident
	√	8. Air crash accident
	√	9. Seismic accident
√		10. Handling of top beryllium reflector
√		11. Core replacement accident
√		12. Design basis accident (DBA)
√		13. Beyond design basis accident (BDBA)
		Auxiliary systems
	√	14. Failure of water level monitor
	√	15. Failure to operate the reactor gas purge system
	√	16. Concurrent operation of reactor water purification system and reactor
		Irradiation systems
√		17. Inadvertent reactivity increase due to rabbit tubes filled with water
	√	18. Explosion of irradiated sample
	√	19 Human error

(a) HEU model validation using measured data from the NIRR-1 reactor

The RELAP5-3D [2.23] thermal-hydraulic model used for these calculations includes the entire MNSR system, including the core, the beryllium reflectors, the water in the vessel and the surrounding pool. Perfect mixing of the coolant water was assumed as it emerges from the top of the core. The core is installed in a tank containing 1.5 m^3 of water. The tank is located in a pool containing 30 m^3 of water. There are no pumps or heat exchangers in the system. All coolant flow is due to natural circulation. Heat removal from the tank is by conduction through the tank wall to the pool water. Heat removal from the pool is by evaporation and conduction to the air, and by conduction through the wall of the pool.

Table 2.42 lists the material properties used in the HEU fuel cases, and Tables 2.43—2.45 list the material properties used in the LEU fuel. The density multiplied by heat capacity used for the helium filled gap in the LEU cases was 10 200 $J \cdot m^{-3} \cdot K^{-1}$. Also, at higher temperatures a small addition was made to the helium thermal conductivity to account for radiation heat transfer. The beryllium properties were the same in the HEU and LEU cases. The Zircaloy-4 properties and the UO_2 properties were obtained from the ANL International Nuclear Safety Center Database [2.24].

In this report, an incipient melting temperature of approximately 640°C is used for the aluminium of the UAl alloy fuel meat and aluminium cladding (Al-303-1) of the HEU fuel rods. An incipient melting temperature of 2865°C is used for the LEU UO_2 fuel pellets and an incipient melting temperature of 1850°C is used for the Zircaloy-4 cladding of the LEU fuel rods.

TABLE 2.42. THERMAL PROPERTIES USED FOR HEU UAl ALLOY FUEL PINS

	Fuel	Gap	Al cladding	Be
Thermal conductivity, $W \times m^{-1} \times K^{-1}$	167.6	0.0282	199.7	200
Density × heat capacity, $J \times m^{-3} \times K^{-1}$	2.24×10^6	10 200	2.42×10^6	3.38×10^6

TABLE 2.43. THERMAL PROPERTIES USED FOR URANIUM DIOXIDE WITH 95% THEORETICAL DENSITY

Temperature (K)	Thermal conductivity ($W \times m^{-1} \times K^{-1}$)	Density × heat capacity ($J \times m^{-3} \times K^{-1}$)
296.15	7.63	2.35×10^6
500	5.78	2.83×10^6
700	4.61	3.00×10^6

TABLE 2.44. THERMAL PROPERTIES OF ZIRCALOY-4

Temperature (K)	Thermal conductivity ($W \times m^{-1} \times K^{-1}$)	Density × heat capacity ($J \times m^{-3} \times K^{-1}$)
295	13.383	1.9×10^6
400	13.987	1.9×10^6
500	14.741	1.9×10^6

TABLE 2.45. THERMAL CONDUCTIVITY OF HELIUM FILLED GAP

Temperature (K)	Thermal conductivity ($W \times m^{-1} \times K^{-1}$)
280	0.1373
340	0.1620
400	0.1796
440	0.1916
500	0.2116
800	0.3121

Reactivity feedback coefficients are discussed in Section 2.10.7.

> "In addition to the negative reactivity feedbacks from increasing core moderator and fuel temperatures, it was necessary to calculate and include positive reactivity feedback from temperature changes in the radial beryllium reflector, and changes in the temperature and density of the water in the tank above the core and at the side of the core." [2.19]

The MCNP code was used to obtain the power distributions in the NIRR-1 MNSR core with 347 active fuel pins and 3 dummy pins. In the HEU core, the pin with peak power has 19% more power than the average pin. In the LEU core, the peak pin has 21% more power than the average pin. The coolant in the peak pin and in the average pin has the same coolant flow area per pin. In the model, the radial beryllium reflector transfers heat to the average pin coolant channel and the coolant down-flow.

Gaps between the bottom and radial beryllium reflectors create flow orifices at the core inlet and outlet. Because these flow orifices are somewhat irregular, measured data for steady state operation of the NIRR-1 reactor was used to determine the best values to use for the orifice coefficients.

(b) Operation at constant power

Figure 2.23 shows the measured and calculated inlet and outlet coolant temperatures and pool temperatures for a run in the NIRR-1 at a constant power of 15 kW. The calculations shown in Fig. 2.23 were completed for a number of values of the orifice coefficients for the core inlet and outlet orifices, with the inlet and outlet orifice coefficients set to the same value. Results for orifice coefficients of 2.35, 2.40 and 2.45 are shown. A value of 2.40 was used in the rod withdrawal cases described below. In the later parts of the transient, heat losses not included in the RELAP5-3D model probably have some impact on the measurements.

In general, the calculated inlet and outlet temperatures agree well with the measurements, except possibly near the end of the transient. This indicates that for most of the transient the RELAP3-3D model accurately accounts for all of the significant heat transfer in the system. In the early part of the transient, from 500 to 3000 s, the rise in the inlet and outlet temperatures is determined mainly by the heat capacity in the water in the vessel. Later in the transient, from 7500 to 17 500 s, the heat generated in the core is transferred through the vessel wall to the pool about as fast as it is generated. In this time span, the heat capacity of the water in the pool dominates the temperature rise. After 17 500 s (4.9 hours), the calculated inlet and outlet temperatures rise toward the top of the experimental data band. This is probably due to heat transfer from the pool to the air above and to the pool wall. These heat transfer paths are not included in the RELAP5-3D model, but they could be included in future models.

At the beginning of operation, when all of the temperatures in the system might be expected to be the same, the measured pool temperature was about 1.5°C above the core inlet and outlet temperatures. During operation, the measured pool temperature was consistently 1.5—2.0°C above the calculated pool temperature. The 1.5—2.0°C degree temperature difference may have occurred because the pool temperature and the vessel temperature were not in equilibrium at the start of operation.

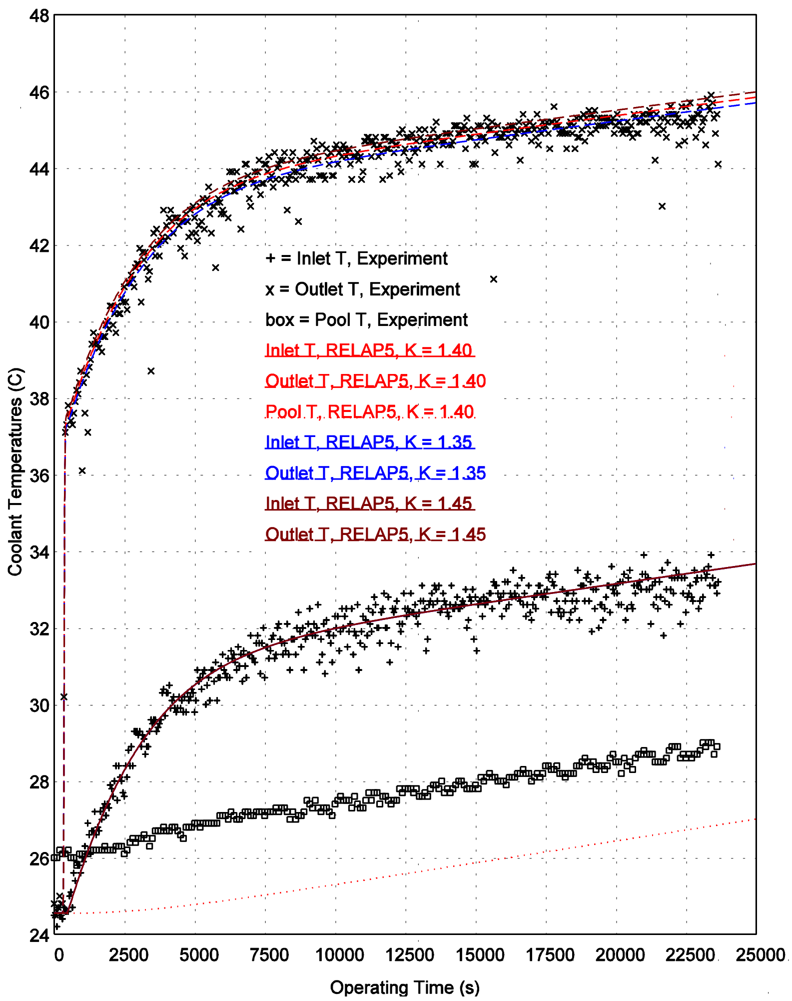

FIG. 2.23. Measured and calculated core inlet and outlet coolant temperatures for NIRR-1 operation at constant power, extended time scale (Courtesy of Argonne National Laboratory, USA).

(c) Rod withdrawal transient with HEU fuel

Figures 2.24 and 2.25 compare experimental measurements and calculated results for the 3.77 mk reactivity insertion with HEU fuel. The calculated results agree well with the measured data. This shows that the RELAP5-3D thermal-hydraulic model and the reactivity feedback coefficients accurately model the NIRR-1 MNSR with HEU fuel.

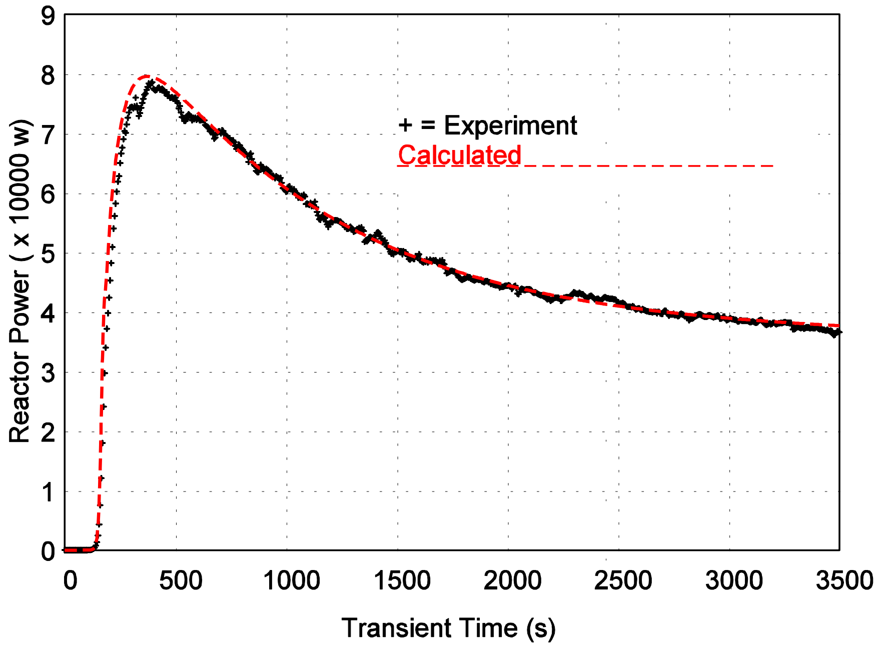

FIG. 2.24. Measured and calculated results, reactor power for 3.77 mk reactivity insertion, HEU core (Courtesy of Argonne National Laboratory, USA).

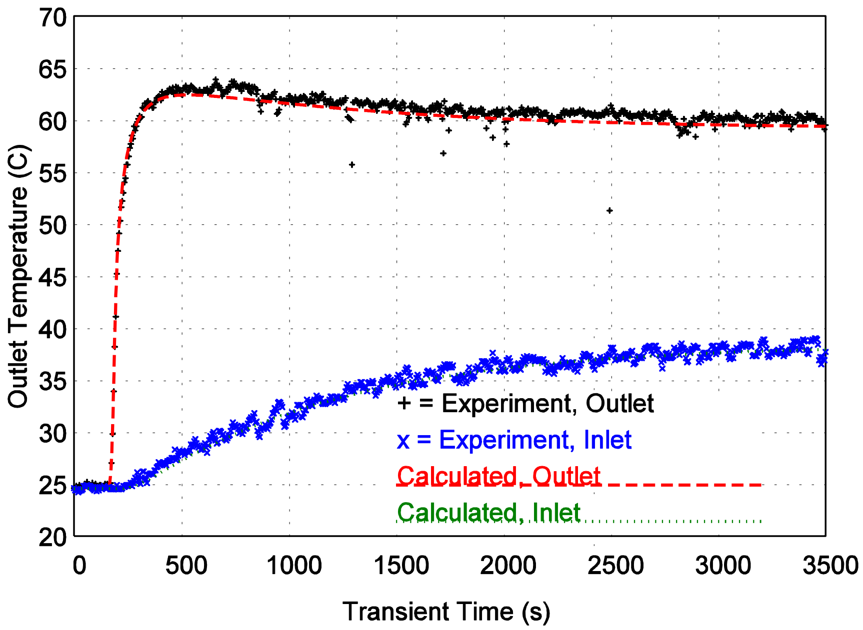

FIG. 2.25. Measured and calculated inlet and outlet temperatures for 3.77 mk reactivity insertion, HEU core (Courtesy of Argonne National Laboratory, USA).

(d) Nominal 3.77 mk reactivity insertions in the HEU and LEU cores

Figures 2.26 and 2.27 show the results of a 3.77 mk reactivity insertion for the HEU case and for the two LEU cases. The powers and peak clad temperatures with LEU fuel are lower than those with HEU fuel. The peak fuel temperatures are significantly higher for the LEU cases because of the lower thermal conductivity of the LEU oxide fuel.

Since the melting temperatures of the fuel and cladding for the LEU fuel are much higher than those for the HEU fuel, the safety margins for this transient are significantly larger for the LEU-fuelled cores. The Al cladding of the HEU fuel begins to melt at about 640°C, whereas the Zircaloy-4 cladding of the LEU fuel begins to melt at about 1850°C. The melting temperature of HEU UAl alloy is about 640°C. The melting temperature of the UO_2 of the LEU fuel is 2865°C.

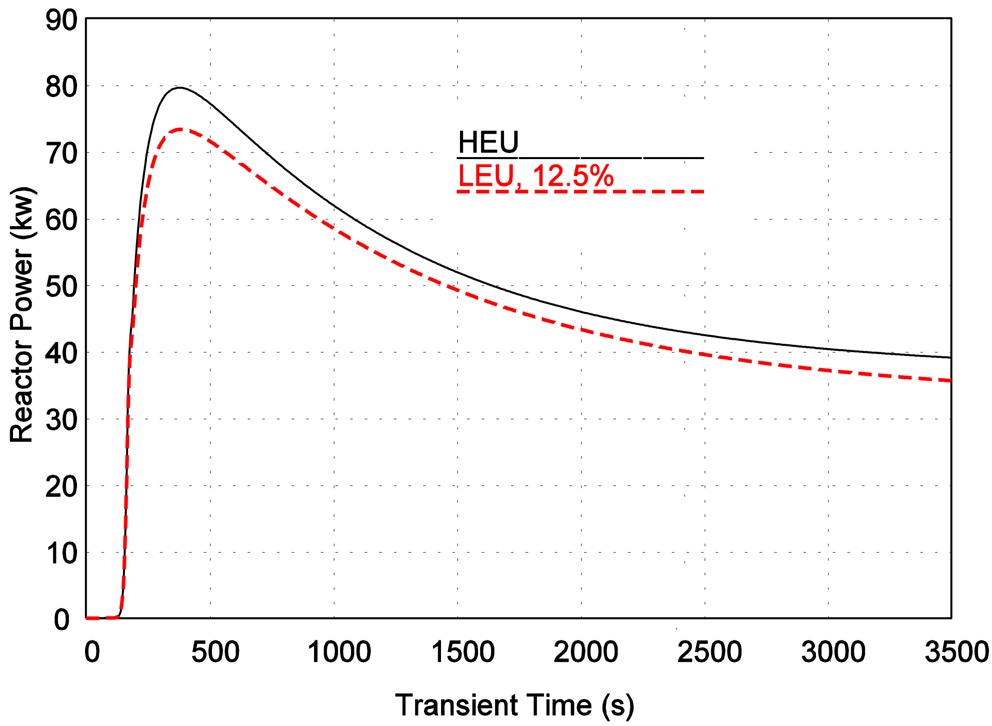

FIG. 2.26. Power vs. time for a 3.77 mk reactivity insertion with HEU and LEU fuel (Courtesy of Argonne National Laboratory, USA).

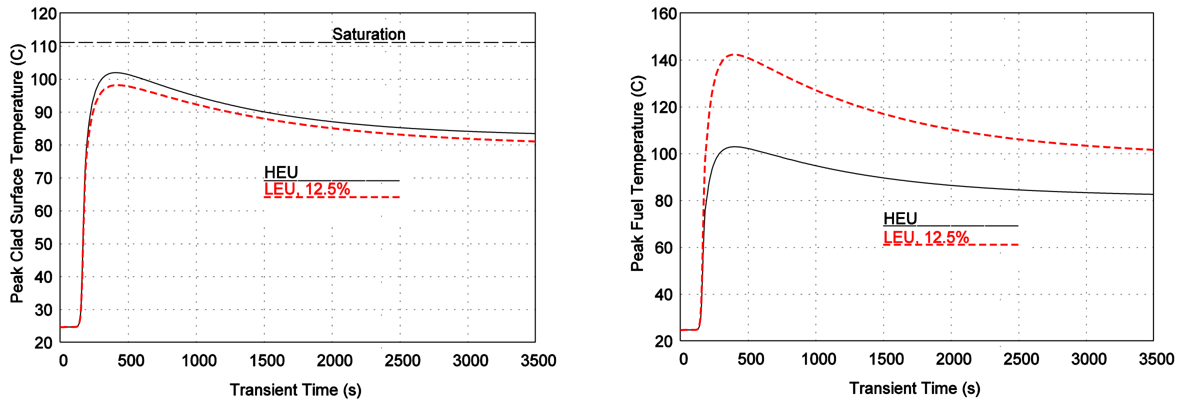

FIG. 2.27. Peak clad surface temperature and peak fuel temperature for a 3.77 mk reactivity insertion with HEU and LEU fuel (Courtesy of Argonne National Laboratory, USA).

(e) Reactivity insertions of 6 mk and 8 mk in the LEU core

For the MNSR design, the maximum allowed reactivity insertion in the operating limits and conditions due to full withdrawal of the control rod is 4 mk. To provide an indication of the margin of safety inherent in the LEU-fuelled core, rod withdrawal transients caused by hypothetical reactivity insertions of 6 mk and 8 mk were also calculated. The results are shown in Figs. 2.28—2.29. The peak power that was reached and the peak fuel and cladding temperatures are shown in Table 2.46. For the slow reactivity insertion of 8 mk, the peak cladding temperature was calculated to be 122°C, far below the incipient melting temperature of 1850°C for Zircaloy-4.

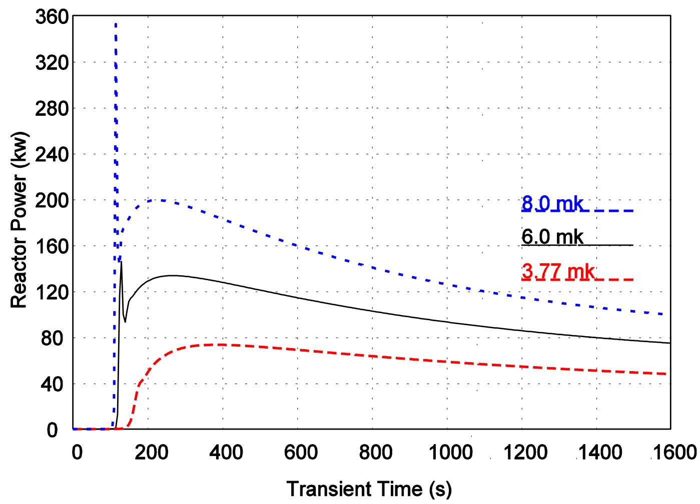

FIG. 2.28. Reactor power for slow reactivity insertions of 3.77 mk, 6 mk, and 8 mk in the generic LEU MNSR (Courtesy of Argonne National Laboratory, USA).

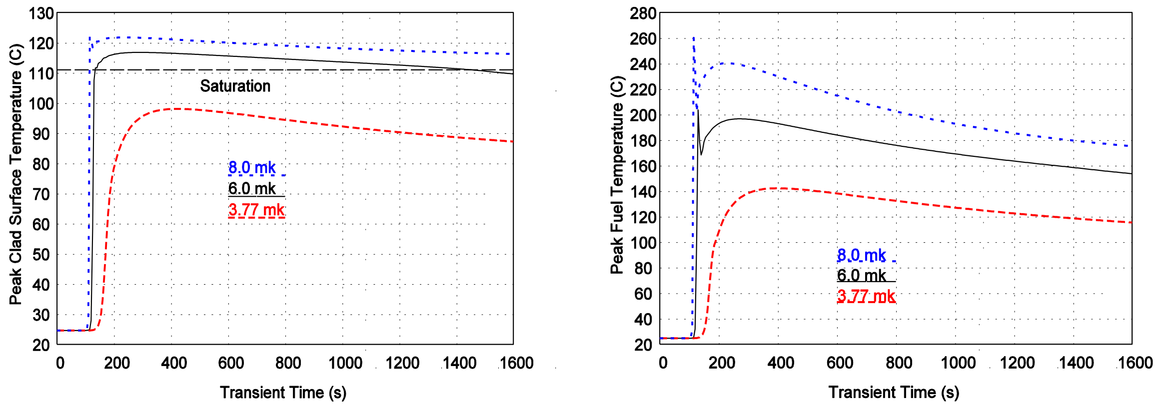

FIG. 2.29. Peak clad temperatures and peak fuel temperatures for reactivity insertions of 3.77 mk, 6 mk, and 8 mk in the generic LEU MNSR (Courtesy of Argonne National Laboratory, USA).

TABLE 2.46. PEAK POWER, PEAK FUEL, AND PEAK CLADDING TEMPERATURES FOR SLOW REACTIVITY INSERTIONS OF 3.77 mk, 6 mk, AND 8 mk IN THE GENERIC LEU CORES

Reactivity insertion (mk)	Peak power (kW)	Peak fuel temperature (°C)	Peak clad temperature (°C)
3.77	73	142	98
6.0	146	204	117
8.0	352	260	122

2.10.8.3. *Inadvertent reactivity insertions*

Slow reactivity insertions of 3.77—8.0 mk are discussed in Sections 2.10.8.2 (a)—(e), and fast reactivity insertions of 4.0–8.0 mk are discussed as part of the core installation accident in Sections 2.10.8.9 (a)—(b).

During operation, except for the addition of beryllium shims and core replacement, reactivity insertions will be less than 4.0 mk, the maximum allowed excess reactivity. Analyses of fast and slow reactivity insertions of ⩽4.0 mk show that the peak temperatures reached in the fuel, and at the surface of the cladding, are far below the melting temperatures of the fuel and cladding for both the generic HEU and LEU cores.

The analyses also show that inadvertent reactivity insertions of 4.0—8.0 mk also result in peak fuel and cladding temperatures that are far below their melting temperatures, and would not result in a release of radioactivity.

2.10.8.4. *Handling of the top beryllium reflector*

Since MNSRs are designed with only a small excess reactivity, top beryllium reflector shim plates are added to compensate for the loss of reactivity due to ^{235}U burnup and ^{149}Sm accumulation. When the cold excess reactivity falls below a specified value, typically 2—3 mk, beryllium shim plates are added to increase the excess reactivity by 1—2 mk up to a maximum of 4 mk.

A detailed procedure for adding the beryllium shims in a safe manner was provided by the CIAE. In this procedure, strings of three cadmium rabbits, and a small polyethylene irradiation capsule with dimensions 17 mm diameter by 56 mm length, filled with a cylindrical sheet of cadmium, are inserted into each of the five inner irradiation tubes. Each string has a reactivity worth of approximately –2.1 mk, and the total negative reactivity added is about –10.5 mk. After this, the control rod (worth around 7 mk) is removed and placed on the side of the beryllium reflector. The beryllium shim tray (worth around 1.6 mk) is then lifted to the upper flange of the upper section of the reactor vessel, where top beryllium shims can be added.

If this procedure is not adhered to and the reactor staff removes the control rod before inserting the cadmium strings, an excess reactivity of 2–3 mk will be introduced. The resulting power excursion will result in peak fuel and cladding temperatures in the HEU and LEU cores that are less severe than those analysed in Sections 2.10.8.2 (a) and (b) for slow inadvertent reactivity insertions, and in Sections 2.10.8.9 (a) and (b) for rapid inadvertent reactivity insertions.

2.10.8.5. Inadvertent reactivity increase due to rabbit tubes filled with water

Based on experiments performed in the zero power testing of GHARR-1 [2.1], filling the five inner irradiation tubes with water resulted in a reactivity increase of 1.95 mk. This reactivity increase is expected to be about the same in other HEU-fuelled MNSRs, and in the LEU replacement cores as well. The analyses of slow reactivity insertions in Sections 2.10.8.2 (b) and (c), and rapid reactivity insertions in Sections 2.10.8.9 (a) and (b) for reactivity insertions of 4 mk and greater, show that an inadvertent reactivity increase of approximately 2 mk due to rabbit tubes filled with water will not lead to melting of the fuel rods and release of radioactivity.

2.10.8.6. Loss of pool water shielding

In this accident scenario, described in the Nigeria NIRR–1 and Ghana GHARR-1 Final Safety Analysis Reports, a major earthquake is assumed to cause a crack on the bottom floor of the pool, resulting in the pool water draining below the level of the core [2.1, 2.2]. Simultaneous loss of water in the reactor vessel is not considered to be credible because the vessel is designed and constructed to support the core while suspended in an empty pool. The reactor is assumed to continue operating, but the power level will decrease because of the increasingly negative reactivity coefficients caused by loss of cooling water to the pool.

The loss of pool water will cause very high gamma radiation fields over the reactor. A loss of pool water accident simulation experiment was carried out at the prototype MNSR at CIAE near Beijing [2.25]. Portable gamma monitors were placed at positions 1—4 (Fig. 2.30), close to the lower end of the defence fence with the sensors sticking into the pool. A fixed gamma monitor was installed at position 5, and sensors were placed on top of the reactor flange and towards the bottom of the pool.

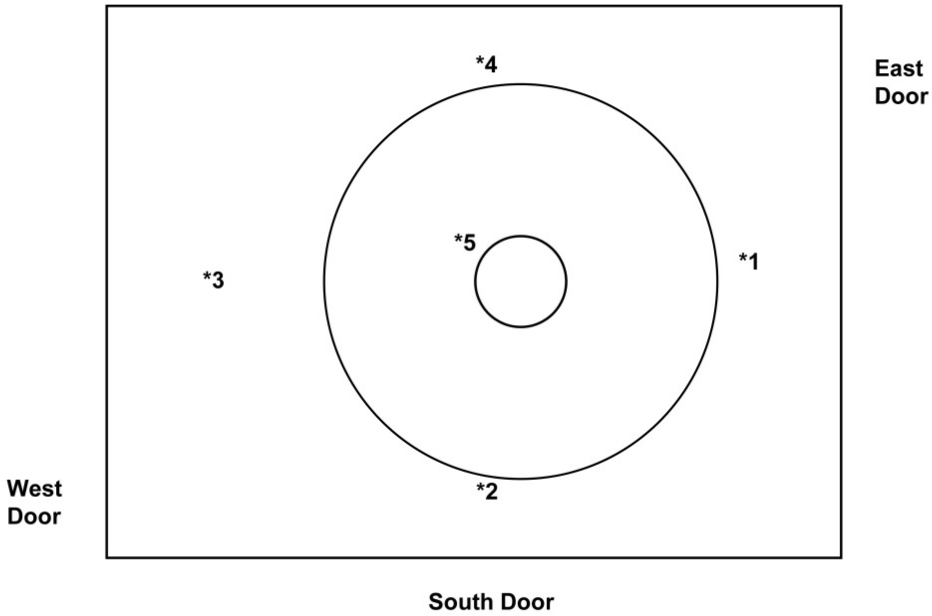

FIG. 2.30. Positions for gamma monitoring for simulating loss of pool water accident (Reproduced from Ref. [2.26] with permission Courtesy of Argonne National Laboratory, USA).

The measured gamma dose rates (mSv/h) for the different monitoring positions are shown in Table 2.47.

TABLE 2.47. GAMMA DOSE RATE (mSv/h) MEASURED AT MONITORING POSITIONS IN THE HEU MNSR PROTOTYPE

Position	1	2	3	4
Measured value	4.0×10^{2}	4.2×10^{2}	4.2×10^{2}	6.2×10^{2}

Position	5	East door	South door	West door
Measured value	1.1×10^{2}	1.6×10^{-2}	2.3×10^{-1}	2.3×10^{-1}

Gamma sources in 18 energy groups were calculated for the generic HEU and LEU cores using the ORIGEN2 code. The 18-group gamma spectra are produced both during the irradiation period and cooling period after shutdown. For a bounding radiological dose evaluation for a hypothetical accident, the maximum values of the gamma spectra over the entire core life history, including both irradiation period and cooling period, need to be determined. The HEU core operated at full power of 30 kW has an estimated core life of approximately 810 FPED, and the LEU core operated at a full power of 34 kW has an estimated lifetime of approximately 903 FPED. The maximally burned fuel rod at end of core life will produce the bounding hypothetical radiological dose. The gamma (photon) source data shown in Table 2.48 indicates that the gamma source for the LEU core is 1.19 times larger than that for the HEU core, because the LEU core has a higher power level and a longer estimated lifetime.

TABLE 2.48. GAMMA SOURCES FOR FUEL ROD WITH MAXIMUM BURNUP AT END OF CORE LIFE IN THE GENERIC HEU345 AND LEU348 CORES

Photon group	Mean energy (MeV)	HEU345 source photons	LEU348 source photons	LEU/HEU ratio
1	1.00×10^{-2}	6.61×10^{12}	8.13×10^{12}	1.23
2	2.50×10^{-2}	1.65×10^{12}	1.90×10^{12}	1.15
3	3.75×10^{-2}	1.38×10^{12}	1.61×10^{12}	1.17
4	5.75×10^{-2}	1.42×10^{12}	1.64×10^{12}	1.16
5	8.50×10^{-2}	1.05×10^{12}	1.49×10^{12}	1.42
6	1.25×10^{-1}	1.09×10^{12}	1.48×10^{12}	1.36
7	2.25×10^{-1}	2.55×10^{12}	3.06×10^{12}	1.20
8	3.75×10^{-1}	1.53×10^{12}	1.77×10^{12}	1.16
9	5.75×10^{-1}	2.61×10^{12}	2.98×10^{12}	1.14
10	8.50×10^{-1}	2.95×10^{12}	3.37×10^{12}	1.14
11	1.25	1.77×10^{12}	2.01×10^{12}	1.14
12	1.75	7.02×10^{11}	7.22×10^{11}	1.03
13	2.25	3.54×10^{11}	4.02×10^{11}	1.14
14	2.75	1.52×10^{11}	1.72×10^{11}	1.13
15	3.50	9.17×10^{11}	1.04×10^{11}	1.13
16	5.00	4.95×10^{10}	5.57×10^{10}	1.13
17	7.00	3.99×10^{8}	4.56×10^{8}	1.15
18	9.50	7.88×10^{14}	9.40×10^{4}	1.19
	Total	2.60×10^{13}	3.09×10^{13}	1.19

As a result, gamma dose rates in an LEU MNSR are expected to be about 2.19 times the dose rates that were measured in the HEU MNSR prototype reactor. These dose rates are shown in Table 2.49. Some reduction in the LEU dose may be expected because gamma rays emanating from the LEU core need to pass through denser material, namely UO_2, instead of UAl alloy.

TABLE 2.49. GAMMA DOSE (mSv/h) RATE EXPECTED AT MONITORING POSITIONS IN AN LEU MNSR

Position	1	2	3	4
Expected value	4.8×10^{2}	5.0×10^{2}	5.0×10^{2}	7.4×10^{2}
Position	**5**	**East door**	**South door**	**West door**
Expected value	1.3×10^{2}	1.9×10^{-2}	2.7×10^{-1}	2.7×10^{-1}

The average dose rate at gamma monitoring positions 1—5 in Table 2.47 for the HEU MNSR Prototype was measured as 4.0×10^2 mSv/h, and is estimated from Table 2.49 to be about 4.7×10^2 mSv/h in the generic LEU core. During operation, the area within the fence on top of the reactor is the controlled area where no individual would be when the accident occurs.

The average dose rate at the east, south and west entrance doors of the reactor hall was measured to be 1.6×10^{-1} mSv/h in the HEU Prototype reactor (Table 2.47), and estimated to be 1.9×10^{-1} mSv/h in the generic LEU reactor (Table 2.49). The exposure of individuals working for eight hours on the main floor of the reactor hall, or in the adjoining room during an emergency would be approximately 1.3 mSv in the HEU case and 1.5 mSv in the LEU case. Both of these doses are far below the recommended maximum effective (whole body) dose of 50 mSv/year prescribed in IAEA Safety Standards No. GSR Part 3[1] [2.25]. Since the reactor would be shut down in the event of loss of pool water, the actual dose would be much smaller. This would not cause any risk to operating personnel.

2.10.8.7. DBA and the maximum credible accident

As the DBA for the generic MNSR, it is postulated that pitting corrosion of the cladding creates cladding failure in one or more fuel rods, such that a hole (or holes) in the cladding are formed totalling 0.5 cm^2 while in the water of the reactor vessel. In normal operation, gaseous fission products from the failed fuel rod(s) would collect in the top space of the reactor vessel. For purposes of this analysis, it is assumed that the reactor continued to operate without replacing the failed fuel rod(s), the gas purge system failed, and a fraction of the fuel rod fission product inventory was released into the pool water by some means. A fraction of this inventory was released into the air of the reactor hall. Furthermore, part of the total fission product content of air in the reactor hall was released to the environment by leakage from the reactor building. Effective (whole body) and thyroid doses are evaluated for this scenario for a reactor building leak rate of 20% per hour and compared with dose limits recommended by IAEA Safety Standards No. GSR Part 3 [2.25].

(a) Radionuclide activities in fuel rod with peak burnup

Calculations were performed to obtain the inventories of halogens, noble gases, alkaline metals, and actinides in the peak power fuel rods for the generic MNSR HEU345 and LEU348 cores. These inventory data are intended to be used for radiological assessment of accident scenarios involving the potential release of radioactive material (e.g., DBA).

Pertinent design data for the generic HEU345 and LEU348 fuel rods are summarized for convenience in Table 2.50. The LEU348 core is designed for a slightly higher total core power, and has a slightly larger peak to average rod power than the HEU345 core. The peak rod powers used for the inventory analysis are 99.66 W and 113.35 W for the generic HEU345 and LEU348 cores, respectively. Based on the estimated core lifetimes, the ^{235}U burnup in the pin with peak burnup is 3.5% for the generic HEU345 core at 810 FPEDs, and 3.3% for the generic LEU348 core at 903 FPEDs.

[1] While the dose limit is 20 mSv/y averaged over 5 years, a dose of 50 mSv in a single year is used for the accident scenarios used in this document.

TABLE 2.50. GENERIC MNSR FUEL ROD PARAMETERS

Parameter	HEU345	LEU348
Reactor power (kW)	30.0	34.0
Number of rods in core	345	348
Uranium density in fuel meat (g/cm^3)	0.92	9.35
Enrichment (%)	90.2	12.5
Fuel meat outer diameter (mm)	4.3	4.3
Fuel rod outer diameter (mm)	5.5	5.5
^{235}U/rod	2.8721	3.8915
^{238}U/rod	0.2872	27.1007
P_{max}/P_{avg} rod power	1.15	1.16
Peak rod power (W)	99.66	113.35
Anticipated core residence (FPED)	810	903

Inventory data were calculated using the ORIGEN2 code [2.10], a zero-dimensional isotope decay and transmutation code. The code solves the transmutation equations using libraries of radioactive decay data and one group cross-section data. The base code libraries allow the tracking of over 100 actinides and nearly 900 fission product nuclides. Precalculated libraries of 1 group cross-section data are available for use in ORIGEN2 for several reactor systems. A standard library for an oxide fuelled light water reactor (LWR), named the PWRUS library, represents the closest potential match to data for the generic MNSR cores.

However, since the neutron spectrum in MNSRs is different from that of an LWR, it is preferable to replace cross section data for some of the nuclides in the library with more appropriate data. In this analysis, one group cross-section data were calculated for the generic MNSR fuel rods using the WIMS–ANL code [2.27]. The calculated one group capture and fission cross sections for the HEU345 and LEU348 rods are compared with the cross section data from the ORIGEN2 PWRUS library in Table 2.51.

TABLE 2.51. ONE GROUP CROSS SECTION DATA (b) FOR GENERIC MNSR FUEL RODS

Nuclide	Capture			Fission		
	PWRUS library[1]	Replacement data[2]		PWRUS library	Replacement data[2]	
		HEU345	LEU348		HEU345	LEU348
^{234}U	20.710	29.775	22.663	0.452	0.5661	0.5764
^{235}U	10.680	15.891	12.247	47.520	80.711	59.75
^{236}U	8.348	9.0647	7.433	0.191	0.33621	0.32749
^{238}U	0.887	5.1894	1.1384	0.093	0.11355	0.1186
^{237}Np	33.280	46.924	39.706	0.495	0.53016	0.5588
^{238}Pu	34.830	68.997	49.836	2.308	3.3731	2.8671
^{239}Pu	69.090	74.765	60.52	121.100	151.83	119.05
^{240}Pu	222.800	260.67	241.63	0.579	0.61888	0.6465
^{241}Pu	42.020	60.101	45.743	125.900	174.79	133.02
^{242}Pu	33.200	31.004	29.887	0.406	0.44785	0.4722
^{241}Am	95.700	149.000	123.000	1.120	1.3673	1.2535
^{135}Xe	221 500	420 000	350000	0	0	0

[1] PWRUS library is a standard PWR library available with the ORIGEN2 code
[2] Replacement cross sections calculated with WIMS–ANL at 400 FPED for the HEU rod and at 450 FPED for the LEU rod.

Radioactive nuclide inventories were calculated for three material groups, i.e., activation products, actinides and daughters, and fission products. The radioactive nuclide activities are produced both during the irradiation period and the cooling period afterward. For a bounding analysis of the radiological dose from a hypothetical accident, the maximum value of the radionuclide activities over the life history of the core, including both irradiation period and cooling period, need to be extracted.

The bounding maximum radioactivity values are summarized in Table 2.52 for four groups of materials: (i) halogens, (ii) noble gases, (iii) alkaline metals, and (iv) actinides for HEU345 and LEU348 rods with peak burnup, respectively. The bounding values are almost always found near the beginning (75 FPED for the HEU345 core or 90 FPED for the LEU348 core) of the irradiation period for halogens (except for ^{82}Br, ^{130}I, and ^{130m}I), and noble gases (except for ^{85}Kr) fission products. However, the bounding maximum activities for alkaline metals, actinides and daughters are almost always found at the end of the irradiation period, 810 FPED for the HEU345 core or 903 FPED for the LEU348 core.

For the halogen and noble gas radioactivities, the concentrations of these short-lived nuclides reach a saturation point within 100 days of operation, as production from fission and destruction by radioactive decay balance. It is noted that the long-lived fission products (notably, ^{85}Kr, $t_{1/2}$=10.8 years) do not reach a saturated concentration. For the alkaline metals and actinides, the concentrations do not generally reach saturation during the irradiation because of their long half-lives. Thus, in order to obtain the bounding values of radiological doses, the maximum values of the radionuclide activities over the entire core life history (including both irradiation period and cooling period) need to be extracted.

TABLE 2.52. MAXIMUM ACTIVITIES (Bq) FOR GENERIC MNSR FUEL RODS WITH PEAK POWER OVER THE ENTIRE CORE LIFE TIME

Radioactive nuclide	HEU345	LEU348	LEU/HEU
^{130}I	7.07×10^{7}	8.44×10^{7}	1.10
^{130m}I	3.15×10^{7}	3.43×10^{7}	1.09
^{131}I	8.88×10^{10}	1.02×10^{11}	1.15
^{132}I	1.32×10^{11}	1.52×10^{11}	1.15
^{133}I	2.08×10^{11}	2.36×10^{11}	1.14
^{134}I	2.35×10^{11}	2.67×10^{11}	1.14
^{135}I	1.94×10^{11}	2.20×10^{11}	1.14
^{136}I	9.44×10^{10}	1.08×10^{11}	1.15
^{82}Br	1.72×10^{7}	1.93×10^{7}	1.12
^{83}Br	1.66×10^{10}	1.89×10^{10}	1.14
^{84m}Br	5.85×10^{8}	6.62×10^{8}	1.13
^{84}Br	3.12×10^{10}	3.54×10^{10}	1.14
^{85}Br	3.89×10^{10}	4.40×10^{10}	1.13
^{86}Br	2.94×10^{10}	3.33×10^{10}	1.13
^{87}Br	6.70×10^{10}	7.59×10^{10}	1.13
^{132}Te	1.32×10^{11}	1.51×10^{11}	1.14
Total halogens	1.27×10^{12}	1.44×10^{12}	1.14
^{83m}Kr	1.66×10^{10}	1.89×10^{10}	1.14
^{85}Kr	1.12×10^{9}	1.41×10^{9}	1.26
^{85m}Kr	3.92×10^{10}	4.44×10^{10}	1.13
^{87}Kr	7.96×10^{10}	8.99×10^{10}	1.13
^{88}Kr	1.12×10^{11}	1.27×10^{11}	1.13
^{89}Kr	1.42×10^{11}	1.61×10^{11}	1.13
^{131m}Xe	9.88×10^{8}	1.01×10^{9}	1.02
^{133m}Xe	6.07×10^{9}	6.92×10^{9}	1.14
^{133}Xe	2.08×10^{11}	2.36×10^{11}	1.14
^{135}Xe	1.83×10^{11}	2.11×10^{11}	1.16
^{135m}Xe	3.50×10^{10}	4.00×10^{10}	1.14
^{137}Xe	1.85×10^{11}	2.10×10^{11}	1.14
^{138}Xe	1.93×10^{11}	2.19×10^{11}	1.13
Total noble gases	1.20×10^{12}	1.37×10^{12}	1.14

TABLE 2.52. MAXIMUM ACTIVITIES (Bq) FOR GENERIC MNSR FUEL RODS WITH PEAK POWER OVER THE ENTIRE CORE LIFE TIME (cont.)

Radioactive nuclide	HEU345	LEU348	LEU/HEU
^{140}Ba	1.92×10^{11}	2.18×10^{11}	1.14
^{141}Ce	1.82×10^{11}	2.06×10^{11}	1.13
^{143}Ce	1.82×10^{11}	2.07×10^{11}	1.13
^{144}Ce	1.44×10^{11}	1.69×10^{11}	1.17
^{134}Cs	4.59×10^{8}	5.29×10^{8}	1.15
^{137}Cs	9.44×10^{9}	1.20×10^{10}	1.27
^{140}La	1.92×10^{11}	2.18×10^{11}	1.13
^{99}Mo	1.85×10^{11}	2.10×10^{11}	1.14
^{95}Nb	1.98×10^{11}	2.26×10^{11}	1.14
^{147}Nd	7.03×10^{10}	8.03×10^{10}	1.14
^{147}Pm	3.01×10^{10}	3.74×10^{10}	1.24
^{143}Pr	1.79×10^{11}	2.02×10^{11}	1.13
^{103}Ru	9.73×10^{10}	1.13×10^{11}	1.16
^{106}Ru	1.01×10^{10}	1.35×10^{10}	1.34
^{89}Sr	1.48×10^{11}	1.67×10^{11}	1.13
^{90}Sr	9.10×10^{9}	1.15×10^{10}	1.26
^{91}Y	1.80×10^{11}	2.03×10^{11}	1.13
^{95}Zr	1.98×10^{11}	2.26×10^{11}	1.14
Total alkalines	2.21×10^{12}	2.52×10^{12}	1.14

TABLE 2.52. MAXIMUM ACTIVITIES (Bq) FOR GENERIC MNSR FUEL RODS WITH PEAK POWER OVER THE ENTIRE CORE LIFE TIME (cont.)

Radioactive nuclide	HEU345	LEU348	LEU/HEU
^{237}U	3.41×10^{9}	1.77×10^{10}	5.18
^{238}Np	3.49×10^{7}	2.98×10^{8}	8.53
^{239}Np	6.07×10^{9}	4.70×10^{11}	77.44
^{240m}Np	4.77×10^{4}	3.02×10^{6}	63.33
^{238}Pu	2.05×10^{5}	2.78×10^{6}	13.53
^{239}Pu	3.63×10^{5}	3.18×10^{7}	87.58
^{240}Pu	2.49×10^{4}	2.02×10^{6}	81.10
^{241}Pu	2.41×10^{5}	1.81×10^{7}	74.85
^{243}Pu	2.95×10^{2}	1.67×10^{4}	56.78
^{241}Am	5.07×10^{3}	3.81×10^{5}	75.18
^{242}Am	4.11×10^{3}	2.84×10^{5}	69.19
^{243}Am	9.58×10^{-2}	5.03	52.51
^{242}Cm	1.45×10^{3}	1.08×10^{5}	74.23
Total actinides	9.51×10^{9}	4.88×10^{11}	51.36

Table 2.52 summarizes the bounding maximum activities of halogens, noble gases, alkaline metals, and actinides in the generic HEU345 and the generic LEU348 fuel rods continuously operating at their peak rod power. Ratios of the LEU348 activities to HEU345 activities are shown for convenience. The higher fission product activities for halogens, noble gases, and alkaline metals in the LEU348 fuel rods relative to the HEU345 fuel rods are primarily due to the 13% higher power level in the LEU348 design. Activities for the average rod in the HEU345 and LEU348 cores can be obtained by dividing the activities in Table 2.52 by the maximum to average rod powers shown in Table 2.50.

The actinide activity in the LEU348 is nearly a factor of 51 times higher than in the HEU345 rod. As shown in Table 2.50, the ^{238}U loading in the LEU348 rods is a factor of 87 higher than in the HEU345 rod. ^{238}U undergoes a neutron capture to form ^{239}U, which quickly decays by β^- emission to ^{239}Np. Subsequent transmutations of ^{239}Np lead to even higher actinides. Table 2.52 shows that the increase in the total higher actinide activity at the end of core life (discharge) is mostly due to the increase of initial ^{238}U concentration in the LEU348 rods. The major contributors, ^{239}Np and ^{237}U, to the actinide activities at end of irradiation are short-lived radionuclides with half-lives in the order of days. Within a few weeks after shutdown, these nuclides will have largely decayed to longer lived ^{238}Pu and ^{239}Pu.

For the purpose of assessing the bounding radiological consequences of a release of actinides from fuel material, the maximum doses would be obtained at the time of discharge. Unless the hypothetical accident scenario assumes that it happens right at the precise moment of discharge, it is reasonable to consider some level of cooling has occurred for accidents involving any kind of operational core access event or maintenance activity. Therefore, any level of cooling assumed after discharge would be helpful to reduce the radiological dose levels due to the decay of these short-lived actinides. The total actinide inventory in the generic LEU348 peak power rod decreases by nearly a factor of 500 from the discharge value following one month of post-irradiation cooling. It is also noted that the differences in the actinide inventory between the generic HEU345 and LEU348 peak power rods decreases with cooling. Consequently, any differences in radiological dose evaluations for hypothetical accidents between the HEU345 core and LEU348 core would be reduced for longer cooling times.

(b) Source term determination

The source term for radioactivity in the air of the reactor hall is determined as the inventory of the fuel rod with peak ^{235}U burnup times: the transfer factor from fuel material to matrix material, the transfer factor from matrix material to water, and the transfer factor from water to air. However, since specific factors for each of these transfers are not available, a combined factor for transfer of fission products from the fuel matrix material to the air of the reactor building is used [2.28]. The fission product inventory for the selected isotopes in the fuel rod with peak ^{235}U burnup, the combined transfer factor, and resulting source term for use in the dose calculations are listed in Table 2.53.

TABLE 2.53. INVENTORY OF THE PEAK HEU FUEL ROD WITH 3.5% ^{235}U BURNUP, THE PEAK LEU FUEL ROD WITH 3.3% ^{235}U BURNUP, TRANSFER FACTORS AND SOURCE TERM FOR THE SCENARIO INVESTIGATED

No.	Isotope	HEU: calculated inventory for one peak power fuel rod (Bq)	LEU: calculated inventory for one peak power fuel rod (Bq)	Transfer factor: matrix material to air [2.28][1]	HEU: source term in air of reactor hall (Bq)	LEU: source term in air of reactor hall (Bq)
			Halogens			
1	^{130}I	7.70×10^{7}	8.44×10^{7}	1×10^{-4}	7.70×10^{3}	8.44×10^{3}
2	^{130m}I	3.15×10^{7}	3.43×10^{7}	1×10^{-4}	3.15×10^{7}	3.43×10^{7}
3	^{131}I	8.88×10^{10}	1.02×10^{11}	1×10^{-4}	8.88×10^{6}	1.02×10^{7}
4	^{132}I	1.32×10^{11}	1.52×10^{11}	1×10^{-4}	1.32×10^{7}	1.52×10^{7}
5	^{133}I	2.08×10^{11}	2.36×10^{11}	1×10^{-4}	2.08×10^{7}	2.36×10^{7}
6	^{134}I	2.35×10^{11}	2.67×10^{11}	1×10^{-4}	2.35×10^{7}	2.67×10^{7}
7	^{135}I	1.94×10^{11}	2.20×10^{11}	1×10^{-4}	1.94×10^{7}	2.20×10^{7}
8	^{136}I	9.44×10^{10}	1.08×10^{11}	1×10^{-4}	9.44×10^{6}	1.08×10^{7}
9	^{82}Br	1.72×10^{7}	1.93×10^{7}	1×10^{-4}	1.72×10^{3}	1.93×10^{3}
10	^{83}Br	1.66×10^{10}	1.89×10^{10}	1×10^{-4}	1.66×10^{6}	1.89×10^{6}
11	^{84m}Br	5.85×10^{8}	6.62×10^{8}	1×10^{-4}	5.85×10^{4}	6.62×10^{4}
12	^{84}Br	3.12×10^{10}	3.54×10^{10}	1×10^{-4}	3.12×10^{6}	3.54×10^{6}
13	^{85}Br	3.89×10^{10}	4.40×10^{10}	1×10^{-4}	3.89×10^{6}	4.40×10^{6}
14	^{86}Br	2.77×10^{10}	3.33×10^{10}	1×10^{-4}	2.77×10^{6}	3.33×10^{6}
15	^{87}Br	6.70×10^{10}	7.59×10^{10}	1×10^{-4}	6.70×10^{6}	7.59×10^{6}
16	^{132}Te	1.32×10^{11}	1.51×10^{11}	1×10^{-4}	1.32×10^{5}	1.51×10^{5}

[1] Reference [2.29] states: "The release of noble gases to the confinement air in actual accidents or tests was 1.5% [2.29] and 0.5% [2.30]. Conservatively, a value of 2.0% was assumed. Release factors for iodine were determined in several experiments resulting in values of 4×10^{-6} [2.30] to 5×10^{-4} [2.31]. In the source term calculation, a value of 1×10^{-4} is used. For aerosols (solids) a release factor of less than 10^{-6} was assumed." A value of 10^{-6} for the aerosols was used here.

TABLE 2.53. INVENTORY OF THE PEAK HEU FUEL ROD WITH 3.5% ^{235}U BURNUP, THE PEAK LEU FUEL ROD WITH 3.3% ^{235}U BURNUP, TRANSFER FACTORS AND SOURCE TERM FOR THE SCENARIO INVESTIGATED (cont.)

No.	Isotope	HEU: calculated inventory for one peak power fuel rod (Bq)	LEU: calculated inventory for one peak power fuel rod (Bq)	Transfer factor: matrix material to air [2.28][1]	HEU: source term in air of reactor hall (Bq)	LEU: source term in air of reactor hall (Bq)
			Noble gases			
17	^{83m}Kr	1.66×10^{10}	1.89×10^{10}	2×10^{-2}	3.32×10^{8}	3.77×10^{8}
18	^{85m}Kr	3.92×10^{10}	4.44×10^{10}	2×10^{-2}	7.84×10^{8}	8.88×10^{8}
19	^{85}Kr	1.12×10^{9}	1.41×10^{9}	2×10^{-2}	2.23×10^{7}	2.81×10^{7}
20	^{87}Kr	7.96×10^{10}	8.99×10^{10}	2×10^{-2}	1.59×10^{9}	1.80×10^{9}
21	^{88}Kr	1.12×10^{11}	1.27×10^{11}	2×10^{-2}	2.24×10^{9}	2.54×10^{9}
22	^{89}Kr	1.42×10^{11}	1.61×10^{11}	2×10^{-2}	2.84×10^{9}	3.22×10^{9}
23	^{131m}Xe	9.88×10^{8}	1.01×10^{9}	2×10^{-2}	1.98×10^{7}	2.02×10^{7}
24	^{133m}Xe	6.07×10^{9}	6.92×10^{9}	2×10^{-2}	1.21×10^{8}	1.38×10^{8}
25	^{133}Xe	2.08×10^{11}	2.36×10^{11}	2×10^{-2}	4.16×10^{9}	4.73×10^{9}
26	^{135m}Xe	3.50×10^{10}	4.00×10^{10}	2×10^{-2}	7.01×10^{8}	7.99×10^{8}
27	^{135}Xe	1.83×10^{11}	2.11×10^{11}	2×10^{-2}	3.66×10^{9}	4.23×10^{9}
28	^{137}Xe	1.85×10^{11}	2.10×10^{11}	2×10^{-2}	3.70×10^{9}	4.20×10^{9}
29	^{138}Xe	1.93×10^{11}	2.19×10^{11}	2×10^{-2}	3.86×10^{9}	4.37×10^{9}

[1] Reference [2.29] states: “The release of noble gases to the confinement air in actual accidents or tests was 1.5% [2.29] and 0.5% [2.30]. Conservatively, a value of 2.0% was assumed. Release factors for iodine were determined in several experiments resulting in values of 4×10^{-6} [2.30] to 5×10^{-4} [2.31]. In the source term calculation, a value of 1×10^{-4} is used. For aerosols (solids) a release factor of less than 10^{-6} was assumed.” A value of 10^{-6} for the aerosols was used here.

TABLE 2.53. INVENTORY OF THE PEAK HEU FUEL ROD WITH 3.5% ^{235}U BURNUP, THE PEAK LEU FUEL ROD WITH 3.3% ^{235}U BURNUP, TRANSFER FACTORS AND SOURCE TERM FOR THE SCENARIO INVESTIGATED (cont.)

No.	Isotope	HEU: calculated inventory for one peak power fuel rod (Bq)	LEU: calculated inventory for one peak power fuel rod (Bq)	Transfer factor: matrix material to air [2.28][1]	HEU: source term in air of reactor hall (Bq)	LEU: source term in air of reactor hall (Bq)
		Alkalines, lanthanides and alkali metals				
30	^{140}Ba	1.92×10^{11}	2.18×10^{11}	1×10^{-6}	1.92×10^{5}	2.18×10^{5}
31	^{141}Ce	1.82×10^{11}	2.06×10^{11}	1×10^{-6}	1.82×10^{5}	2.06×10^{5}
32	^{143}Ce	1.82×10^{11}	2.07×10^{11}	1×10^{-6}	1.82×10^{5}	2.07×10^{5}
33	^{144}Ce	1.44×10^{11}	1.69×10^{11}	1×10^{-6}	1.44×10^{5}	1.69×10^{5}
34	^{134}Cs	4.59×10^{8}	5.29×10^{8}	1×10^{-6}	4.59×10^{2}	5.29×10^{2}
35	^{137}Cs	9.44×10^{9}	1.20×10^{10}	1×10^{-6}	9.44×10^{3}	1.20×10^{4}
36	^{140}La	1.92×10^{11}	2.18×10^{11}	1×10^{-6}	1.92×10^{5}	2.18×10^{5}
37	^{99}Mo	1.85×10^{11}	2.10×10^{11}	1×10^{-6}	1.85×10^{5}	2.10×10^{5}
38	^{95}Nb	1.98×10^{11}	2.26×10^{11}	1×10^{-6}	1.98×10^{5}	2.26×10^{5}
39	^{147}Nd	7.03×10^{10}	8.03×10^{10}	1×10^{-6}	7.03×10^{4}	8.03×10^{4}
40	^{147}Pm	3.01×10^{10}	3.74×10^{10}	1×10^{-6}	3.01×10^{4}	3.74×10^{4}
41	^{143}Pr	1.79×10^{11}	2.02×10^{11}	1×10^{-6}	1.79×10^{5}	2.02×10^{5}
42	^{103}Ru	9.73×10^{10}	1.13×10^{11}	1×10^{-6}	9.73×10^{4}	1.13×10^{5}
43	^{106}Ru	1.01×10^{10}	1.35×10^{10}	1×10^{-6}	1.01×10^{4}	1.35×10^{4}
44	^{89}Sr	1.48×10^{11}	1.67×10^{11}	1×10^{-6}	1.48×10^{5}	1.67×10^{5}
45	^{90}Sr	9.10×10^{9}	1.15×10^{10}	1×10^{-6}	9.10×10^{3}	1.15×10^{4}
46	^{91}Y	1.80×10^{11}	2.03×10^{11}	1×10^{-6}	1.80×10^{5}	2.03×10^{5}
47	^{95}Zr	1.98×10^{11}	2.26×10^{11}	1×10^{-6}	1.98×10^{5}	2.26×10^{5}

[1] Reference [2.29] states: "The release of noble gases to the confinement air in actual accidents or tests was 1.5% [2.29] and 0.5% [2.30]. Conservatively, a value of 2.0% was assumed. Release factors for iodine were determined in several experiments resulting in values of 4×10^{-6} [2.30] to 5×10^{-4} [2.31]. In the source term calculation, a value of 1×10^{-4} is used. For aerosols (solids) a release factor of less than 10^{-6} was assumed." A value of 10^{-6} for the aerosols was used here.

TABLE 2.53. INVENTORY OF THE PEAK HEU FUEL ROD WITH 3.5% ^{235}U BURNUP, THE PEAK LEU FUEL ROD WITH 3.3% ^{235}U BURNUP, TRANSFER FACTORS AND SOURCE TERM FOR THE SCENARIO INVESTIGATED (cont.)

No.	Isotope	HEU: calculated inventory for one peak power fuel rod (Bq)	LEU: calculated inventory for one peak power fuel rod (Bq)	Transfer factor: matrix material to air [2.28][1]	HEU: source term in air of reactor hall (Bq)	LEU: source term in air of reactor hall (Bq)
			Actinides			
48	^{237}U	3.41×10^{9}	1.77×10^{10}	1×10^{-6}	3.41×10^{3}	1.77×10^{4}
49	^{238}Np	3.49×10^{7}	2.98×10^{8}	1×10^{-6}	3.49×10^{1}	2.98×10^{2}
50	^{239}Np	6.07×10^{9}	4.70×10^{11}	1×10^{-6}	6.07×10^{3}	4.70×10^{5}
51	^{240m}Np	4.77×10^{4}	3.02×10^{6}	1×10^{-6}	4.77×10^{-2}	3.02×10^{0}
52	^{238}Pu	2.05×10^{5}	2.78×10^{6}	1×10^{-6}	2.05×10^{-1}	2.78×10^{0}
53	^{239}Pu	3.63×10^{5}	3.18×10^{7}	1×10^{-6}	3.63×10^{-1}	3.18×10^{1}
54	^{240}Pu	2.49×10^{4}	2.02×10^{6}	1×10^{-6}	2.49×10^{-2}	2.02×10^{0}
55	^{241}Pu	2.41×10^{5}	1.81×10^{7}	1×10^{-6}	2.41×10^{-1}	1.81×10^{1}
56	^{243}Pu	2.95×10^{2}	1.67×10^{4}	1×10^{-6}	2.95×10^{-4}	1.67×10^{-2}
57	^{241}Am	5.07×10^{3}	3.81×10^{5}	1×10^{-6}	5.07×10^{-3}	3.81×10^{-1}
58	^{242}Am	4.11×10^{3}	2.84×10^{5}	1×10^{-6}	4.11×10^{-3}	2.84×10^{-1}
59	^{243}Am	9.58×10^{-2}	5.03×10^{0}	1×10^{-6}	9.58×10^{-8}	5.03×10^{-6}
60	^{242}Cm	1.45×10^{3}	1.08×10^{5}	1×10^{-6}	1.45×10^{-3}	1.08×10^{-1}

[1] Reference [2.29] states: "The release of noble gases to the confinement air in actual accidents or tests was 1.5% [2.29] and 0.5% [2.30]. Conservatively, a value of 2.0% was assumed. Release factors for iodine were determined in several experiments resulting in values of 4×10^{-6} [2.30] to 5×10^{-4} [2.31]. In the source term calculation, a value of 1×10^{-4} is used. For aerosols (solids) a release factor of less than 10^{-6} was assumed." A value of 10^{-6} for the aerosols was used here.

(c) Evaluation of radiological consequences

For assumptions for dose calculations, a spreadsheet was used to calculate data for evaluation of the doses [2.32]. A close approximation to the doses calculated using this spreadsheet can be obtained using the basic equations and methodology described in the Research Reactor Core Conversion Guidebook [2.33].

The following assumptions were made for the input:

i. Source term as determined in Section 2.10.8.7 (b);
ii. Release of fission products occurs in a single phase of one hour duration;
iii. The release height for the fission products is ground level (0 m). The dimensions of the reactor building are: height: 8.5 m, width: 7.1 m, length: 7.2 m, volume: 434.52 m^3;
iv. A conservative meteorological model was used, fixing the meteorological conditions to Pasquill stability class F with 1 m/s wind speed and uniform direction for a period of 0—8 hours [2.34]. Additionally, a Pasquill stability class F with a wind speed of 1 m/s and a variable direction within a 22.5° sector for a time period of 8—24 hours was utilized;

v. For distances below 100 m from the reactor, the atmospheric dispersion in air and dose values are identical to the corresponding values at 100 m;

vi. The ventilation system is shut down at the time of the accident, so that no credit is taken for the reactor filtration system.

The results in this evaluation include:

(1) Doses for exposure of the last staff member leaving the reactor hall after the postulated accident;

(2) Doses for exposure of a member of the public present at the site fence;

(3) Doses for exposure of the member of the public living closest to the reactor.

Dose calculations are normally made using specific information describing each site and location relative to surrounding permanent residences. Since existing HEU MNSRs have a wide variety of local conditions and individual regulatory bodies, dose calculations were done for several exposure times and distances in an attempt to cover most situations. Individual MNSRs need to use data specific to their site.

The first individual case of exposure during the considered accident is that of the staff members that are present in the reactor hall during the accident. It is assumed that the last staff member evacuates the reactor hall after five minutes. This time is adequate to take the necessary actions specified in the operating procedures. Doses were also calculated for evacuation times of 10 and 30 minutes. The dose rate and the activity concentrations in the air of the reactor hall during these five minutes was based on an assumed volume method in which the radiological material is dispersed evenly in the containment or confinement volume over a specified time period; one hour is used. To obtain the dose for five minutes, the dose rate in mSv/h was divided by 12 (60 minutes/12 = 5 minutes).

The effective (whole body) doses and thyroid doses that were calculated are shown in Table 2.54. For a typical evacuation time of five minutes, the effective (whole body) doses were 0.43 mSv in the HEU core and 0.49 mSv in the LEU core, in accord with the higher power level and longer lifetime of the LEU core. These doses are far less than the effective (whole body) dose limit of 50 mSv/year recommended by IAEA Safety Standards No. GSR Part 3 [2.25]. Similarly, the thyroid doses were calculated to be 0.85 mSv and 0.97 mSv in the HEU and LEU cores, respectively. These doses are far less than the thyroid dose limit of 1250 mSv/year recommended by IAEA Safety Standards No. GSR Part 3 [2.25].

TABLE 2.54. COMPARISON OF CALCULATED DOSES WITH DOSE LIMITS SPECIFIED BY IAEA SAFETY STANDARDS No. GSR PART 3 [2.25] FOR KEY EXPOSED INDIVIDUALS FOR A BUILDING LEAK RATE OF 20% PER HOUR

Exposed individual	Exposure time	Distance	Effective (whole body) dose			Thyroid dose		
			Calculated dose (mSv)		Dose limits (mSv)	Calculated dose (mSv)		Dose limits (mSv)
			HEU	LEU	IAEA SS No. GSR Part 3 [2.25]	HEU	LEU	IAEA SS No. GSR Part 3 [2.25]
Maximum exposed worker	5 min 10 min 30 min		0.43 0.86 2.58	0.49 0.98 2.94	50/year [1]	0.85 1.70 5.11	0.97 1.94 5.82	1250/year
Maximum exposed member of public	2 h	100 m 300 m 500 m	1.18×10^{-3} 5.72×10^{-4} 2.37×10^{-4}	1.34×10^{-3} 6.52×10^{-4} 2.71×10^{-4}	1/year	3.25×10^{-3} 1.58×10^{-3} 6.55×10^{-4}	3.71×10^{-3} 1.80×10^{-3} 7.47×10^{-4}	25/year
	4 h	100 m 300 m 500 m	1.63×10^{-3} 7.89×10^{-4} 3.28×10^{-4}	1.86×10^{-3} 9.02×10^{-4} 3.74×10^{-4}		5.05×10^{-3} 2.45×10^{-3} 1.02×10^{-3}	5.76×10^{-3} 2.80×10^{-3} 1.16×10^{-3}	
	8 h	100 m 300 m 500 m	1.94×10^{-3} 9.43×10^{-4} 3.91×10^{-4}	2.22×10^{-3} 1.08×10^{-3} 4.48×10^{-4}		6.83×10^{-3} 3.32×10^{-3} 1.38×10^{-3}	7.79×10^{-3} 3.78×10^{-3} 1.57×10^{-3}	
Maximum exposed permanent resident	24 h	300 m 600 m 1000 m 10 000 m	9.28×10^{-4} 2.84×10^{-4} 1.23×10^{-4} 4.37×10^{-6}	1.06×10^{-3} 3.24×10^{-4} 1.41×10^{-4} 5.00×10^{-6}	1/year	2.66×10^{-3} 8.13×10^{-4} 3.53×10^{-4} 1.25×10^{-5}	3.04×10^{-3} 9.28×10^{-4} 4.03×10^{-4} 1.43×10^{-5}	25/year
Additional doses calculated for a hypothetical building leak rate of 100% per hour to establish an upper bound								
Maximum exposed worker	5 min	-	0.43	0.49	50/year	0.85	0.97	1250/year
Maximum exposed member of public	2 h	100 m	3.45×10^{-3}	3.93×10^{-3}	1/year	8.90×10^{-3}	1.02×10^{-2}	25/year
Maximum exposed permanent resident	24 h	300 m	1.77×10^{-3}	2.02×10^{-3}	1/year	3.95×10^{-3}	4.50×10^{-3}	25/year

[1] While the does limit is 20 mSv/y averaged over 5 years, a dose of 50 mSv in a single year is used for the accident scenarios used in this document.

The dose for the maximum exposed member of the public was evaluated for the case that a person stands during the accident at a fence that separates the reactor site from the public area. Doses were computed for locations closest to the reactor at distances of 100 m, 300 m, and 500 m. Further, it is assumed that the person stays at the location for two hours, but cases were also calculated for four hours and eight hours. After this time, the area at the public perimeter of the site is assumed to be evacuated by the security staff. No ingestion is assumed to take place during the considered time period. Doses computed for two hours are sufficient to consider all effects due to inhalation. The results are shown in Table 2.54.

The effective (whole body) doses were calculated to be 1.18×10^{-3} mSv for the HEU core and 1.34×10^{-3} mSv for the LEU core in the case with an exposure time of two hours at a distance of 100 m from the reactors, assuming a building leak rate of 20% of volume per hour. These doses are far less than the effective (whole body) dose limit of 1 mSv/year recommended by IAEA Safety Standards No. GSR Part 3 [2.25]. For the same conditions, thyroid doses of 3.25×10^{-3} and 3.71×10^{-3} mSv were obtained for the HEU and LEU cores respectively. These doses are far less than the thyroid dose limit of 25 mSv/year recommended by IAEA Safety Standards No. GSR Part 3 [2.25].

Doses were calculated for cases in which the closest permanent resident is assumed to be 300 m, 600 m, 1000 m, and 10 000 m using the assumptions listed in Section 1.10.8.7 (c). The wind is assumed to blow in the direction of the permanent residence as described in the assumptions. The doses are computed for 24 hours, which is sufficient to consider all effects due to inhalation. These results are shown in Table 2.54.

The effective (whole body) doses were calculated to be 9.28×10^{-4} for the HEU core and 1.06×10^{-3} mSv for the LEU core, assuming that the residence is located 300 m from the reactor and building leak rate is 20% per hour. These doses are far less than the effective (whole body) dose limit of 1 mSv/year recommended by IAEA Safety Standards No. GSR Part 3 [2.25]. For the same conditions, thyroid doses of 2.66×10^{-3} and 3.04×10^{-3} mSv were calculated for the HEU and LEU cores respectively. These doses are far less than the thyroid dose limit of 25 mSv/year recommended by IAEA Safety Standards No. GSR Part 3 [2.25].

The dose calculation in Table 2.54 incorporated an assumed building leakage rate of 20% per hour. A building leakage rate of 100% per hour is not considered to be credible. Nonetheless, additional dose calculations were done for representative cases with a building leakage rate of 100% per hour in order to establish an upper bound on the doses that may be expected due to varying this parameter. Again, the calculated doses are far below the dose limits recommended in IAEA Safety Standards No. GSR Part 3 [2.25].

Considering the conservative approach taken in i—v. of Section 2.10.8.7 (c) for calculation of the radionuclide inventory and the meteorological conditions, doses for more realistic conditions will be significantly lower than those that were calculated.

2.10.8.8. BDBA and maximum hypothetical accident

The BDBA is sometimes called the maximum hypothetical accident. It is described for purposes of emergency planning and is always an accident that is more severe than the DBA.

This accident is considered with the following assumptions [2.1, 2.2]:

— The reactor building collapses;
— The reactor vessel water and the pool water leak at a rate of 4 m^3/hr;
— The reactor core is exposed to air after six hours;
— The HEU reactor was operating at 30 kW and the LEU reactor was operating at 34 kW;
— The reactor has been operating for ten years at full power, 2.5 hours a day, five days a week; and
— The reactor scrams at the beginning of the accident sequence.

Under these conditions, the HEU or the LEU cores would be cooled by natural circulation of air and by thermal radiation. The cores would not melt. Any exposure will be external exposure emanating from the unshielded core.

Fission product activities for unshielded generic HEU and LEU cores were calculated using the ORIGEN2 code [2.10] with the operating history shown in Fig. 2.31. Since ORIGEN2 input allows only ten time steps to be entered for each run, an approximation must be made to the assumed ten year operating history. The power history used for the HEU core based on a power level of 30 kW is shown in Fig. 2.31. It was selected to obtain a reasonable estimate of the total activity for fission product with long, intermediate, and short half-lives. The same operating history was used for the LEU core operated at a power level of 34 kW.

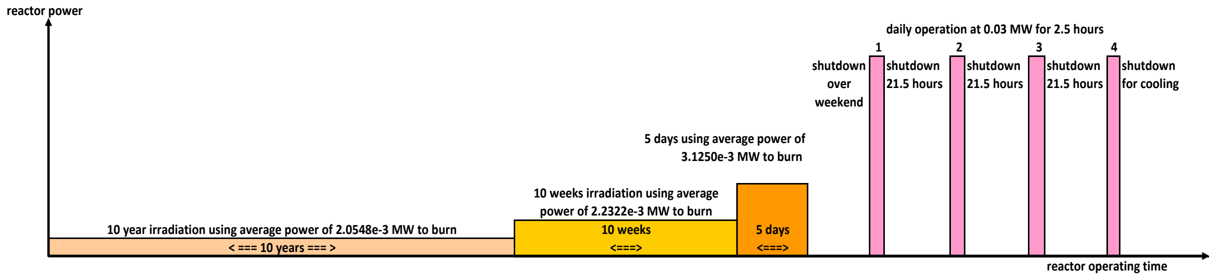

FIG. 2.31. Reactor power history and approximations use in ORIGEN2 for MNSR BDBA analyses (Courtesy of Argonne National Laboratory, USA).

Table 2.55 compares the total activity of core fission products that were calculated for the generic HEU and LEU cores using the above reactor power history with the corresponding data in two MNSR Final SARs [2.1, 2.2]. This comparison is quite good, given that the reports simply state values of the total fission product activity with no justification of how the data was obtained. The data in Table 2.55 are plotted in Figure 2.32.

TABLE 2.55. ESTIMATED AND CALCULATED CORE FISSION PRODUCT ACTIVITY WITH COOLING TIME

	Total activity of fission products in core (TBq)		
Cooling time	MNSR SAR estimate [2.1, 2.2]	Generic HEU core calculated	Generic LEU core calculated
1 min	1400	2109	2521
1 h	170	508	611
6 h	99	200	240
12 h	91	146	178
1 d	80	107	132
5 d	65	61	72
10 d	58	49	56
30 d	44	32	37
60 d	—	24	27
90 d	—	19	22

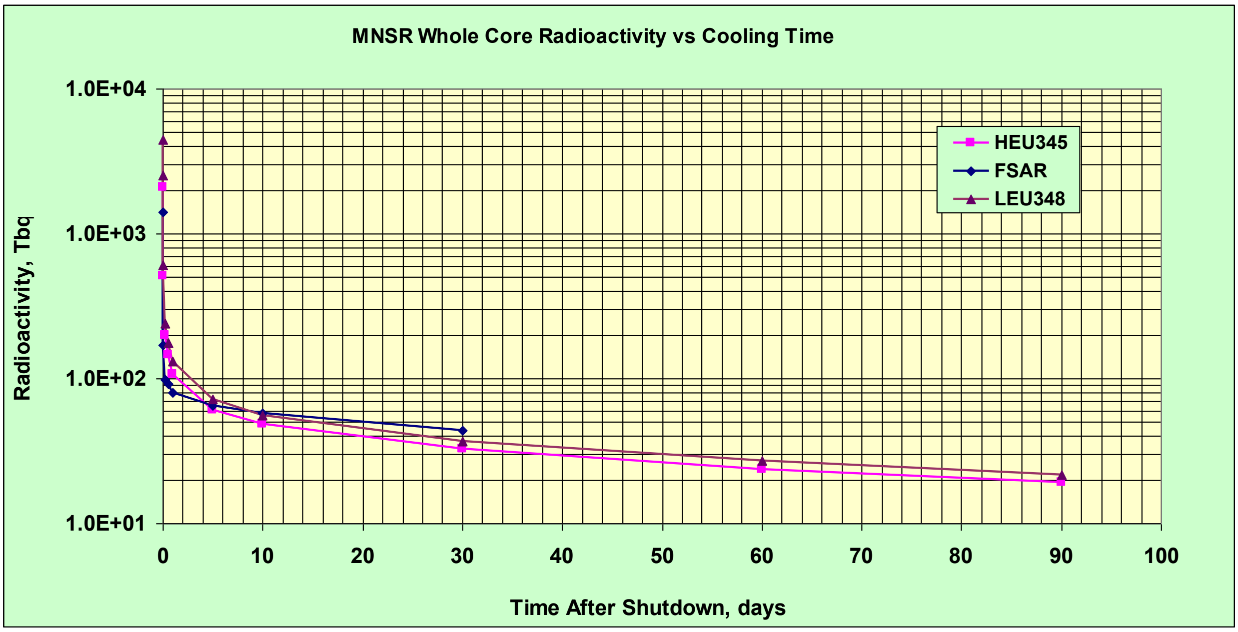

FIG. 2.32. MNSR whole core fission product activity versus cooling time (Courtesy of Argonne National Laboratory, USA).

Gamma dose rates from the Final Safety Analysis Reports of two HEU MNSRs [2.1, 2.2] at different locations for six hours, one day, and 30 days after the BDBA are shown in Table 2.56, along with estimated gamma dose rates for the generic LEU core. The gamma source for the LEU core is estimated to be 1.2 times higher than for the HEU core based on the fission product activities shown in Table 2.55. The reason for this factor of 1.2 is that the LEU core has a higher power level and a longer lifetime.

TABLE 2.56. GAMMA DOSE RATES AT DIFFERENT LOCATIONS AFTER BDBA

Time after accident	Radiation dose rate (mSv/h)				
	In the reactor building		Outside the reactor building		
	Top of reactor restricted	Reactor hall	Balcony, 10 m away	Office, 20 m away	Office, 50 m away
HEU core (from References [2.1, 2.2])					
6 h	1.7×10^{2}	8.9×10^{-1}	1.6×10^{-2}	7.6×10^{-3}	2.7×10^{-3}
1 d	1.2×10^{2}	6.7×10^{-1}	1.1×10^{-2}	5.3×10^{-3}	1.9×10^{-3}
30 d	5.0×10^{-1}	3.3×10^{-1}	4.8×10^{-3}	2.2×10^{-3}	7.9×10^{-4}
LEU core (estimated)					
6 h	2.0×10^{2}	10.7×10^{-1}	1.9×10^{-2}	9.1×10^{-3}	3.2×10^{-3}
1 d	1.4×10^{2}	8.0×10^{-1}	1.3×10^{-2}	6.4×10^{-3}	2.3×10^{-3}
30 d	6.0×10^{-1}	4.0×10^{-1}	5.8×10^{-3}	2.6×10^{-3}	9.5×10^{-4}

The effective (whole body) dose limit for the maximum exposed worker recommended in IAEA Safety Standards No. GSR Part 3 [2.25] is 50 mSv per year. Except for the easily controlled restricted area immediately above the core, all dose rates are low and would permit emergency operations to proceed.

2.10.8.9. HEU core removal and LEU core installation reactivity insertion accident scenarios

(a) Analysis of rapid reactivity insertions in the generic HEU and LEU cores using the RELAP5 version 3.3 code

Detailed procedures have been developed by the CIAE for removal of the HEU core and installation of the LEU core [2.36]. Inadvertent reactivity insertions may occur if these procedures are not performed in the prescribed sequence. Analyses are done here to determine the power level and temperatures that would be reached for hypothetical rapid reactivity insertions that may occur in the generic HEU and LEU cores during conversion from HEU to LEU fuel.

Several experiments involving rapid insertion of reactivity greater than 4 mk were performed in Slowpoke-1 and Slowpoke-2 reactors at Chalk River Laboratories in Canada in the 1970s [2.36]. The largest reactivity insertions were 6.48 mk in 0.8 s in a Slowpoke-1 reactor, and 6.05 mk in a Slowpoke-2 reactor.

MNSR and Slowpoke reactors have very similar designs, but are not identical. To demonstrate validity of the RELAP5 model for rapid reactivity insertions in MNSRs, a comparison is made in Fig. 2.33 of the measured power profile resulting from a rapid insertion of 6.48 mk in a Slowpoke-1 experiment, with calculated power profiles for the same 6.48 mk reactivity insertions in 0.5 s in the generic HEU and LEU MNSRs. The results show that the calculated generic MNSR results are comparable with the measured Slowpoke-1 data.

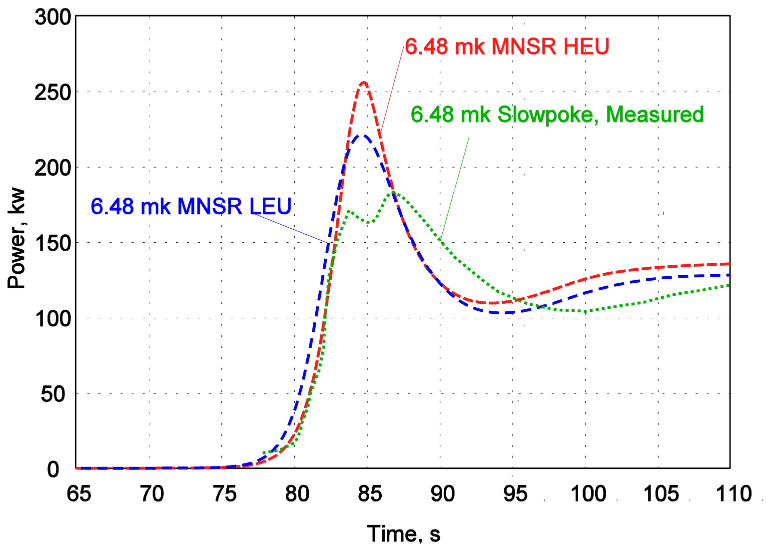

FIG. 2.33. Comparison of power profiles measured for a rapid reactivity insertion of 6.48 mk in a Slowpoke-1 reactor with calculated power profiles for the same rapid reactivity insertion in the generic HEU and LEU MNSRs (Courtesy of Argonne National Laboratory, USA).

Only coolant and moderator temperatures were measured in the Slowpoke experiments [2.36]. Figure 2.34 shows calculated temperature profiles in the fuel and at the surface of the cladding for the MNSR HEU and LEU cores. The peak temperatures reached in the UAl fuel and Al cladding of the HEU core were 129°C and 124°C, respectively. This is far below the aluminium incipient melting temperature of approximately 640°C. In the LEU MNSR core, the peak temperature in the LEU UO_2 fuel was calculated to be 239°C, which is far below the incipient melting temperature of 2865°C for UO_2. The peak temperature at the surface of the Zircaloy-4 cladding was calculated to be 121°C, far below its incipient melting temperature of 1850°C.

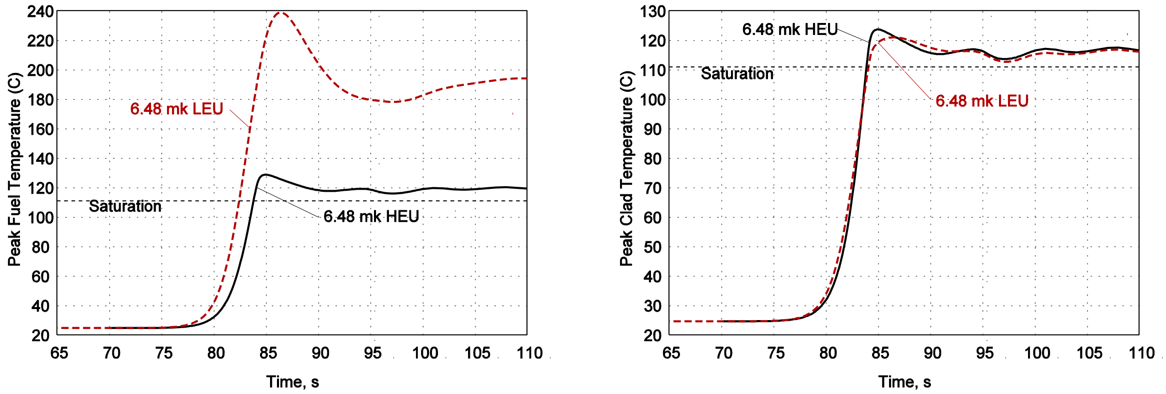

FIG. 2.34. Calculated temperature profiles in the fuel and at the cladding surface in the fuel rod with peak power for rapid reactivity insertions of 6.48 mk in the generic HEU and LEU cores (Courtesy of Argonne National Laboratory, USA).

On this basis, the RELAP5 model for the generic HEU and LEU MNSRs was used to calculate additional rapid reactivity insertions of 4 mk, 8 mk, and 9 mk. The purpose was to establish an envelope of reactivity insertions which would not lead to melting of fuel rods, either in the event of an accident involving a net positive insertion of reactivity during removal of the HEU core, or installation of the LEU core. Peak fuel and cladding temperatures are shown in Fig. 2.35 for a rapid insertion of 8 mk in the HEU and LEU reactors.

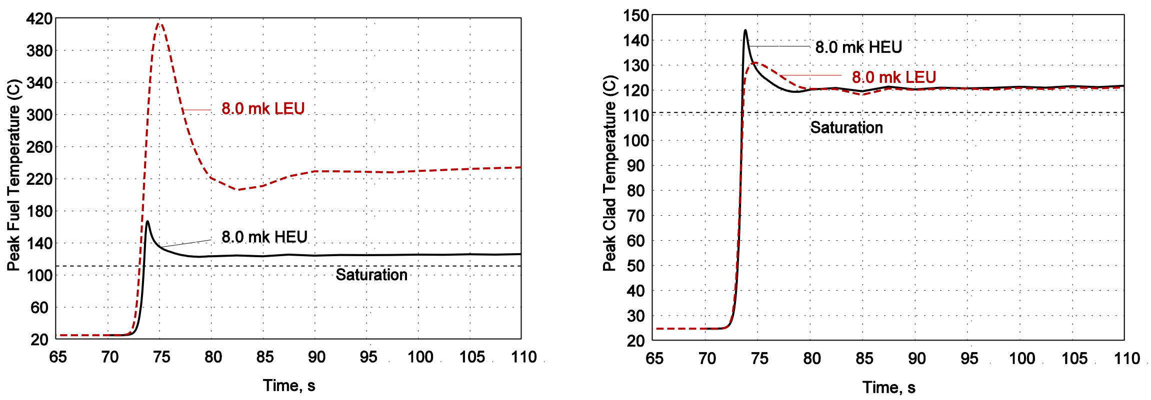

FIG. 2.35. Fuel and cladding temperature profiles for rapid insertions of 8 mk in the generic HEU and LEU reactors (Courtesy of the Argonne National Laboratory, USA).

Peak reactor power, and peak fuel and cladding temperatures in the fuel rod with peak power are shown in Table 2.57 for rapid insertions of 4–9.25 mk in the HEU core and 4–11 mk in the LEU core. Again, the peak cladding temperature in the HEU core is to be compared with an incipient melting temperature of approximately 640°C for aluminium, and the peak cladding temperature in the LEU core is to be compared with an incipient melting temperature of 1850°C for Zircaloy-4. Similarly, the peak fuel temperatures are to be compared with approximately 640°C for the HEU UAl alloy fuel, and 2865°C for the LEU UO_2 fuel.

TABLE 2.57. CALCULATED PEAK FUEL AND CLADDING TEMPERATURES FOR RAPID REACTIVITY INSERTIONS IN THE GENERIC HEU AND LEU MNSRS

Rapid reactivity insertion (mk)	Peak power (kW)		Peak clad temperature (°C)		Peak fuel temperature (°C)	
	HEU	LEU	HEU	LEU	HEU	LEU
4.0	83	77	104	101	105	148
6.48	256	221	124	121	129	239
8.0	1213	727	144	131	167	414
9.0	6028	2656	234	138	259	614
9.25	8668	—	299	—	305	—
10.0	—	9559	—	146	—	889
11.0	—	26 179	—	157	—	1111

For rapid reactivity insertions greater than 9.25 mk for the HEU core and 11 mk in the LEU core, RELAP5 predicts that the critical heat flux (CHF) or DNB will be reached and that temperatures in the fuel and the cladding will rise rapidly and could lead to melting of the fuel.

Since experiments have not been performed to verify the behaviour of an MNSR for reactivity insertions greater than approximately 4 mk, it would be prudent to consider only reactivity insertions below prompt critical (8.57 mk in the HEU core and 8.45 mk in the LEU core), for use in potential accident scenarios.

(b) Analysis of rapid reactivity insertions in the generic LEU core using the PARET/ANL version 7.5 code

Analyses of rapid reactivity insertion transients for the generic LEU core were also performed using the PARET/ANL Version 7.5 code using the same input data that was used in the calculations using the RELAP5 Version 3.3 code [2.37]. Peak power levels as a function of reactivity insertion that were computed using the two codes are in good agreement, as shown in Fig. 2.36. Peak temperatures in the fuel and cladding that are shown in Fig. 2.37 are also in good agreement.

The PARET/ANL results in Fig. 2.37 show temperatures calculated at both the inner and outer surfaces of the Zircaloy-4 cladding. Both of these temperatures, along with the temperature at the cladding surface calculated using RELAP5 Version 3.3, are far below the incipient melting temperature of 1850°C for Zircaloy-4.

(c) Analysis of reactivity insertion scenarios for removal of the HEU core

A step by step procedure for removing the current HEU core and installing a fresh LEU core was provided by the CIAE [2.35]. A description of the steps, the change in reactivity of the core, and the net excess reactivity after each step are provided in Appendix IV for the generic HEU and LEU cores.

If all steps in the procedure are performed in the specified sequence, the HEU and LEU cores will remain in a deep subcritical state, even if they were inadvertently dropped into the radial beryllium reflector to put the core into its maximum reactive state.

Three hypothetical accident scenarios for the HEU core removal operation and three hypothetical accident scenarios for the LEU core installation were evaluated in the unlikely event that the core changing procedures are not followed in the prescribed sequence.

The operations in the procedure that maintain the core in a deep subcritical state during core changing are the insertion of strings of four cadmium rabbits into the five inner irradiation positions in the beryllium reflector. In the NIRR-1 reactor in Nigeria, each string of four cadmium rabbits has a reactivity worth of –2.48 mk [2.38]. Insertion of a string of cadmium rabbits into each of the five inner irradiation positions would reduce the reactivity by 12.4 mk. It is also very important to insert the neutron and gamma detectors into the slant tubes outside the vessel to monitor changes in the neutron and gamma doses in the specified sequence. This would allow early detection of inadvertent increases in reactor power.

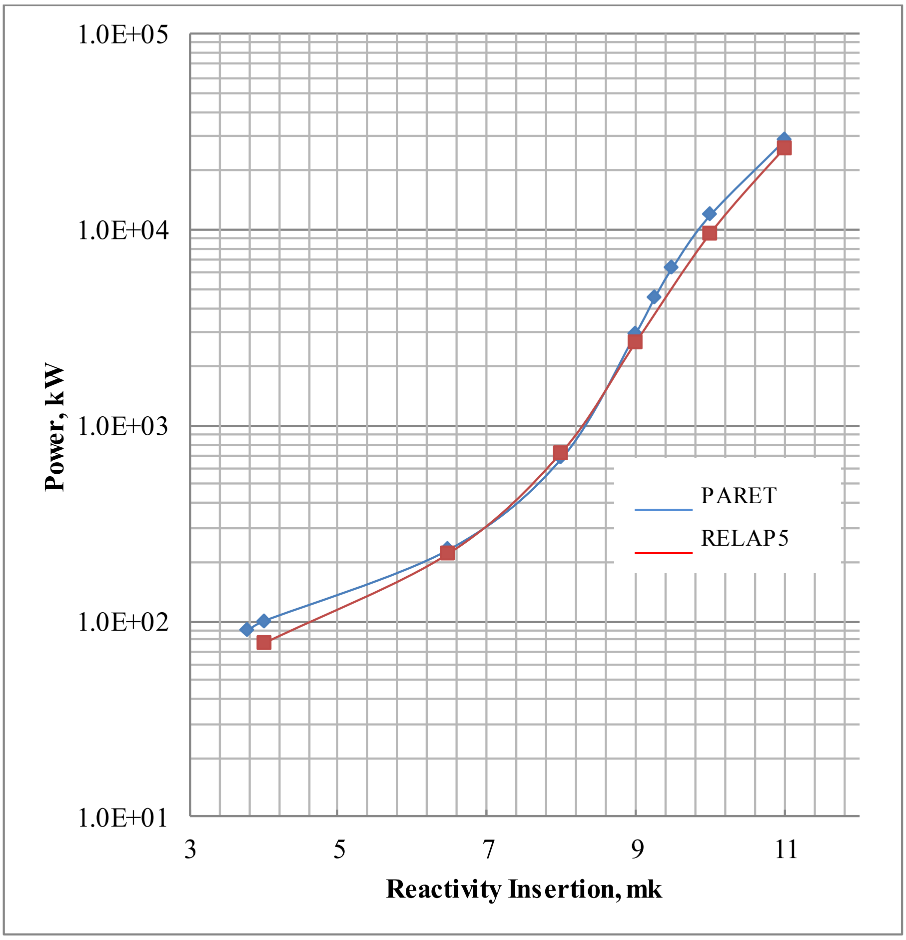

FIG. 2.36. Comparison of peak power calculated using RELAP5 and PARET/ANL for rapid reactivity insertions in the generic LEU core (Courtesy of Argonne National Laboratory, USA).

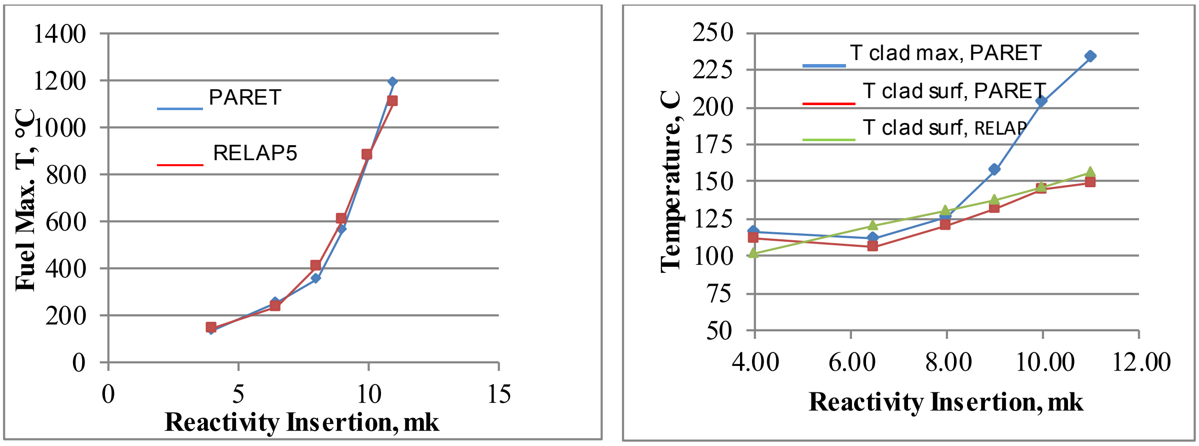

FIG. 2.37. Comparison of peak fuel and cladding temperatures calculated using RELAP5 and PARET/ANL for rapid reactivity insertions in the generic LEU core (Courtesy of Argonne National Laboratory, USA).

In the first core removal accident scenario, it was assumed that the reactor staff failed to insert all five strings of cadmium rabbits as specified during removal of the HEU core, and also failed to address increases in the neutron and gamma doses as the core approached criticality and additional excess reactivity was inserted. This scenario will result in a net positive reactivity insertion of about 5.6 mk, which is less than the excess reactivity needed to reach prompt critical, which is 8.57 mk in the HEU core. The RELAP5 transient analyses described in Section 2.10.8.9 (a) indicate that melting of the fuel would not be initiated under these circumstances. However, it is very important that the five strings of cadmium rabbits are inserted in the prescribed sequence.

The maximum excess reactivity of 4 mk was assumed at the beginning of this scenario. However, individual MNSRs may begin with a lower excess reactivity since the HEU cores will be partially burned. In addition, the reactivity worth of individual components that are removed or reinstalled in the core changing process may have smaller or larger reactivity worths in each MNSR. The conclusion is that each MNSR needs to be evaluated individually.

In the second core removal scenario, it was assumed that the reactor staff failed to insert four of the five strings of cadmium rabbits before removal of the HEU core, and also failed to address increases in the neutron and gamma doses as the core approached criticality and additional excess reactivity was inserted. Since the worth of each cadmium rabbit string is approximately –2.48 mk, the net positive reactivity insertion would be about 3.1 mk. In this case, the peak fuel and cladding temperatures would be far below their incipient melting temperatures, as described in the analyses shown in Sections 2.10.8.9 (a) and (b). There would be no damage to the fuel and no release of radioactivity,

In the third core removal scenario, it was assumed that the reactor staff failed to insert three of the five strings of four cadmium rabbits, each worth about –2.48 mk, into the five inner irradiation positions during step three of procedure for removal of the HEU core. The result is that the excess reactivity would reach 0.65 mk. The peak fuel and cladding temperatures would be far below their incipient melting temperatures, as described in the analyses shown in Sections 2.10.8.9 (a) and (b). There would be no damage to the fuel and no release of radioactivity.

(d) Analysis of reactivity insertion accident scenarios for installation of the LEU core

Three similar hypothetical reactivity insertion accident scenarios were also evaluated for installation of the LEU core, assuming that the procedures for removal of the HEU core had been followed and that the HEU core had been safely removed.

In the first LEU core installation scenario, it was assumed that the reactor staff inadvertently removed the five strings of cadmium rabbits from the inner irradiation positions immediately after installation of the LEU core in the radial beryllium reflector, and before replacement of the aluminium shim tray and newly designed control rod. The staff also failed to address increases in the neutron and gamma doses as the core approached criticality and additional excess reactivity was inserted.

In this case, the net positive rapid reactivity insertion would be about 4.7 mk. The analyses shown in Sections 2.10.8.9 (a) and (b) indicate that incipient melting of the fuel would not occur. There would be no damage to the fuel and no release of radioactivity. However, it is important to ensure that the operations specified in the LEU core installation procedures are performed in the proper sequence.

In the second installation scenario, it was assumed that the reactor staff removed four of the five strings of cadmium rabbits from the inner irradiation positions after installation of the LEU core in the radial beryllium reflector, and before replacement of the aluminium shim tray and newly designed control rod. The staff also failed to address increases in the neutron and gamma doses as the core approached criticality and additional excess reactivity was inserted. The net positive reactivity insertion would be about 2.2 mk. In this case, the peak fuel and cladding temperatures would be far below their incipient melting temperatures, as described in Sections 2.10.8.9 (a) and (b). There would be no damage to the fuel and no release of radioactivity.

In the third installation scenario, it was assumed that the reactor staff failed to insert three of the five strings of cadmium rabbits into the inner irradiation positions in the sequence specified in the core installation procedures. In this case, the core remains subcritical throughout the installation process. There would be no damage to the fuel and no release of radioactivity.

The aforementioned analyses highlight the importance of following the removal and installation procedures in the correct sequence for HEU core removal and LEU core installation. This is particularly important for monitoring changes in the neutron and gamma doses, and the insertion and removal of the cadmium rabbits in the beryllium reflector.

REFERENCES TO SECTION 2

[2.1] CENTRE FOR ENERGY RESEARCH AND TRAINING, Nigeria Research Reactor-1: Final Safety Analysis Report, CERT/NIRR-1/001, Ahmadu Bello University, Zaria (2005).

[2.2] AKAHO, E.H.K., et al., Ghana Research Reactor-1, Final Safety Analysis Report, GAEA-NNRI-RT-90, National Nuclear Research Institute, Legon-Accra (2003).

[2.3] INTERNATIONAL ATOMIC ENERGY AGENCY, Summary Report on 2nd RCM on MNSR Conversions, IAEA, Vienna (2008).

[2.4] X-5 MONTE CARLO TEAM, MCNP-A General Monte Carlo N-Particle Transport Code, Version 5, Volumes I, II and III, LA-UR-03-1987/LA-CP-03-0245/LA-CP-03-0284, Los Alamos National Laboratory, Los Alamos (2003).

[2.5] LI, YG., The Physics Experimental Study for In-Hospital Neutron Irradiator (IHNI), Proc. International Meeting on Reduced Enrichment for Research and Test Reactors, Prague, 2007, Argonne National Laboratory, Argonne (2007).

[2.6] MATOS, J.E., LELL, R., (Proc. 2005 International Meeting on Reduced Enrichment for Research and Test Reactors, Boston, 2005), Argonne National Laboratory, Argonne (2006).

[2.7] MATOS, J.E., Argonne National Laboratory, presented at First Research Coordination Meeting for the IAEA Coordinated Research Project on Conversion of Miniature Neutron Source Reactors (MNSR) from HEU to LEU Fuel, Vienna, 2006.

[2.8] OLSON, A.P., A Users Guide for the REBUS-PC Code, Version 1.4, ANL/RERTR/TM02-32, Argonne National Laboratory, Argonne (2001).

[2.9] LIAW, J.R., MATOS, J.E., MNSR Flux Performance and Core Lifetime Analysis with HEU and LEU Fuels, Proc. International Meeting on Reduced Enrichment for Research and Test Reactors, Prague, 2007, Argonne National Laboratory, Argonne (2007).

[2.10] CROFF, A.G., ORIGEN2: A Versatile Computer Code for Calculating the Nuclide Compositions and Characteristics of Nuclear Materials, Nucl. Techn. 62 (1983) 335; CROFF, A.G., A User's Manual for the ORIGEN2 Computer Code, ORNL/TM-7175, Oak Ridge National Laboratory, Oak Ridge (1980).

[2.11] OLSON, A.P. and KALIMULLAH, M., A Users Guide to the PLTEMP/ANL V4.1 Code, Global Threat Reduction Initiative (GTRI) – Conversion Program, Nuclear Engineering Division, Argonne National Laboratory, Chicago, IL, USA (April 5, 2011).

[2.12] RELAP5/MOD3.3 Code Manual Volume I: Code Structure, System Models, and Solution Methods, NUREG/CR-5535/Rev. P3-Vol I, US Nuclear Regulatory Commission, Washington, DC (2003).

[2.13] SHI, S., MNSR Thermal Hydraulics, MNSR Training Manual, China Institute of Atomic Energy, Beijing, 1993 (unpublished).

[2.14] AMPOMAH-AMOAKO, E., AKAHO, E.H.K., ANIM-SAMPONG, S., NYARKO, B.J.B., Transient Analysis of Ghana Research Reactor-1 using PARET/ANL Thermal Hydraulic Code, Nucl. Eng. and Design 239 (2009) 2479–2483.

[2.15] KALIMULLAH, M., DIONNE, B., FELDMAN, E.E., MATOS, J.E., OLSON, A.P., Estimating Hot Channel Factors for a Generic MNSR Using Rodded Fuel Cooled by Natural Circulation, Proc. Intl. Mtg. on Reduced Enrichment for Research and Test Reactors (RERTR), Santiago, 2011, Argonne National Laboratory, Argonne (2012).

[2.16] DUNN, F.E., MATOS, J.E., Thermal Hydraulic Safety Margins for MNSR HEU and LEU Cores, presented at IAEA Workshop on Conversion of MNSRs to LEU, Vienna, 2007.

[2.17] AHMED, Y.A., BALOGUN, G.I., JONAH, S.A., FUNTUA, I.I., The Behavior of Reactor Power and Flux Resulting from Changes in Core-Coolant Temperature for a Miniature Neutron Source Reactor, Annals of Nuclear Energy 35 (2008) 2417–2419.

[2.18] CAROLINA POWER AND LIGHT COMPANY, Final Safety Analysis Report of Shearon Harris Nuclear Power Plant, New Hill (1987) 4.4.2–4.

[2.19] DUNN, F.E., THOMAS, J., LIAW, J., MATOS, J.E., MNSR Transient Analyses and Thermal Hydraulic Safety Margins for HEU and LEU Cores Using the RELAP5-3D Code, Proc. International Meeting on Reduced Enrichment for Research and Test Reactors, Prague, 2007, Argonne National Laboratory, Argonne (2007).

[2.20] BRIESMEISTER, J.F., MCNP – A General Monte Carlo N-Particle Transport Code, Version 4C, Ed., LA-13709-M (2000).

[2.21] INTERNATIONAL ATOMIC ENERGY AGENCY, Safety of Research Reactors, IAEA Safety Standards Series No. NS-R-4, IAEA, Vienna (2005).

[2.22] JONAH, S., Center for Energy Research and Training, private communication, 2012.

[2.23] THE RELAP5-3D CODE DEVELOPMENT TEAM, RELAP5-3D Code Manual, Version 2.3, INEEL-EXT-98-00834, Idaho National Laboratory, Idaho Falls (2005).

[2.24] ARGONNE NATIONAL LABORATORY, International Nuclear Safety Center database ANL, Argonne (2012).

[2.25] INTERNATIONAL ATOMIC ENERGY AGENCY, Radiation Protection and Safety of Radiation Sources: International Basic Safety Standards, IAEA Safety Standards No. GSR Part 3, IAEA, Vienna (2014).

[2.26] GUO, C., Performance Study and Improvements of the Miniature Neutron Source Reactor, MNSR Training Materials, China Institute of Atomic Energy, Beijing (1993).

[2.27] DEEN, J.R., WOODRUFF, W.L., COSTESCU, C.I., LEOPANDO, L.S., WIMS-ANL User Manual, Rev. 3, ANL/RERTR/TM-23, Argonne National Laboratory, Argonne (1999).

[2.28] INTERNATIONAL ATOMIC ENERGY AGENCY, Derivation of the Source Term and Analysis of the Radiological Consequences of Research Reactor Accidents, IAEA Safety Reports Series No. 53, IAEA, Vienna (2008) 100–101.

[2.29] MAIN, J.M., Compte-rendu de l'incident de fusion de plaques d'un element combustible a SILOE, CEA Report INT/Pi(R) 760-775/68, Atomic Energy Commission, Paris (1968) (in French).

[2.30] DADILLON, J., GEISSE, G., Taux d'emmission et comportement de la contamination liberee par la fusion de plaque combustible dans le Coeur d'une pile piscine, SESR/EDC Nr. 67/34 (1967) (in French).

[2.31] PETITPIERRE, F., Mesure de l'emission du iode du bassin Saphir, TM-SR-107 (1976) (in French).

[2.32] PFEIFFER, P.A., Microsoft Excel Spreadsheet Model for Dose Calculations, DRAFT SSDOSE 2.2, 2008.

[2.33] INTERNATIONAL ATOMIC ENERGY AGENCY, Research Reactor Core Conversion Guidebook, Volume 2: Analysis (Appendices A–F), IAEA-TECDOC-643, IAEA, Vienna (1992) 155.

[2.34] US ATOMIC ENERGY COMISSION, U.S. Atomic Energy Commission Regulatory Guide 1.4, Rev. 2, AEC, Germantown (1974).

[2.35] Li, Y., Physical Steps in Converting MNSR Prototype Unit to LEU, Removal of Existing HEU Core and Insertion of LEU Core, presented at Third Research Coordination Meeting of the IAEA Coordinated Research Project on Conversion of Miniature Neutron Source Reactors (MNSR) from HEU to LEU Fuel, Vienna, 2012.
[2.36] KAY, R.E., HILBORN, J.W., POULSEN, N.B., The Self-Limiting Power Excursion Behaviour of the Slowpoke Reactor, Results of Experiments and Qualitative Explanation, AECL-4470, Chalk River Nuclear Laboratories, Deep River (1976).
[2.37] OLSON, A.P., A Users Guide to the PARET/ANL Code, Version 7.5, ANL/RERTR/TM-11-38, Ver. 7.5, Argonne National Laboratory, Argonne (2011).
[2.38] JONAH, S., NIRR-1, Nigeria, private communication, February 2012.

3. CONVERSION ANALYSIS OF CHINA'S MNSRs

3.1. INTRODUCTION

China has two operational MNSRs, MNSR IAE and MNSR-SZ, which were designed and constructed by CIAE in 1984 and 1988 respectively. They are enriched to approximately 90% ^{235}U fuel in UAl_4 form, have aluminium alloy cladding, metal beryllium reflectors, and light water as the moderator and coolant. These MNSRs are mainly used for neutron activation analysis (NAA), testing and training.

In order to verify the calculation method, the reactor physics and thermal parameters of MNSR IAE and MNSR-SZ with HEU fuel were calculated, and the results were compared with experimental results. Using the HEU calculation method, LEU calculations were performed, and dynamic features of both HEU and LEU were analysed.

Monte Carlo code was employed to perform calculations of k_{eff}, worth of the top beryllium reflector, worth of the central control rod, and neutron flux in the inner irradiation site of the HEU-fuelled prototype MNSR, MNSR IAE, and the MNSR-SZ in Shenzhen. RELAP-5 code was used to perform the thermal analysis of these two MNSRs.

The dynamic parameters of the reactors corresponding to a 3.6 mk step reactivity insertion for MNSR IAE and a 3.51 mk step reactivity insertion for MNSR-SZ are given. A comparison was made between the theoretical calculations and the experiments results, which are agreeable.

Without changing the core dimensions of MNSR IAE and MNSR-SZ, but substituting high enriched uranium (HEU) fuel with low enriched uranium (LEU) and Al cladding with zircaloy cladding, k_{eff} and the neutron flux were calculated. Finally, thermal dynamic features under a condition of 4.0 mk excess reactivity were analysed.

3.2. MNSR DESCRIPTION

3.2.1. Critical assembly for MNSR IAE

The critical assembly includes: the reactor core, a side beryllium reflector, a bottom reflector and a top beryllium reflector (see Fig. 3.1 and Table 3.1).

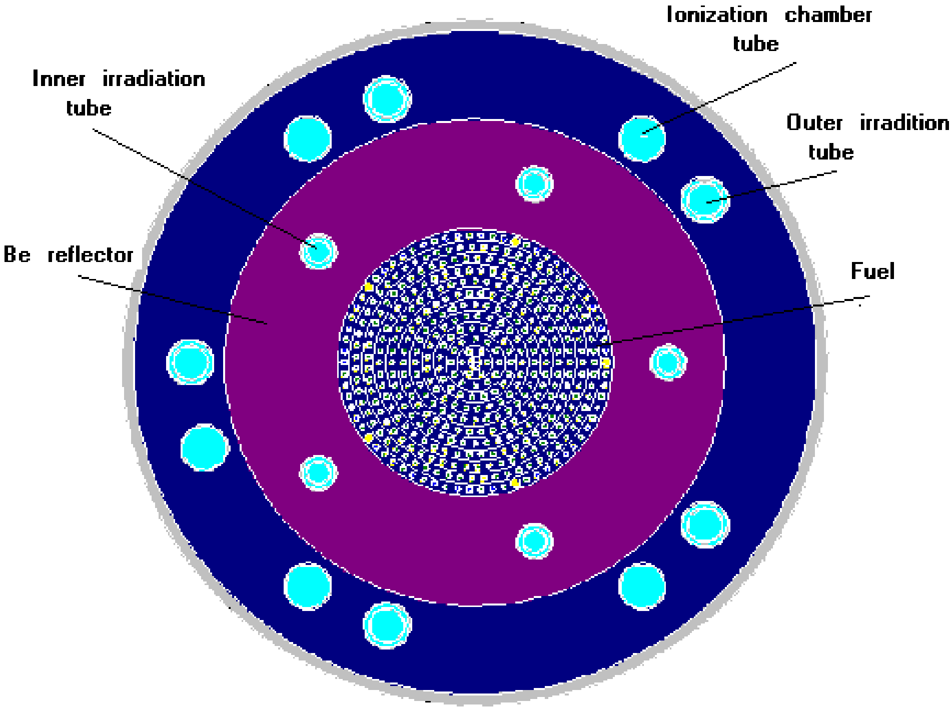

FIG. 3.1. The geometric diagram in x–y plane from MCNP (Courtesy of China Institute of Atomic Energy (CIAE), China).

3.2.1.1. Reactor core

The upper and lower grid plates are linked by five tie rods. Concentrically arranged in the core are 11 rows of 417 lattices, with the central lattice reserved for the central control rod. The five tie rods are uniformly arranged at the eleventh row, while 35 fuel elements of ^{238}U are in the outermost circle. The remaining 376 lattices are for fuel elements, shown in Fig. 3.2.

UAl_4 is used as the fuel meat with a density of 3.403 g/cm^3 and dimensions of 4.0 mm×250 mm. ^{235}U enrichment is 90.3%. The cladding material is aluminium alloy with wall thickness of 0.5 mm and 270 mm in length. End plugs of 11 mm and 9 mm are placed at the top and bottom, respectively.

The central control rod consists of: 1) a guide tube with 9 mm ID, 12 mm OD and 278 mm length; 2) a cadmium rod with 3.7 mm outer diameter and 290 mm length; and 3) a stainless steel tube with 5 mm outer diameter, 0.5 mm wall thickness, and 450 mm total length.

The fuel cage has a diameter of 242 mm and a height of 263 mm. Its top and lower core plates are fabricated from an aluminium alloy, with thickness of 3.5 mm at the top and 5 mm at the lower core plate.

3.2.1.2. Side beryllium reflector

The dimensions are 242 mm ID, 440 mm OD and 260 mm in height.

3.2.1.3. Bottom beryllium reflector

The dimensions are 340 mm in diameter and 50 mm in thickness, with a central hole 20 mm in diameter.

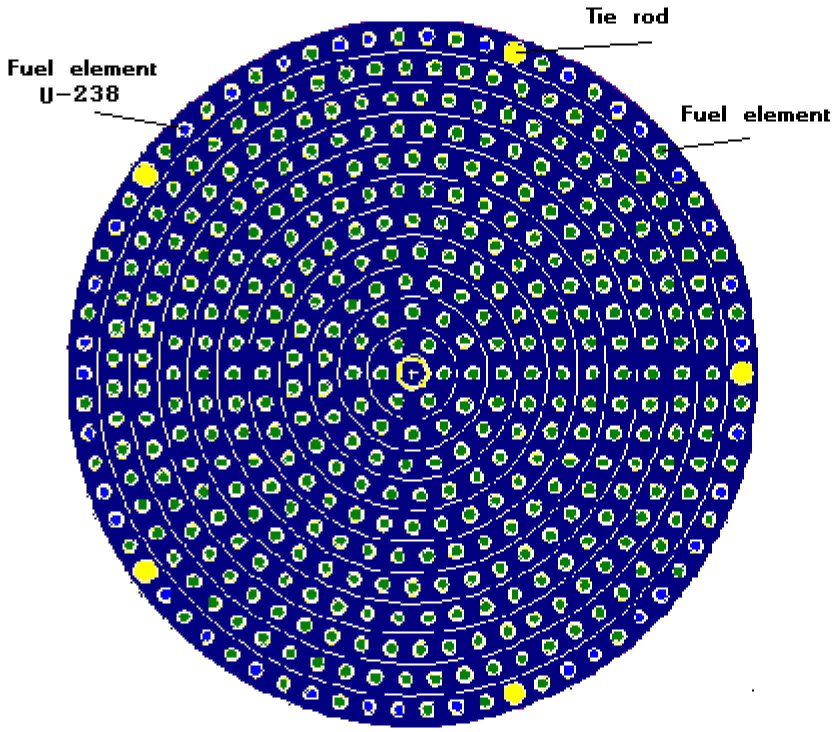

FIG. 3.2. The fuel element arrangement (Courtesy of China Institute of Atomic Energy (CIAE), China).

3.2.1.4. *Top beryllium reflector*

The aluminium alloy tray for the top beryllium reflector has an ID of 266 mm, an OD of 270 mm, a height of 115 mm, and a bottom thickness of 2 mm.

The dimensions of the top beryllium reflector are 265 mm in diameter, 20 mm hole diameter and 109.5 mm in total thickness. There are no top beryllium reflectors at initial loading.

3.2.1.5. *Irradiation sites*

There are five inner irradiation sites, uniformly and vertically arranged locations in the side beryllium reflector at a radius of 170 mm. The irradiation tube, fit for rabbit samples, penetrates the irradiation site at a depth of 190 mm. The outer thimble of the irradiation tube has an outer diameter of 32 mm and an ID of 29 mm, while the inner thimble is 22 mm in OD and 19 mm in ID.

There are five outer irradiation sites external to the side reflector, uniformly and vertically arranged at a radius of 250 mm. The insertion depth is 190 mm. The outer thimble has an OD of 42 mm and an ID of 39 mm, while the inner thimble OD is 34 mm and 31.0 mm ID.

3.2.1.6. *Five ionization chamber tubes*

The five ionization chamber tubes are arranged in the same circle with a radius of 255 mm. The OD of the tube is 56.0 mm, and the ID is 52.0 mm.

TABLE 3.1. THE MAIN PARAMETERS OF THE MNSR IAE CORE

Fuel type	HEU	LEU
Fuel material	UAl_4	UO_2
Enrichment of ^{235}U (%)	90.3	12.5
Density of meat (g/cm^3)	3.403	10.6
Meat diameter (mm)	4.0	4.0
Fuel meat length (mm)	250	250
Cladding material	Al	Zr-4
Cladding diameter (mm)	5.0	5.0
Number of fuel rods	376	362
Number of dummy elements	35	49
Central control rod guide tube		
Inner diameter (mm)	9	9
Outer diameter (mm)	12	12
Length (mm)	278	278
Central control rod		
Cd rod outer diameter (mm)	3.7	3.7
Length (mm)	290	290
External Cd rod stainless steel tube		
Outer diameter (mm)	5	5
Wall thickness (mm)	0.5	0.5
Length (mm)	450	450
Irradiation sites		
Inner irradiation sites	5	5
Outer irradiation sites	5	5
Side Be reflector		
Inner diameter (mm)	242	242
Outer diameter (mm)	440	440
Height (mm)	260	260
Bottom Be reflector		
Diameter (mm)	340	340
Thickness (mm)	50	50
Top Be reflector		
Diameter (mm)	265	265
Total thickness (mm)	109.5	109.5

3.2.2. Critical assembly for MNSR-SZ

3.2.2.1. Critical assembly

The critical assembly includes the core and side bottom and top beryllium reflectors as shown in Figs 3.3–3.4 and Table 3.2.

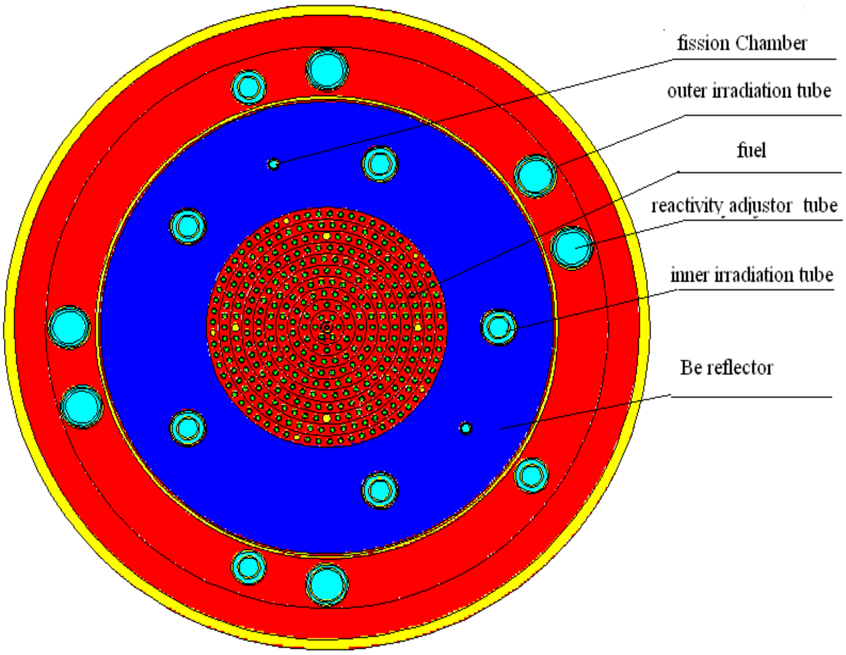

FIG. 3.3. The MNSR-SZ critical assembly geometric diagram in x–y plane from MCNP (Courtesy of China Institute of Atomic Energy (CIAE), China).

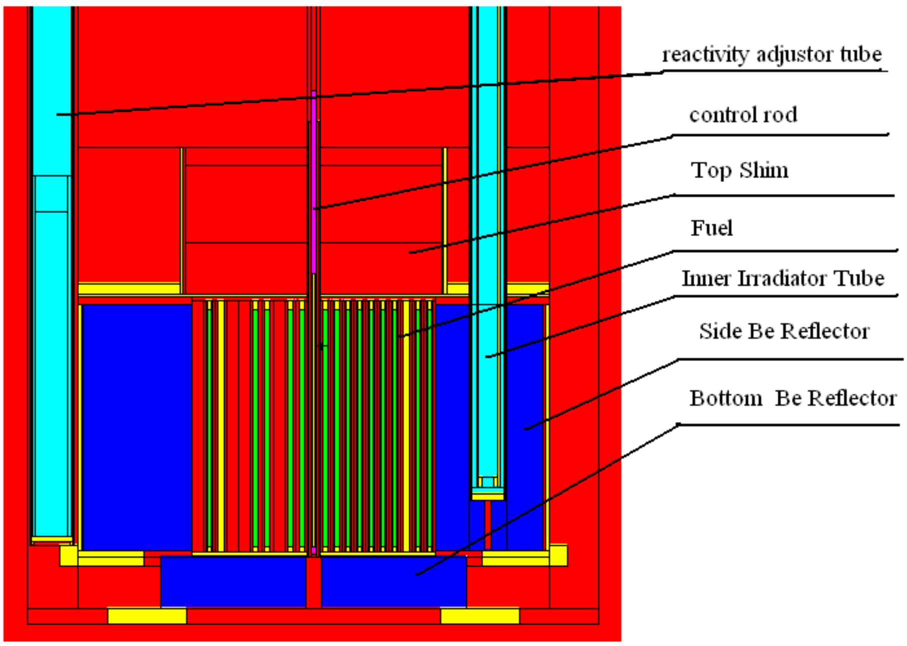

FIG. 3.4. The MNSR-SZ critical assembly geometric diagram in x–z plane from MCNP (Courtesy of China Institute of Atomic Energy (CIAE), China).

3.2.2.2. *Reactor core*

The upper and lower grid plates of the fuel cage are linked by four tie rods. Concentrically arranged around the core are 10 rows of 351 lattices. The central lattice is reserved for the central control rod. The four tie rods are uniformly arranged at the eighth row. In the outermost circle are five dummy rods. The remaining 345 lattices are for fuel elements, as shown in Fig. 3.5.

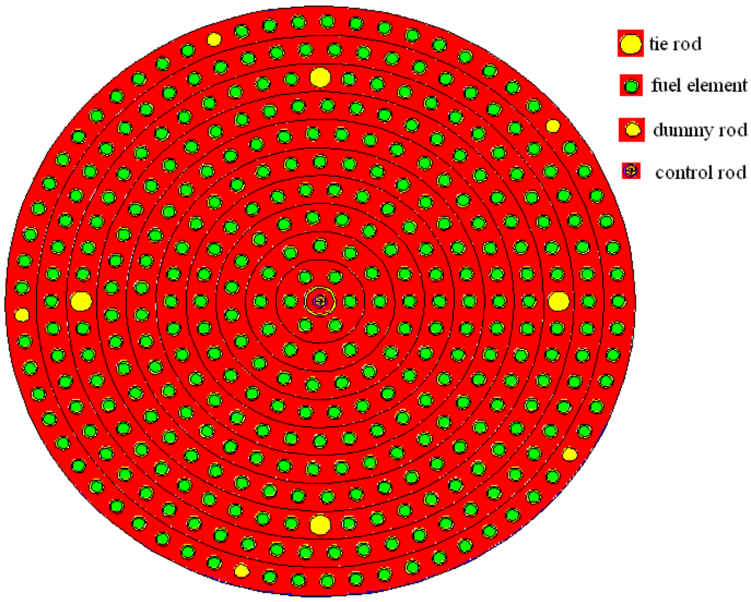

FIG. 3.5. The MNSR-SZ fuel element arrangement (Courtesy of China Institute of Atomic Energy (CIAE), China).

UAl_4 is used as the fuel meat with a density of 3.456 g/cm^3, and its dimensions are 4.3 mm×230 mm. The fuel is enriched to 90.2% ^{235}U. The cladding material is an aluminium alloy with a thickness of 0.6 mm, and length of 248 mm. A 9 mm end plug is at each end.

The central control rod consists of: 1) a guide tube of 9 mm ID, 12 mm OD and 258 mm in length; 2) a cadmium tube with an OD of 3.9 mm, an ID of 1.9 mm and a length of 266 mm; an Al rod inside the cadmium tube of dimensions 1.9×290 mm; and 3) an exterior stainless steel tube with a 5 mm outer diameter, 0.5 mm wall thickness and a total length of 450 mm.

The fuel cage has a diameter of 230 mm and a height of 241 mm. The top core and lower core plates are made of an aluminium alloy with a top thickness of 3 mm, and a lower thickness of 5 mm.

3.2.2.3. *Side beryllium reflector*

The side beryllium reflector ID is 231 mm, the OD is 435 mm, and the height is 238.5 mm.

3.2.2.4. *Bottom beryllium reflector*

The bottom beryllium reflector is 290 mm in diameter, 50 mm in thickness, with a central hole 20 mm in diameter.

The distance between the upper surface of the bottom beryllium reflector and the lower surface of the side beryllium reflector is 6 mm, which is the inlet orifice.

3.2.2.5. *Top beryllium reflector*

The aluminium alloy tray for the top beryllium reflector has an ID of 246 mm, OD of 252 mm, height of 145 mm, and bottom thickness of 2 mm.

The distance between the bottom surface of the tray and the upper surface of the side beryllium reflector is 7.5 mm, which is the outlet orifice.

The top beryllium reflectors are 243 mm in diameter, 20 mm in hole diameter and 109.5 mm in total thickness. At initial loading there are no top beryllium reflectors.

3.2.2.6. *Irradiation sites*

There are five inner irradiation positions uniformly and vertically arranged in the side beryllium reflector at a radius of 165 mm from the reactor centre. The irradiation rabbit tube penetrates the irradiation site at a depth of 190 mm. The OD of the outer thimble of the irradiation tube is 34 mm, and of the ID is 31. The inner thimble has an OD of 22 mm and an ID of 19 mm.

Five outer irradiation sites are uniformly and vertically arranged outside the side beryllium reflector, at a radius of 240 mm for the larger rabbit tube and 235 mm for the smaller rabbit tube. The insertion depth is 190 mm.

The larger rabbit tube is comprised of an aluminium alloy. The OD of the outer thimble is 42 mm and of the ID 39 mm, while the inner thimble has an OD of 34 mm and an ID of 31 mm.

3.2.2.7. *Four reactivity regulator tubes*

Four reactivity regulator tubes are arranged in a circle at a radius of 240 mm. The OD of each tube is 42 mm, and the ID is 39 mm.

3.2.2.8. *Fission chamber tubes*

Two fission chamber tubes are arranged outside the side reflector at a radius of 165 mm. The insertion depth is 190 mm, and the OD is 10 mm and ID is 8 mm.

TABLE 3.2. THE MAIN PARAMETERS OF THE MNSR-SZ CORE

Fuel type	HEU	LEU
Fuel material	UAl_4	UO_2
Enrichment of ^{235}U (%)	90.2	12.5
Density of meat (g/cm^3)	3.456	10.6
Meat diameter (mm)	4.3	4.3
Fuel meat length (mm)	230	230
Cladding material	Al	Zr-4
Cladding diameter (mm)	5.5	5.5
Number of fuel rods	345	345
Number of dummy elements	5	5
Central control rod guide tube		
Inner diameter (mm)	9	9
Outer diameter (mm)	12	12
Length (mm)	258	258
Central control rod meat		
Cd rod outer diameter (mm)	3.9	3.9
Cd rod inner diameter (mm)	1.9	1.9
Length (mm)	266	266
External Cd rod stainless steel tube		
Outer diameter (mm)	5	5
Wall thickness (mm)	0.5	0.5
Length (mm)	450	450
Irradiation sites		
Inner irradiation sites	5	5
Outer irradiation sites	5	5
Side Be Reflector		
Inner diameter (mm)	231	231
Outer diameter (mm)	435	435
Height (mm)	238.5	238.5
Bottom Be reflector		
Diameter (mm)	290	290
Thickness (mm)	50	50
Top Be reflector		
Diameter (mm)	243	243
Total thickness (mm)	109.5	109.5

3.3. CALCULATED RESULTS FOR THE HEU CORE

3.3.1. MNSR IAE

The core centre was set as the origin (0, 0, 0) for the design of the MCNP input card. The worth of the central control rod (see Fig. 3.6), the worth of the top beryllium reflectors (see Fig. 3.7), k_{eff} and dynamic features under step insertions of 3.6 mk excess reactivity (see Fig. 3.8) were calculated.

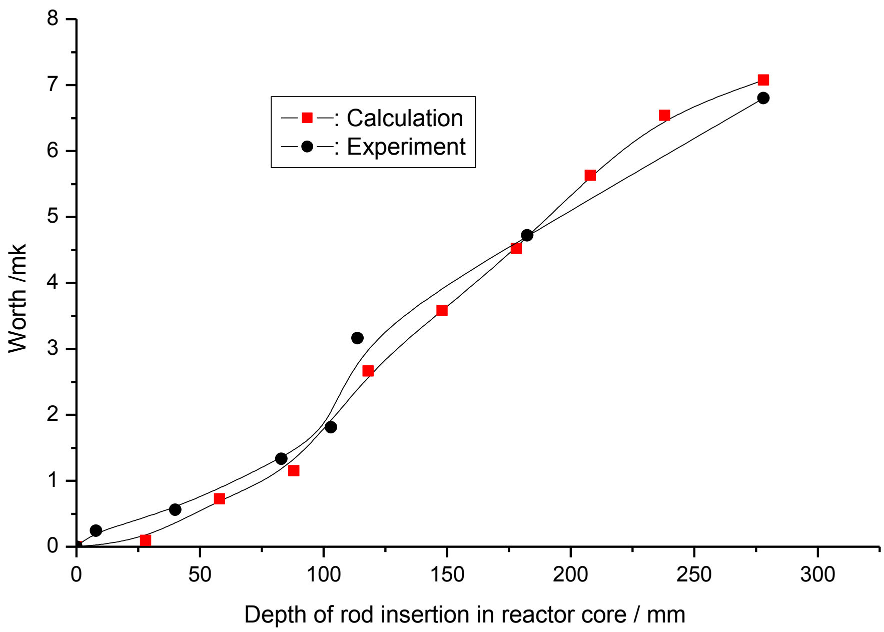

FIG. 3.6. The worth of the central control rod vs depth of insertion (Courtesy of China Institute of Atomic Energy (CIAE), China).

The values of k_{eff} calculated and derived from experiment are 1.00431±0.0005 and 1.00453 (modified), respectively. The total worths of the central control rod by calculation and experiment are 7.07 mk and 6.98 mk respectively. The total worths of the top beryllium reflectors by calculation and experiment are 15.07 mk and 14.45 mk respectively.

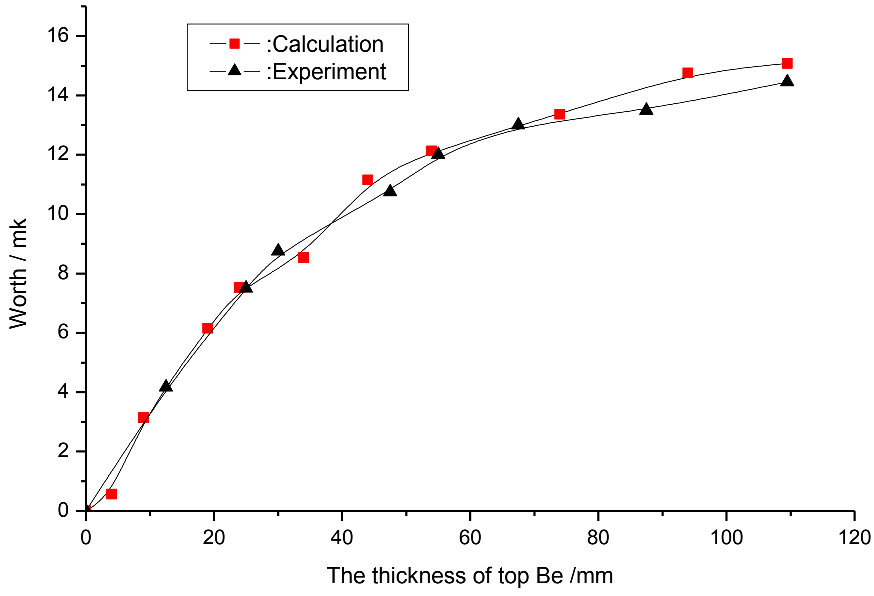

FIG. 3.7. The worth of the top beryllium reflectors vs thickness (Courtesy of China Institute of Atomic Energy (CIAE), China).

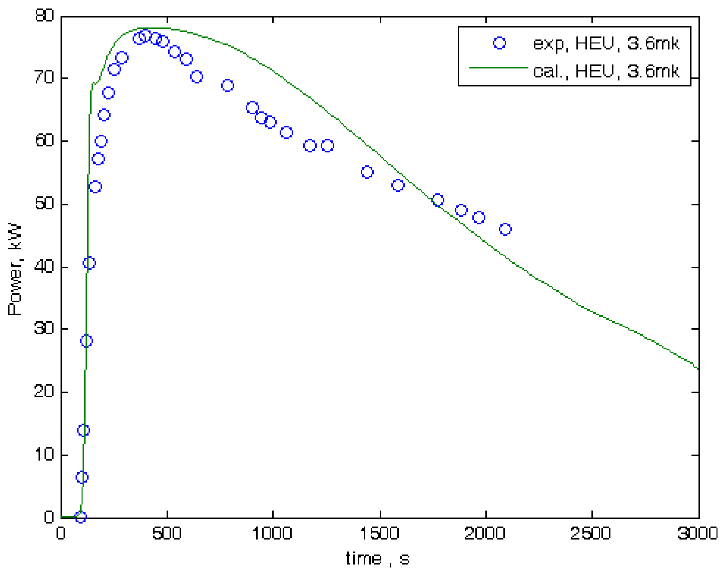

FIG. 3.8. Experimental (exp) and calculated (cal) power transient following 3.6 mk step increase in reactivity (Courtesy of China Institute of Atomic Energy (CIAE), China).

When a positive reactivity of 3.6 mk is added by step insertions, the maximum peak powers by calculation and experiment are 78.2 kW and 76.0 kW respectively. The corresponding temperature of the cladding at 78.2 kW is 92.5°C.

3.3.2. MNSR-SZ

The core centre was set as the origin (0, 0, 0) for the design of the MCNP input card. The worth of the central control rod (see Fig. 3.9), the worth of the top beryllium reflector (see Fig. 3.10), and k_{eff} and the dynamic features of step insertions of 3.51 mk reactivity (see Fig. 3.11) were calculated.

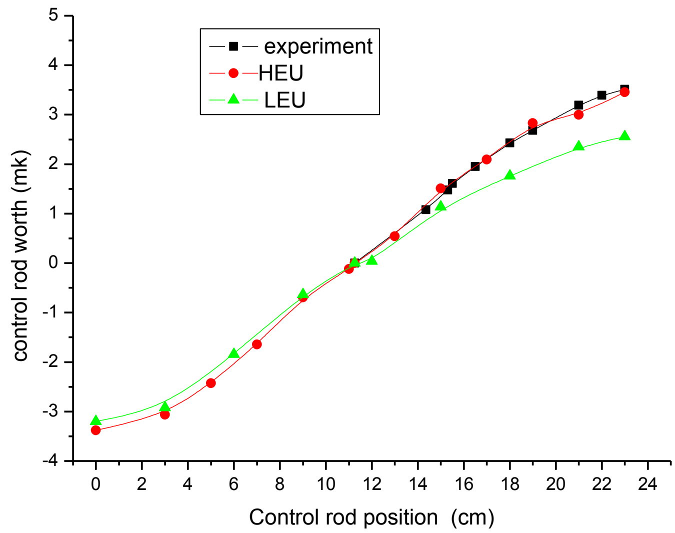

FIG. 3.9. The worth of the central control rod vs depth of insertion (Courtesy of China Institute of Atomic Energy (CIAE), China).

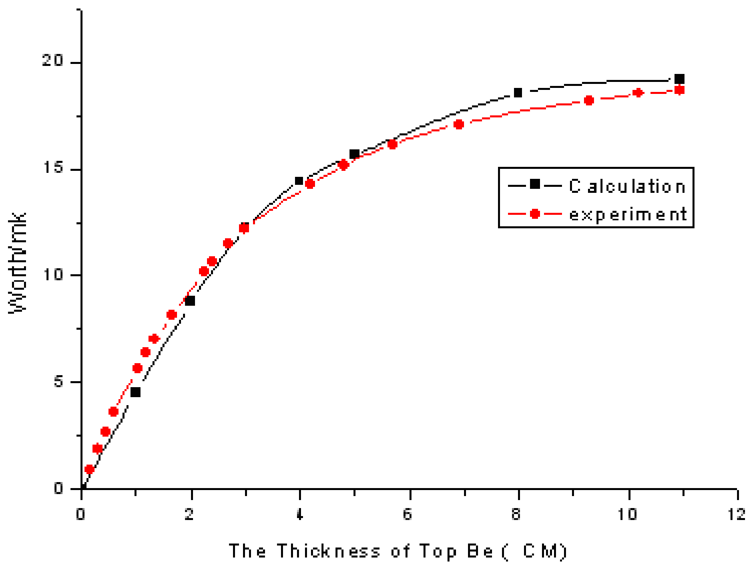

FIG. 3.10. The worth of the top Be reflectors vs thickness (Courtesy of China Institute of Atomic Energy (CIAE), China).

The calculated and experimental values of k_{eff} with the control rod at its critical position are 1.004557±0.0004 and 1.00113 (modified), respectively. The critical position of MNSR-SZ is 112.5 mm. The total worths of the central control rod by calculation and experiment are 8.0 mk and 7.1 mk respectively. The experimental worth of the control rod from the critical position to the top of the rod is 3.51 mk. The calculated result is 3.76 mk. The total worths of the top beryllium reflectors by calculation and experiment are 19.18 mk and 18.68 mk respectively.

When a positive reactivity of 3.51 mk is inserted into the reactor core in steps, with an initial temperature of 20°C, the maximum peak power is calculated to be 60.8 kW, and the corresponding maximum temperature of the cladding is 87.0°C.

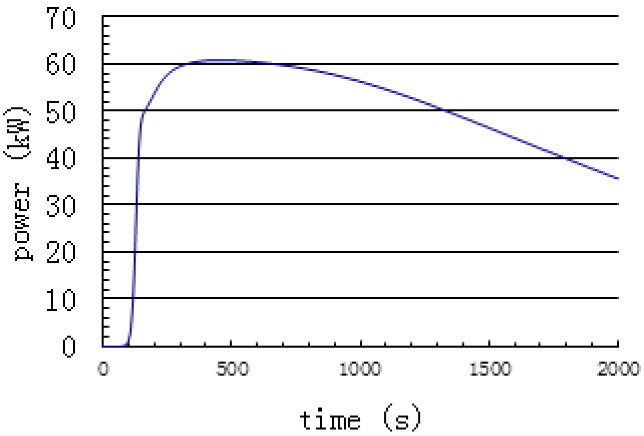

FIG. 3.11. Power transient following 3.51 mk step increase in reactivity (Courtesy of China Institute of Atomic Energy (CIAE), China).

3.4. LEU CORE CALCULATION RESULTS

3.4.1. Overview

Using the established MCNP model for the MNSR core with HEU, the physics parameters of the MNSR IAE and MNSR-SZ cores with LEU were calculated. These included clean cold excess reactivity, the worth of the control rod and top beryllium plate, shutdown margin and loading of fuel.

The LEU core has similar dimensions to the current HEU fuel pins. The pellet and cladding ODs are 4.3 mm and 5.5 mm respectively, and the ODs of the meat and cladding are 4.0 mm and 5.0 mm respectively for MNSR IAE fuel. UO_2 serves as the fuel meat and Zircaloy-4 as the cladding material.

3.4.2. MNSR-IAE

Tables 3.3, 3.4 and 3.5 list the characteristics for fuel, the central control rod, and the top beryllium plate. With unchanged core materials and dimensions, except for the substitution of HEU UAl_4 fuel meat with LEU of UO_2 fuel meat (12.5% ^{235}U) and Al alloy cladding with zircaloy cladding, the neutron flux distribution of the core (Fig. 3.12), neutron flux in the inner irradiation site, k_{eff}, worth of the control rod and dynamic features of step insertions of 4 mk reactivity (Fig. 3.13) were calculated.

TABLE 3.3. MNSR IAE CHARACTERISTICS OF FUEL OPTIONS

Fuel type	Enrichment (%)	Density of meat (g/cm^3)	Meat diameter (mm)	Cladding diameter (mm)	Number of fuel rods	k_{eff}
HEU	90.3	3.403	4.0	Al/5.0	376	1.0043
HEU	90.3	3.403	4.0	Al/5.0	376	1.0045[1]
LEU	12.5	10.6	4.0	Zircaloy-4/5.0	376/362	1.01738/1.00367

[1] Experiment results (modified)

TABLE 3.4. MNSR IAE CHARACTERISTICS OF THE CENTRAL CONTROL ROD

Fuel type	Cd rod outer diameter (mm)	Cd rod inner diameter (mm)	Cd length (mm)	External Cd rod stainless steel tube (mm)	Stainless steel tube thickness (mm)	Control rod total length (mm)	Control rod worth (mk)
HEU	3.7	1.9	290	5.0	0.5	450	7.07
HEU	3.7	1.9	290	5.0	0.5	450	6.98[1]
LEU	3.7	1.9	290	5.0	0.5	450	5.72

[1] Experiment results (modified)

TABLE 3.5. MNSR IAE CHARACTERISTICS OF THE TOP Be PLATE

Fuel type	Enrichment (%)	Diameter (mm)	Total thickness (mm)	k_{eff}
HEU	90.3	243	109.5	15.07
HEU	90.3	243	109.5	14.45[1]

[1] Experiment results (modified)

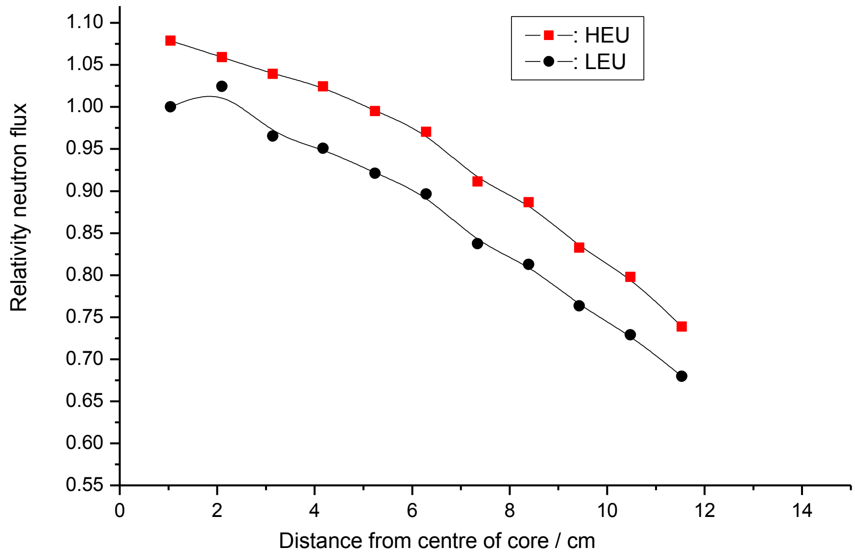

FIG. 3.12. The neutron flux distribution in the core for MNSR IAE with HEU and LEU (Courtesy of China Institute of Atomic Energy (CIAE), China).

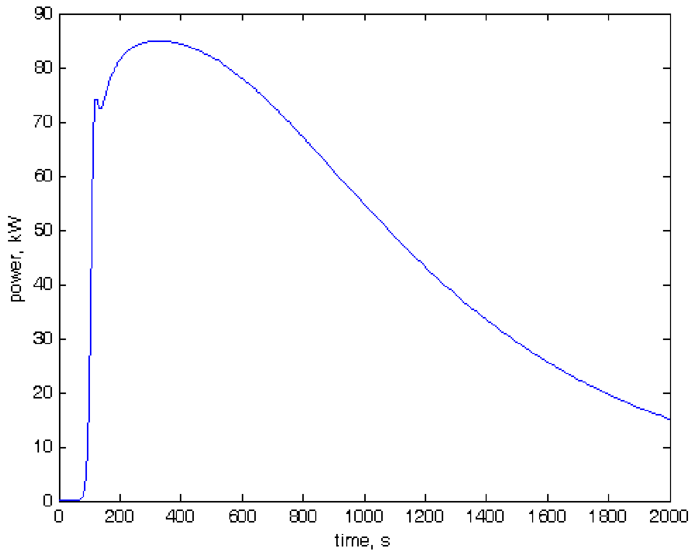

FIG. 3.13. Power transient following 4 mk step increase in reactivity for an LEU core (Courtesy of China Institute of Atomic Energy (CIAE), China).

For HEU and LEU cores, the neutron fluxes in the inner irradiation site for a given power are 4.4912×10^{-4} and 4.1596×10^{-4} neutron/cm^2.

For an LEU core, if k_{eff} is 1.01738, the fuel loading would be 376 fuel rods of ^{235}U and 35 fuel rods of ^{238}U; if k_{eff} is 1.00367, the fuel loading would be 362 fuel rods of ^{235}U and 49 fuel rods of ^{238}U. The worth of the central control rod is 5.7208 mk.

When a positive reactivity of 4 mk is inserted into the reactor core by steps, the maximum peak power is 85.5 kW at 330 s. The corresponding maximum temperature of the cladding is 97.3°C, as seen in Table 3.6.

TABLE 3.6. MNSR IAE CHARACTERISTICS OF REACTIVITY RELEASE

Fuel type	Enrichment (%)	Reactivity release (mk)	Peak time (s)	Max. peak power (kW)	Cladding temperature (°C)
HEU	90.3	3.6	—	78.2	92.5
HEU	90.3	3.6	—	76	
LEU	12.5	4	330	85.5	97.3

3.4.3. MNSR-SZ

Tables 3.7, 3.8 and 3.9 list the characteristics for fuel, the central control rod, and the top beryllium plate. With unchanged core materials and dimensions, except for substituting HEU of UAl_4 fuel meat with LEU of UO_2 fuel meat (12.5% of ^{235}U) and cladding of Al alloy with zircaloy, the neutron flux distribution of the core (Fig. 3.14), neutron flux in the inner irradiation site, k_{eff} and the dynamic features of step insertions of 4 mk reactivity (Figs 3.15 and 3.16) are calculated.

For HEU, the neutron flux is 5.26561×10^{-4} neutron/cm^2 in the inner irradiation site. For LEU, the neutron flux at the same inner irradiation position is 4.72904×10^{-4}. At the same power level, the neutron flux in the inner irradiation site for an LEU core is 11.35% lower than that with an HEU core.

For an LEU core with 345 fuel rods, equivalent to an HEU fuel load, if the enrichment of ^{235}U is 12.5%, the calculated k_{eff} is equal to 1.005476±0.0006.

At the same power level, the neutron flux in the inner irradiation site for an LEU core is 11.35% lower than that with an HEU core.

TABLE 3.7. MNSR-SZ CHARACTERISTICS OF FUEL OPTIONS

Fuel type	Enrichment (%)	Density of meat (g/cm^3)	Meat diameter (mm)	Cladding diameter (mm)	Number of fuel rods	k_{eff}
HEU	90.2	3.456	4.3	Al/5.5	345	1.0045
HEU	90.2	3.456	4.3	Al/5.5	345	1.0011[1]
LEU	12.5	10.6	4.3	Zircaloy-4/5.5	345	1.0054

[1] Experiment results (modified)

TABLE 3.8. MNSR-SZ CHARACTERISTICS OF THE CENTRAL CONTROL ROD

Fuel type	Cd rod outer diameter (mm)	Cd rod inner diameter (mm)	Cd length (mm)	External Cd rod stainless steel tube (mm)	Stainless steel tube thickness (mm)	Control rod total length (mm)	Control rod worth (mk)
HEU	3.9	1.9	266	5.0	0.5	450	7.999
HEU	3.9	1.9	266	5.0	0.5	450	7.1[1]
LEU	3.9	1.9	266	5.0	0.5	450	5.75

[1] Experiment results (modified)

TABLE 3.9. MNSR-SZ CHARACTERISTICS OF THE TOP Be PLATE

Fuel type	Enrichment (%)	Diameter (mm)	Total thickness (mm)	k_{eff}
HEU	90.3	243	109.5	19.18
HEU	90.3	243	109.5	18.68[1]

[1] Experiment results (modified)

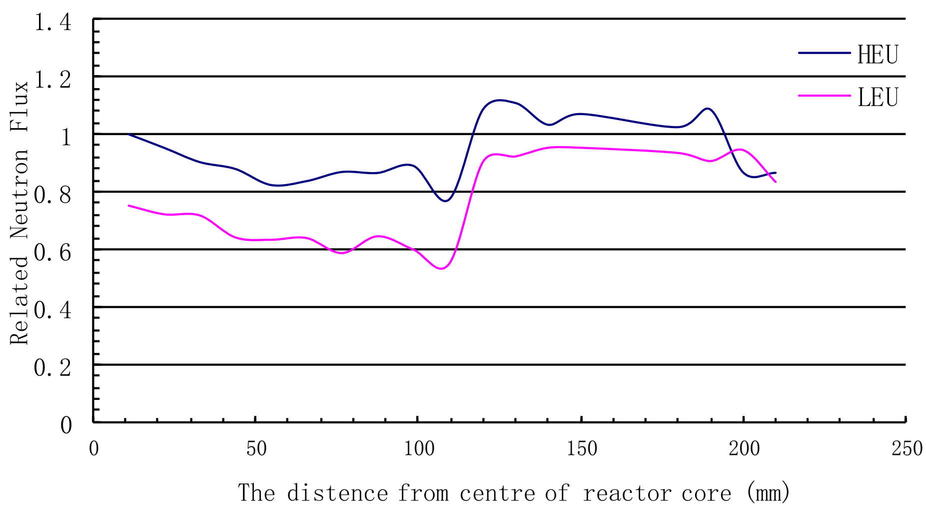

FIG. 3.14. The neutron flux distribution in the core for MNSR with HEU and LEU (Courtesy of China Institute of Atomic Energy (CIAE), China).

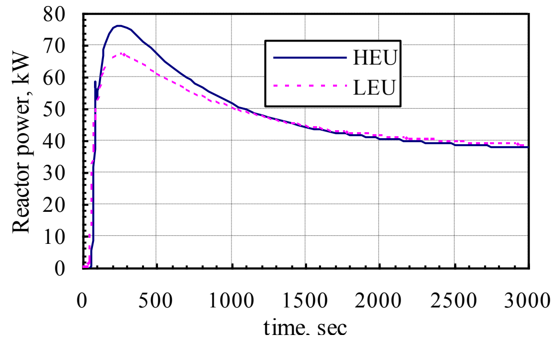

FIG. 3.15. Power transient following 4.0 mk step increase for MNSR with HEU and LEU core (Courtesy of China Institute of Atomic Energy (CIAE), China).

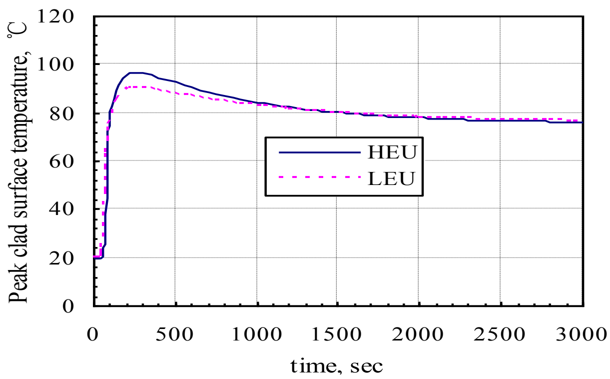

FIG. 3.16. Cladding surface temperature following 4.0 mk step increase for MNSR with HEU and LEU core (Courtesy of China Institute of Atomic Energy (CIAE), China).

When a positive reactivity of 4.01 mk is inserted to the reactor core by steps, with an initial temperature of 20°C, the maximum peak power is 66.5 kW, and the corresponding maximum temperature of the surface of the cladding is 90.2°C. This is listed in Table 3.10 below.

TABLE 3.10. MNSR-SZ CHARACTERISTICS OF REACTIVITY RELEASE

Fuel type	Enrichment (%)	Reactivity release (mk)	Peak time (s)	Max. peak power (kW)	Cladding temperature (°C)
HEU	90.3	3.51	20	60.8	87.0
LEU	12.5	4.01	20	66.5	90.2

3.5. RADIOLOGICAL CONSEQUENCE ANALYSIS

3.5.1. DBA

3.5.1.1. Accident scenario

The accident begins with a hole in one fuel pin due to pit corrosion. Gaseous fission products are released to the reactor water and accumulate at the top of the reactor vessel. The fission products are released to the environment without any retention through the operation of the gas purge system.

3.5.1.2. Calculation assumptions

In the dose release calculation, the following assumptions are proposed:

a) Release factor from pitted fuel:
- Inert gases are 0.03;
- ^{3}H and I are 0.02 each;
- Cs is 0.03; and
- Other elements can be ignored.

b) Release factor from the reactor water:
- Inert gases are 1;
- I isotopes are 5×10^{-4};
- Cs is 1×10^{-4}; and
- ^{3}H is 0.1

The following formula is used for nuclide release:

$$Q = Q_0 k_1 k_2 e^{-\lambda t} \tag{3.1}$$

where
- Q is the nuclide release in DBA (Bq);
- Q_0 is the assumed amount of fission products when accident happened (Bq);
- k_1 is the release factor from the broken fuel pin;
- k_2 is the release factor from the reactor water;
- λ is the nuclide decay factor (day^{-1});
- t is the time from the beginning of the hole, to fission product release (day).

3.5.1.3. Release

Using the above mentioned calculation formula, the characteristics of the release due to a DBA is listed in Table 3.11.

TABLE 3.11. RELEASE DUE TO A DBA

Nuclide	Q_0 (Bq)	k_1	k_2	Q (Bq)
^{85}Kr	4.48×10^7	0.03	1	1.34×10^6
^{85}mKr	3.35×10^3	0.03	1	1.01×10^2
^{88}Kr	2.62	0.03	1	∼0
^{131}I	1.68×10^9	0.02	5×10^{-4}	1.68×10^4
^{133}I	5.21×10^8	0.02	5×10^{-4}	5.21×10^3
^{131m}Xe	7.19×10^7	0.03	1	2.16×10^6
^{133}Xe	3.89×10^9	0.03	1	1.16×10^8
^{133m}Xe	8.96×10^7	0.03	1	2.69×10^6
^{135}Xe	5.24×10^6	0.03	1	1.57×10^5
^{135m}Xe	2.09×10^3	0.03	1	6.27×10^1
^{134}Cs	2.30×10^6	0.03	10^{-4}	6.9
^{137}Cs	9.33×10^8	0.03	10^{-4}	2.80×10^3
^{91}Sr	2.25×10^7	—	—	0
^{95}Zr	4.64×10^9	—	—	0
^{99m}Tc	4.17×10^9	—	—	0
^{103}Ru	2.04×10^9	—	—	0
^{127}Te	1.04×10^8	—	—	0
^{3}H	1.23×10^9	0.02	0.1	2.46×10^6

3.5.2. BDBA

3.5.2.1. Accident scenario

The reactor is operated for 10 years, and subsequently shut-down for one month. The BDBA occurs during unloading of the fuel cage, when all fuel pins are found to be broken and all gas fission products are released to the environment.

3.5.2.2. Calculation assumptions

In the dose release calculation, the following assumptions are proposed: all fuel rods are broken, and all gas fission products are released to the environment, within 100 m of the accident location.

The following formula is used for nuclide release:

$$Q = Q_0 k_1 k_2 k_3 e^{-\lambda t} \tag{3.2}$$

where

Q is the nuclide release in a DBA (Bq);

Q_0 is the assumption of the fission products when the accident happens (Bq);

k_1 is the release factor from the broken fuel;

k_2 is the release factor from the reactor water;
k_3 is the percentage of broken fuel rods (%);
λ is the nuclide decay factor (day^{-1}); and
t is the time from the reactor shutdown to the unloading operation (day).

3.5.2.3. Release

Using the above mentioned calculation formula, the characteristics of the release due to the BDBA is listed in Table 3.12.

TABLE 3.12. RELEASE DUE TO A BDBA

Nuclide	Q_0 (Bq)	k_1	k_2	k_3 (%)	Q (Bq)
^{3}H	1.22×10^{9}	0.02	0.1	100	2.44×10^{6}
^{83m}Kr	~0	0.03	1	100	~0
^{85}Kr	3.26×10^{10}	0.03	1	100	9.78×10^{8}
^{88}Kr	~0	0.03	1	100	~0
^{131}I	7.16×10^{10}	0.02	5×10^{-4}	100	7.16×10^{5}
^{133}I	2.20×10^{2}	0.02	5×10^{-4}	100	~0
^{135}I	~0	0.03	5×10^{-4}	100	~0
^{131m}Xe	3.59×10^{9}	0.03	1	100	1.08×10^{8}
^{133}Xe	5.57×10^{10}	0.03	1	100	1.67×10^{9}
^{133m}Xe	1.21×10^{7}	0.03	1	100	3.63×10^{5}
^{135}Xe	~0	0.03	1	100	~0
^{135m}Xe	~0	0.03	1	100	~0
^{137}Cs	3.21×10^{11}	0.03	10^{-4}	100	9.63×10^{5}
^{134}Cs	7.70×10^{8}	0.03	10^{-4}	100	2.31×10^{3}
^{95}Zr	6.35×10^{11}	—	—	100	0
^{99m}Tc	1.33×10^{9}	—	—	100	0
^{103}Ru	5.04×10^{11}	—	—	100	0
^{127}Te	5.49×10^{9}	—	—	100	0

3.5.3. Calculation results

For an MNSR, the supposed main accidents are leakage by one fuel pin (DBA), and an unloading operation accident (BDBA).

According to the above calculations, a pitted fuel pin accident could cause a maximum personal effective dose rate to the public of 1.65×10^{-5} mSv. The unloading operation accident could cause a maximum personal effective dose rate for the public of 9.92×10^{-4} mSv.

3.6. CONCLUSION

For an HEU core, the calculation results agree with the experimental results. Through the comparison of the calculation results both of HEU and LEU cores with unchanged core dimensions, UO_2 with an enrichment 12.5% ^{235}U can meet the requirements of critical mass and excess reactivity.

At the same power level, the neutron flux at an inner irradiation site for a generic LEU core is approximately 10% lower than that for the MNSR-IAE HEU core or MNSR-SZ HEU core. The power therefore for the LEU core should be around 10% higher in order to retain a neutron flux of 1.0×10^{12} $cm^{-2}s^{-1}$ at the inner irradiation site. However, for either MNSR with the LEU core, a neutron flux of approximately 8.0×10^{11} $cm^{-2}s^{-1}$ at an inner irradiation site is enough for NAA, and a power level of 30 kW for an LEU-fuelled MNSR is therefore acceptable.

An MNSR with an LEU core also maintains inherent safety upon a step insertion of excess reactivity of 4 mk in total.

For the MNSR DBA and BDBA, the environmental effect is small, as the dose rate to the public is acceptable, and an MNSR with an LEU core also remains safe.

4. ANALYSIS FOR CORE CONVERSION OF GHANA RESEARCH REACTOR-1 FROM HEU TO LEU FUEL

4.1. INTRODUCTION

The Ghana Research Reactor-1 (GHARR-1) is a commercial version of the MNSR and belongs to the class of tank-in-pool type reactors [4.1]. It is under-moderated with an H/U atom ratio of 197. This ratio will reduce to about 145 due the conversion of the fuel from HEU to LEU. Thermal power is rated at 30 kW with a corresponding peak thermal neutron flux of 1.0×10^{12} cm^{-2}s^{-1}. To maintain this flux, the thermal power of the LEU core must be increased to a nominal 34 kW. The cold clean excess reactivity of the fresh core is about 4 mk, which has been licensed and will be maintained. Cooling is achieved by natural convection using light water. Presently, the GHARR-1 core consists of a UAl alloyed HEU fuel assembly with fuel elements arranged in ten concentric rings about a central control rod guide tube that houses the reactor's only control rod. The control rod's reactivity worth is about -7 mk, providing a core shutdown margin of -3 mk. The small core has a low critical mass. However, its relatively large negative temperature coefficient of reactivity is capable of boosting its inherent safety properties [4.2]. The small size of the core facilitates neutron leakage and escape in both axial and radial directions. To minimize such losses and thereby conserve neutron economy, the core is heavily reflected on the side and underneath the fuel cage by a thick annulus and slab of beryllium material. Regulated shims of beryllium to the top tray can compensate for loss of reactivity due to axial neutron leakage.

GHARR-1 was obtained under a Project Supply Agreement between the IAEA, CIAE and the Government of Ghana in 1994 [4.3]. It began operation on 15 March 1995 and has since been used for NAA, experiments and personnel training in nuclear science and technology. The reactor fuel is enriched to 90.2%.

The objective of this study was to design an LEU core with similar operational capabilities as the original HEU core, and with acceptable safety margins under both normal and accident conditions. In order to provide comparisons between the proposed LEU core and the initial GHARR-1 HEU core, thorough analyses were performed for both cores. The proposed LEU core consists of UO_2 fuel elements clad in Zircaloy-4 alloy. The control element of the control rod material will remain unchanged, but the diameter of the absorber material will increase, leaving the diameter of the control rod unchanged.

In the following sections of the document, it is revealed that throughout the lifetime of the proposed LEU core:

- The shutdown margin meets technical specification limits;
- Reactivity coefficients meet required limits and are comparable to the existing HEU core;
- Fuel integrity is maintained under all operating conditions;
- Dose to the public from BDBA is below maximum permissible limits; and
- There will be no trade-off in the thermal neutron fluxes in the experimental channels. This will be achieved by increasing the power of the LEU core by 13%.

4.1.1. Reactor facility changes

Two facility changes are required for this conversion. The current UAl_4 HEU fuel elements will be replaced with UO_2 LEU fuel elements containing 88 wt% uranium, enriched to 12.5% ^{235}U. The dimensions of the LEU fuel elements are identical to the HEU fuel. In addition, the proposed LEU fuel has obtained approval from CIAE, the manufacturer of the MNSR. Table 4.3 provides a detailed description of the proposed LEU fuel. Also, the shutdown margin of the control rod will be improved by increasing the cadmium component.

4.1.2. Operation license and procedural changes

The GHARR-1 operating license must be amended to allow possession of both the LEU and HEU fuel inventories during conversion, as stated in section 17.3 of the facility's Safety Analysis Report (SAR) [4.2]. Significant proposed changes to the technical specifications include:

— Changing all references to fuel type from UAl_4 in Al matrix to UO_2 fuel;
— Review of the characteristics of the central control rod; and
— Review of provisions regulating the amount of reactor fuel to be held by NNRI during the conversion exercise.

4.1.3. Characteristics of reference GHARR-1 LEU core

The GHARR-1 LEU core base model was established from the reference HEU core base model.

The core layout was kept the same. Only the components within the fuel cage (fuel pins, dummy pins, tie rods, and top and bottom grid plates) and the control rod design were different between these two reference models. All other core and reactor structure components were kept the same. A control rod design with a larger outer diameter for the cadmium absorber was also implemented for the LEU core as shown in Table 4.1. Uranium isotopes used in the generic models are compared in Table 4.2. Comparison of key core parameters between the HEU and LEU models are shown in Table 4.3.

TABLE 4.1. CONTROL ROD AND GUIDE TUBE DESIGN PARAMETERS IN MNSR MODELS

Parameter	HEU (mm)	LEU (mm)
Outer diameter of cadmium	3.9	4.5
Thickness of stainless steel cladding	0.5	0.5
Thickness of water gap	2.0	1.7
Thickness of guide tube	1.5	1.5
Material of guide tube	LT-21	Zircaloy-4

TABLE 4.2. COMPARISON OF REFERENCE GHARR-1 HEU AND LEU FUEL URANIUM ISOTOPES

Uranium isotope	HEU (wt%)	LEU (wt%)
^{235}U	90.2	12.5
^{238}U	8.3	87.65
^{234}U	1.0	0.2
^{236}U	0.5	0.25
Total	100.0	100.0

TABLE 4.3. COMPARISON OF KEY PARAMETERS FOR REFERENCE GHARR-1 HEU AND LEU CORES

Key parameters	HEU	LEU
Fuel meat	UAl_4	UO_2
^{235}U total core loading (g)	~998	~1358
^{235}U enrichment (wt%)	90.2	12.5
^{234}U content (wt%)	1.0	0.2
^{236}U content (wt%)	0.5	0.25
Density of meat (g/cm^3)	3.456	10.6
Meat diameter (mm)	4.3	4.3
Cladding diameter (mm)	5.5	5.5
Thickness of He gap (mm)	None	0.05
Cladding material	Al-303-1	Zircaloy-4
Number of fuel rods	344	348
Material for grid plates	LT-21	Zircaloy-4
Top shim tray (not modelled)	LT-21	LT-21
Number of dummy elements	6	2
Material for dummy elements	Al-303-1	Zircaloy-4
Number of tie rods	4	4
Material for tie rods	Al-303-1	Zircaloy-4
Adjuster guide tubes	4	4

In an actual LEU MNSR, adjustments to the excess reactivity are likely to be required to compensate for differences between the reactor design data and the manufacturer's as-built materials and geometry data. Some of the most important of these differences are in the as-built ^{235}U, ^{234}U and ^{236}U loadings, and the as-built impurity levels in the fuel meat. The adjuster rods would be made available to make these adjustments, depending on the results of the low power experiments that are planned at CIAE before the reactor is shipped to the customer's site, as well as choices made by the customer.

The results of the design, safety, and accident analyses performed for the conversion of the GHARR-1 from the use of HEU to LEU is highlighted in this report

4.2. CORE CONVERSION ANALYSES

GHARR-1 is a 30 kW(th) MNSR located at Kwabenya, a village in the Greater Accra Region of Accra, Ghana. GHARR-1 changes required for this conversion include the replacement of the current HEU fuel with the LEU fuel of 12.5% enrichment, and increasing the diameter of the cadmium control rod absorber. Furthermore, the number of fuel pins may be increased if necessary in order to obtain the licensed core excess reactivity.

4.2.1. Neutronics analyses

4.2.1.1. Method of analysis

The 3-D GHARR-1 Monte Carlo model for both HEU and LEU were simulated to estimate some reactor physics parameters, such as nuclear criticality and core reactivities and neutron flux distribution in selected locations of the reactor. In particular, neutron transport simulations were performed for a fresh core (zero burnup). The GHARR-1 Monte Carlo model was further simulated for total control rod withdrawal and full insertion determine control rod worth and shutdown margins. Simulations were also performed for different positions of the control rod for the control rod calibration curve shown in Fig. 4.1. The radius of control rod for the LEU is slightly increased as proposed for the core conversion of MNSRs. The TOTNU total fission card in MCNP was utilized to simulate a fresh core without the delay neutrons to estimate the delayed neutron fraction. The reactivity coefficients were estimated for the fuel as well as the moderator by variation of different parameters in the input decks. The reactivity worth of various components stated in the HEU SAR were also re-evaluated for the HEU core and estimated for the LEU core as well.

The S(αβ) thermal neutron scattering laws for moderators were applied in the GHARR-1 Monte Carlo model to treat thermal neutron scattering in beryllium and hydrogen in light water for the reflector material and water regions respectively.

4.2.1.2. Results and discussion

(a) Criticality results

The criticality results for both the HEU and LEU are shown in Table 4.4. The multiplication factors, k_{eff}, and (unsurprisingly) the reactivities are quite comparable with values stated in the HEU SAR. The delayed neutron fractions for the two cores as estimated by MCNP are 3.3% and 3.9% higher than the MNSR manufacturer's quoted value of 0.00808 [4.4] respectively. Nevertheless, the two compare well with the delayed neutron fraction of 0.00837 reported for NIRR-1 [4.5].

TABLE 4.4. COMPARISON OF CRITICALITY RESULTS FOR HEU AND LEU

Criticality result	HEU SAR	HEU	Sigma	LEU	Sigma
K_{eff} control rod completely withdrawn	—	1.00375	0.00005	1.00385	0.00004
K_{eff} control rod fully inserted	—	0.99680	0.00004	0.99714	0.00004
Core excess reactivity (mk)	4.0	3.74	0.05	3.84	0.04
Delayed neutron fraction β_{eff} ($\times 10^3$)	8.5	8.347	0.0641	8.395	0.0566
Prompt neutron lifetime Λ (s)	8.52×10^{-5}	8.46×10^{-5}	0.06×10^{-5}	7.39×10^{-5}	0.06×10^{-5}
Control rod worth, (mk)	6.80	6.95	0.018	6.74	0.017
Shutdown margin, (mk)	3.0	3.21	0.012	2.87	0.011

The design control rod worth of the reactor is 6.8 mk, and the shutdown margin is 3.0 mk for maintaining the reactor in safe shutdown conditions. The total cold excess reactivity to be compensated by the control rod is about 4.0 mk [4.2]. The MCNP calculation of the control rod worth is about 10.5% more for the HEU core. Both the HEU and LEU cores have shutdown margin close to 3 mk.

(b) Integral and differential control rod worth

The exact effect of control rods on reactivity can be determined experimentally. For example, a control rod can be withdrawn in small increments such as 1 cm, and the change in reactivity can be determined following each increment of withdrawal. By plotting the resulting reactivity versus the rod position, a graph obtained for both cores is shown in Fig. 4.1.

Differential control rod worth is the reactivity change per unit movement of a rod and is normally expressed as ρ/cm or δk/k/cm. The chart for the differential control rod worth is shown in Table 4.5 for both the HEU and LEU cores. Figure 4.1 depicts integral control rod worth over the full range of withdrawal. The integral control rod worth is the total reactivity worth of the rod at that particular degree of withdrawal, and is usually defined to be greatest when the rod is fully withdrawn. The integral rod worth at a given withdrawal is merely the summation of the entire differential rod worth up to that point of withdrawal. It is also the area under the differential rod worth curve at any given withdrawal position. The highest differential control rod worth occurred below the middle of the core.

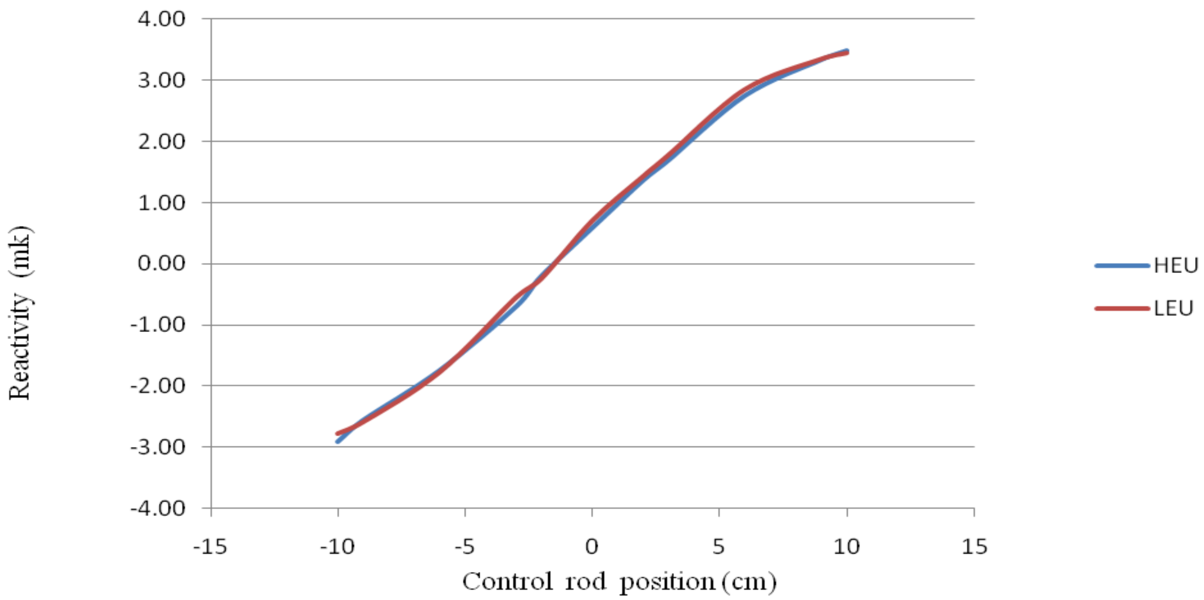

FIG. 4.1. The integral control rod curve (Courtesy of National Nuclear Research Institute (NNRI), Ghana).

TABLE 4.5. DIFFERENTIAL CONTROL ROD WORTH VALUES

Rod position (cm)	Differential reactivity (mk)	
	HEU	LEU
–10	0.3220	0.8754
–9	0.3519	0.0804
–6	0.8135	0.8135
–3	1.0425	1.2228
–2	0.5005	0.3403
0	0.7897	0.9195
2	0.8383	0.7583
3	0.2692	0.3190
6	1.0056	1.0750
9	0.7553	0.4969
10	0.1291	0.2085
12.4	0.4664	0.4764

(c) Flux distributions

Measurement of neutron flux and neutron energy spectrum parameters in the inner irradiation sites can be utilized to determine linearity, repeatability and stability of the neutron measurement system, which includes detectors and secondary instruments.

The LB1120 miniature fission chamber is employed as a neutron detector for the reactor. It is small and can be put into the side annulus. This detector could measure the linear absolute neutron flux over four to five decades with both gold and manganese foils [4.2].

The average flux distributions in the inner irradiation channels, outer irradiation channels and fission chambers for both HEU and LEU at 30 kW are shown in Figs 4.2–4.4. Figure 4.5 then compares the average flux distribution for LEU and HEU at nominal powers. The centre of the core is equidistant from the inner irradiation channels and the fission chamber used in measuring the neutron flux.

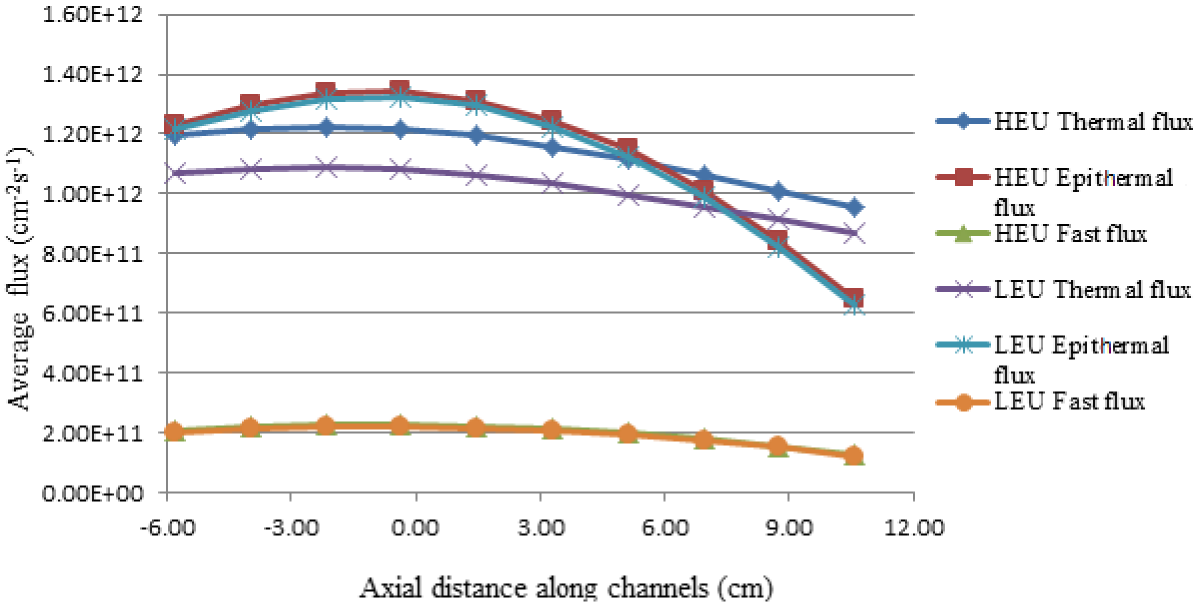

FIG. 4.2. Comparison of average flux distribution in inner irradiation channel at 30 kW (Courtesy of National Nuclear Research Institute (NNRI), Ghana).

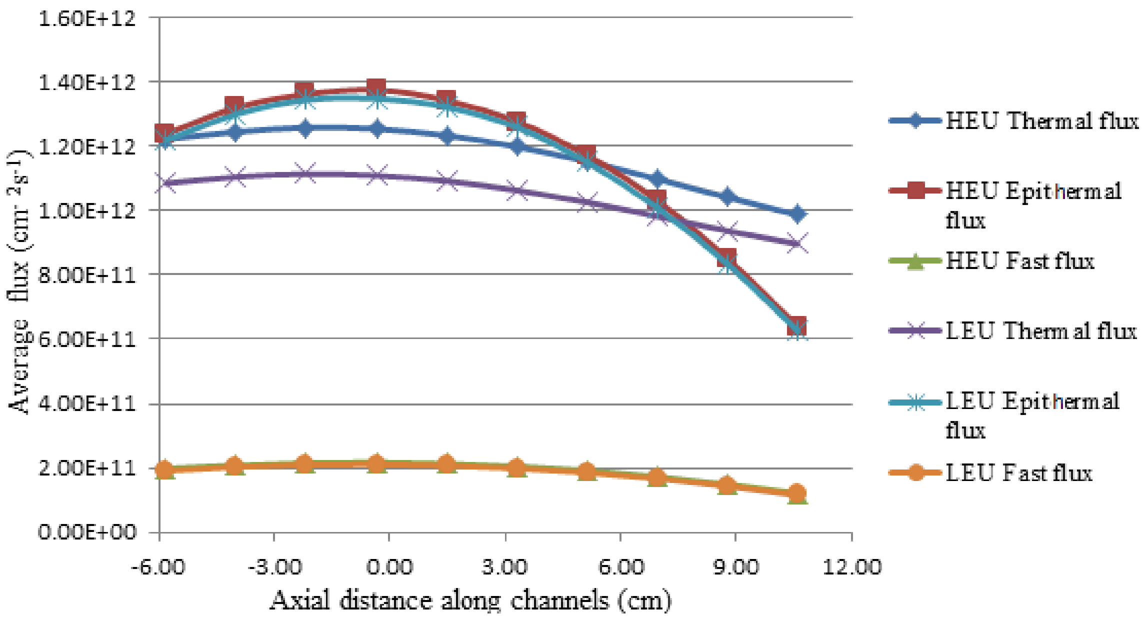

FIG. 4.3. Comparison of flux distribution in fission chamber at 30 kW (Courtesy of National Nuclear Research Institute (NNRI), Ghana).

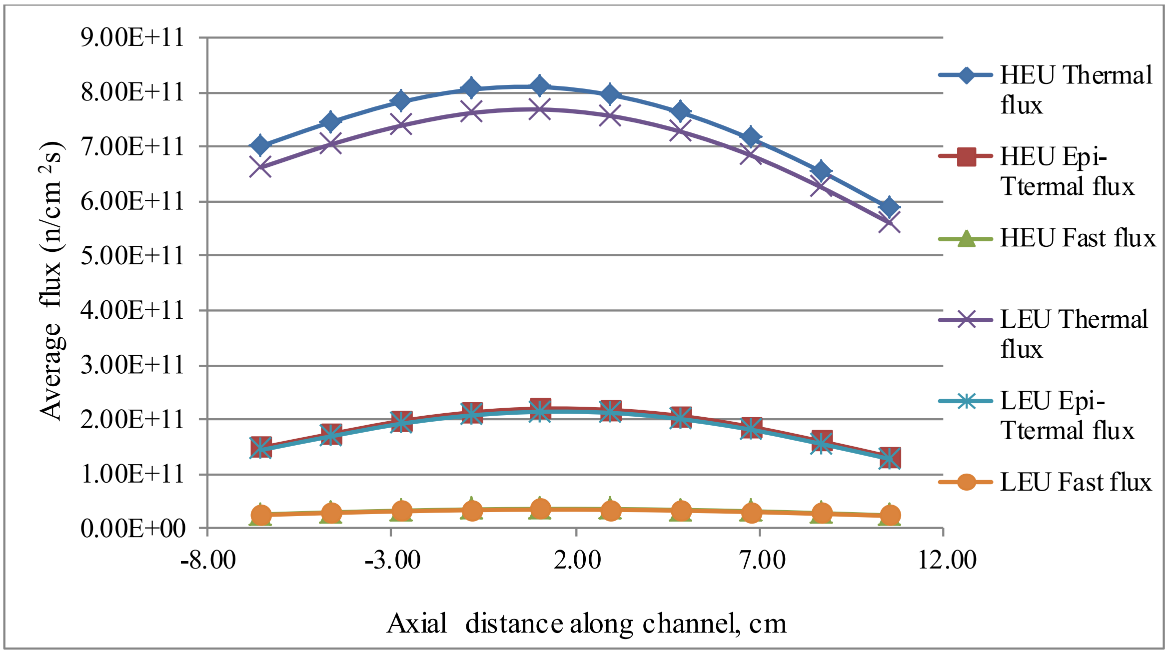

FIG. 4.4. Comparison of average flux distribution in outer irradiation channel at 30 kW (Courtesy of National Nuclear Research Institute (NNRI), Ghana).

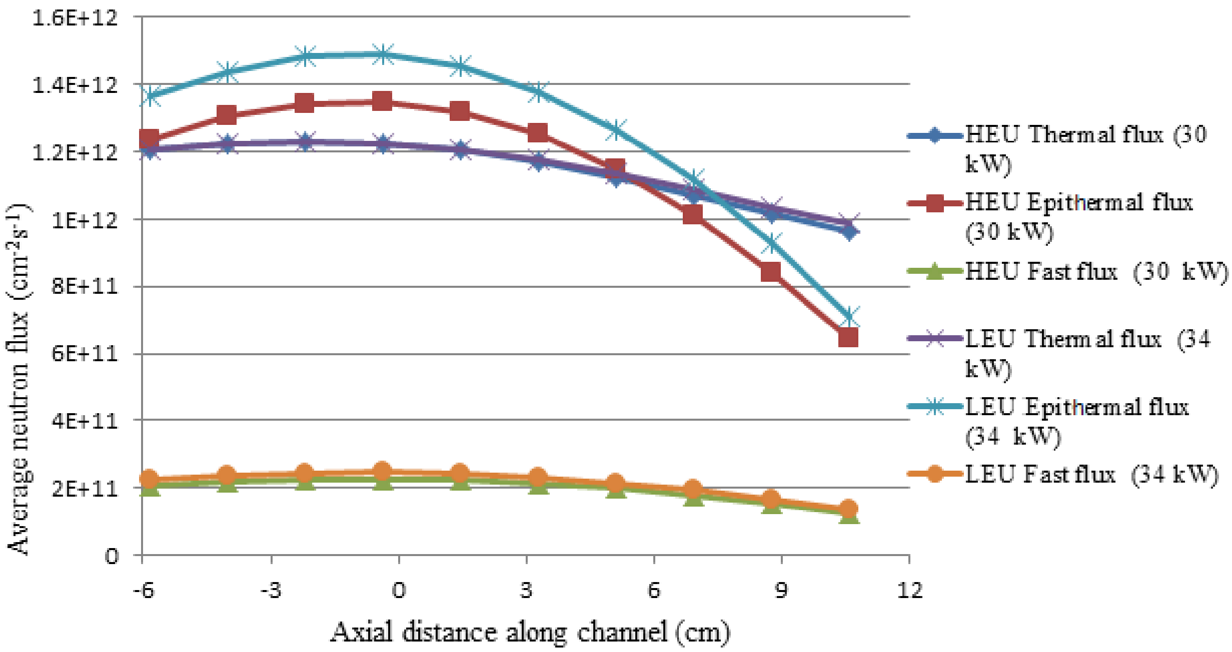

FIG. 4.5. Comparison of average flux distribution in inner irradiation channel at nominal powers (Courtesy of National Nuclear Research Institute (NNRI), Ghana).

To avoid compromising the thermal neutron flux, especially in the inner irradiation channel, the power of the LEU core is to be increased by 13%. This is to compensate for the fall in neutron flux at 30 kW. Based on the LEU to HEU ratio of the average thermal neutron flux in the inner irradiation channel at 30 kW, the power of LEU core is increased to 34 kW. This is to normalize the thermal neutron flux ratio in the inner irradiation channels to a unit; hence the two profiles of the thermal flux are almost superimposed as observed in Figure 3.5. The effects of power increase for the LEU core on the neutron fluxes in the fission chamber and outer irradiation channels are shown in Figs 4.6 and 4.7.

The peak fluxes in the inner irradiation channels are listed in Table 4.6. The decreases in the peak fluxes as a result of the core conversion are in the range of 10% to 13%, with an average of about 11%. This supports the increase in power of the LEU core by about 13% to compensate for the estimated decrease in neutron flux.

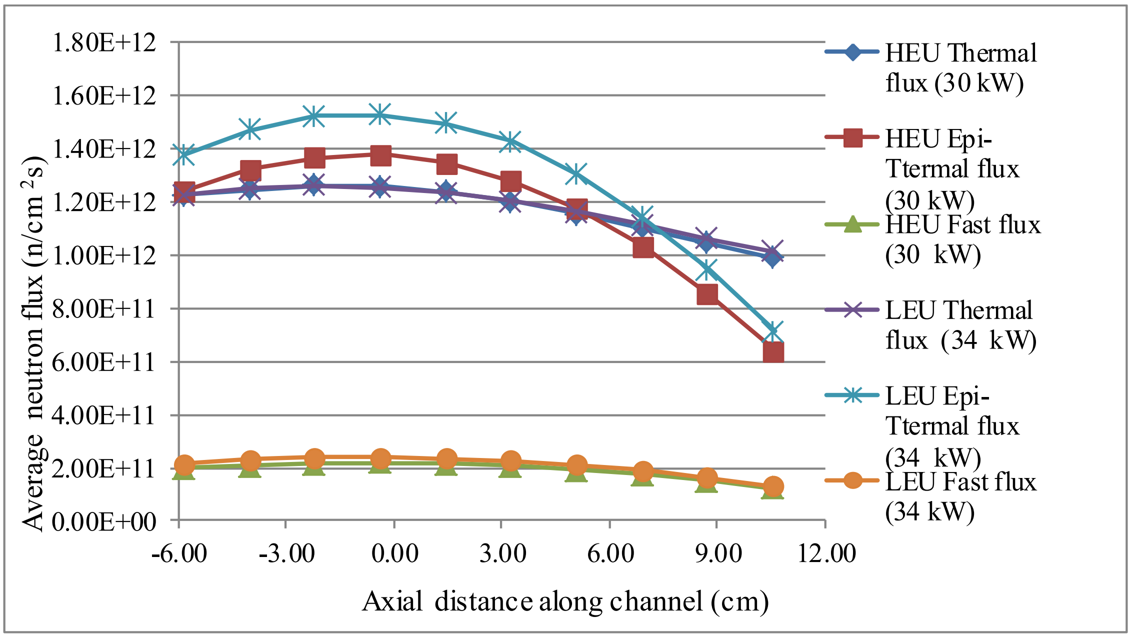

FIG. 4.6. Comparison of average flux distribution in fission chamber at nominal powers (Courtesy of National Nuclear Research Institute (NNRI), Ghana).

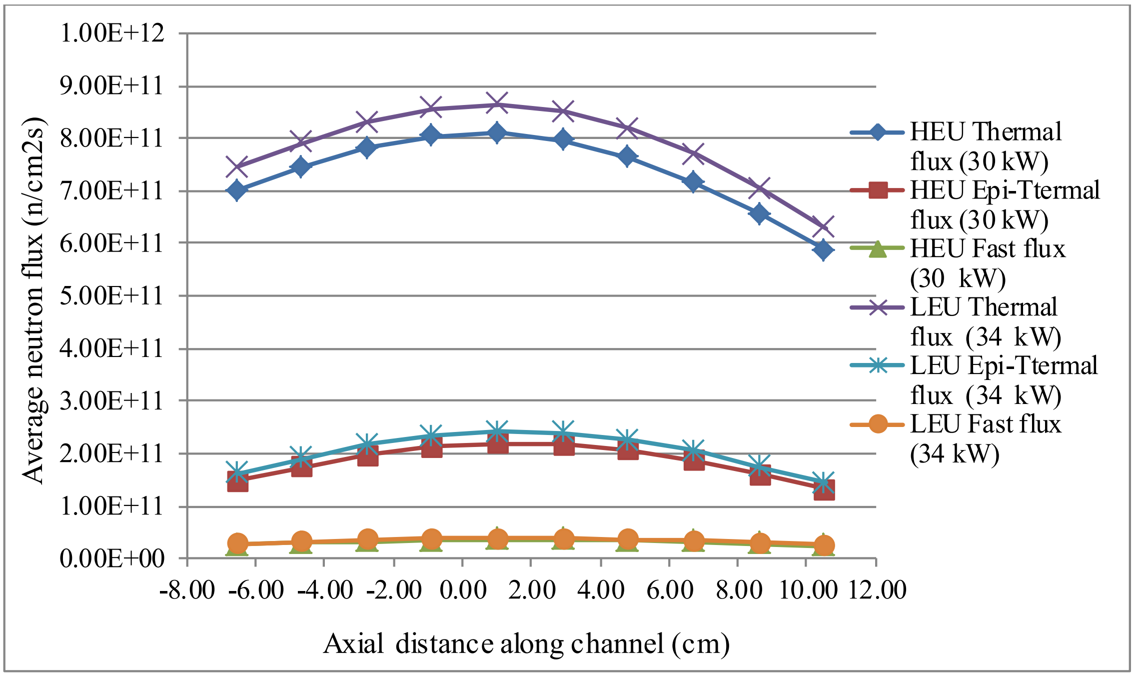

FIG. 4.7. Comparison of average flux distribution in outer irradiation channel at nominal powers (Courtesy of National Nuclear Research Institute (NNRI), Ghana).

TABLE 4.6. PEAK FLUX IN THE INNER IRRADIATION CHANNELS

Channels (MCNP)	HEU 30 kW ($\times10^{12}$ cm^{-2}s^{-1})	LEU 30 kW ($\times10^{12}$ cm^{-2}s^{-1})	LEU 34 kW ($\times10^{12}$ cm^{-2}s^{-1})
Cell 971	1.220 ± 0.0018	1.087 ± 0.0017	1.223 ± 0.0017
Cell 933	1.231 ± 0.0018	1.091 ± 0.0018	1.228 ± 0.0017
Cell 935	1.217 ± 0.0018	1.100 ± 0.0018	1.238 ± 0.0018
Cell 937	1.253 ± 0.0018	1.098 ± 0.0018	1.236 ± 0.0018
Cell 939	1.221 ± 0.0018	1.097 ± 0.0018	1.235 ± 0.0018
Average	1.228 ± 0.0006	1.095 ± 0.0018	1.232 ± 0.0018

The MCNP5/MCNPX code is capable of computing the axial power profiles of the fuel pins in the core. Comparison of peak power profile for the two cores is shown in Fig. 4.8; the axial power profile of the LEU core at 34 kW is also included. The axial power profiles are important for thermal-hydraulic analyses, and thermal-hydraulic codes such as PARET and PLTEMP that require both peak and average power profile for computation of safety margins, transients, etc.

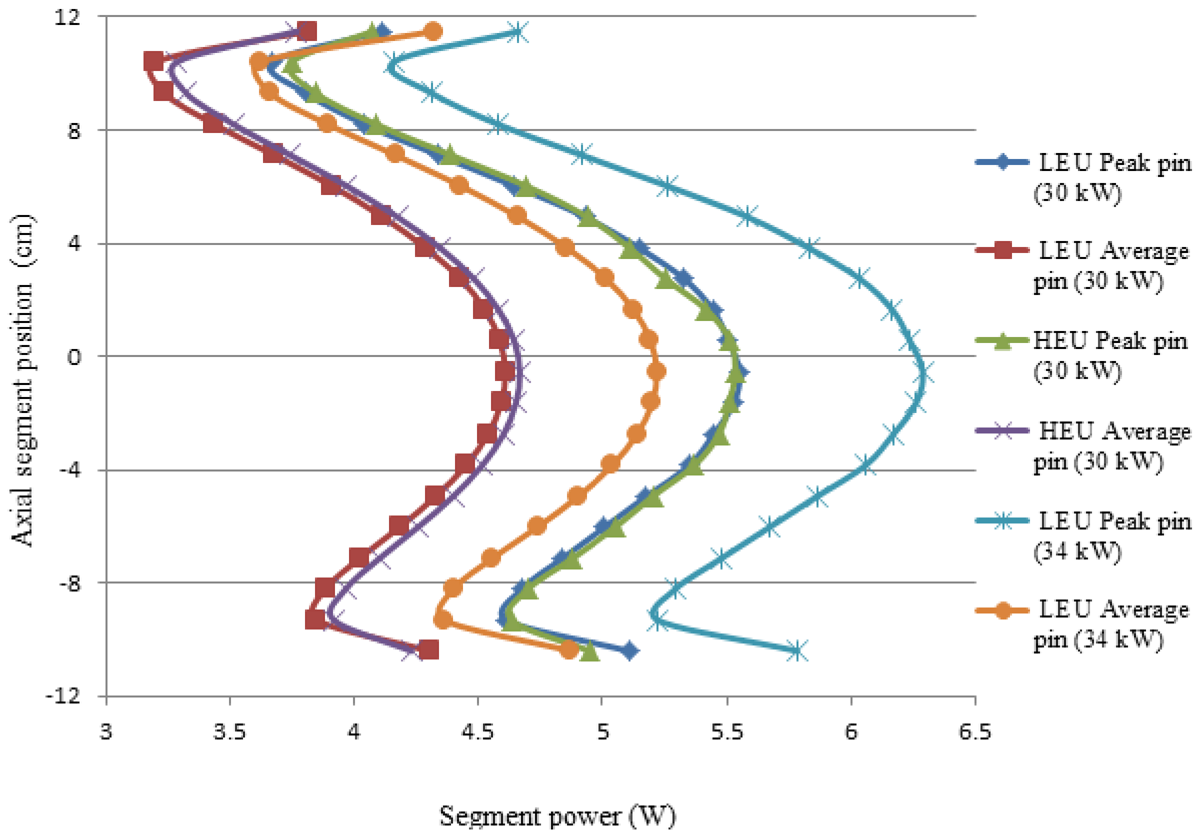

FIG. 4.8. Peak power pin axial profile (21 segments) (Courtesy of National Nuclear Research Institute (NNRI), Ghana).

(d) Reactivity coefficients

Changes in the physical properties of the materials in the reactor alter its reactivity. Reactivity coefficients are useful in quantifying the reactivity change that will occur due to the change in a physical property such as the temperature of the moderator [4.6]. The temperature coefficient can be conveniently considered to consist of three partial contributions: nuclear, density and volume temperature coefficients [4.7]. Some reactivity coefficients evaluated for the core conversion are shown below.

The fuel temperature coefficient for both cores at various temperatures is shown in Table 4.7. The LEU fuel demonstrates consistency as the coefficients computed are all negative, and hence the core is more inherently stable than the HEU core.

TABLE 4.7. FUEL TEMPERATURE COEFFICIENT

Temperature (°C)	HEU (mk/°C)	LEU (mk/°C)
126.85	$1.02 \pm 0.001 \times 10^{-3}$	$-6.69 \pm 0.005 \times 10^{-3}$
226.85	$4.80 \pm 0.020 \times 10^{-4}$	$-9.57 \pm 0.004 \times 10^{-3}$
326.85	$-9.71 \pm 0.002 \times 10^{-5}$	$-10.2 \pm 0.003 \times 10^{-3}$
526.85	$-9.79 \pm 0.002 \times 10^{-5}$	$-9.92 \pm 0.002 \times 10^{-3}$
Average	3.26682×10^{-4}	$-9.08 \pm 0.002 \times 10^{-3}$

The moderator temperature coefficient for light water was computed in three ways. First, only the temperature card was varied, and the results are shown in Table 4.8.

TABLE 4.8. MODERATOR TEMPERATURE COEFFICIENT (PARTIAL)

Temperature (°C)	HEU (mk/°C)	LEU (mk/°C)
30	$-6.75 \pm 0.049 \times 10^{-2}$	$-3.37 \pm 0.026 \times 10^{-2}$
32	$-4.96 \pm 0.030 \times 10^{-2}$	$-3.89 \pm 0.025 \times 10^{-2}$
40	$-6.10 \pm 0.052 \times 10^{-2}$	$-3.77 \pm 0.015 \times 10^{-2}$
50	$-1.88 \pm 0.008 \times 10^{-2}$	$-3.74 \pm 0.010 \times 10^{-2}$
60	$-6.14 \pm 0.017 \times 10^{-2}$	$-3.48 \pm 0.007 \times 10^{-2}$
70	$-5.99 \pm 0.013 \times 10^{-2}$	$-3.64 \pm 0.006 \times 10^{-2}$
100	$-6.35 \pm 0.007 \times 10^{-2}$	$-3.95 \pm 0.004 \times 10^{-2}$
Average	$-5.45 \pm 0.020 \times 10^{-2}$	$-3.69 \pm 0.008 \times 10^{-2}$

Secondly, the density of the moderator changes by the introduction of a void in the reactor moderator. The density of the water in the coolant cell changes with a change in temperature. The density decreases from 0.99825 g/cm^3 to 0.95838 g/cm^3, when temperature increases from 20°C to 100°C. The void coefficients of reactivity for the HEU and LEU cores in this range are shown in Table 4.9.

TABLE 4.9. MODERATOR VOID COEFFICIENT

Temperature (°C)	HEU (mk/°C)	LEU (mk/°C)
25	$-1.27 \pm 0.021 \times 10^{-1}$	$-1.03 \pm 0.017 \times 10^{-1}$
30	$-1.01 \pm 0.009 \times 10^{-1}$	$-0.88 \pm 0.007 \times 10^{-1}$
50	$-1.15 \pm 0.003 \times 10^{-1}$	$-1.22 \pm 0.003 \times 10^{-1}$
60	$-1.28 \pm 0.003 \times 10^{-1}$	$-1.34 \pm 0.003 \times 10^{-1}$
100	$-1.77 \pm 0.002 \times 10^{-1}$	$-1.86 \pm 0.002 \times 10^{-1}$
Average	$-1.30 \pm 0.008 \times 10^{-1}$	$-1.27 \pm 0.007 \times 10^{-1}$

Finally, the temperature and density were both varied simultaneously, as shown in Table 4.10. This is the most viable result amongst the three.

TABLE 4.10. MODERATOR TEMPERATURE COEFFICIENT

Temperature (°C)	HEU (mk/°C)	LEU (mk/°C)
50	–0.15883	–0.18768
60	–0.18148	–0.20405
70	–0.39561	–0.40581
100	–0.24293	–0.25832
Average	–0.24471	–0.26397

The three means of computing the moderator coefficient for both the HEU and LEU show comparable results. Water was used as the moderator in all cases.

(e) Worth of the top beryllium reflector

The purpose of calculating the worth of beryllium shims was to determine the reactivity increase. This was achieved by adding shim pieces of different thickness that will compensate the reactivity losses due to the burnup of ^{235}U, as well as ^{149}Sm poisoning. The total thickness available is 109.5 mm, which corresponds to a total reactivity worth of about 18 mk. Figures 4.9 and 4.10 show the comparison of experimental and calculated shim worth of HEU with that of calculated LEU. The differential reactivity added by the shim decreases with the increasing thickness of the shim.

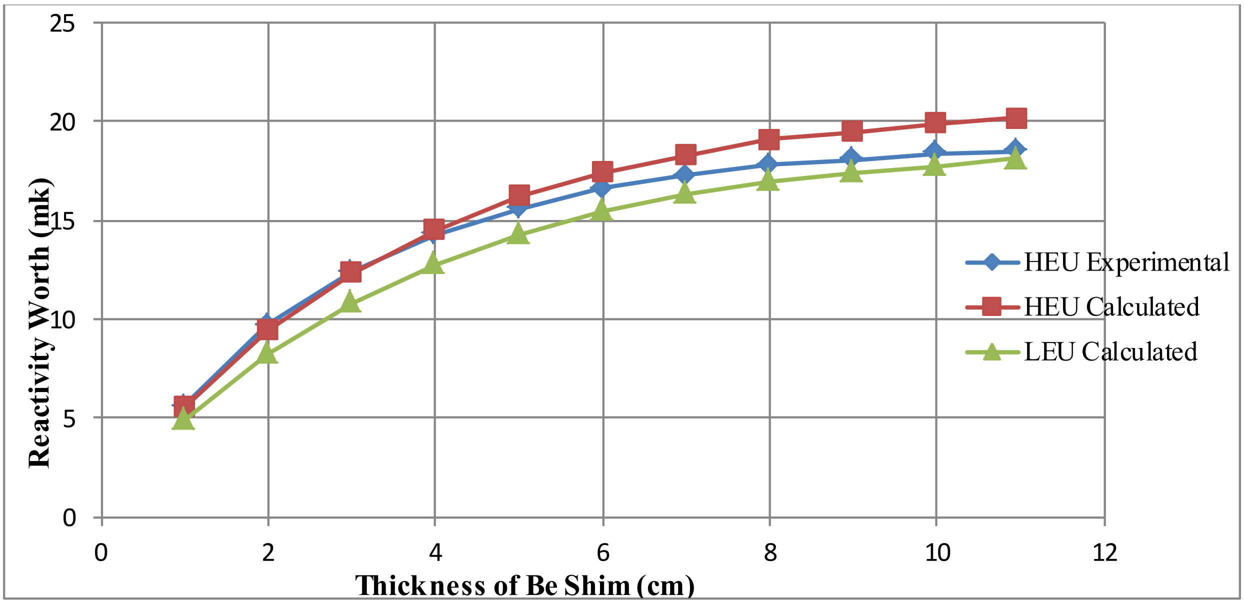

FIG. 4.9. Reactivity worths of top beryllium shims for HEU and LEU cores (Courtesy of National Nuclear Research Institute (NNRI), Ghana).

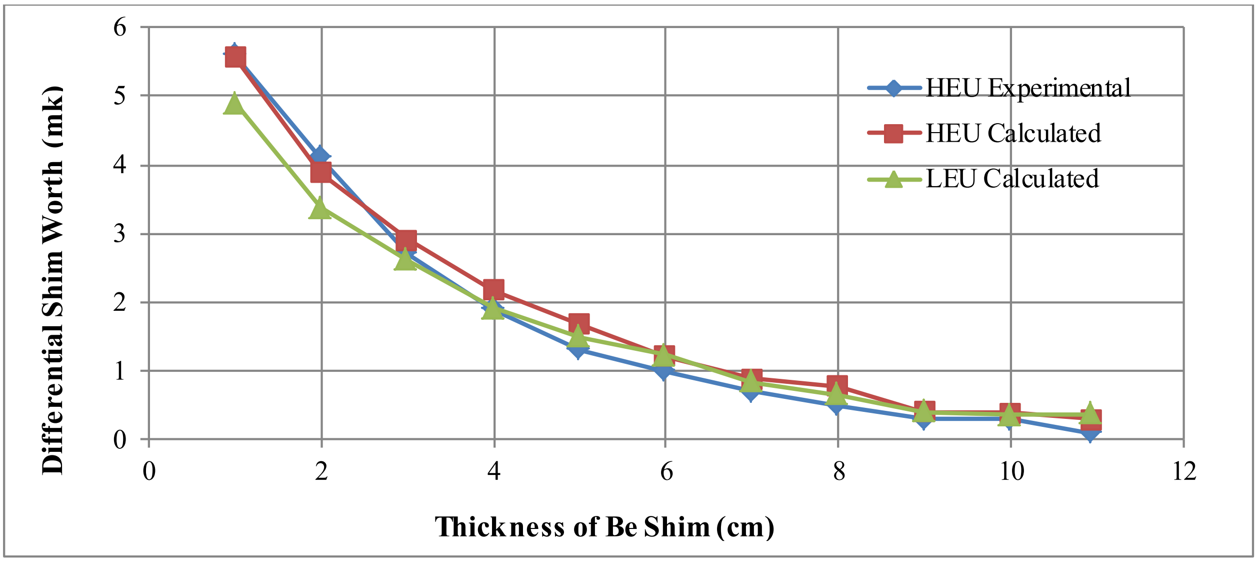

FIG. 4.10. Differential reactivity worth of top beryllium shims for HEU and LEU cores (Courtesy of National Nuclear Research Institute (NNRI), Ghana).

4.2.1.3. Core lifetime analysis

An R-Z diffusion theory model using the REBUS-3 code was developed to identify the basic fuel depletion characteristics of the GHARR-1 core. Various parts of the core were homogenized. Xenon worth, rate of fuel depletion and fuel cycle length were obtained by performing simple reactivity rundown calculations. A newly loaded fresh core with the control rod fully withdrawn is depleted at a fixed power level for a given length of time. Cross-sections were generated using the WIMS/ANL code. Results of burnup analyses are shown in Table 4.11.

TABLE 4.11. XENON WORTH AND REACTIVITY CHANGE RATES

Parameters	HEU, 15 kW/30 kW	LEU, 17 kW/34 kW
Equilibrium Xe worth (mk)	2.013/3.827	1.617/3.099
Fuel depletion (mk/day)	0.0250/0.0489	0.0198/0.0389
Hours to operate before adding shim	1631.8/835.1	2059.5/1049.9
Core lifetime (years)	46 at 15 kW	57 at 17 kW

The GHARR-1 core has a very small window of excess reactivity, approximately 1.7 mk, for operation between 4.0 mk and 2.3 mk. Based on the above reactivity rundown study, one finding is that the equilibrium xenon worth is high compared to the allowed excess reactivity window for typical reactor operation. Consequently, GHARR-1 cannot be operated continuously to allow xenon to accumulate to its equilibrium level. As per its design, GHARR-1 can only operate for a very short operational time, no more than approximately 4.5 hours per day at half power, or no more than around 2.5 hours per day at full power to avoid excessive xenon build up.

4.2.2. Thermal-hydraulic analyses

The thermal-hydraulic design of the reactor is closely related to neutronic calculations and the structural design [4.2]. The geometrical dimensions of the fuel element, fuel element temperatures, coolant pressure, temperatures and velocities are analytically shortened to satisfy the requirements of reactor safety during all operational states.

The core region of GHARR-1 is located 4.7 m under water, close to the bottom of a watertight reactor vessel. The quantity of water is 1.5 m^3 in the vessel, which serves as a radiation shield, moderator and as a primary heat transfer medium. In addition, heat can be extracted from the water in the vessel by means of a water-cooling coil located near the top of the vessel. The water-filled reactor vessel is in turn immersed in a water-filled pool of 30 m^3. Cold water is drawn through the inlet orifice by natural convection. The water flows past the hot fuel elements and comes out through the core outlet orifice. The hot water rises to mix with the large volume of water in the reactor vessel and to the cooling coil. Heat passes through the walls of the container to the pool water. A diagrammatic representation of the heat transfer mechanism is represented in Fig. 4.11.

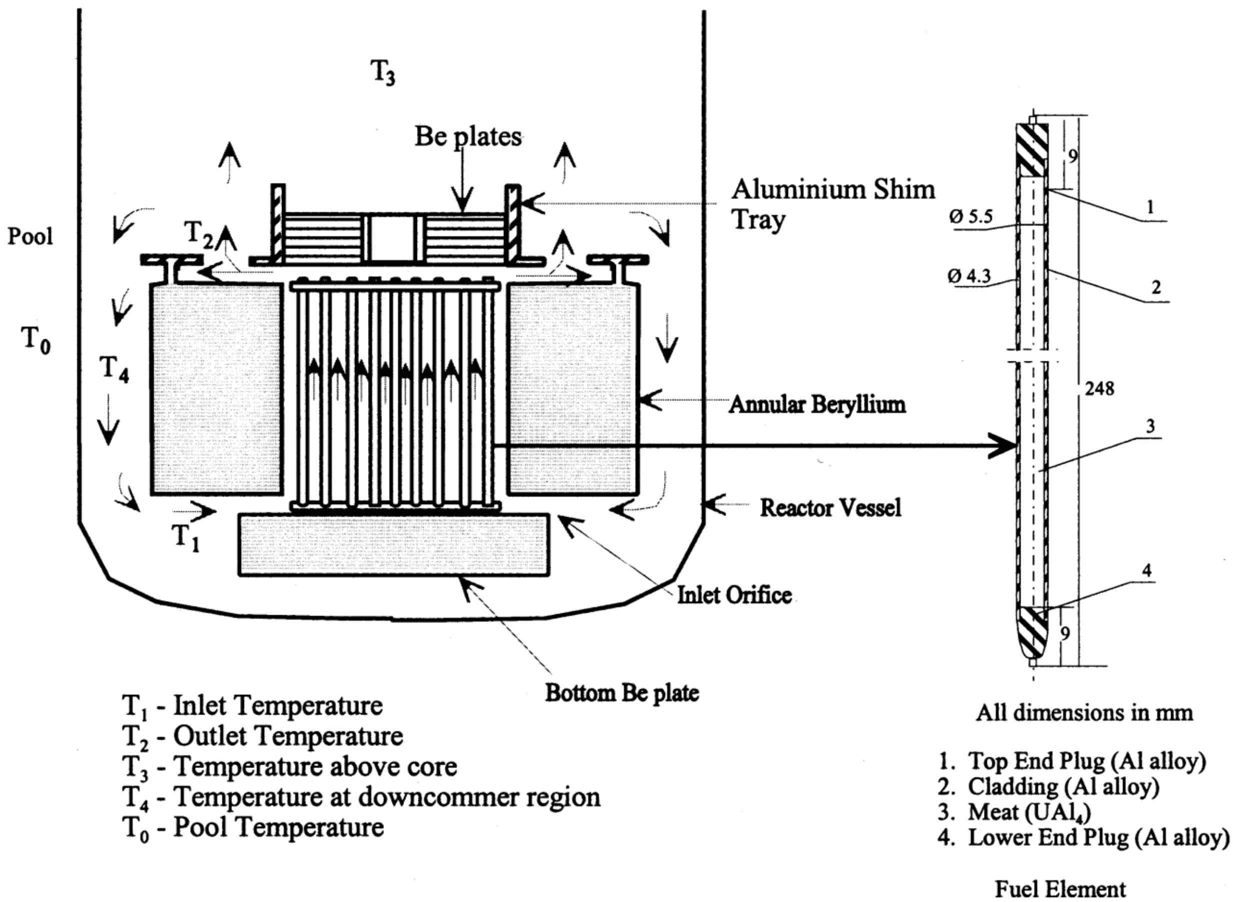

FIG. 4.11. A schematic diagram of the coolant flow pattern (Reproduced from Ref. [4.8] with permission courtesy of National Nuclear Research Institute (NNRI), Ghana).

The core inlet flow orifice impedes the natural circulation of water through the core. Its area is designed so that the highest power achieved during the design basis self-limiting power excursion can cause no damage to the core or present any hazard to nearby staff.

The GHARR-1 reactor has a small core, and the coolant flow in the core is at the transient phase from laminar flow to turbulent flow. The flow transition will occur when there is an increase in power. The closer to the upper part of elements, the stronger the turbulence becomes. The buoyancy force in natural circulation must overcome the friction. Calculations show that the friction resistance is small, about 10% of the total resistance. Meanwhile, the inlet resistance is about 70% of the total resistance and thus has a great effect on the state of flow. An appropriate choice for the inlet flow orifice is a very important factor in the thermal-hydraulic design. As the inlet orifice gets smaller, the flow velocity and in turn the turbulence in the core will increase. As a result, the heat transfer from fuel element to coolant will be improved. However, a smaller inlet orifice will cause an increase in resistance and a decrease in flow rate resulting in a rapid increase of temperature. Minimizing temperature rise is an essential condition. A temperature rise that is too high will cause a relatively large temperature effect, and make the excess reactivity used for compensating xenon poisoning too small, and thus the operable time will be reduced. The relationship obtained using the thermal-hydraulic test data is expressed in the form [4.2]:

$$\Delta T = 6.81 P^{(0.59+0.0019T_i)} T_i^{-0.35} \tag{4.1}$$

where

P is the reactor power in kW,
T_i is the coolant temperature (°C), and
ΔT is the temperature difference between the inlet and outlet coolant in the core.

It is evident from this relationship that the increase in the temperature difference between the inlet and outlet coolant ΔT will increase with increasing reactor power, and decrease with the inlet coolant temperature.

The water in the reactor is not pressurized and relies upon natural convection; therefore issues surrounding depressurization or coolant flow pump failure are not considered. A water cooled coil of limited heat removal capacity will eventually remove the thermal energy generated in the core. Due to the fact that the reactor possesses limited excess reactivity and reactivity feedback characteristics, any significant deterioration in heat removal capability will eventually result in an automatic decrease in reactor power.

The temperature in an operating reactor varies from point to point within the system. As a consequence, there is always one fuel rod, usually near the centre of the reactor that has the maximum fuel temperature at some point along its length. This temperature is determined by the power level of the reactor, the design of the coolant system, and the nature of the fuel [4.9]. One major design of a reactor coolant system is to provide for the removal of heat produced at the desired power level while ensuring that the maximum fuel temperature is always below this predetermined value. This then ensures a good safety margin. Under subcooled flow boiling conditions, the boiling crisis is often called the DNB. The heat flux at which the boiling crisis occurs is named the critical heat flux CHF [4.10]. In general, thermal performance improvements are highly desirable, so there is a need to predict CHF accurately in the earliest stages of a new product design. In the case of a nuclear reactor core, CHF margin gain (e.g. using improved fuel assembly design) can allow power uprate and enhanced operating flexibility [4.11]. Most metal finishing operations score tiny grooves on the surface of the fuel pin, and also typically involve some chattering or bouncing action, which hammers small holes into the surface. When a fuel pin surface is wet, liquid is prevented by surface tension from entering these holes, so small gas or vapour pockets are formed. These little pockets are sites at which bubble nucleation occurs [4.9]. The ONB is not a limiting criterion in the design of a fuel element. However, it is a heat transfer regime which should be identified for proper hydraulic and heat transfer considerations, i.e., single-phase flow versus two-phase flow. For reactor design purposes, acceptable data on burn-out heat flux are needed since DNB is potentially a limiting design constraint. Optimization of core cooling against other neutronic, economic, and materials constraints can best be accomplished by judicious use of standard, experimentally deduced DNB correlations [4.12]. The parameter most used to evaluate the failure margin by boiling crisis is the critical heat flux ratio (CHFR), or departure from nucleate boiling ratio (DNBR). This is the ratio of the calculated CHF to the most limiting heat flux condition in the reactor [4.13].

4.2.2.1. Method of analysis

Both the steady state and transients were analysed for the two cores under the thermal-hydraulic design. PLTEMP/ANL and PARET codes were used for the steady state and transient analyses respectively. Some of values obtained were compared with those stated in the current HEU SAR.

(a) Steady state

Four input data files were used in the PLTEMP/ANL V4.1 code to calculate the safety margins in the steady state operation of GHARR-1 with a HEU core. In addition, an input file giving the axial power shape of the modelled fuel pin, the average power pin, and the peak power pin in the HEU core were used with the four input data files. Another set of four similar input data files were used to calculate steady-state safety margins of GHARR-1 with an LEU core at both 30 kW and 34 kW. In addition, an input file giving the axial power shape of the modelled fuel pin was also used with each set of the four input data files, as required by the PLTEMP/ANL V4.1 code.

One set of input files will model one average fuel pin of the 344 or 348 fuel pins in the HEU or LEU core respectively, with a reactor power of 15 kW and a coolant inlet temperature of 24.5°C. The pin is modelled as a solid rod of radius 2.15 mm in a 0.6 mm thick cladding, without any gap resistance in the case of HEU core. This input data file was used to calibrate the hydraulic resistance in the PLTEMP/ANL model to reproduce an experimentally measured coolant temperature rise of 13°C (from 24.5—37.5°C).

Another input data file uses the above determined value of the hydraulic resistance coefficient, and models one average fuel pin in the HEU and LEU cores when the reactor is operating at the nominal reactor power of 30 kW. The purpose of this input data file is to adjust the coolant channel inlet temperature so that the coolant exit temperature is 70°C. The next input data file uses the above adjusted values of the hydraulic resistance coefficient and the channel inlet temperature, and models the peak power pin of the core, with six HCFs. The purpose of this input data file is to determine the maximum allowed operating reactor power with all HCFs applied.

The final set of input data files is identical to the third set of input data files, except that five of the HCFs have been set to 1.0 in order to calculate the maximum allowed reactor power without HCFs. The HCF for power was kept unchanged at its actual value because the ratio of the peak pin to the average pin power is certain. Using this input data file, the pin power was raised and adjusted so that the minimum ONBR on the cladding outer surface is exactly 1.0. The minimum ONBR occurs in axial node 10. When this minimum ONBR is 1.0, the pin power multiplied by the number of pins gives the maximum allowed operating reactor power of the core without HCFs.

Six HCFs, defined below, are used in the PLTEMP/ANL V4.1 code to calculate research reactor safety margins. These factors are different in natural circulation flow from those in forced flow. The basic reason for this is that in natural circulation the coolant flow is induced by the power produced in the pin, thus softening the effect of pin power on inlet to outlet coolant temperature rise, whereas this is not the case in forced flow. In forced flow, the pressure drop induces the coolant flow [4.14]. The HCFs for forced flow over research reactor fuel plates have already been formulated [4.15]. Table 4.12 shows the type of uncertainties included in each of the six HCFs. The uncertainties of pool water level and pin heated length are not included.

TABLE 4.12. UNCERTAINTIES INCLUDED IN THE SIX HCFS

No.[1]	Uncertainty type	FPOWER	FFLOW	FNUSLT	FBULK	FFILM	FFLUX
1	Neutronics calculation of power density in a pin, u_1				×	×	×
2	^{235}U mass per pin, u_2				×	×	×
3	UO_2 pellet radius, u_3					×	×
4	U enrichment in a pellet, u_{10}					×	×
5	UO_2 pellet density, u_{11}						
6	Fuel pin radius, u_{12}				×	×	×
7	Fuel pin pitch, u_{13}				×	×	
8	Flow redistribution among channels, u_6				×		
9	Reactor power measurement uncertainty, u_7	×					
10	Flow uncertainty due to uncertainty in friction factor, u_8		×				
11	Heat transfer coefficient uncertainty due to uncertainty in Nu number correlation, u_9			×			

[1] 1–8 are for local or random uncertainties, while 9–11 represent system-wide uncertainties

System wide and global HCFs are described in Section 2.10.6.1.

(b) Results and discussion

The reactor power for ONBR=1 without HCFs is 65.72 kW for HEU and 67.75 kW for LEU. The reactor power at ONBR=1 with all six HCFs is 51.6 kW and 53 kW for the HEU and LEU core respectively. The minimum DNBR with all six HCFs is 8.9 for the HEU and 8.5 for the LEU core.

The ONBR and DNBR computed so far show there is no boiling in both cores; this indicates the limits of operating power for both the HEU and LEU cores. The maximum allowed operating power assumes that the power measuring instrument is perfect without any error. The results also indicated good safety margins for the boiling point of the coolant and the melting points of both the fuel and cladding.

Thermal-hydraulic parameters obtained from further studies undertaken on both the HEU and LEU cores at nominal reactor powers are show in Tables 4.13 and 4.14. The results of the calculations for the clad surface and coolant temperatures using an inlet temperature of 30°C and a coolant pressure of 1 bar are also shown.

TABLE 4.13. COMPARISON OF HEU AND LEU STEADY STATE PARAMETERS USING PLTEMP/ANL

Parameter	HEU, 344 rods	LEU, 348 rods	LEU, 348 rods
Power (kW)	30.0	30.0	34.0
Core flow rate (kg/S)	1.1×10^{-3}	1.1×10^{-3}	1.2×10^{-3}
Peak fuel temp. (°C)	104	n.a.	142
Max. clad surface temp. (°C)	77.3	95.0	98.3
Max. coolant temp. (°C)	53.1	53.4	57.1

n.a.: not available.

For the LEU core the nominal power is raised to 34 kW in order to meet the flux level of 1×10^{12} $cm^{-2}s^{-1}$. Hence the computations, using PLTEMP, were done for the LEU core at this power and the steady state parameters were also compared with those of HEU and LEU at 30 kW in Table 4.13.

The melting point of UAl_4 and UO_2 fuels are 650°C and 2800°C respectively, and those of Al and Zircaloy-4 claddings are 600°C and 1850°C respectively. The peak fuel temperature for the LEU core is increased by a factor of 1.37, while the melting points of the respective fuels are increased by a factor of 4.3. The peak clad surface temperature is increased by a factor of 1.27 but the melting point of Zircaloy-4 for the LEU is higher than that of Al for the HEU core by a factor of 3.08. These give wider safety margins. Additionally, the core is located at a depth of 6 m thus increasing the boiling point of water at that pressure to about 113°C.

TABLE 4.14. COMPARISON OF COMPUTED COOLANT OUTLET TEMPERATURES AT VARIOUS POWERS AND INLET TEMPERATURES

Power (kW)	Inlet temperature (°C)	Measured HEU outlet temperature (°C)	Calculated HEU outlet temperature (°C)	LEU outlet temperature (°C)
0.3	32.0	32.6	33.2	33.2
	35.0	—	36.1	36.1
3	32.0	—	37.0	37.0
	37.0	—	41.7	41.7
	39.0	42.0	43.6	43.6
15	30.0	—	43.9	44.0
	37.0	48.5	50.0	50.2
	42.0	—	54.6	54.7
30	30.0	—	51.4	51.7
	34.0	53.0	54.7	55.4
	37.0	—	57.3	57.5
	42.0	—	61.6	61.9

The safety settings of the reactor ensure that protective action will correct an abnormal situation before a safety limit is exceeded [4.3]. For the HEU, the safety system settings for reactor thermal power, *P*, height of water above the top of the core, *H*, and ΔT are as follows:

- — *P(max)* = 36 kW
- — *H(min)* = 465 cm
- — $\Delta T(max)$ = 21°C

The effect of inlet temperature on temperature difference, as computed by PLTEMP, for both HEU and LEU is shown in Table 4.15.

TABLE 4.15. EFFECT OF INLET TEMPERATURE ON TEMPERATURE DIFFERENCE AT NOMINAL OPERATING POWER FOR THE HEU AND LEU CORES

T_{in} (°C)	30 kW		36 kW	
	HEU, ΔT (°C)	LEU, ΔT (°C)	HEU, ΔT (°C)	LEU, ΔT (°C)
10	24.10	29.15	27.00	32.28
15	21.63	27.16	24.20	30.20
20	20.20	25.59	22.66	28.54
30	18.60	23.26	20.97	26.03
35	18.30	22.37	20.63	25.07
40	18.03	21.61	20.54	24.24

4.2.2.2. Transients analysis

Program for the Analysis of Reactor Transients, or PARET, code was developed for testing methods and models and for subsequent applications in the analysis of transient behaviour in research reactors [4.16]. The code was originally developed for the analysis of the SPERT-III experiments for temperatures and pressures typical of power reactors [4.17]. Subsequently, the code has been modified to address some aspects of reactor thermal-hydraulic analysis, including a selection of flow instability, DNB, single and two-phase heat transfer correlations, and flow rates. Essentially, the code provides a coupled thermal-hydraulic and point kinetics capability with continuous reactivity feedback, and an optional voiding model which estimates the voiding produced by subcooled boiling [4.18]. For PARET applications, the reactor core can be represented by one to four regions. Each region may have different power generation, coolant mass flow rate, and hydraulic parameters as represented in a single fuel pin with its associated coolant channel. The heat transfer in each fuel element is computed on the basis of a one-dimensional conduction solution, providing for a maximum of 21 axial segments.

The hydrodynamics solution is also one-dimensional for each of the two channels at each time node [4.19]. The heat transfer could take place by natural or forced convection, nucleate, transition, or stable film boiling and the coolant could range from subcooled liquid through the two phase regime, and up to and including superheated steam, and allows for coolant flow reversal [4.20]. The code has been used for transient analysis of GHARR-1 [4.21]. PARET code was utilized for the transient analysis in order to compare the reactor power, fuel temperature and clad temperature for the two cores. Results are shown in Figs 4.12—4.14.

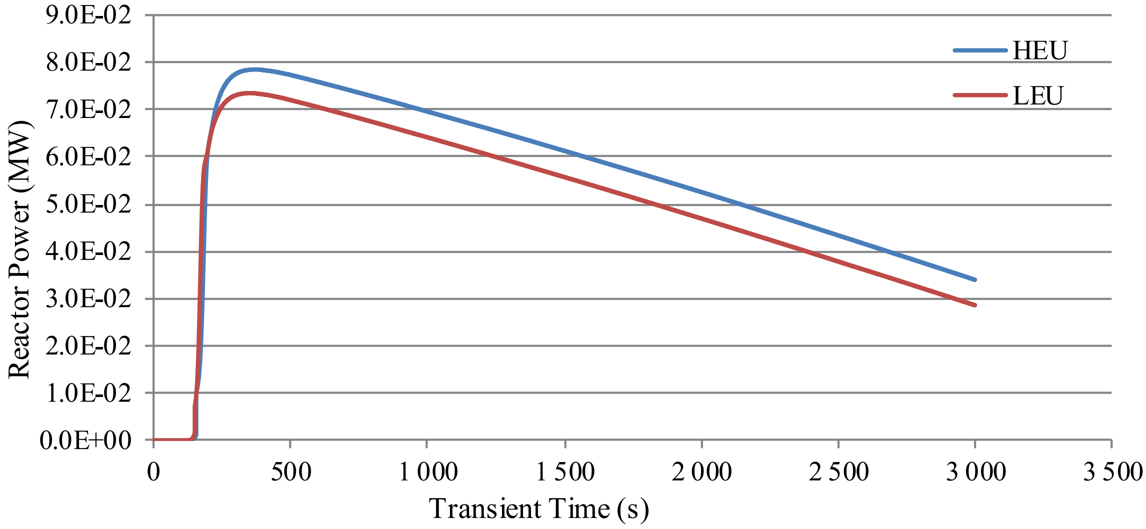

FIG. 4.12. Time vs. power for a 3.8 mk reactivity insertion with HEU and LEU fuel (Courtesy of National Nuclear Research Institute (NNRI), Ghana).

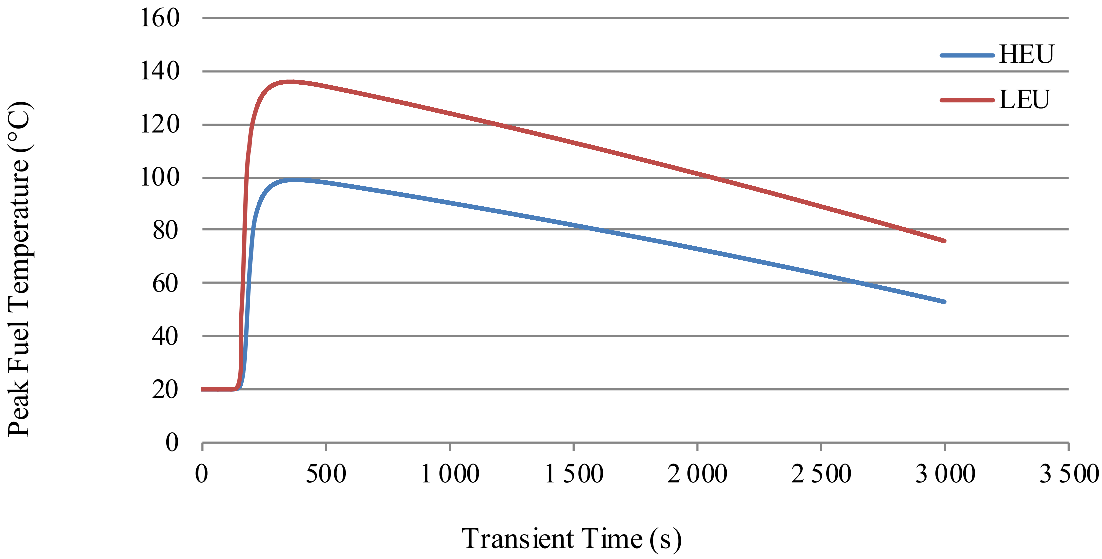

FIG. 4.13. Fuel temperature comparison of HEU and LEU cores for 3.8 mk reactivity transient (Courtesy of National Nuclear Research Institute (NNRI), Ghana).

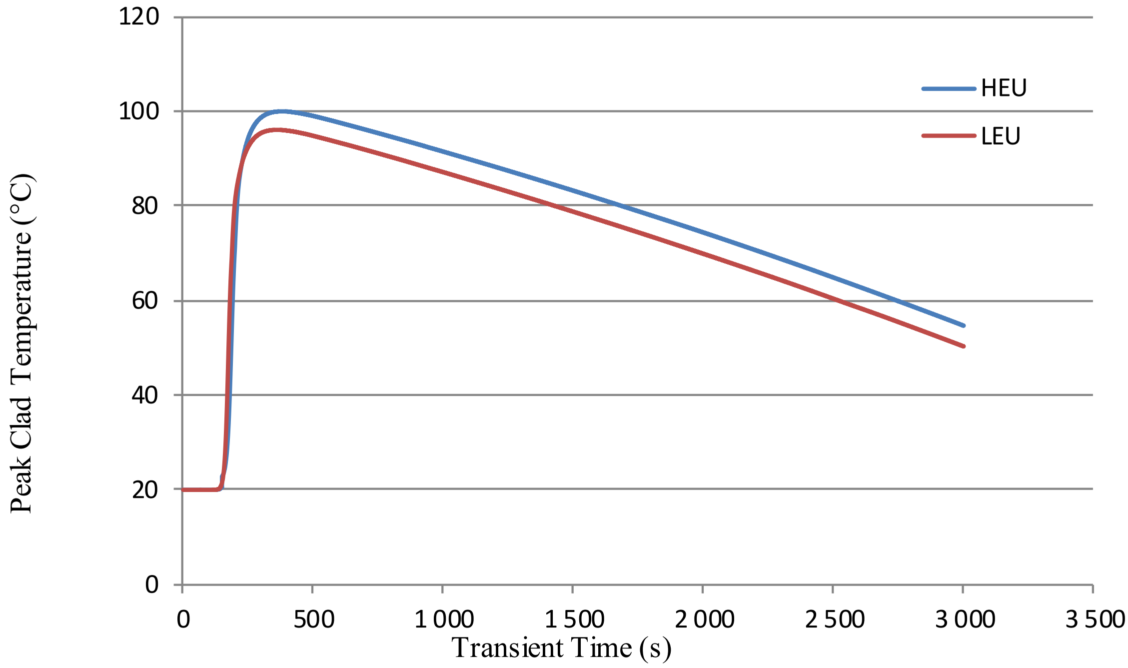

FIG. 4.14. Clad surface temperature comparison of HEU and LEU cores for 3.8 mk reactivity transient (Courtesy of National Nuclear Research Institute (NNRI), Ghana).

Hypothetical reactivity insertions for 6 mk and 8 mk were also performed to show the inherent safety margin of the LEU core. The results are shown in Figs 4.15—4.17 for the reactor power, fuel temperature and clad temperature respectively.

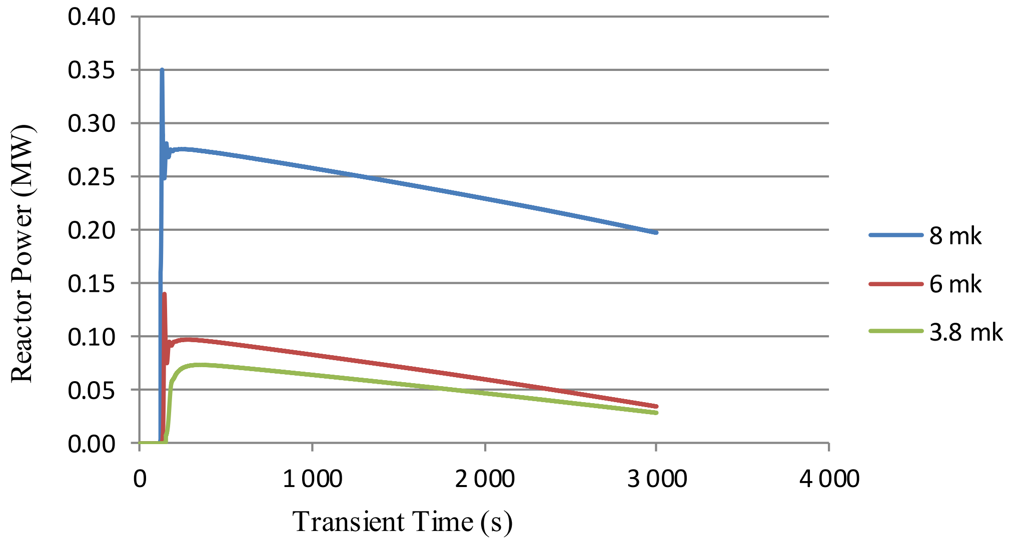

FIG. 4.15. Reactor power for reactivity insertions of 3.8 mk, 6 mk and 8 mk for LEU (Courtesy of National Nuclear Research Institute (NNRI), Ghana).

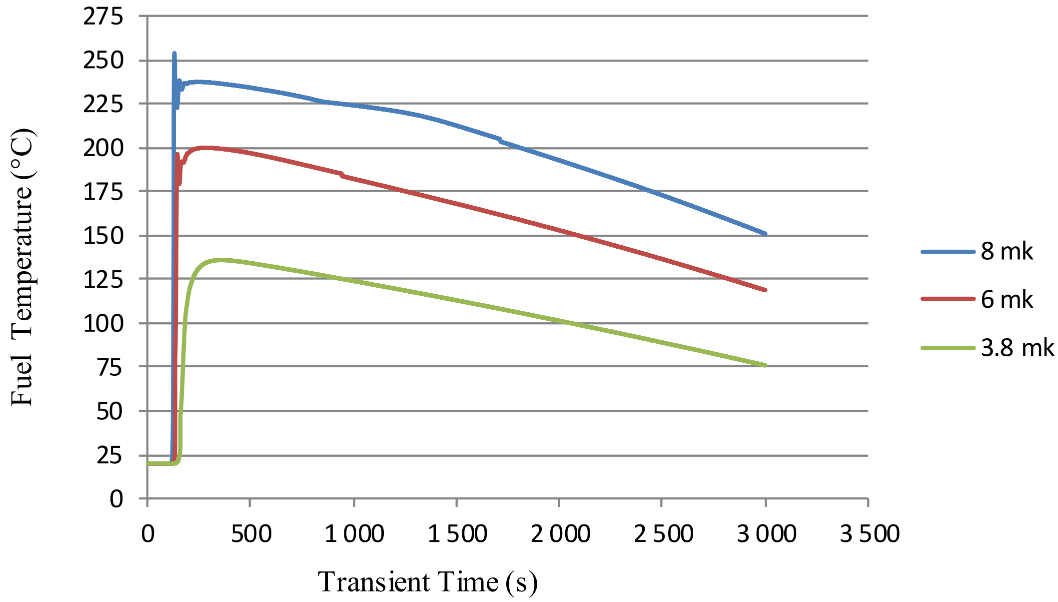

FIG. 4.16. Fuel Temperature for reactivity insertions of 3.8 mk, 6 mk and 8 mk for LEU (Courtesy of National Nuclear Research Institute (NNRI), Ghana).

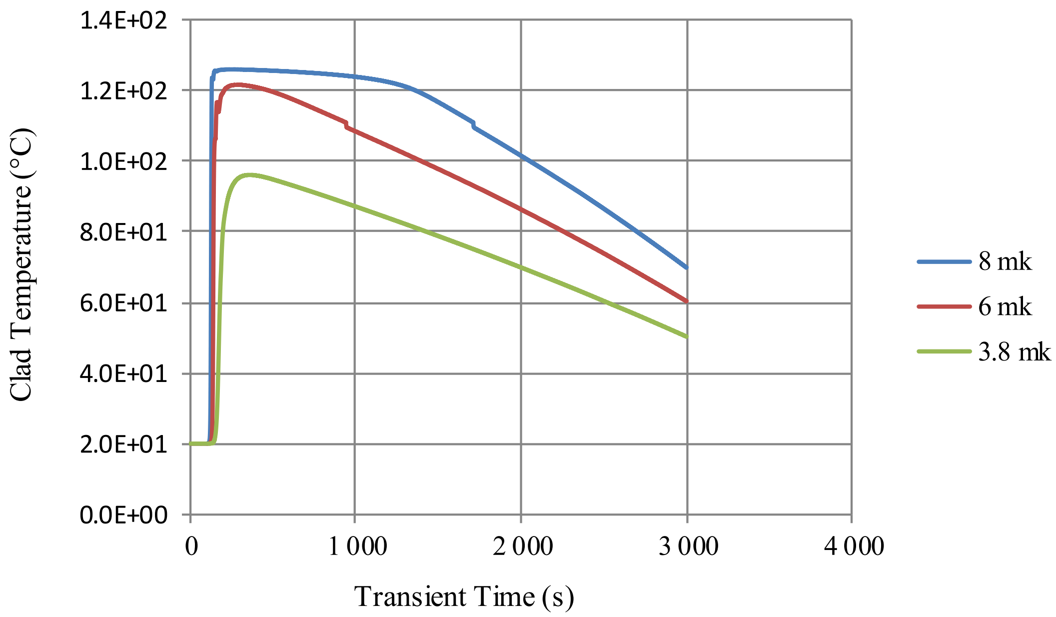

FIG. 4.17. Clad temperature for reactivity insertions of 3.8 mk, 6 mk and 8 mk for LEU. (Courtesy of National Nuclear Research Institute (NNRI), Ghana)

The peak temperature for the fuel as shown in Table 3.16 is far below its melting point of 2800°C, and that of the clad is also far below its melting point of 1850°C, indicating good safety margins.

TABLE 4.16. PEAK POWER, PEAK FUEL TEMPERATURE AND PEAK CLAD TEMPERATURE FOR VARIOUS REACTIVITY INSERTIONS

Reactivity insertion (mk)	Peak power (kW)	Peak fuel temperature (°C)	Peak cladding temperature (°C)
3.8	73.5	136	96.1
6.0	140	200	122
8.0	350	254	126

4.3. RADIOLOGICAL CONSEQUENCES ANALYSES

For the purpose of understanding the nature of severe accidents and assessment of accident scenarios involving the release of radioactive material at the GHARR-1 facility, the source term inventory of the core during normal operation must be known. Inventory data for GHARR-1 HEU and LEU cores were calculated for the SAR, which is based on the assumption that a hypothetical accident results in the release of some portion of the inventory of radioactive materials to the atmosphere. The DBA and BDBA scenarios for GHARR-1 HEU and LEU cores are analysed and presented in the following sections.

4.3.1. DBA

4.3.1.1. Scenario

It was assumed that pit corrosion of the cladding has created cladding failure in one or more fuel elements, such that a hole or holes in the cladding totaling 0.5 cm can exist.

It should be recognized that the control of reactor water quality is such that clad failures are not expected. In addition, monitoring of the reactor vessel water will be performed periodically and this should permit the discovery of clad failures well before they reach this size. Table 4.17 presents the concentration of radionuclides that could appear in the reactor vessel water because of the aforementioned leak.

A fraction of the fuel rod fission product inventory is released into the pool water and a fraction of this inventory is released into the air of the reactor hall. Furthermore, part of the total fission product content of air in the reactor hall is released to the environment by leakage from the reactor building. Effective (whole body) and thyroid doses are evaluated for this scenario for reactor building leak rates of 20% per hour and 100% per hour.

4.3.1.2. Fission inventory and source term determination

The fission product inventory was calculated using ORIGEN 2.2 (ORIGIN 2.2 Code, RSICC Collection, USA). Burnup and power distribution data were obtained from the neutronic analysis. It was assumed conservatively that the LEU core operated continuously at a power level of 34 kW for its estimated life time of 903 FPEDs.

The peak and the average rod power used for the inventory analysis were 112.97 W and 97.70 W for the LEU core. The ^{235}U burnup at the end of core life for both the fuel rod with maximum burnup, and the fuel rod with average burnup, is calculated to be 3.3% and 2.9% respectively for the LEU core. From the calculated fission product inventory, the most important isotope which contributes to the doses was selected. The source term for radioactivity in the air of the reactor hall is the inventory of one fuel assembly multiplied by the transfer factor from the fuel to the matrix material, the transfer factor from the matrix material to water and the transfer factor from water to air. However, since specific factors for each of these transfers are not available, a combined factor for transfer of fission products from the fuel matrix material to the air of the reactor building is used. The fission product inventory for the selected isotopes in one fuel assembly, the combined transfer factor, and the resulting source term for use in the dose calculation are presented in Table 4.17.

TABLE 4.17. PIT CORROSION FISSION PRODUCT INVENTORY

Nuclide	Half-life	Inventory in pool water (Bq/cm^3)		Transfer factor: matrix material to air[1]	Inventory in reactor hall (Bq/cm^3)
		HEU	LEU	LEU	
^{131}I	8.06 d	9.6×10^3	1.02×10^{11}	1×10^{-4}	1.02×10^7
^{132}I	2.26 d	4×10^{-1}	1.52×10^{11}	1×10^{-4}	1.52×10^7
^{133}I	20.9 h	1.5×10^4	2.36×10^{11}	1×10^{-4}	2.36×10^7
^{135}I	6.7 h	1.1×10^3	2.20×10^{11}	1×10^{-4}	2.20×10^7
^{90}Sr	28.1 y	1.7×10^3	1.15×10^{10}	1×10^{-6}	1.15×10^4
^{95}Zr	65.5 d	3.0×10^3	2.26×10^{11}	1×10^{-6}	2.26×10^5
^{95}Nb	35.0 d	4.8×10^3	2.26×10^{11}	1×10^{-6}	2.26×10^5
^{137}Cs	35.17 d	2.7×10^3	1.20×10^{10}	1×10^{-6}	1.20×10^4
^{140}Ba	12.8 d	1.2×10^4	2.18×10^{11}	1×10^{-6}	2.18×10^5
^{140}La	40.27 h	2.4×10^4	2.18×10^{11}	1×10^{-6}	2.18×10^5
^{85}Kr	10.76 y	2.21	1.41×10^9	0.02	2.81×10^7
^{133}Xe	5.29 d	2.3×10^4	2.36×10^{11}	0.02	4.73×10^9
^{135}Xe	9.5 h	3.3×10^3	2.11×10^3	0.02	4.23×10^9

[1] Transfer factors were obtained from IAEA Safety Reports Series No. 53 [4.22].

Based on the source term for radioactivity in the air of the reactor hall in Table 4.17, radiation doses were calculated for exposed workers, members of the public, and permanent residents.

4.3.1.3. *Assumptions for dose calculations*

A spreadsheet based on the methodology described by Pfeiffer [4.23] was used to calculate data for evaluation of doses with the following assumptions:

— Source term as determined in Section 4.3.1.2;
— Release of fission products occurs in a single phase of one hour duration;
— The release height for the fission products is ground level. The dimensions of the reactor building are: height: 8.0 m, width: 7.0 m, length: 7.0 m, and volume: 392.0 m^3;
— A conservative meteorological model was used fixing the meteorological conditions to Pasquill stability class F, with 1 m/s wind speed of uniform direction for a time period 0–8 hours. Additionally, a Pasquill stability class F with a wind speed of 1 m/s of a variable direction within a 22.5 sector for a time period of 8–24 hours was utilized;
— For distances below 100 m from the reactor, the atmospheric dispersion in air and dose values are identical to the corresponding values at 100 m; and
— The ventilation system is shut down at the time of accident to prevent any effect by the reactor filtration system.

4.3.1.4. *Calculated results*

(a) Dose for maximum exposed worker

The first individual case of exposure during the considered accident is that of the staff members that are present in the reactor hall during the accident. It is assumed that the last staff member evacuates the reactor hall after five minutes. This time is adequate to take the necessary actions specified in the operating procedures. The dose rate and the activity concentrations in the air of the reactor hall during these five minutes was based on an assumed volume method, in which the radiological material is dispersed evenly in the containment volume over a specified time period. To obtain the dose for 5 minutes this dose rate value, which is computed in mSv per hour, was divided by 12 (60 minutes/12 = 5 minutes). The results are shown in Table 4.18 for both whole body and thyroid doses.

(b) Dose for maximum exposed member of the public

The dose for the maximum exposed member of the public was evaluated for the case that a person stands at a distance of about 100 m from the accident site, for two hours. After this time the area at the public perimeter of the site is assumed to be evacuated by the security staff. No ingestion is assumed to take place during the considered time period. The doses are computed for two hours, which is sufficient to consider all effects due to inhalation. The results are shown in Table 4.18 for both whole body and thyroid doses.

(c) Dose for maximum exposed permanent resident

The closest permanently inhabited house is more than 300 m from the GHARR-1 reactor. Radiation doses for a person living 300 m away is considered, based on the postulated accident scenario. The calculation uses the assumptions listed in Section 4.3.1.3. The wind is assumed to blow in the direction of the closest house as described in the assumptions. The doses are computed for 24 hours, which is sufficient to consider all effects due to inhalation. The results are shown in Table 4.18 for both whole body and thyroid doses.

TABLE 4.18. CALCULATED DOSES FOR THREE EXPOSED INDIVIDUALS

Exposed individual	Exposure time	Effective (whole body) dose		Thyroid dose	
		Calculated dose (mSv)	Dose limits (mSv/yr)	Calculated dose (mSv)	Dose limits (mSv/yr)
		LEU	GRPB-3	LEU	IAEA SS No. GSR Part 3 [2.24]
Maximum exposed worker	5 min	0.49	50[c]	0.97	1250
Maximum exposed member of the public (100 m away)	2 h	1.34×10^{-3} [a] 3.93×10^{-3} [b]	5	3.71×10^{-3} [a] 1.02×10^{-2} [b]	25
Maximum exposed permanent resident (300 m away)	24 h	1.06×10^{-3} [a] 2.02×10^{-3} [b]	1	3.04×10^{-3} [a] 4.50×10^{-3} [b]	25

[a] Calculated dose exposures for building leak rate of 20%
[b] Calculated dose exposures for building leak rate of 100%
[c] While the dose limit is 20 mSv/y averaged over 5 years, a dose of 50 mSv in a single year is used for the accident scenarios used in this document

The calculated effective (whole body) and thyroid doses for exposed workers and the members of the public are below the set limits by the Radiation Protection Board of Ghana Atomic Energy Commission. Considering the conservative approach taken for the calculation of the fission product inventory, for which the source term was based on the peak power pin and assumed to be the same in all 348 pins, as well as the meteorological conditions, doses for more realistic conditions will be significantly lower than the calculated values.

4.3.2. BDBA

The BDBA is not expected to occur and is therefore not analysed. It is described for purposes of emergency planning only, as it is always an accident more severe than the DBA. The accident is considered with the following assumptions:

— The reactor building collapses;
— The reactor vessel water and the pool water leak at a rate 4 m^3/hr;
— The reactor core is exposed to air after six hours;
— The reactor was operating at 34 kW; and
— The reactor has operated for 903 FEPD (equivalent to the core lifetime at 3.3% burnup).

Under these conditions, the reactor core would be cooled by natural circulation of air and by thermal radiation. The core would not melt and any exposure will be external exposure due to the unshielded core. In the event that pit corrosion totals an area of 5 cm^2 during this accident, the calculated fission product inventory of the core as a function of time is presented in Table 4.19.

TABLE 4.19. ACTIVITY OF CORE FISSION PRODUCTS (FP) WITH TIME

Cooling time	Estimated, total activity of core FP mixture (TBq)	
	HEU	LEU
1 min	1.4×10^{3}	2.07×10^{1}
1 h	1.7×10^{2}	2.02×10^{1}
6 h	1.7×10^{1}	1.80×10^{1}
12 h	9.1×10^{1}	1.62×10^{1}
1 day	8.0×10^{1}	1.39×10^{1}
5 days	6.5×10^{1}	8.62×10^{-1}
10 days	5.8×10^{1}	6.54×10^{-1}
30 days	4.4×10^{1}	3.61×10^{-1}

Assuming isotropic point sources, calculations have been performed for dose rates at various points at the top of the reactor pool, in the reactor hall and controlled area around the collapsed building. The results are presented in Table 4.20.

TABLE 4.20. GAMMA DOSE RATES AT DIFFERENT POSITIONS FOR THE HEU AND LEU CORES

Time after accident	γ radiation dose rate (mSv/h)					
	In the building				Out of the building	
	Top of reactor restricted		Reactor hall		Balcony 10 m away from core centre	
	HEU	LEU	HEU	LEU	HEU	LEU
6 h	1.7×10^{2}	2.0×10^{2}	8.9×10^{-1}	10.7×10^{-1}	1.6×10^{-2}	1.9×10^{-2}
1 day	1.2×10^{2}	1.4×10^{2}	6.7×10^{-1}	8.0×10^{-1}	1.1×10^{-2}	1.3×10^{-2}
30 days	5.0×10^{2}	6.0×10^{-1}	3.3×10^{-1}	4.0×10^{-1}	4.8×10^{-2}	5.8×10^{-3}

The effective (whole body) dose limit for the maximum exposed worker recommended in IAEA Safety Standards No. GSR Part 3 [4.24] is 50 mSv per year. Except for the easily controlled restricted area immediately above the core, all dose rates are low and would permit emergency operations to proceed.

4.4. CONCLUSION

Ghana is committed to ensuring the success of the US National Nuclear Security Administration's Global Threat Reduction Initiative HEU to LEU conversion programme, and 12.5% enriched UO_2 has been chosen as the fuel for GHARR-1's LEU core. For a core excess reactivity of 4 mk, 348 fuel pins would be appropriate for the GHARR-1. Results indicate that the flux distribution in the inner irradiation channels will not be compromised if the power of LEU core is increased to 34 kW. The properties of UO_2 and Zircaloy-4 will increase the safety of the LEU core relative to the HEU core due to their higher melting points. Zircaloy-4 will increase core lifetime because it is more resistant to corrosion. The GHARR-1 core using UO_2 12.5% fuel can be operated for 23 shim cycles, with a cycle length of 2.5 years, for over 57 years at a 16.5 kW power level. All 23 LEU cycles meet the approximate 4.0 mk excess reactivity required at the beginning of the cycle. For comparison, the MNSR HEU reference core can also be operated for 23 shim cycles, but with a cycle length of exactly two years for just over 46 years at a 15.0 kW power level. It is concluded that the GHARR-1 core with LEU UO_2 fuel enriched to 12.5% and a power level of 34 kW can be operated approximately 25% longer than the current HEU core operated at 30 kW. Both cores will have the same value of thermal neutron flux in their experimental positions.

Acknowledgment

Ghana's NNRI acknowledges with gratitude the financial support of IAEA for the award of Research Contract Number 13946. They also appreciate fellowships sponsored by US Department of Energy and particularly thank the staff of the Nuclear Engineering Section of Argonne National Laboratory, especially, J. Roglans-Ribas, J.E. Matos, J.R. Liaw, M. Kalimullah, J. Morman and S.C. Mo for hosting fellowships, and the importance they assigned to this project.

REFERENCES TO SECTION 4

[4.1] YAN, Y.W., Reactor Complex of Miniature Neutron Source Reactor Training Document, China Institute of Atomic Energy, China (1993).

[4.2] AKAHO, E.H.K., ANIM-SAMPONG, S., DODOO-AMOO, D.N.A., EMI-REYNOLDS, G., Safety Analysis Report for Ghana Research Reactor -1; GEAC-NNRI-RT-26 (1995).

[4.3] INTERNATIONAL ATOMIC ENERGY AGENCY, Project and Supply Agreement, Information Circular, INFCIRC/468, IAEA, Vienna, (1995).

[4.4] CHENZHAN G., Experimental of Adding Top Beryllium Shims for MNSR, MNSR Training Materials, CIAE Technical Report, China (1993).

[4.5] JONAH, S., et al, Monte Carlo simulation of core physics parameters of the Nigeria Research Reactor-1, Annals of Nuclear Energy 34 (2007) 953-957.

[4.6] U.S. DEPARTMENT OF ENERGY, Fundamentals Handbook: Nuclear Physics and Reactor Theory, DOE-HDBK-1019/2-93, Washington, D.C. (1993).

[4.7] LIVERHANT, S.E., Elementary Introduction to Nuclear Reactor Physics; John Wiley and Sons (1960).

[4.8] AKAHO, E.H.K., MAAKUU, B. T., Simulations of Reactivity Transients in a Miniature Neutron Source Reactor Core, Nuclear Engineering and Design, (2002) 213, 31-42.

[4.9] LAMARSH, J.R., BARATTA, A.J., Introduction to Nuclear Engineering (3rd edition), Prentice-Hall (2001).

[4.10] BUTTERWORTH, D., HEWITT, G.F., Two Phase Flow and Heat Transfer, Harwel Series: Oxford University Press, (1978).

[4.11] LE CORRE, J.-M., YAO, S.-C., AMON, C.H.; Two-phase flow regimes and mechanisms of critical heat flux under subcooled flow boiling conditions (2009). Nuclear Engineering and Design 240 (2010) 245–251.

[4.12] INTERNATIONAL ATOMIC ENERGY AGNCY, Research Reactor Core Conversion from the Use of Highly Enriched Uranium to the Use of Low Enriched Uranium Fuels Guide book, IAEA-TECDOC-233, IAEA, Vienna (1980) Appendix A.

[4.13] GRAVES, H.W., Jr., Nuclear Fuel Management, John Wiley and Sons, (1979).

[4.14] OLSON, A.P., KALIMULLAH, M., A Users Guide to the PLTEMP/ANL V4.1 Code, Global Threat Reduction Initiative (GTRI) Program, Nuclear Engineering Division, Argonne National Laboratory, Chicago, IL, USA, (2011).

[4.15] WOODRUFF, W.L., Evaluation and Selection of Hot Channel (Peaking) Factors for Research Reactors Applications," CONF-8709189–2, Intl. Mtg. on Reduced Enrichment for Research and Test Reactors (RERTR), Buenos Aires, Argentina, September 28 to October 2, (1987).

[4.16] WOODRUFF, W.L, The PARET code and the analysis of the SPERT I transients, Argonne National Laboratory. RERTR/TM-4 (1982).

[4.17] OBENCHAIM, C.F., PARET – A Program for the Analysis of Reactor Transients, IDO-17282 (1969).

[4.18] OLSON, A.P., Jonah, S.A., MNSR Transient Analysis and Thermal-Hydraulic Safety Margins for HEU and LEU Cores using PARET, in Intl. Mtg. on Reduced Enrichment for Research and Test Reactors, Prague, Czech Republic, Sep. 23-27, (2007).

[4.19] CLANCY, B.E., CONNOLLY, J.W., HARRINGTON, B.V., An analysis of power transients observed in SPERT I reactors. Part I. Transients in aluminium plate-type reactors initiated at ambient temperature, AAEC, E345 (1975).

[4.20] NUCLEAR ENERGY AGENCY, Data Bank, Computer program services, Computer program NESC0555 PARET-ANL(NESC), http://www.oecd-nea.org/tools/abstract/detail/nesc0555/

[4.21] AMPOMAH-AMOAKA, E., AKAHO, E.H.K., ANIM-SAMPONG, S., NYARKO, B.J.B., Transient Analysis of Ghana Research Reactor-1 Using PARET/ANL Thermal–Hydraulic Code, Nuclear Engineering and Design 239 (2009) 2479–2483.

[4.22] INTERNATIONAL ATOMIC ENERGY AGENCY, Derivation of the Source Term and Analysis of the Radiological Consequences of Research Reactor Accidents, IAEA Safety Reports Series No. 53, IAEA, Vienna (2008) 100–101.

[4.23] PFEIFFER, P.A., Analysis Method for Dose Assessment, draft ANL/RERTR/TM-08-01, Version 1.1 (2008).

[4.24] INTERNATIONAL ATOMIC ENERGY AGENCY, Radiation Protection and Safety of Radiation Sources: International Basic Safety Standards, IAEA Safety Standards No. GSR Part 3, IAEA, Vienna (2014).

5. ANALYSIS REPORT FOR CONVERSION OF THE NIGERIAN MNSR NIRR-1 TO LEU FUEL: 2006–2012

5.1. INTRODUCTION

The Nigeria MNSR named Nigeria Research Reactor-1 (NIRR-1), is a low power research reactor with a nominal thermal power of 31 kW. It is a small, safe nuclear facility that employs HEU fuel, a light water moderator and coolant, and a beryllium reflector. Cooling is achieved via natural convection. The reactor is designed, manufactured and installed by CIAE. It is designed for use in universities, hospitals and research institutes mainly for NAA, limited production of short lived radioisotopes, and training. The reactor is located at the Centre for Energy Research and Training (CERT), Ahmadu Bello University, Zaria, Nigeria.

The main specifications of NIRR-1 are shown in Table 5.1. The reactor is a tank-in-pool type reactor. The reactor complex contains five major components. These are the reactor assembly, control console, auxiliary systems, irradiation system and pool. The reactor assembly consists of the reactor core, beryllium reflector, small fission chambers for detecting neutron flux, one central control rod and its drive mechanism, and thermocouples for measuring inlet and outlet temperatures of the coolant. Five inner irradiation tubes are installed within the beryllium annulus, while five outer irradiation tubes are also installed outside the beryllium annulus. The reactor vessel is a cylindrical aluminium alloy container, 0.6 m in diameter and 5.6 m high. The container, which is built in two sections, is suspended in a stainless steel-lined pool of water made of reinforced concrete. The core consists of fuel elements arranged in a fuel cage. The cage is inside an annular beryllium reflector and rests on a lower beryllium reflector plate. The volume of the vessel is 1.5 m^3. The fuel elements consist of an enriched uranium–aluminium alloy extrusion, clad with aluminium. They are arranged in ten multi-concentric circle layers at a pitch distance of 10.95 mm. The element cage consists of two grid plates, four tie rods and a guide tube for the control rod. The grid plates and tie rods are connected by screws. The total number of lattice positions is 350, and the number of fuel elements is 347. The remaining positions are filled with dummy aluminium elements. A detailed desciption of NIRR-1, including relevant diagrams, can be found in the NIRR-1 Final Safety Analysis Report [5.1].

The beryllium annulus and lower reflector are spaced to form the lower orifice, which controls water flow through the core. The top plate of the core and annulus are spaced to form the upper orifice.

TABLE 5.1. MAIN SPECIFICATIONS OF NIRR-1

Type	Tank in pool
Nominal core power	31 kW_{th}
Coolant and moderator	Deionized light water
Loading of ^{235}U in core	1006.65 g
Reflector	Metallic beryllium
Excess reactivity-cold, clean	3.77 mk
Daily operation fluence in inner irradiation sites	$<9 \times 10^{15}$ cm^{-2}
Fuel life in core	$>3.24 \times 10^{19}$ cm^{-2}
Neutron flux at inner irradiation sites	1×10^{12} $cm^{-2}s^{-1}$, stability ±1%, horizontal and vertical variation <3%
Number of irradiation sites	10 sites (5 inner and 5 outer), 6 sites connected (4 inner and 2 outer)
Control rod	1 stainless steel clad cadmium absorber
Reactor operation mode	Manual and automatic
Temperature in irradiation sites	Inner site <54°C; outer sites <40°C (at pool temperature of 20°C).
Core reactivity temperature coefficient	-0.1 mk/°C for core temperature of 15—40°C
Average radiation dose in reactor hall	<1 μSv/h

An aluminium tray holds the upper reflector, which is designed to hold semicircular beryllium shims. Beryllium shims can be added when needed to compensate for fuel burnup and fission product poisoning. The reactor is designed to have a self-limiting power excursion characteristic. A fail-safe principle is adopted in the design of the reactor control system. The control console consists of the reactor control system, the radiation monitoring system readouts, a monitoring panel of auxiliary system and a power supply system for the console. There are two control modes for the reactor. In the first mode, start-up or shutdown of the reactor is controlled manually by the operator. In the second mode, the reactor is controlled automatically by the computer. A microcomputer closed loop control system has been developed for the reactor with an IBM compatible computer. In addition to controlling the reactor, the system also acts as a data acquisition and reactivity monitoring system.

The reactor incorporates several auxiliary systems. For example, two purification systems for the reactor vessel and pool water are used for controlling water quality. A reactor gas purge system is employed to pump out the gas accumulated in the top space of the reactor vessel. There are also monitoring systems for water temperature and level, and a radiation detecting system for measuring the dose level at the top of the reactor vessel, the working area of the reactor hall and the reactor water deionizer column. Other auxiliary systems for the utilization of the reactor have been installed such as pneumatic transfer systems. The system known as type A is suitable for irradiation for medium and long time periods. Type B, a multifunction capsule transfer system, is coupled to four irradiation tubes. A multi-channel analyser computer system is available for NAA.

The report contains the results of design and safety analyses performed by CERT under the aegis of the IAEA CRP, 2006–2012, for the conversion of NIRR-1 from the use of HEU fuel to LEU fuel under nominal and accident conditions. In order to provide comparisons between the proposed LEU core and the initial HEU core, thorough analyses were performed for both cores.

5.2. NEUTRONICS STUDIES

Under the neutronics studies, MCNP code was used for the neutronics analysis of the HEU core in order to establish the MCNP HEU model. The established model was used to qualify LEU fuels for the conversion of NIRR-1 from HEU to LEU. Furthermore, a computational method was developed to assess the impact of conversion to LEU on utlization. In order to address the single point failure posed by the use of a single control rod in both the commercial and prototype MNSR, the inclusion of two additional control rods in the design of MNSR facilities was carried out using the established MNCP model of NIRR-1.

5.2.1. MCNP HEU model

MCNP was used for the neutronics analysis of the HEU core in order to establish the MCNP HEU model. Detailed geometry of the HEU-fuelled core of the reactor was created in a three dimensional Cartesian coordinate system. An MCNP input deck was constructed using engineering drawings of the reactor. The core centre was taken as the origin (0, 0, 0) in the x and y planes, and the centre of the fuel pin in the z plane. Individual cells were defined explicitly for each of the following reactor components: 347 fuel pins and three aluminium dummies, a control rod, the light water moderator, grid plates, beryllium reflectors, a shim tray, irradiation channels, reactivity regulators, fission chambers and the start-up guide tube (also known as the slant tube). The temperature measuring devices were defined as separate cells, and all details of the aluminium support structure, reactor vessel, reactor pool and stainless steel liner were included. Geometric representation of the reactor in the input deck was read by MNCP code, and the result is depicted in Fig. 5.1.

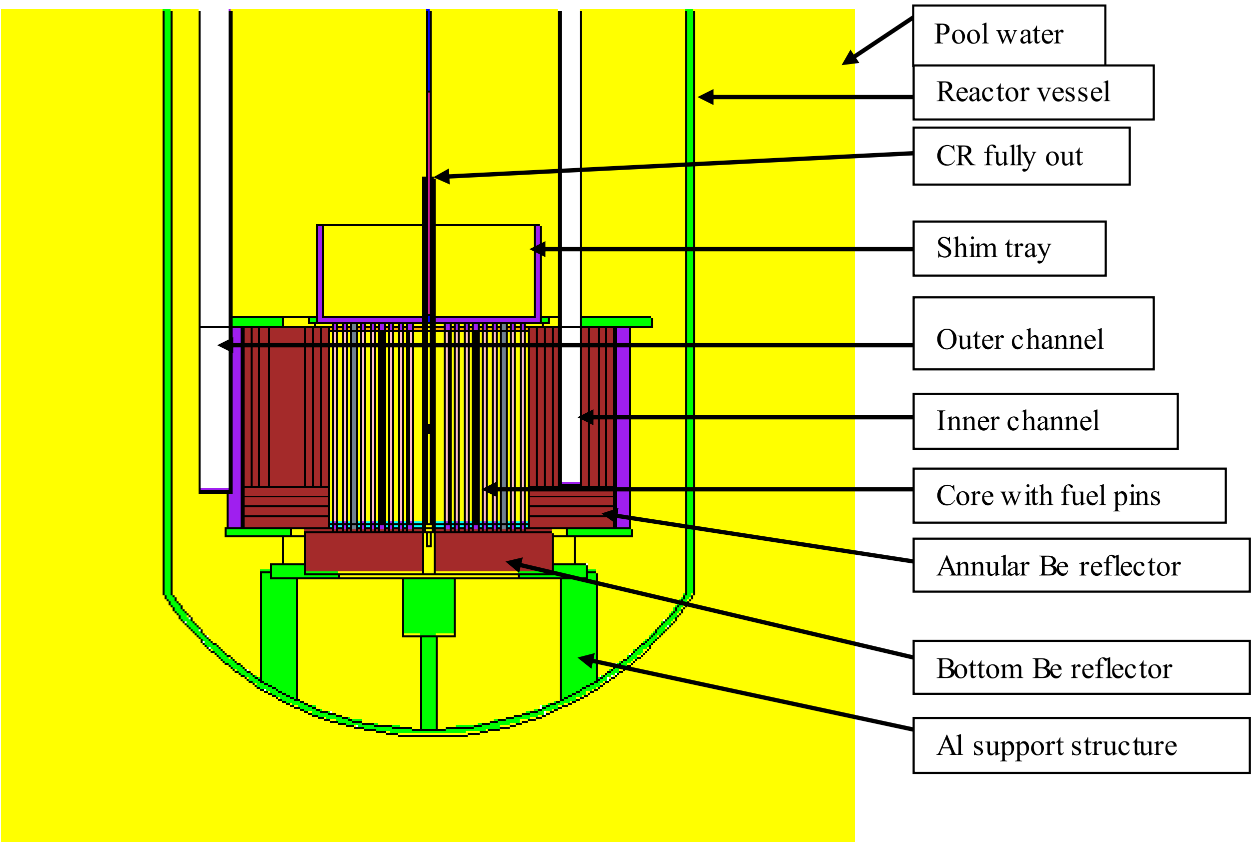

FIG. 5.1. A geometric representation of NIRR-1 in x–y plane from MCNP (Reproduced from Ref. [5.4] with permission courtesy of Centre for Energy Research and Training, Nigeria).

The MCNP physical model for an HEU-fuelled NIRR-1 was used to calculate the clean cold core excess reactivity, control rod worth, shut-down margin, delayed neutron fraction, neutron flux and energy spectrum in the irradiation channels. Results obtained were benchmarked by data in the Final SAR published by Jonah, et al. [5.2].

5.2.2. LEU feasibility search

A major objective of the MCNP modelling of NIRR-1 was to perform a feasibility study for conversion to LEU. Subsequently, a number of LEU fuel options were investigated for NIRR-1 in particular and an MNSR in general. In this regard, five LEU fuels described in Table 5.2 were used to substitute the HEU in the original input deck. Since NIRR-1 is specifically designed for NAA, conversion to LEU should not compromise its utilization capacity, especially the neutron flux and spectrum distributions. Consequently, the methodology and MCNP model that were used in the neutronic analysis of the HEU were also used to search for the LEU options. The first step in the conversion study was to determine the impact of replacing HEU fuel with LEU in the same core configuration.

TABLE 5.2. CHARACTERISTICS OF FUELS CONSIDERED IN THIS STUDY

Fuel type	Density of meat (g/cm^3)	Meat diameter (mm)	Cladding thickness (mm)	^{235}U core loading (g)	k_{eff}
HEU U–Al, 90.2%	3.456/0.92	4.3	Al/0.6	1085	1.00476
LEU U_3Si–Al, 19.75%	6.41/4.42	4.74	Al/0.38	1228	1.00476
LEU U_3Si, 19.75%	7.394/5.49	4.3	Al/0.6	1257	1.00476
LEU U_9Mo, 19.75%	8.21/5.95	4.3	Al/0.6	1361	1.00478
LEU UO_2 pellets, 347 pins, 12.45%	10.6/9.35	4.3	Zr/0.6	1349	1.00476
LEU UO_2 pellets, 206 pins, 19.75%	10.6/9.35	4.3	Zr/0.6	1270	1.00476

From results obtained, it was determined that the conversion of NIRR-1 to LEU would be feasible with UO_2 fuel enriched to 12.5%. For an LEU-fuelled core, however, the reactor power level would have to be raised by 10% from the current value of 31 kW in order to match the nominal flux level for MNSRs. Similarly, the control rod must be redesigned to compensate for the loss of reactivity worth in order to increase the shutdown margin for an LEU core. A detailed methodology used, and the results obatined can be found in Jonah, et al. [5.3].

The LEU core arrangement is identical to the HEU core except that: 1) the LEU fuel elements are all 12.5 wt% ^{235}U enriched UO_2 pellets clad with Zircaloy-4; 2) the number of LEU fuel elements is 348 with two Zircaloy-4 dummy elements completing the 350 lattice positions; 3) the LEU fuel element cage is two Zircaloy-4 grid plates; and 4) differing dimensions of the control rod. A comparison of the main characteristics of the HEU and LEU cores are given in Table 5.3. Results of neutronics data obtained for the HEU core and the proposed LEU core are provided in Table 5.4 for the flux performance, and Table 5.5 for the reactivity worth of a top beryllium shim. Furthermore, the reactivity worth of top beryllium shims for the HEU core, measured and calculated, are compared with calculated data for the LEU core in Fig. 5.2.

TABLE 5.3. A COMPARISON OF THE MAIN SPECIFICATIONS OF THE HEU CORE AND PROPOSED LEU CORE OF NIRR-1

SPECIFICATION	HEU	LEU
Type	Tank in pool	Tank in pool
Nominal core power (kW_{th})	31	34
Coolant/Moderator	Deionized light water	Deionized light water
Loading of ^{235}U in core (g)	1006.65	1357.86
Reflector	Metallic beryllium	Metallic beryllium
Excess reactivity: cold, clean (mk)	3.77	4.02
Neutron flux at inner irradiation sites	1×10^{12} $cm^{-2}s^{-1}$, stability ±1%, horizontal and vertical variation <3%	1.04×10^{12} $cm^{-2}s^{-1}$, stability ±1%, horizontal and vertical variation <3%
Daily operation fluence in inner irradiation sites	$<9 \times 10^{15}$ cm^{-2}	$<9 \times 10^{15}$ cm^{-2}
Fuel life in core (fluence)	$>3.24 \times 10^{19}$ cm^{-2}	$>3.24 \times 10^{19}$ cm^{-2}
Number of irradiation sites	10 sites (5 inner and 5 outer)	10 sites (5 inner and 5 outer)
Control rod	1 stainless steel clad cadmium absorber	1 stainless steel clad cadmium absorber
Reactor operation modes	Manual and automatic	Manual and automatic
Temperature in irradiation sites	Inner site < 54°C; outer sites <40°C at pool temperature of 20°C	Inner site < 54°C; outer sites <40°C at pool temperature of 25°C
Core reactivity temperature coefficient	–0.1 mk/°C for core temperature 15–40°C	–0.1 mk/°C for core temperature 15–40°C
Average radiation dose in reactor hall (μSv/h)	<1	<1

TABLE 5.4. COMPARISON OF NEUTRON FLUX DATA AT INNER IRRADIATION CHANNELS (IC), OUTER IRRADIATION CHANNELS, FISSION CHAMBERS AND SLANT TUBE IN NIRR-1

Location	Thermal 0–0.625 eV		Epithermal 0.625 eV–0.825 MeV		Fast 0.825–20 MeV	
	Inner IC	Outer IC	Inner IC	Outer IC	Inner IC	Outer IC
HEU 90.2%	1.16±0.01	0.66±0.01	1.29±0.01	0.19±0.01	0.27±0.01	0.04±0.03
UO_2 12.45%	1.04±0.01	0.62±0.01	1.26±0.01	0.18±0.01	0.26±0.01	0.04±0.03
Location	Fission chamber	Slant tube	Fission chamber	Slant tube	Fission chamber	Slant tube
HEU 90.2%	1.19±0.01	0.026±0.02	1.33±0.01	0.004±0.05	0.26±0.01	0.002±0.04
UO_2 12.45%	1.06±0.01	0.024±0.02	1.28±0.01	0.003±0.05	0.25±0.01	0.002±0.04

TABLE 5.5. COMPARISON OF REACTIVITY WORTH OF THE TOP BERYLLIUM REFLECTOR FOR HEU AND LEU CORES

Thickness of top Be reflector (cm)	HEU (δk, mk)		LEU (δk, mk)
	Measured	Calculated MCNP	Calculated MCNP
1	5.6	5.32	5.45
2	9.7	9.18	9.26
3	12.4	12.2	11.59
4	14.3	14.44	13.65
5	15.6	16.05	15.23
6	16.6	17.35	16.38
7	17.3	18.17	17.29
8	17.8	18.82	17.84
9	18.1	19.41	18.35
10	18.4	19.72	18.70
10.95	18.5	20.00	18.95

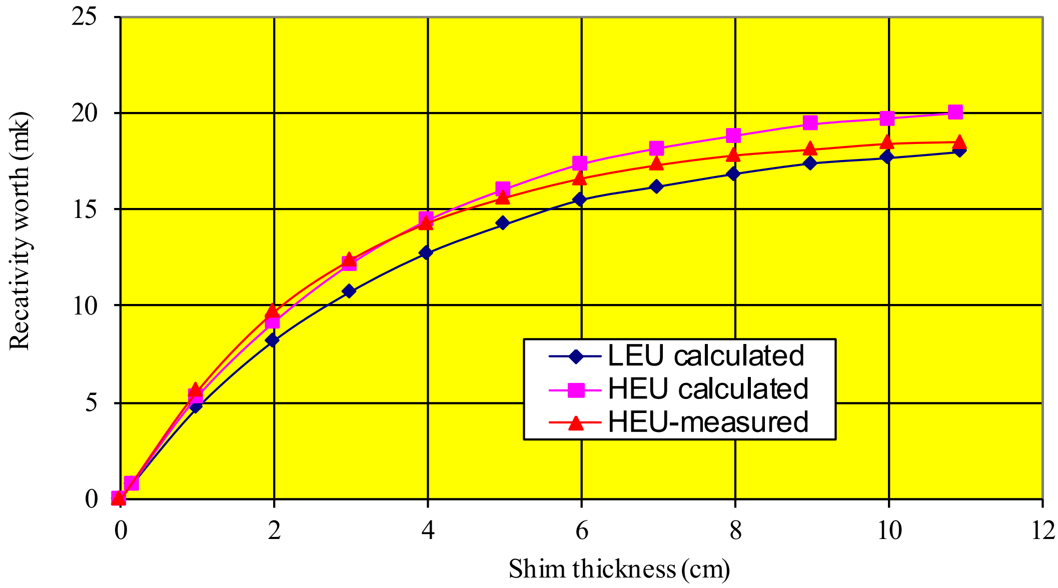

FIG. 5.2. Reactivity worths of top beryllium shims for HEU and LEU cores (Reproduced from Ref. [5.2] with permission courtesy of Centre for Energy Research and Training, Nigeria).

5.2.3. Impact of conversion on utilization

In order to further assess the performance of the proposed LEU fuel with respect to NAA, a computational method has been developed for the calculation of neutron spectrum parameters in the irradiation channels. MCNP code was used to calculate the neutron spectral distributions in a 640 group energy structure from 10^{-10} MeV to 20 MeV. The calculated data in combination with the neutron capture cross-section data of some dosimetry reactions extracted from the ENDF-VII data library was used to determine the cadmium ratios, which were then used to deduce the f and α parameters in the inner and outer channels of the current HEU core, as well as the proposed LEU core. In order to verify the calculations, measured experimental data for the current HEU core is compared to the calculations. The simulated energy-dependent neutron flux distributions obtained by MNCP in an inner and outer irradiation channel of NIRR-1 HEU core are displayed in Fig. 5.3. The methodology and details of the computational procedures have been published by Jonah, et al. [5.4]. A summary of results obtained depicted in Table 5.6 indicate slightly 'hardened' neutron spectra distributions in the inner and outer irradiation channels of the proposed LEU core with no significant impact on utilization.

TABLE 5.6. COMPARISON OF NEUTRON SPECTRUM PARAMETERS OF NIRR-1 HEU AND LEU CORES

	α		f	
Core	Inner	Outer	Inner	Outer
HEU (experiment)	–0.052±0.002	0.029±0.005	19.2±0.5	48.3±3.3
HEU (calculated)	–0.056±0.004	0.021±0.005	17.2±1.1	46.7±2.9
LEU (calculated)	–0.047±0.006	0.028±0.006	14.7±0.7	43.7±2.8

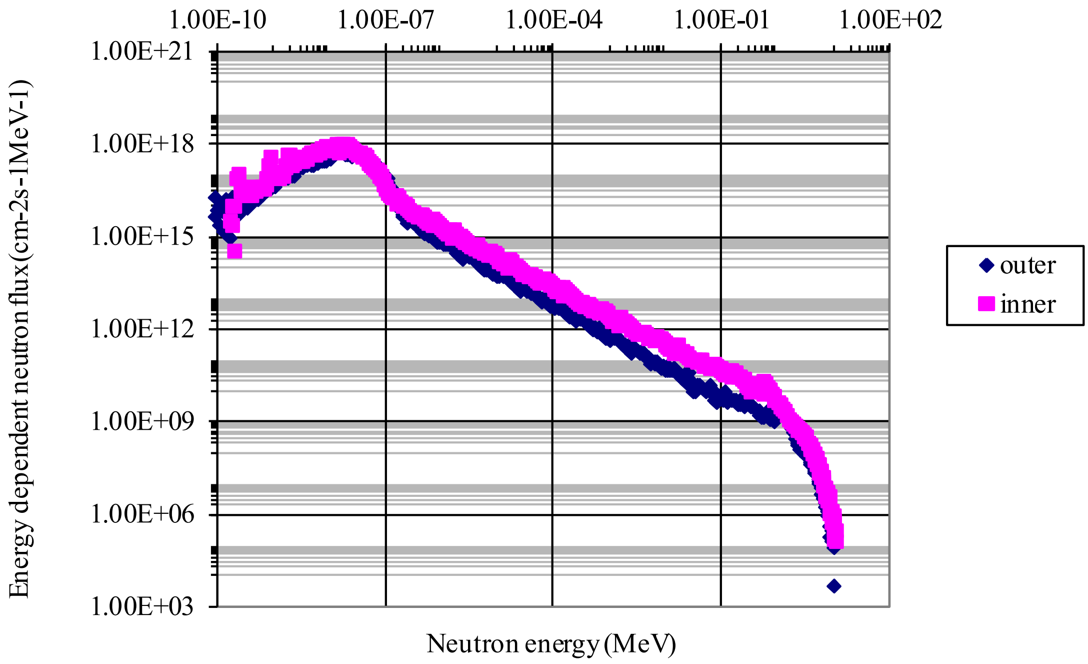

FIG 5.3. Comparison of MCNP simulated energy dependent neutron flux distributions in an inner and an outer irradiation channel of NIRR-1 (Reproduced from Ref. [5.4] with permission courtesy of Centre for Energy Research and Training, Nigeria).

5.2.4. Neutronics analysis of two additional control rods for improved MNSR safety

All MNSR facilities are equipped with a single control rod.This serves to both compensate for the excess reactivity necessary for long term core operation and also to adjust the power level of the reactor, in order to bring the core to power, follow load demands and shut down the reactor. Because the movement of the single control rod is controlled by mechanical clutches, it is possible for the mechanical systems to malfunction. Therefore, this may prevent the control rod from performing its intended functions, especially the safety function. In the case of malfunction of the single control rod such as the rod being stuck, emergency shutdown of the reactor is achieved by pumping cadmium rabbits and strings into irradiation channels. Pumping of cadmium rabbits may not be achievable if there is pressure failure. There is a possibility of single point failure which could lead to excessive power excursion and ultimately to radiation exposure of personnel in the process of inserting the cadmium strings. Even though the MNSR is inherently safe due to the high negative temperature coefficient of reactivity, which provides self limiting power excursion characteristics, reactor safety experts have recommended redundancies in design to enhance reliability of systems important to safety.

Consequently, in order to satisfy the current single-point failure posed in MNSR design, the MCNP code was used to simulate NIRR-1 HEU and the proposed LEU cores with two additional control rods to enhance safety. The two additional safety rods are of the same material composition as the main central control rod, but with differing dimensions. The following reactor core physics parameters impacting on safety of the reactor were calculated: control rod worth for each rod; core excess reactivity; shutdown margin; and some kinetic parameters. Details of the methodology adopted in the design of additional safety rods for the current HEU core and proposed LEU core are contained in Ibrahim et al., 2012 [5.5].

Results displayed in Table 5.7 indicate that it would be possible to introduce additional safety control rods to enhance the safety of the MNSR, with little or no modification to the existing core configuration.

TABLE 5.7. MODIFIED AND UNMODIFIED NEUTRONICS DATA FOR NIRR-1 HEU CORE

Parameter	Modified	Unmodified
Rods-out (k_{eff})	1.00474±0.00021	1.00476 ±0.00021
Main Rod-In (k_{eff})	0.99712±0.00021	0.99712±0.00021
A-In k_{eff}	1.00164±0.00021	No data
B-In k_{eff}	1.00170±0.00021	No data
A and B-In (k_{eff})	0.99856±0.00021	No data
Core excess reactivity ρ_{ex} (mk)	4.72±0.05	4.74±0.05
Worth of each rod (mk)	Main A B 7.62 3.12 3.04	7.61
Worth for ASCRs (mk)	6.16	
Shutdown margin (mk)		
Main CR	2.90	2.87
A and B	1.44	No data
$B_{eff} \times 10^{-3}$	8.37±0.09	8.37±0.09
Φ_{th}(n/cm^{2}s) × 10^{12}inner	1.16±0.01	1.16±0.01
Φ_{th}(n/cm^{2}s) × 10^{12} outer	0.66±0.01	0.66±0.01

5.3. THERMAL-HYDRAULICS STUDIES

Under the thermal-hydraulics investigations, the PLTEMP/ANL code version 4.1 [5.6] was used to calculate some steady state parameters of HEU and LEU cores for NIRR-1. Data obtained for the HEU core compare well with measured data and those from the manufacturer. For the transient analyses of the two cores, PARET/ANL code version 7.3 [5.7] was used to simulate reactivity insertion transients, including the insertion of 3.77 mk reactivity This is the maximum credible insertion demonstrated during the on-site commissioning of NIRR-1.

5.3.1. Steady state temperature and heat flux parameters using PLTEMP code

PLTEMP/ANL code version 4.0 (2010) was used to perform thermal-hydraulic analysis of the NIRR-1 HEU core and the proposed UO_2 LEU fuel core, with 348 fuel pins at a nominal power of 34 kW. The steady state operational parameters and safety margins were detemined for the two cores. Measured data for an HEU core having 347 fuel pins in the core configuration at a nominal power of 31 kW were used to validate the calculated data. The steady state operational parameters include fuel, cladding and coolant temperatures as functions of power. Safety parameters such as peak heat flux, minimum CHF, minimum flow instability power ratio (FIR) and margin to ONB were also studied.

The PLTEMP/ANL series of codes have been frequently used to perform thermal-hydraulic analysis of research reactors for the determination of steady state operational parameters and safety margins. The steady state operational parameters include fuel, clad, and coolant temperatures as functions of power. The code also calculates radial and axial distributions of fuel, cladding and coolant temperatures in a fuel assembly. The fuel assembly consists of several coaxial fuel tubes cooled by light water or heavy water flowing in the annular gaps, i.e. coolant channels, between adjacent fuel tubes. The number of coolant channels in the fuel assembly is always one more than the number of fuel tubes. This difference is required in the code input data. The innermost boundary of the first channel and the outermost boundary of the last channel are assumed to adiabatic in the multi-tube radial heat transfer model of the code.

Results in Table 5.8 show that measured data for the current HEU core compare well with calculated data obtained by the PLTEMP code using the 2006 CHF Look-up Table in Ref. [5.8]. Table 5.9 contains the calculated thermal-hydraulic steady state operational characteristics and safety margins for NIRR-1, with the proposed UO_2 LEU fuel in 348 pins.

TABLE 5.8. COMPARISON OF STEADY STATE THERMAL-HYDRAULIC DATA AND SAFETY MARGINS FOR NIRR-1

Parameters	Reactor power 31 kW		Reactor power 15.5 kW	
	Measured	PLTEMP	Measured	PLTEMP
T_{in} (°C)	24.5	24.5	24.5	24.5
T_{out} (°C)	45.2	44.13	37.72	36.93
T_{clad} (°C)	—	99.75	—	70.18
$ONBR_{min}$	—	1.234	—	1.807
$DNBR_{min}$	>2.5 (CIAE)	11.41	—	18.49
FIR	—	4.476	—	6.284
Core flow (kg/s)	—	0.3755	—	0.2891

Data was obtained using the Bergles–Rohsenow boiling correlation option and 2006 CHF Look-up Table with iteration option ITRNCHF enabled [5.8].

TABLE 5.9. CALCULATED STEADY STATE THERMAL-HYDRAULIC DATA AND SAFETY MARGINS FOR LEU-FUELLED NIRR-1

Parameters	Reactor power 34 kW	Reactor power 17 kW
T_{in} (°C)	24.5	24.5
T_{out} (°C)	44.45	37.61
T_{clad} (°C)	108.8	75.9
$ONBR_{min}$	1.10	1.79
$DNBR_{min}$	10.92	18.48
FIR	4.32	6.70
Core flow (kg/s)	0.389	0.299

5.3.2. Transient analysis using PARET code

The PARET code, which was originally developed for the analysis of the SPERT-III experiments for temperatures and pressures typical of power reactors, provides a coupled thermal, hydrodynamic and point kinetic capability [5.9]. It presents a convenient means of assessing the various models and correlations proposed for use in the analysis of research reactor behaviour. Among other things, the provision of a simple external loop model in version 7.5 of the PARET/ANL code allows the simulation of heat flow regimes that are particular to MNSRs. Consequently, a thermal-hydraulic closed loop can now be modelled. This is an improvement over old versions of the code that was previously used in this work.

In the input file, control rod reactivity insertion is simulated with rate and delay time settings, including trip points for overpower. In this investigation, an input file of NIRR-1 HEU model was constructed from the Final SAR [5.1], while the kinetic parameters and reactivity feedback coefficients were obtained from MCNP runs performed on the reference HEU model [5.2]. A two channel model was utilized with one fuel pin taken as the hottest channel, while the remaining 346 fuel pins were assumed as the average channel. Axial power distribution was represented by 21 mesh points, and a radial power peaking factor of 1.24, determined from neutronics calculations by the MCNP, was used. Data of thermal conductivity and heat capacity of the fuel meat and aluminium clad was obtained from IAEA TECDOC 643 [5.10]. All calculations have been carried out with a coolant inlet temperature of 24.5°C and inlet pressure of 1.7237 bar, corresponding to the pressure head of the water in the reactor vessel above the inlet orifice.

For reactivity insertion transients, a period of 3500 s was used with all protection and safety circuits switched off. A time delay of 0.15 s was taken between attainment of the trip level and the start of shutdown reactivity insertion. During the commissioning of NIRR-1, step and ramp reactivity insertions of 2.23 mk and 3.77 mk, i.e. the clean cold core excess reactivity, were investigated. To achieve the step insertion of 2.23 mk reactivity, cadmium rabbits of equivalent reactivity worth were pumped out of the system using the pneumatic transfer system. To achieve the reactivity insertion of 3.77 mk the control rod was fully withdrawn as rapidly as possible from the fully inserted position. Details of the reactivity insertion measurements performed to demonstrate the inherent safety features of the reactor have been enumerated in the Final SAR. In the case of a 0.32 mk insertion performed for safeguards, the reactor was manually operated at a power level of 3 W, and the control rod was withdrawn by approximately 8 mm from the critical position, which is equivalent to a reactivity insertion of 0.32 mk. Results obtained for the HEU core have been published [5.11]. A comparison of calculated and measured data for the power excursion profiles for the reactivity insertions of 3.77 mk and 2.23 mk are shown in Figures 5.4—5.5 respectively. Furthermore, the calculated power excursion characteristics for the HEU and LEU cores are displayed in Fig. 5.6.

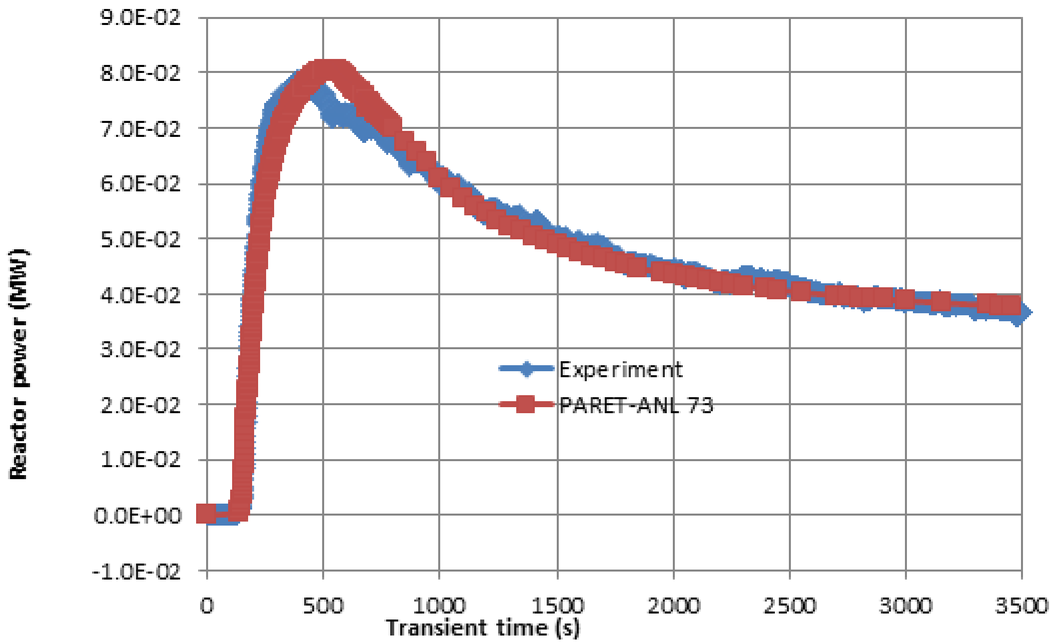

FIG. 5.4. Comparison of measured and calculated power excursion for reactivity insertion of 3.77 mk in NIRR-1 (Reproduced from Ref. [5.11] with permission courtesy of Centre for Energy Research and Training, Nigeria).

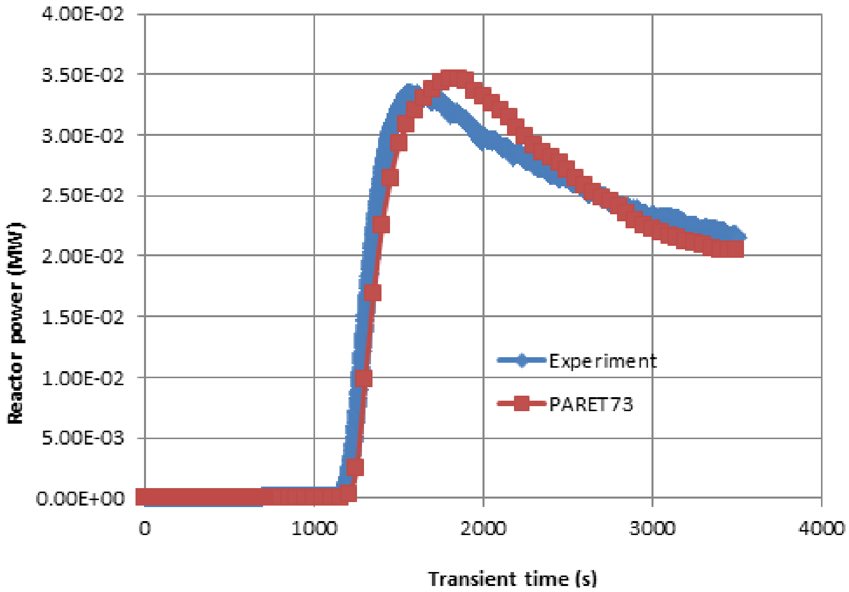

FIG. 5.5. Comparison of measured and calculated power excursion for a reactivity insertion of 2.23 mk in NIRR-1 (Reproduced from Ref. [5.11] with permission courtesy of Centre for Energy Research and Training, Nigeria).

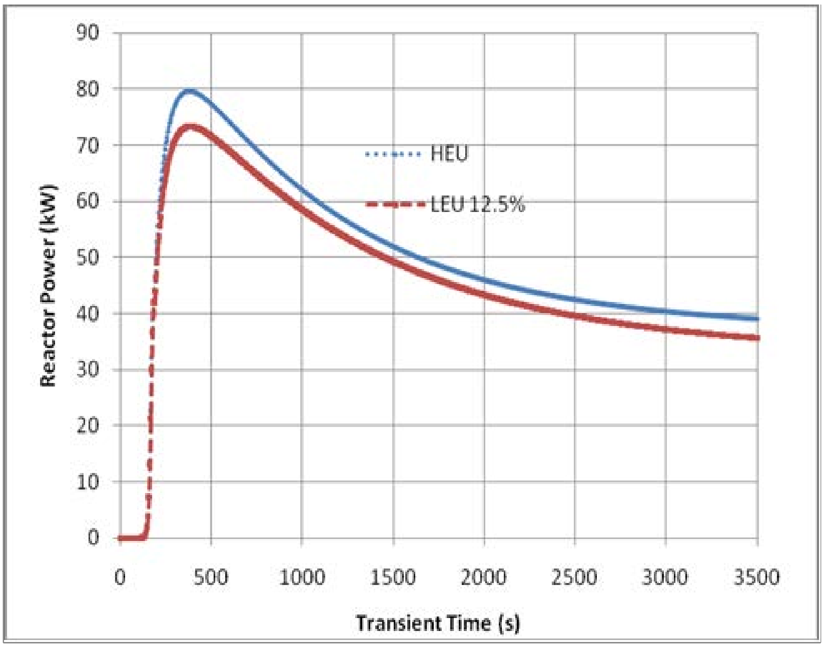

Fig. 5.6. Time vs power for a 3.77 mk reactivity insertion with HEU and LEU fuel (Reproduced from Ref. [5.12] with permission courtesy of Centre for Energy Research and Training, Nigeria).

5.4. RADIOLOGICAL CONSEQUENCES ANALYSES

For the purpose of understanding the nature of severe accidents and assessment of accident scenarios involving the release of radioactive material at the NIRR-1 facility, the source term inventory of the core during the normal operation must be known. Inventory data for NIRR-1 HEU and LEU cores were calculated for the SAR for research reactors, and is based on the assumption that a hypothetical accident results in the release of some portion of the inventory of radioactive materials to the atmosphere. In this section, the DBA and BDBA analyses scenarios for NIRR-1 HEU and LEU cores.

5.4.1. DBA

5.4.1.1. Scenario

The DBA for NIRR-1involves pitting corrosion of the cladding, creating cladding failure in one or more fuel rods such that a hole or holes are formed totaling 0.5 cm^2 while in the water of the reactor vessel. A fraction of the fuel rod fission product inventory is released into the pool water, and a fraction of this inventory is released into the air of the reactor hall. Furthermore, part of the total fission product content of air in the reactor hall is released to the environment by leakage from the reactor building. Effective (whole body) and thyroid doses are evaluated for this scenario for reactor building leak rates of 20% per hour and 100% per hour, and compared with dose limits prescribed in the Nigeria Basic Ionizing Radiation Regulations (NiBIRR) [5.13].

5.4.1.2. Fission inventory and source term determination

The fission product inventory was calculated using the ORIGEN 2.2 [5.14]. Burnup and power distribution data were obtained from the neutronic analysis. It was assumed conservatively that the LEU core operated continuously at power level of 34 kW for its estimated life time of 903 FPEDs.

The peak and the average rod power used for the inventory analysis were 112.97 kW and 97.70 kW for the LEU core. The ^{235}U burnup at the end of core life for the fuel rod with maximum burnup, and the fuel rod with average burnup, are calculated to be 3.3% and 2.9% respectively for the LEU core. From the calculated fission product inventory, the most important isotope which contributes to the doses was selected. The source term for radioactivity in the air of the reactor hall is the inventory of one fuel assembly multiplied by the transfer factor from the fuel to the matrix material, the transfer factor from the matrix material to water and the transfer factor from water to air. However, since specific factors for each of these transfers are not available, a combined factor for transfer of fission products from the fuel matrix material to the air of the reactor building is used. The fission product inventory for the selected isotopes in one fuel assembly, the combined transfer factor and the resulting source term for use in the dose calculation are presented in Table 5.10.

TABLE 5.10. PIT CORROSION SCENARIO FISSION PRODUCT INVENTORY

Nuclide	Half-life	Inventory in pool water (Bq/cm^3)		Transfer factor: matrix material to air	Inventory in reactor hall (Bq/cm^3)
		HEU	LEU	LEU	
^{131}I	8.06 d	9.6×10^3	11.52×10^3	1×10^{-4}	1.15
^{132}I	2.26 d	4.0×10^{-1}	4.8×10^{-1}	1×10^{-4}	4.8×10^{-5}
^{133}I	20.9 h	1.5×10^4	1.8×10^4	1×10^{-4}	1.8
^{135}I	6.7 h	1.1×10^3	1.32×10^3	1×10^{-4}	1.32×10^{-1}
^{90}Sr	28.1 y	1.7×10^3	1.7×10^3	1×10^{-6}	1.7×10^{-3}
^{95}Zr	65.5 d	3.0×10^3	3.6×10^3	1×10^{-6}	3.6×10^{-3}
^{95}Nb	35.0 d	4.8×10^3	5.4×10^3	1×10^{-6}	5.4×10^{-3}
^{137}Cs	35.17 d	2.7×10^3	3.2×10^3	1×10^{-6}	3.2×10^{-3}
^{140}Ba	12.8 d	1.2×10^4	1.4×10^4	1×10^{-6}	1.4×10^{-2}
^{140}La	40.27 h	2.4×10^4	2.9×10^4	1×10^{-6}	2.9×10^{-2}
^{85}Kr	10.76 y	2.21	2.65	0.02	5.3×10^{-2}
^{133}Xe	5.29 d	2.3×10^4	2.8×10^4	0.02	5.60×10^3
^{135}Xe	9.5 h	3.3×10^3	4.0×10^3	0.02	8.0×10^1

Based on the source term for radioactivity in the air of the reactor hall in Table 5.10, radiation doses were calculated for exposed workers, members of the public, and permanent residents.

5.4.1.3. Assumptions for dose calculations

A spreadsheet based on the methodology described by Pffeifer, [5.15–5.16], was used to calculate data for evaluation of doses with the following assumptions:

— Source term is as determined in Section 5.4.1.2;
— Release of fission products occurs in a single phase of one hour duration;
— The release height for the fission products is the ground level. The dimensions of the reactor building are: height: 8.5 m; width: 7.1 m; length: 7.2 m; and volume: 434.52 m^3;
— A conservative meteorological model was used fixing the meteorological conditions to Pasquill stability class F, with 1 m/s wind speed of uniform direction for a time period 0-8 hours. Additionally, a Pasquill stability class F with a wind speed of 1 m/s of a variable direction within a 22.5° sector for a time period of 8–24 hours was utilized;
— For distances below 100 m from the reactor, the atmospheric dispersion in air and dose values are identical to the corresponding values at 100 m; and
— The ventilation system is shut down at the time of accident, so that the reactor filtration system is not in use for this scenario.

5.4.1.4. *Calculated results*

(a) Dose for maximum exposed worker

The first selected case of exposure is that of the staff members present in the reactor hall during the accident. It is assumed that the last staff member evacuates the reactor hall after five minutes. This time is adequate to take the necessary actions specified in the operating procedures. The dose rate and the activity concentrations in the air of the reactor hall during these five minutes was based on an assumed volume method in which the radiological material is dispersed evenly in the containment or confinement volume over a specified time period of one hour. To obtain the dose for five minutes the dose rate value, which is computed in mSv per hour, was divided by 12 (60 minutes / 12 = 5 minutes). The effective (whole body) dose and thyroid dose calculated are 5.9×10^{-7} mSv and 1.2×10^{-6} mSv, respectively. These results are summarized in Table 5.11.

(b) Dose for maximum exposed member of the public

The dose for the maximum exposed member of the public was evaluated for the case that a person stands during the accident at the fence that separates the CERT site from the public area. The location closest to the NIRR-1 reactor is at a distance of about 100 m. Further, it is assumed that the person stays there for two hours. After this time the area at the public perimeter of the CERT site is assumed to be evacuated by the security staff. No ingestion is assumed to take place during the considered time period. The doses are computed for two hours, which is sufficient to consider all effects due to inhalation. The effective (whole body) doses calculated are 1.3×10^{-6} mSv and 3.9×10^{-6} mSv for building leak rates of 20% and 100% per hour, respectively. For the thyroid doses, a value of 3.7×10^{-6} mSv was obtained for a building leak rate of 20% per hour and 1.0×10^{-7} mSv for a building leak rate of 100% per hour. These results are summarized in Table 5.11.

(c) Dose for maximum exposed resident

Since the closest permanently inhabited house is approximately 300 m from the NIRR-1 reactor, the radiation doses for a person living there is considered, based on the postulated accident scenario. The calculation uses the assumptions listed in Section 5.1.2. The wind is assumed to blow in the direction of the closest house as described in the assumptions. The doses are computed for 24 hours, which is sufficient to consider all effects due to inhalation. The effective (whole body) doses calculated are 1.1×10^{-6} mSv and 2.0×10^{-6} mSv for building leak rates of 20% and 100% per hour, respectively. For the thyroid doses, a value of 8.9×10^{-6} mSv was obtained for a building leak rate of 20% per hour and 4.5×10^{-7} mSv for a building leak rate of 20% per hour. These results are summarized in Table 5.11.

TABLE 5.11. CALCULATED DOSES FOR THREE EXPOSED INDIVIDUALS

Exposed individual	Exposure time	Effective (whole body) dose			Thyroid dose		
		Calculated dose (mSv)		Dose limits (mSv/yr)	Calculated dose (mSv)		Dose limits (mSv/yr)
		HEU	LEU	NiBIRR/ IAEA SS No. GSR Part 3 [5.17]	HEU	LEU	NiBIRR/ IAEA SS No. GSR Part 3 [5.17]
Maximum exposed worker	5 min	5.2×10^{-7}	5.9×10^{-7}	50	1.0×10^{-6}	1.2×10^{-6}	1250
Maximum exposed member of the public	2 h	1.2×10^{-6} [a] 3.5×10^{-6} [b]	1.3×10^{-6} [a] 3.9×10^{-6} [b]	1	3.3×10^{-6} [a] 8.9×10^{-6} [b]	3.7×10^{-6} [a] 1.0×10^{-7} [b]	25
Maximum exposed resident	24 h	9.3×10^{-7} [a] 1.8×10^{-8} [b]	1.1×10^{-6} [a] 2.0×10^{-6} [b]	1	2.3×10^{-6} [a] 4.0×10^{-6} [b]	8.9×10^{-6} [a] 4.5×10^{-7} [b]	25

[a]Calculated dose exposures for building leak rate of 20%.
[b]Calculated dose exposures for building leak rate of 100%.

The calculated effective (whole body) and thyroid doses for exposed workers and the members of the public are below the limits set by NiBIRR. Considering the conservative approach taken for the calculation of the fission product inventory (source term based on the peak power pin and was assumed to be the same in all 348 pins) and the meteorological conditions, doses for more realistic conditions will be significantly lower than the calculated values.

The airborne radioactivity released to the environment has been calculated for the combined events of the failed fuel condition assumed above, and a year of reactor operation with a failed gas purge system. The results are presented in Table 5.12.

TABLE 5.12. INVENTORIES OF RELEASES TO THE ENVIRONMENT

Nuclide	Activity (Bq)	
	HEU	LEU
^{85}Kr	3.1×10^{3}	3.7×10^{3}
^{85m}Kr	4.5×10^{4}	5.4×10^{4}
^{88}Kr	2.6×10^{3}	3.1×10^{3}
^{131m}Xe	1.1×10^{5}	1.3×10^{5}
^{133m}Xe	1.1×10^{6}	1.3×10^{6}
^{90}Sr	2.3×10^{2}	2.8×10^{2}
^{131}I	1.3×10^{7}	1.6×10^{7}
^{132}I	6.2×10^{3}	7.4×10^{3}
^{133}I	2.2×10^{6}	2.6×10^{6}
^{135}I	1.5×10^{6}	1.8×10^{6}
^{137}Cs	7.5×10^{3}	9.0×10^{3}

It can be seen from Tables 5.10 and 5.12 that the activities are higher for the LEU case, as expected. This is because of the conservative approach taken for the calculation of the fission product inventory. The values for HEU, however, were provided by the manufacturer. The assumptions used for the calculations were not provided. The power for the LEU was also raised by 10% to 34 kW.

5.4.2. BDBA

The BDBA is sometimes called the maximum hypothetical accident. The BDBA is not expected to occur and is therefore not analysed. It is described for purposes of emergency planning only, as it is always an accident more severe than the DBA.

The accident is considered with the following assumptions:

— The reactor building collapses;
— The reactor vessel and pool leak water at a rate of 4 m^3/hr;
— The reactor core is exposed to air after six hours;
— The reactor was operating at 34 kW; and
— The reactor has operated for 903 FEPD (equivalent to the core lifetime at 3.3% burnup).

Under these conditions, the reactor core would be cooled by natural circulation of air and thermal radiation. The core would not melt and radiation exposure is in the form of external exposure from the unshielded core. For the event of pit corrosion totalling an area of 5 cm^2 during this accident, the calculated fission product inventory of the core as a function of time is presented in Table 5.13.

TABLE 5.13. ACTIVITY OF CORE FISSION PRODUCTS WITH TIME

Cooling time	Estimated, total activity of core fission product mixture (TBq)	
	HEU	LEU
1 min	1.4×10^3	1.7×10^3
1 h	1.7×10^2	2.0×10^2
6 h	9.9×10^1	1.2×10^2
12 h	9.1×10^1	1.1×10^2
1 day	8.0×10^1	9.6×10^1
5 days	6.5×10^1	7.8×10^1
10 days	5.8×10^1	7.0×10^1
30 days	4.4×10^1	5.3×10^1

Assuming isotropic point sources, calculations have been performed for dose rates at various points at the top of the reactor pool, in the reactor hall, and the controlled area around the collapsed building. The results are presented in Table 5.14.

TABLE 5.14. GAMMA DOSE RATES AT DIFFERENT POSITIONS FOR THE HEU AND THE LEU CORES

Time after accident	γ radiation dose (mSv)					
	In the building				Out of the building	
	Top of reactor restricted		Reactor hall		Balcony 10 m away from core centre	
	HEU	LEU	HEU	LEU	HEU	LEU
6 h	1.7×10^{2}	2.0×10^{2}	8.9×10^{-1}	1.1	1.6×10^{-2}	1.9×10^{-2}
1 day	1.2×10^{2}	1.4×10^{2}	6.7×10^{-1}	8.0×10^{-1}	1.1×10^{-2}	1.3×10^{-2}
30 days	5.0×10^{2}	6.0×10^{2}	3.3×10^{-1}	4.0×10^{-1}	4.8×10^{-2}	5.8×10^{-2}

It can be seen from Table 5.14 that lower dose rates were observed in the LEU case.

5.5. SUMMARY AND CONCLUSION

Nigeria is a signatory to the Nuclear Non-Proliferation Treaty and as part of the non-proliferation programme, there is a global effort to convert this type of research reactor to LEU. The work performed under the CRP indicates that the NIRR-1 HEU core will be replaced by LEU fuel consisting of UO_2 with a nominal enrichment of 12.5%. The report contains the results of the design, safety and accident analyses performed for the conversion of NIRR-1 from the use of HEU to LEU fuel. The changes required for the conversion are to replace the current HEU fuel pins with LEU fuel enriched to 12.5% in ^{235}U, increase the diameter of the cadmium absorber central control rod and increase the operating power level from 31 to 34 $kW_{th.}$ The reactor control systems, auxiliary systems and facility support systems currently in operation will not be modified and are described in the current approved FSAR for the NIRR-1. This conversion safety analysis report presents the results that address steady state operations with the LEU core, neutronic and thermal-hydraulic, and the consequences of postulated accidents that could be affected by the core change. Based on the results obtained under this CRP, the conversion of the NIRR-1 to LEU fuel does not present any new potential accidents nor does the conversion increase the consequences of any of the postulated design basis accidents identified in the current approved safety analysis report. After the conversion, steady state analysis demonstrates that the reactor can be safely operated with the LEU UO_2 fuel at the increased power of 34 kW_{th}.

REFERENCES TO SECTION 5

[5.1] CENTRE FOR ENERGY RESEARCH AND TRAINING, NIRR-1 Final Safety Analysis Report (SAR), CERT, Zaria (2005).

[5.2] JONAH, S.A., LIAW, J.R., MATOS, J.E., Monte Carlo Simulation of Core Physics Parameters of Nigerian Research Reactor-1. Annals of Nuclear Energy 34 (2007) 953–957.

[5.3] JONAH, S.A., IBIKUNLE, K, LI, Y., A Feasibility Study of Low Enrichment Uranium (LEU) fuels for MNSR conversion using MCNP, Annals of Nuclear Energy, 36 (2009) 1285–1286.

[5.4] JONAH, S.A., IBRAHIM, Y.V., AJUJI, A.S., ONIMISI, M.Y., The impact of HEU to LEU conversion of commercial MNSR. Determination of neutron spectrum parameters in irradiation channels of NIRR-1 using MCNP code. Annals of Nuclear Energy, 39 (2012) 15–17.

[5.5] IBRAHIM, Y.V., ODOI, H.C., NJINGA, R.L., ADELEYE, M.O., JONAH, S.A., Monte Carlo Simulation of additional safety control rod for commercial MNSR to enhance safety, Annals of Nuclear Energy (2012).

[5.6] OLSON, A.P., KALIMULLA, M.A., Users Guide to the PLTEMP/ANL V4.1 Code, Global Threat Reduction Initiative (GTRI) Conversion Program, Argonne National Laboratory, Argonne, IL (2010).

[5.7] OLSON, A.P., Program for the Analysis of Reactor Transients, A Users Guide to the PARET/ANL V7.3 Code, Argonne National Laboratory, Argonne, IL (2009).

[5.8] GROENVELD, D.C., et al., The 2006 CHF Look-up Table, Nuclear Engineering and Design 237 (2007) 1909–1922.

[5.9] OBENCHAIN, C.F., PARET – A Program for the Analysis of Reactor Transients, AEC Research and Development Report, Reactor Technology, IDO-17282, Phillips Petroleum Company, Idaho (1969).

[5.10] INTERNATIONAL ATOMIC ENERGY AGENCY, Research Reactor Core Conversion Guidebook, Vol. 4, IAEA-TECDOC-643, IAEA, Vienna (1992) Fuels Appendices I–K.

[5.11] JONAH, S.A., Measured and simulated reactivity insertion transients characteristics of NIRR-1. Annals of Nuclear Energy, 38 (2011) 295–297.

[5.12] OLSON, A., JONAH, S.A., MNSR transient analyses and thermal-hydraulic safety margins for HEU and LEU cores using PARET, Proc. of the 29th International Meeting on Reduced Enrichment for Research and Test Reactors (RERTR), Prague, (2007).

[5.13] NIGERIAN NUCLEAR REGULATORY AUTHORITY, NiBIRR - Nigerian Basic Ionizing Radiation Regulations, The Federal Government Press, Lagos (2006).

[5.14] OAK RIDGE NATIONAL LABORATORY, The ORIGEN 2.2 Code, RSICC Computer Collection CCC-371, Oak Ridge.

[5.15] PFEIFFER, P.A., Analysis Method for Dose Assessment, DRAFT ANL/RERTR/TM-08- 01, Version 1.1 (2008).

[5.16] PFEIFFER, P.A., Microsoft Excel Spreadsheet Model for Dose Calculations, DRAFT SSDOSE 1.1 (2008).

[5.17] INTERNATIONAL ATOMIC ENERGY AGENCY, Radiation Protection and Safety of Radiation Sources: International Basic Safety Standards, IAEA Safety Standards No. GSR Part 3, IAEA, Vienna (2014).

6. THERMAL-HYDRAULIC AND TRANSIENT ANALYSIS OF THE EXISTING HEU CORE AND PROPOSED LEU CORES FOR THE IRAN ENTC MNSR USING PARET/ANL CODE

6.1. SCOPE

This report presents the results of steady state thermal-hydraulic and transient analysis of the Iranian Esfahan Nuclear Technology Centre (ENTC) MNSR, both with the existing HEU fuel and proposed LEU fuel, to investigate the inherent safety of this reactor under various conditions. The transient analysis is performed considering a reactivity insertion accident, and the thermal-hydraulic parameters, e.g. maximum temperature of the fuel, cladding and coolant, was computed to ensure compliance within the permissible limits.

6.2. METHODOLOGY

In order to carry out the steady state thermal-hydraulic and transient analyses, PARET computer code was employed. PARET [6.1] is basically a coupled neutronic–hydrodynamic heat transfer code, employing point kinetics in one-dimensional hydrodynamics and one-dimensional heat transfer. The PARET model consists of a water cooled core represented by a maximum of four fuel elements and associated coolant channels. In this study the core was divided into two regions. One region represents the hottest fuel rod with its associated flow channel and the other represents a fuel rod with a core average heat flux. This channel is divided into 19 segments in the axial direction and seven nodes in the radial direction.

In a typical thermal-hydraulic analysis, the nuclear and engineering effects can be accounted for by the use of HCFs, such as nuclear HCFs accounting for the radial and axial power peaking (F_r^N, F_a^N) in the core, and the engineering HCF (F_q^E) that arises from some engineering subfactors such as fuel fabrication tolerance. The maximum heat flux is calculated by the average heat flux at full power multiplied by the power peaking factor (F_q). The power peaking factor is determined by neutronics calculations in real conditions. The total peaking factor is the product of the radial, axial, and engineering factors, considered in a conservative manner. Therefore, according to Eq. 6.1:

$$F_q = F_r^N F_a^N F_q^E \tag{6.1}$$

Hence the maximum heat flux at the hot channel is the product of the average heat flux in the core and F_q. The required power distribution and hot channel radial and axial factors were computed by our previous neutronics calculations, and the engineering factor is omitted. The axial power profile of the HEU [6.2] and LEU cores [6.3], obtained from neutronic analysis, are given in Figs 6.1—6.3.

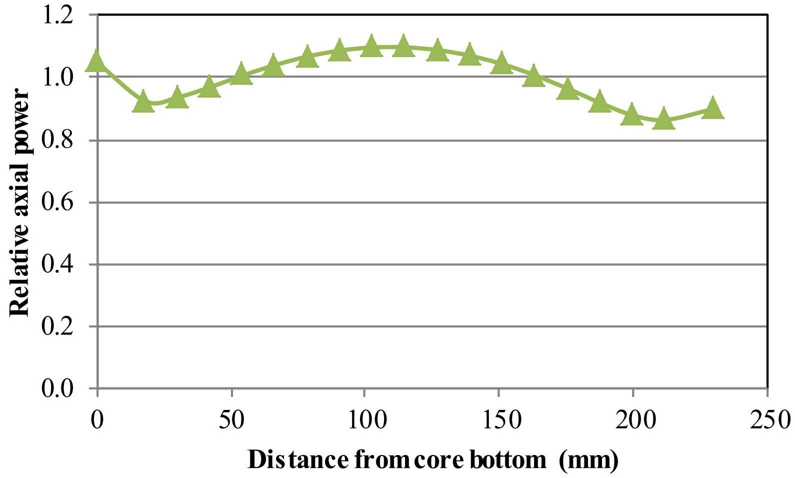

FIG. 6.1. Axial power peaking factor for the existing HEU core (Courtesy of Nuclear Science and Technology Research Institute (NSTRI), Islamic Republic of Iran).

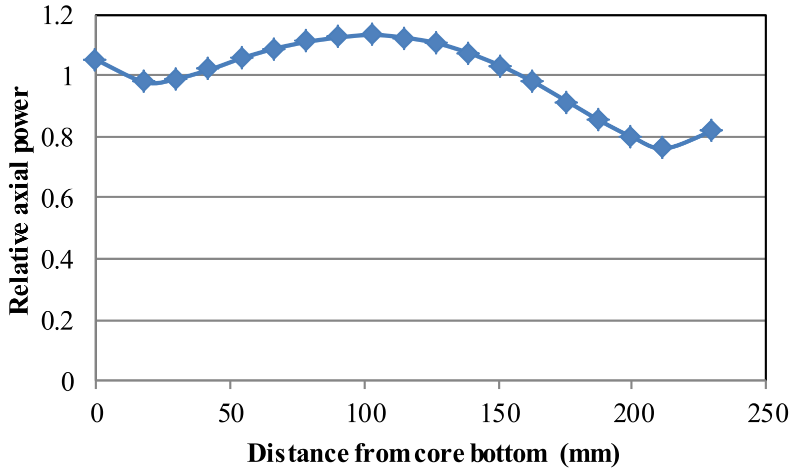

FIG. 6.2. Axial power peaking factor for the proposed LEU 12.6% core (fuel pin diameter 5.5 mm) (Courtesy of Nuclear Science and Technology Research Institute (NSTRI), Islamic Republic of Iran).

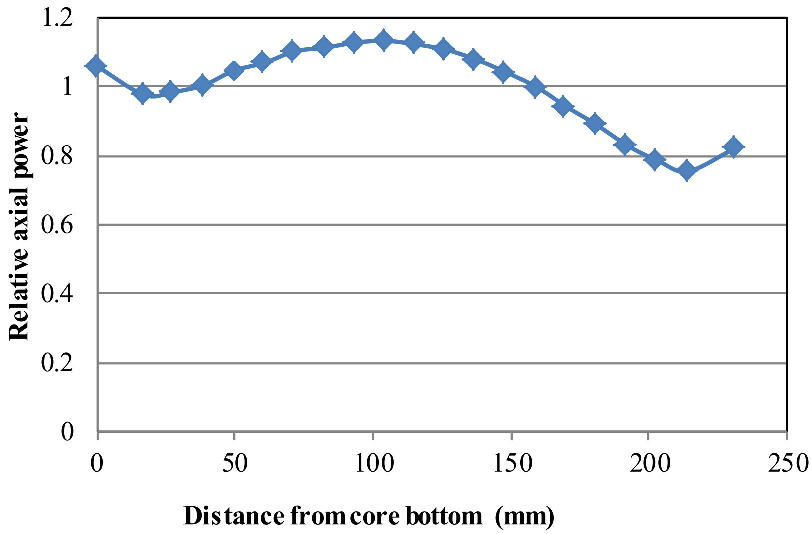

FIG. 6.3. Axial power peaking factor for the proposed LEU 12.3% core (fuel pin diameter 5.1 mm) (Courtesy of Nuclear Science and Technology Research Institute (NSTRI), Islamic Republic of Iran).

First, in this research the thermal-hydraulic analysis of the cores with different fuel types are performed at steady state operating conditions presented in Table 6.1. Thereafter, transient analysis is performed under a reactivity insertion accident. In this case, a 4 mk ramp positive reactivity is inserted into the core, and the core parameters such as maximum reactor power and maximum temperature of the fuel, cladding and coolant are computed.

In this analysis, it is assumed that about 90% of the total fission energy is deposited in the fuel, about 4% is produced in the moderator, about 1% is produced in other reactor materials and the remaining 5% is carried away by neutrinos. Reactivity feedback coefficients, prompt neutron lifetime and effective delayed neutron fraction were taken from the SAR [6.4] and literature describing the respective HEU and LEU fuels. The kinetics parameters and reactivity feedback coefficients of the existing HEU core and the proposed LEU cores are presented in Table 6.2. The values of coolant mass flow rate were taken from the reactor SAR [6.4]. For the HEU core the melting points of both the UAl_4–Al fuel and aluminium cladding are about 650°C. However, for the LEU core the values for UO_2 fuel and Zircaloy-4 cladding are 2800°C and 1850°C respectively.

TABLE 6.1. CHARACTERISTICS OF THE EXISTING AND PROPOSED CORES

Parameter	Existing HEU	Proposed LEU (12.6%)	Proposed LEU (12.3%)
Fuel rod diameter (mm)	5.5	5.5	5.1
Enrichment (%)	90.2	12.6	12.3
Coolant inlet temperature (°C)	20	20	20
Inlet pressure (bar)	1.5	1.5	1.5
Operating power (kW)	30	33	33
Fuel type	UAl_4	UO_2	UO_2
Cladding	Al	Zr	Zr

TABLE 6.2. THE KINETICS PARAMETERS AND REACTIVITY FEEDBACK COEFFICIENTS

Parameter	HEU existing core	LEU proposed core (5.5 mm and 12.6%)	LEU proposed core (5.1 mm and 12.3%)
Prompt neutron generation time (μs)	80.91	47.00	50.50
Effective delayed neutron fraction (βeff)	0.00808	0.00845	0.00832
Moderator temperature coefficient (%Δk/k/°C)	–0.01539	-3.966×10^{-3}	-4.198×10^{-3}
Void/density coefficient (%Δk/k/°C)	–0.326	–0.356	–0.348
Doppler coefficient (%Δk/k/°C)	-2.7×10^{-4}	-1.395×10^{-3}	-1.342×10^{-3}

Material properties of the existing HEU fuel (UAl_4–Al) are computed according to the IAEA Research Reactor Core Conversion Guidebook [6.5]. The volumetric heat capacity and thermal conductivity of the fuel and cladding are computed as follows:

i. For the HEU fuel heat capacity, we use the heat capacity, C_p, of UAl_4, 0.473+0.00024T, and a temperature range of 20—600°C. Eq. 6.2 is therefore:

$$Volumetric\ heat\ capacity = C_p\rho \tag{6.2}$$

where

$$C_p\rho = (0.473 + 0.00024T)3.456 = 1.634688 \times 10^6 + (8.2944 \times 10^2 T)\ \frac{J}{m^3K}$$

ii. For the thermal conductivity of the fuel, Eq. 6.3 is used:

$$k = 2.17 - 2.76W_u \tag{6.3}$$

where

k is the thermal conductivity of fuel meat (W/cmK), and W_U is the weight fraction of uranium in the fuel meat. Therefore the value of k will be:

$$k = 2.17 - 2.76(0.2763) = 1.4074\,\frac{W}{cmK}$$

iii. For the Al cladding (C_p=0.892+0.0046T) of the HEU core, we can write:

$$Volumetric\ heat\ capacity = (0.892 + 0.00046T)2.7 = 2.84084 \times 10^6 + 1.242 \times 10^3 T\ \frac{J}{m^3 K}$$

and

$$K_{Al} = 180\ \frac{W}{mK}$$

Tables 6.3 and 6.4 list the material properties used in the LEU fuel cases. The Zircaloy-4 and UO_2 properties were obtained from the International Nuclear Safety Centre database [6.6].

TABLE 6.3. THERMAL PROPERTIES USED FOR URANIUM DIOXIDE WITH 95% THEORETICAL DENSITY

Temperature (K)	Thermal conductivity (W/mK)	Volumetric heat capacity (J/m^{3}K)
296.15	7.63	2.35×10^6
500	5.78	2.83×10^6
700	4.61	3.00×10^6

TABLE 6.4. THERMAL PROPERTIES OF ZIRCALOY-4

Temperature (K)	Thermal conductivity (W/mK)	Volumetric heat capacity (J/m^{3}K)
295	13.383	1.9×10^6
400	13.987	1.9×10^6
500	14.741	1.9×10^6

6.3. RESULTS AND DISCUSSION

In this section the results of steady state thermal-hydraulic analysis at nominal conditions for the HEU core and two proposed LEU cores are presented. Also the variation of the power, reactivity and temperature of the fuel, cladding and coolant after insertion of 4 mk positive reactivity, which is equal to the cold core excess reactivity, are investigated.

6.3.1. HEU core

The axial temperature distribution of the fuel centre, cladding surface and coolant along the hot channel is shown in Fig. 6.4. As shown, the temperature difference between the fuel centre and cladding is too low, which arises from the use of aluminium alloy in fuel material. The maximum fuel and cladding temperature of the hot rod at a steady state power level of 30 kW is computed to be 58.02°C and 57.75°C respectively. The temperature difference across the core is 20.17°C and 22.58°C along the average and hot channels, respectively, which is in good agreement with data reported in the SAR [6.4]. The computed results of steady state thermal-hydraulic analysis for the HEU and LEU cores are given in Table 6.5.

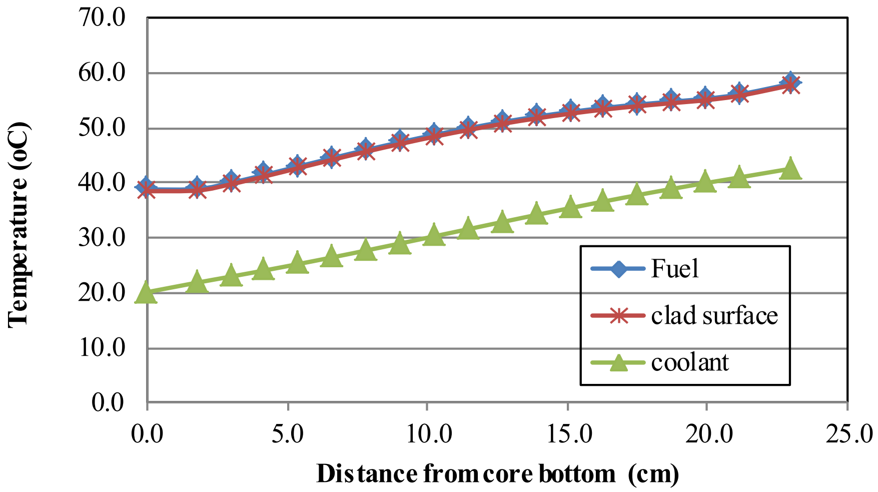

FIG. 6.4. Axial temperature distribution in fuel, clad surface, and coolant along the hot channel of HEU core at steady state power level of 30 kW (Courtesy of Nuclear Science and Technology Research Institute (NSTRI), Islamic Republic of Iran).

Transient analysis is performed under a reactivity insertion accident, and the variations of thermal-hydraulic parameters of the HEU core are investigated during the transient time. The results of the PARET code for transient analysis of a 4 mk ramp reactivity insertion are given in Table 6.6. Additionally, Figures 6.5 and 6.6 show the variation of the power and maximum temperature of fuel, cladding and coolant in the core.

Calculations indicate that the maximum power in this transient is about 88 kW, and the maximum heat flux in the core increases from 2.46 W/cm^2 (at 30 kW) to 6.5 W/cm^2 (at 88 kW), which is much smaller than the critical heat flux. The minimum burnup ratio is 49. Also, the maximum cladding surface temperature is 104.7°C, which remains 6.4°C below the water saturation temperature. The results show that no boiling occurred in the core.

TABLE 6.5. RESULTS OF STEADY STATE THERMAL-HYDRAULIC ANALYSIS OF ENTC MNSR

Parameter	HEU (existing core)	LEU proposed core (5.5 mm and 12.6%)	LEU proposed core (5.1 mm and 12.3%)
Fuel pin diameter	5.5	5.5	5.1
Enrichment (%)	90.2	12.6	12.3
Operating power (kW)	30	33	33
Inlet coolant temperature (°C)	20	20	20
Pressure at core inlet (kPa)	1.5	1.5	1.5
Saturation temperature in core (°C)	111.5	111.5	111.5
Power peaking factors			
Radial	1.12	1.131	1.139
Axial	1.10	1.133	1.132
Temperatures at steady state conditions (°C)			
Coolant temperature rise across core	20.17	21.15	20.4
Coolant temperature rise across hot channel	22.58	23.9	23.22
Maximum cladding temperature	57.75	61.6	62.22
Maximum fuel centre line temperature	58.02	66.71	67.06
Heat flux (W/cm^2)			
Average	1.997	2.49	2.36
Maximum	2.46	2.82	3.05
Critical heat flux (Mirshak correlation)	334.12	334.5	335.29
Minimum margin to CHF	135.82	118.62	109.93

TABLE 6.6. RESULTS OF REACTIVITY INSERTION 4 mk RAMP FOR ENTC MNSR

Parameter	HEU 4 mk ramp	Proposed LEU (12.6%) 4 mk ramp	Proposed LEU (12.3%) 4 mk ramp
Maximum power (kW)	88.16	67.6	69.92
Maximum fuel temperature (°C)	105.43	107.1	111.18
Maximum clad surface temperature (°C)	104.71	97.19	100.76
Maximum coolant temperature (°C)	52.13	60.1	59.93

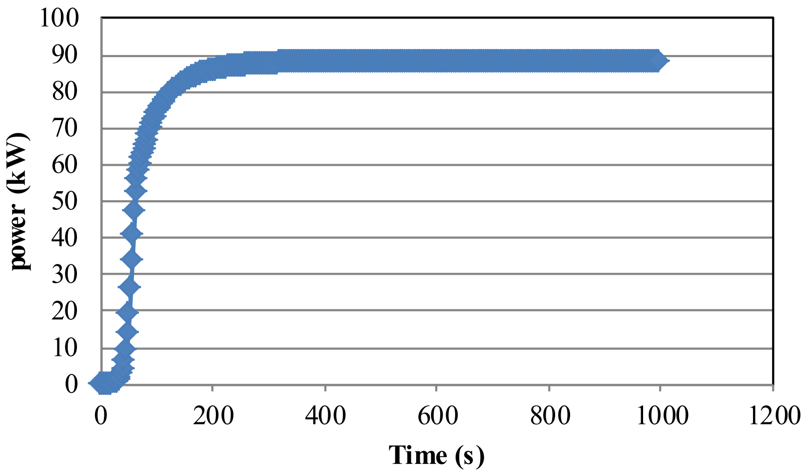

FIG. 6.5. Transient power history during a 4 mk ramp reactivity insertion in the HEU core (Courtesy of Nuclear Science and Technology Research Institute (NSTRI), Islamic Republic of Iran).

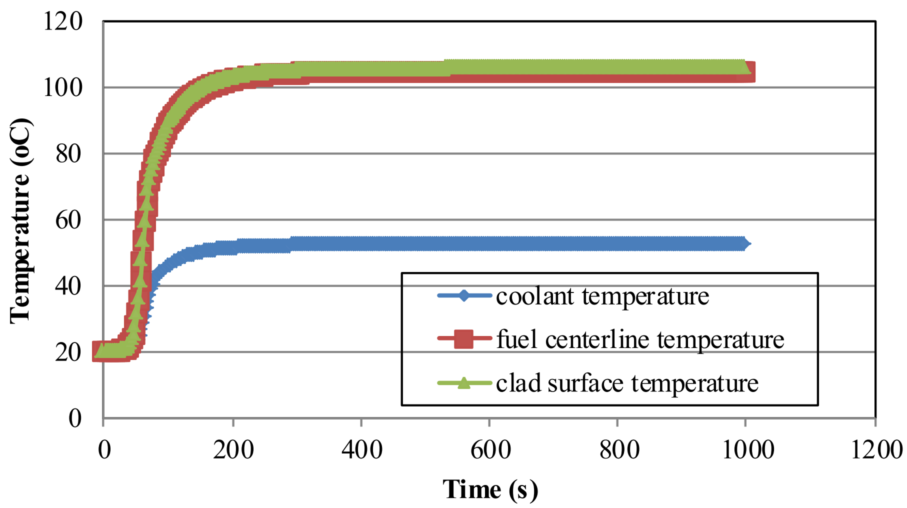

FIG. 6.6. Temperature history in a 4 mk ramp reactivity insertion transient in the HEU core (Courtesy of Nuclear Science and Technology Research Institute (NSTRI), Islamic Republic of Iran).

6.3.2. LEU cores

In a subsequent experiment two proposed LEU cores are considered, and a steady state and transient thermal-hydraulic analysis is performed to investigate their safety margins. The first core is enriched to 12.6% and has a fuel pin of 5.5 mm diameter, and the second core is enriched to 12.3% and has a fuel pin of 5.1 mm diameter. The detailed data for these cores is presented in Table 6.1. In order to achieve the same level of neutron flux, especially in irradiation sites, an increase to 33 kW in the maximum power rating of the LEU cores has been suggested.

The results of steady state analysis at a power level of 33 kW performed for the two LEU cores are presented in Table 6.5. The results show that the maximum cladding temperature is 61.6°C and 62.2°C along the hot channel for the 12.6% and 12.3% enriched LEU cores, respectively. Comparing the LEU calculated data shows an increase in cladding and fuel temperature by increasing the steady state power level of the reactor. However, the cladding temperature would be far below the temperature required to commence boiling in the LEU cores. The maximum fuel centre line temperature in the LEU cores is also much smaller than the fuel melting point. The axial distribution of the fuel centre, cladding and coolant exit temperatures across the hot channel are illustrated in Figures 6.7 and 6.8 for both LEU cores, 12.6% and 12.3% enriched, respectively. The temperature difference across the core is 21.15°C and 23.9°C along the average and hot channel for the 12.6% enriched core, respectively. These temperatures are 20.4°C and 23.22°C for the 12.3% enriched core.

For an LEU core with 12.6% enrichment and 5.5 mm fuel pin diameter, transient analysis results from a 4 mk ramp reactivity insertion is illustrated in Figures 6.9—6.11. The history of reactivity during the transient is presented in Fig. 6.9. As shown in Fig. 6.10 the maximum power reaches 67.6 kW. The variations of maximum temperature of the fuel centre line, cladding surface and coolant exit in the core during transient time are shown in Fig. 6.11. During the transient, the maximum temperature of fuel and cladding is 97.2°C and 60.1°C, respectively. Results show that this core has a sufficient safety margin to the melting points of the fuel and cladding. Additionally, the maximum cladding surface temperature obtained is 14.3°C below the coolant saturation temperature, and no boiling occurs in the core.

In the case of an LEU core with 12.3% enrichment and 5.1 mm fuel pin diameter, the calculation results for transient analysis for a 4 mk reactivity insertion are presented in Figures 6.12—6.13. The peak fuel centre line and clad surface temperature during transient are 111.18°C and 100.76°C, respectively. The maximum power during the transient is about 70 kW.

Comparing the results of transient analysis for the HEU and LEU cores (shown in Table 6.6) indicates that the LEU cores attain a lower peak power than the HEU core due to a larger Doppler coefficient, and consequently the maximum cladding surface temperature is smaller.

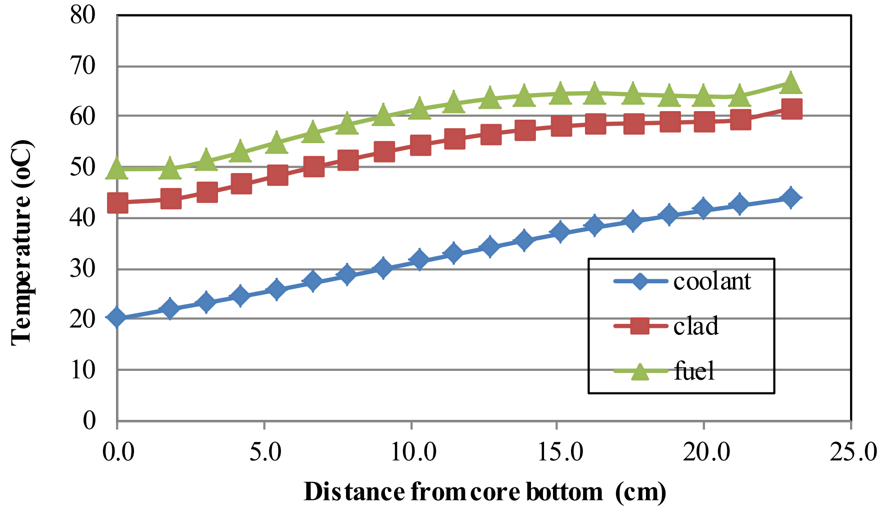

FIG. 6.7. Axial distribution of temperature in a hot channel for a 12.6% enriched LEU core at a steady state power level of 33 kW (Courtesy of Nuclear Science and Technology Research Institute (NSTRI), Islamic Republic of Iran).

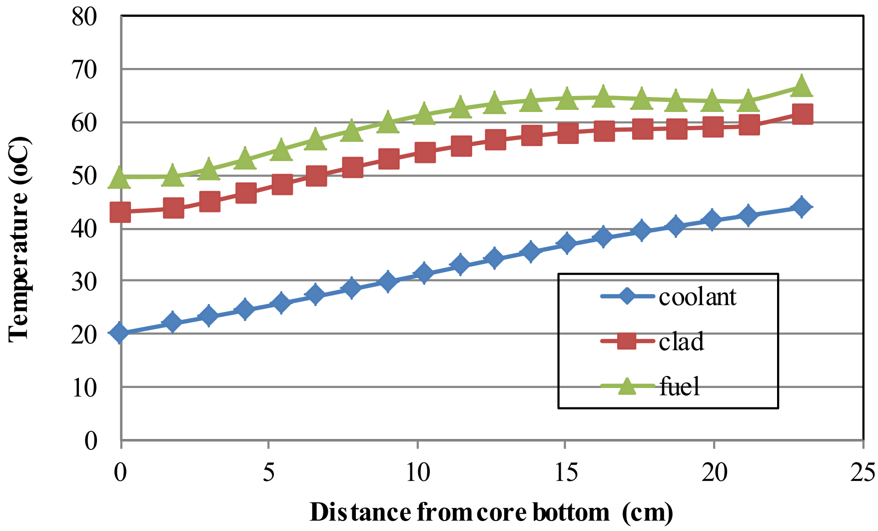

FIG. 6.8. Axial distribution of temperature in a hot channel for a 12.3% enriched LEU core at a steady state power level of 33 kW (Courtesy of Nuclear Science and Technology Research Institute (NSTRI), Islamic Republic of Iran).

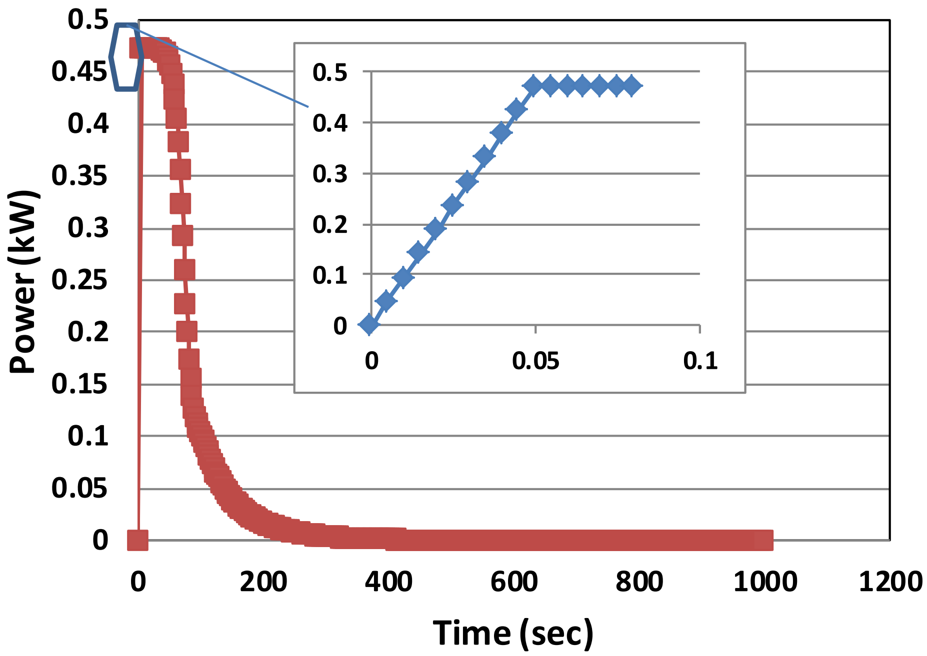

FIG. 6.9. Reactivity history in a transient from a 4 mk ramp reactivity insertion in a 12.6% enriched LEU core (Courtesy of Nuclear Science and Technology Research Institute (NSTRI), Islamic Republic of Iran).

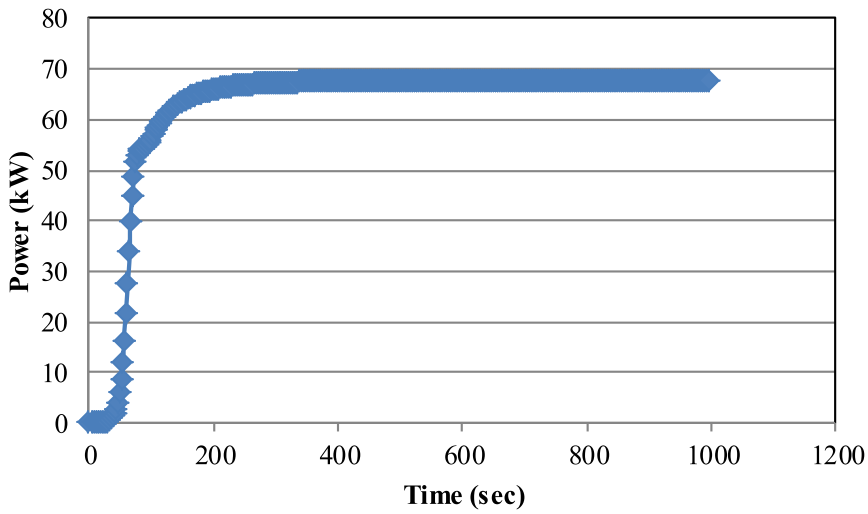

FIG. 6.10. Power history in a transient from a 4 mk ramp reactivity insertion in a 12.6% enriched LEU core (Courtesy of Nuclear Science and Technology Research Institute (NSTRI), Islamic Republic of Iran).

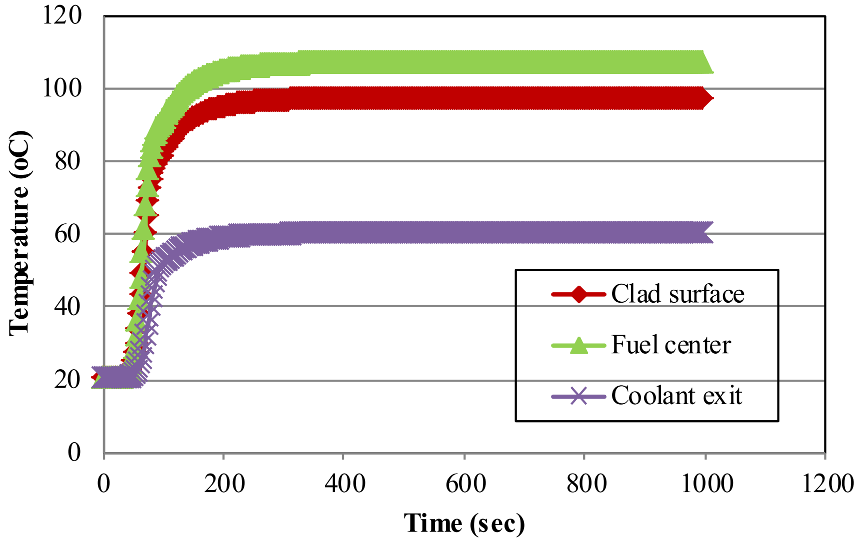

FIG. 6.11. Temperature history in a transient from a 4 mk ramp reactivity insertion in a 12.6% enriched LEU core (Courtesy of Nuclear Science and Technology Research Institute (NSTRI), Islamic Republic of Iran).

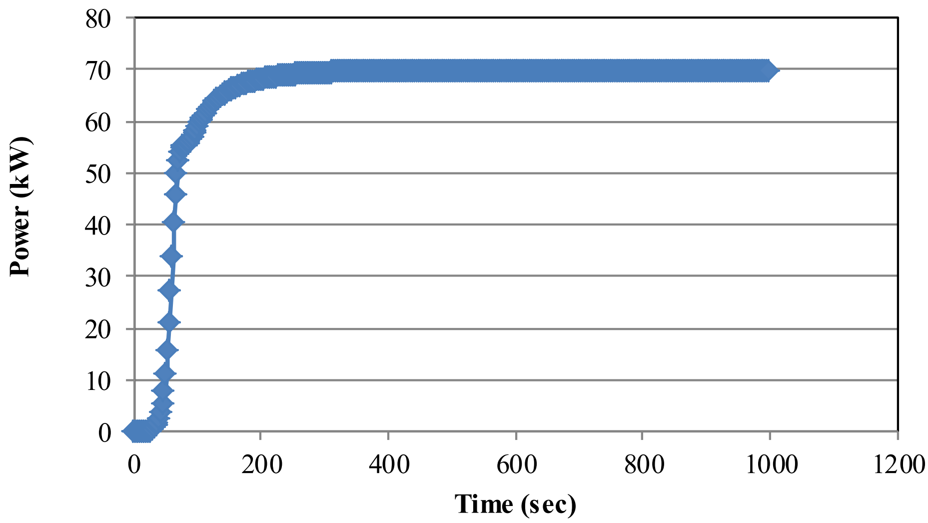

FIG. 6.12. Power history in a transient from a 4 mk ramp reactivity insertion in a 12.3% enriched LEU core (Courtesy of Nuclear Science and Technology Research Institute (NSTRI), Islamic Republic of Iran).

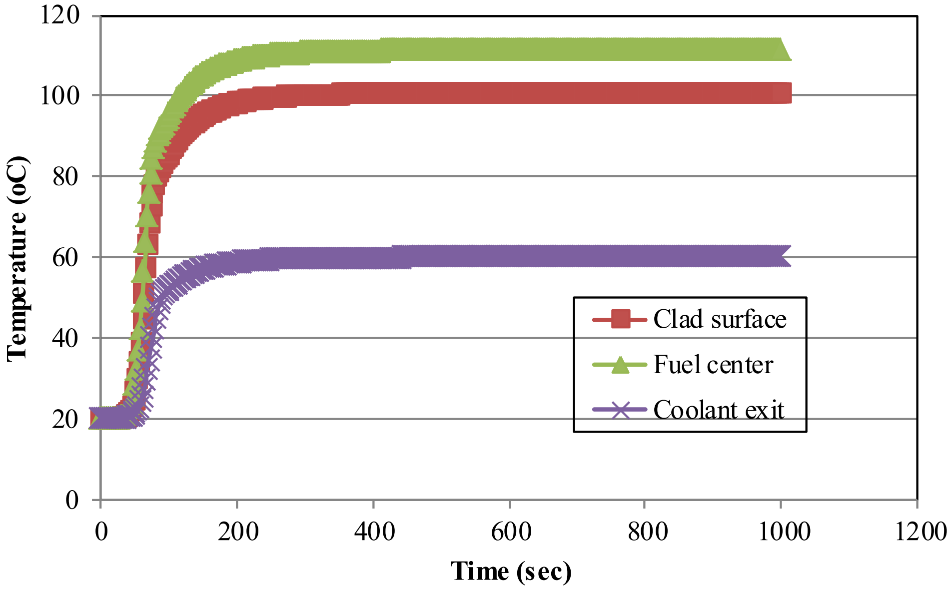

Fig. 6.13. Temperature history in a transient from a 4 mk ramp reactivity insertion in a 12.3% enriched LEU core (Courtesy of Nuclear Science and Technology Research Institute (NSTRI), Islamic Republic of Iran).

REFERENCES TO SECTION 6

[6.1] OBENCHAIN, C.F., PARET - A Program for the Analysis of Reactor Transients, Idaho National Engineering Laboratory, Idaho Falls (1969).

[6.2] FAGHIHI, F., MIRVAKILI, S.M., Burn up calculations for the Iranian miniature reactor: a reliable and safe research reactor, Nuclear Engineering and Design 239, (2009) 1000–1009.

[6.3] BOKHARI, I., PERVEZ, S., Safety analysis for core conversion (from HEU to LEU) of Pakistan research reactor-2 (PARR-2), Nuclear Engineering and Design 240, (2010) 123–128.

[6.4] CHENGZHAN, G., YONGCHUN G., Safety Analysis Report for Miniature Neutron Source Reactor (MNSR), China Institute of Atomic Energy Report RPT4-S-430, CIAE, Beijing (1994).

[6.5] INTERNATIONAL ATOMIC ENERGY AGENCY, Research Reactor Core Conversion Guidebook, Volume 4: Fuels, IAEA-TECDOC-643/4, IAEA, Vienna (1992).

[6.6] DUNN, F.E., et al., MNSR Transient Analyses and Thermal Hydraulic Safety Margins for HEU and LEU Cores Using the RELAP5-3D Code, Pres. 2007 International Meeting On Reduced Enrichment for Research and Test Reactors, Prague, 2007, Argonne National Laboratory, Argonne (2007).

7. ANALYSIS OF CORE CONVERSION FROM HEU TO LEU FUEL FOR PAKISTAN RESEARCH REACTOR-2 (PARR-2)

7.1. INTRODUCTION

The Pakistan Research Reactor-2 (PARR-2) is a 30 kW MNSR that is cooled, moderated and shielded by demineralized light water. The reactor assembly is comprised of an HEU core, beryllium reflectors, and one central control rod. The core is enclosed in a cylindrical aluminium alloy vessel with 0.6 m diameter and 5.7 m height (Fig. 7.1). The vessel is suspended in a reactor pool of size 6.0 m × 3.5 m, and 7.0 m in depth. The reactor has an inherent power peaking characteristic with a self-limiting power of 87 kW, with a 4 mk reactivity release in a cold clean core.

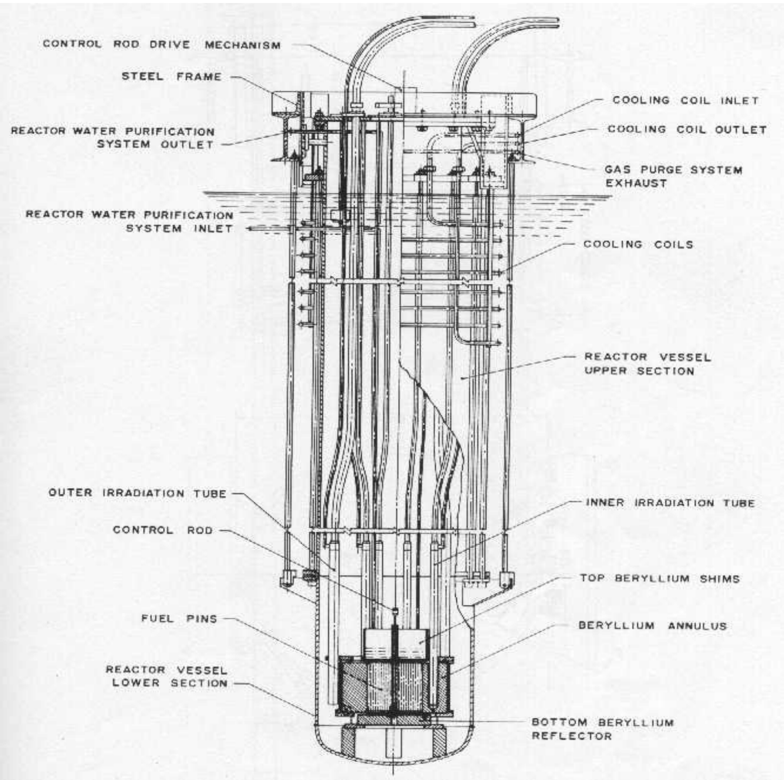

FIG. 7.1. Reactor vessel cross-section of PARR-2 (Reproduced from Ref. [7.1] with permission courtesy of Pakistan Institute of Nuclear Science and Technology (PINSTECH), Pakistan).

Ten irradiation sites are available for experimentation (Fig. 7.2). Five of these are located inside the beryllium annulus, called inner sites, while the rest surround it and are called outer sites. The diameter of each of the five inner and three outer irradiation tubes is 22 mm, while the two other outer tubes are 34 mm in diameter. The maximum thermal neutron flux of 1×10^{12} and 5×10^{11} $cm^{-2}\times s^{-1}$ is available at the inner and outer sites, respectively, at the rated power of 30 kW. Access to the neutron flux is through pneumatic irradiation tubes. The reactor is equipped with monitoring and process instrumentation. Reactor control and flux regulation are accomplished either by manual or automatic controls provided on the reactor console or through a microcomputer-based control system.

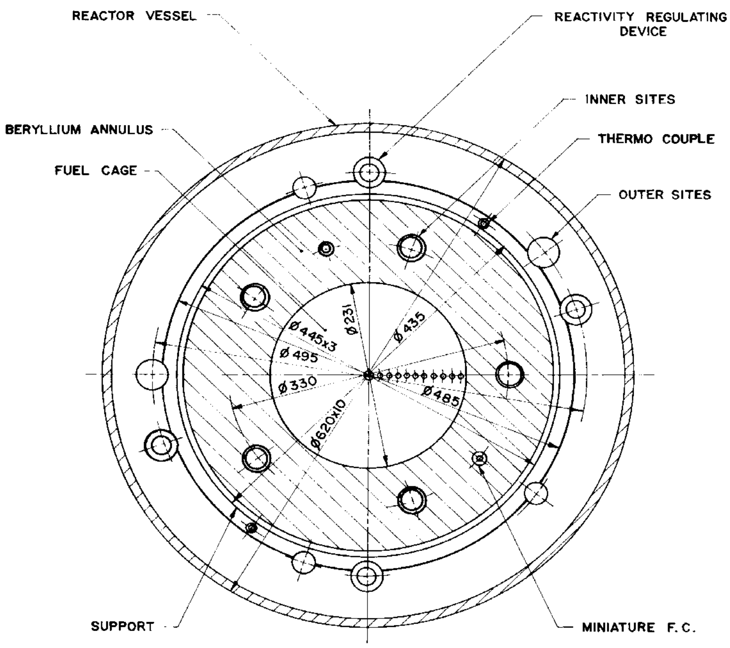

FIG. 7.2. Location of inner and outer irradiation sites of PARR-22 (Reproduced from Ref. [7.1] with permission courtesy of Pakistan Institute of Nuclear Science and Technology (PINSTECH), Pakistan).

The core of PARR-2 is an under-moderated array with hydrogen to ^{235}U atomic ratio of about 201.2 at 20°C that provides strong negative temperature and void coefficient of reactivity. The excess reactivity of 4.0 mk in the cold clean core is much less than the effective delayed neutron fraction of 0.00795, which therefore eliminates the possibility of a prompt critical accident. Heat from the core is removed primarily by natural convection and is transferred to the pool water, which serves as the heat sink. As shown in Fig. 7.3, the water enters the core through the lower orifice of 6 mm height, heats and expands, then rises and leaves the core through an upper orifice of 7.5 mm height. It then descends within the reactor vessel and transfers heat through the walls to the pool water. The reported mass flow rates in the Final SAR [7.2] at 30 kW and 87 kW are 0.34 kg/s and 0.6 kg/s, respectively.

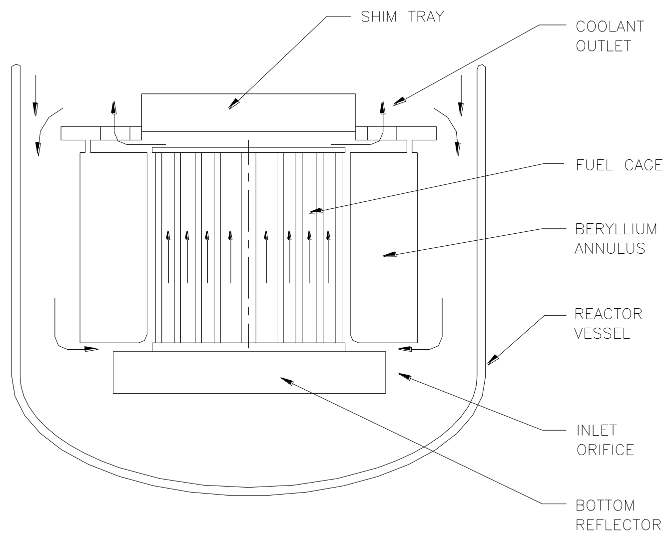

FIG. 7.3. Coolant flow direction in PARR-2 (Reproduced from Ref. [7.3] with permission courtesy of Pakistan Institute of Nuclear Science and Technology (PINSTECH), Pakistan).

The PARR-2 core consists of 344 fuel pins arranged in concentric arrays and forms a square cylinder with a diameter of 230 mm. Upper and lower grid plates secure the fuel pins to form a fuel cage. The fuel pins are fixed to the bottom grid plate by slightly conical self-locking fittings and are free to expand through the upper grid plate. Within the grid plates, four of the 354 holes are used for fixing tie bolts to keep the fuel cage intact, while the remaining six holes are occupied by aluminium dummy pins. The fuel meat is a uranium–aluminium alloy of UAl_4–Al composition and 90.2% enriched in ^{235}U. The fuel pins are 4.3 mm in diameter with cladding material of 0.6 mm thick aluminium alloy (303-Al). The total length of a fuel pin is 248 mm, with an active length of 230 mm. Each fuel pin contains 2.9 g of ^{235}U. The core has a guide tube in the centre, which facilitates the movement of a 3.9 mm diameter cadmium control rod, with stainless steel cladding material that is 0.5 mm thick.

The fuel cage is surrounded by a 100 mm thick metallic beryllium annulus and rests on a 50 mm thick bottom beryllium reflector. The core is reflected on the top by beryllium shim plates. These shims are of a 'D' shape with varying thickness and are added periodically in the shim tray for the compensation of long term reactivity changes. The beryllium reflector is followed by light water [7.2].

Presently, the issues of nuclear safeguard protocols and non-proliferation treaties are essential. LEU fuel will be the reactor fuel in the future. In the foreseeable future, PARR-2 will be converted to use LEU. Since the main purpose of PARR-2 is NAA, the conversion to LEU fuel must not affect its utilization capabilities. Studies conducted by Jonah et al [7.4] showed that high-density LEU fuel (UO_2) could be recommended to gain the required excess reactivity of 3.5 mk to 4 mk for this design.

7.2. NEUTRONIC ANALYSIS

In this study LEU UO_2 fuel with zircaloy cladding is analysed. The existing HEU core of PARR-2 is also analysed to validate the reactor model. Three LEU cores have been analysed, with the basic criterion of 4 mk excess reactivity available in a cold clean core. One LEU core contains the same number of fuel pins and the same dimensions as that in the HEU core. The enrichment for this core is calculated to be 12.6%. The other proposed LEU core has the same number of fuel pins as the HEU core, but the diameter of the fuel meat is 4.2 mm and the diameter of fuel pin including cladding is 5.1 mm. The enrichment for this core is calculated to be 12.3%. The final LEU core contains the same number of fuel pins with the same dimensions as the HEU core, but the cladding material, grid plate and control rod guide tube material is changed from aluminium to Zircaloy-4. Additionally, the control rod absorber cadmium thickness is increased from 3.9 mm to 4.5 mm. The enrichment of this core is calculated to be 12.46%. Design parameters of all analysed cores are shown in Table 7.1.

TABLE 7.1. DESIGN PARAMETERS OF THE PARR-2

Fuel	Core 1 (existing HEU core)	Core 2 (proposed LEU core)	Core 3 (proposed LEU core)	Core 4 (proposed LEU core)
	UAl_4–Al	UO_2	UO_2	UO_2
U^{235} enrichment (%)	90.2	12.6	12.3	12.46
Cladding material	Aluminium	Zircaloy-4	Zircaloy-4	Zircaloy-4
Coolant	H_2O	H_20	H_20	H_20
Moderator	H_2O	H_20	H_20	H_20
Fuel pin diameter (mm)	5.5	5.5	5.1	5.5
Fuel meat diameter (mm)	4.3	4.3	4.2	4.3
Clad thickness (mm)	0.6	0.6	0.45	0.6
Height of core (mm)	230	230	230	230
Total number of fuel pins	344	344	344	344
Orifice size (mm)				
Inlet	6	6	6	6
Outlet	7.5	7.5	7.5	7.5
Control rod and guide tube design parameters (mm)				
Outer diameter of cadmium	3.9	3.9	3.9	4.5
Thickness of stainless steel cladding	0.5	0.5	0.5	0.5
Thickness of water gap	2.0	2.0	2.0	1.7
Thickness of guide tube	1.5	1.5	1.5	1.5
Material of guide tube	Aluminium	Aluminium	Aluminium	Zircaloy-4
Grid plate material	Aluminium	Aluminium	Aluminium	Zircaloy-4

7.2.1. Methodology

Standard nuclear reactor codes WIMSD [7.5] and CITATION [7.6] are used for neutronic analysis of the PARR-2 cores. WIMSD is employed for macroscopic cross-section generation, while core modelling is performed with CITATION. WIMSD uses 69 groups and a multi-region integral transport theory to solve the neutron transport equation for the lattice cells. CITATION uses a finite difference scheme to solve the neutron diffusion equation in one, two and three dimensions. A representative unit fuel cell of a PARR-2 core is modelled in WIMSD for analysis of each core. Although the materials and dimensions of each region of the unit cell differ among the four analysed cores, the unit cell in WIMSD possesses four annuli. The central region of the cell contains the fuel material. Around the fuel meat there is cladding. The third annulus contains water as the moderator. The outermost region is the structural material of the core, which includes the aluminium dummy pins and tie bolts of the fuel cage. Hence this unit cell is representative of the entire core. Utilizing this super unit cell model, ten energy group calculations for group constants of fuel material are performed, the results of which are listed in Table 7.2. The last three groups are considered to be thermal. Cross-sections are calculated for the beryllium reflector, grid plate, reflecting water, irradiation positions, shim tray, control rod follower and control rod absorber material.

TABLE 7.2. TEN ENERGY GROUPS STRUCTURE FOR GENERATION OF CROSS-SECTIONS

Group number	Energy boundaries (eV)
1	10×10^6—0.821×10^6
2	0.821×10^6—0.3025×10^6
3	0.3025×10^6—0.183×10^6
4	0.183×10^6—367.262
5	367.262—1.15
6	1.15—0.972
7	0.972—0.625
8	0.625—0.14
9	0.14—0.05
10	<0.05

These macroscopic cross-sections are employed in CITATION. Modelling of the core was performed in xyz geometry utilizing the three-dimensional option. The PARR-2 core model in CITATION is shown in Fig. 7.4. The same reactor model was used for the analysis of the HEU and proposed LEU cores of PARR-2. As the PARR-2 core is of square cylindrical shape, its modelling in *x-y-z* geometry by CITATION code is achieved by conserving the total area of the core and beryllium reflector. In this regard, effort is made to simulate the actual system as closely as possible. The irradiation sites, fission chambers and control rod guide tube are modelled using the same principle.

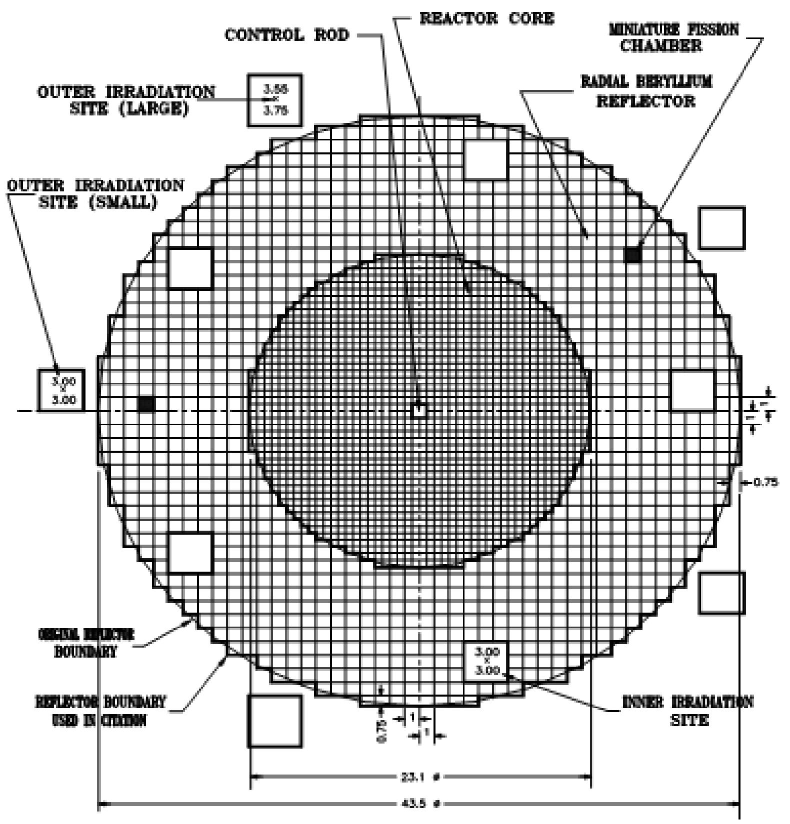

FIG. 7.4. PARR-2 core modelling employed in CITATION2 (Reproduced from Ref. [7.1] with permission courtesy of Pakistan Institute of Nuclear Science and Technology (PINSTECH), Pakistan).

7.2.2. Results and discussion

As the finite difference diffusion theory-based code CITATION is used for the global core calculations of the PARR-2 HEU core, the reactor model developed for the HEU core was used as a benchmark for neutronic calculations of LEU-fuelled cores. Table 7.3 shows the criticality position and k_{eff} values at different positions of the control rod for HEU and LEU fuels. It can be seen that the criticality position and shutdown margins are lower for core 2 and core 3 due to the higher density of uranium in the fuel material and spectrum hardening in the LEU fuel. In the LEU fuel, spectrum hardening causes a decrease in the thermal neutron flux at the central control rod position, and hence the absorption cross-section of the control rod decreases. Therefore, use of the same control rod as in the HEU core results in a decreased control rod worth for the LEU-fuelled core. In order to enhance the shutdown margin and control rod worth, the thickness of the neutron absorber control rod is increased in core 4. Therefore core 4 represents about the same value of control rod worth as for the operating HEU core.

TABLE 7.3. COMPARISON OF CORE REACTIVITY

Core	Fuel material/ enrichment	U density (g/cm^3)	Amount of U^{235} in core (g)	Criticality position (cm)	Excess reactivity (mk)	Shutdown margin (mk)	Control rod worth (mk)
1	UAl alloy/ 90.2%	0.92	995	9	4.046	–2.344	–6.39
2	UO_2 fuel/ 12.6%	9.35	1353	7	4.007	–1.43	–5.437
3	UO_2 fuel/ 12.3%	9.35	1264	7	4.16	–1.498	–5.658
4	UO_2 fuel/ 12.46%	9.35	1339	8.5	4.012	–2.375	–6.387

Originally, ten energy group calculations are performed through CITATION. For comparison of flux levels, ten group fluxes are condensed to three group (thermal, epithermal, fast) fluxes at a nominal reactor power of 30 kW. A power level of 30 kW results in lower thermal flux values at the irradiation sites and fission chambers for LEU UO_2 fuel as compared to HEU fuel, as shown in Tables 7.4 and 7.5.

TABLE 7.4. FLUX AT INNER IRRADIATION SITES AND FISSION CHAMBERS

Core	Fuel material	Reactor power (kW)	Flux at inner sites ($cm^{-2}s^{-1}$)			Flux at fission chambers ($cm^{-2}s^{-1}$)		
			Fast (0.821 MeV–10 MeV)	Epithermal (0.625 eV–0.821 MeV)	Thermal (0 eV–0.625 eV)	Fast (0.821 MeV–10 MeV)	Epithermal (0.625 eV–0.821 MeV)	Thermal (0 eV–0.625 eV)
1	UAl alloy pin diameter 5.5 mm/ 90.2%	30	1.40×10^{11}	5.72×10^{11}	1.02×10^{12}	1.46×10^{11}	6.67×10^{11}	1.09×10^{12}
2	UO_2 fuel pin diameter 5.5 mm/ 12.6%	30	1.35×10^{11}	5.58×10^{11}	9.36×10^{11}	1.40×10^{11}	6.50×10^{11}	9.96×10^{11}
		33	1.48×10^{11}	6.14×10^{11}	1.03×10^{12}	1.54×10^{11}	7.15×10^{11}	1.10×10^{12}
3	UO_2 fuel pin diameter 5.1 mm/ 12.3%	30	1.33×10^{11}	5.49×10^{11}	9.41×10^{11}	1.39×10^{11}	6.40×10^{11}	1.00×10^{12}
		33	1.47×10^{11}	6.04×10^{11}	1.04×10^{12}	1.52×10^{11}	7.04×10^{11}	1.10×10^{12}
4	UO_2fuel pin diameter 5.5 mm/ 12.46%	30	1.24×10^{11}	5.16×10^{11}	9.16×10^{11}	1.37×10^{11}	6.36×10^{11}	9.81×10^{11}
		33	1.36×10^{11}	5.68×10^{11}	1.01×10^{12}	1.51×10^{11}	6.99×10^{11}	1.08×10^{12}

TABLE 7.5. FLUX AT OUTER IRRADIATION SITES

Core	Fuel material	Reactor power (kW)	Flux at three small outer sites ($cm^{-2}s^{-1}$)			Flux at two large outer sites ($cm^{-2}s^{-1}$)		
			Fast (0.821 MeV–10 MeV)	Epithermal (0.625 eV–0.821 MeV)	Thermal (0 eV–0.625 eV)	Fast (0.821 MeV–10 MeV)	Epithermal (0.625 eV–0.821 MeV)	Thermal (0 eV–0.625 eV)
1	UAl alloy pin diameter 5.5 mm/ 90.2%	30	3.20×10^{10}	1.22×10^{11}	5.30×10^{11}	2.88×10^{10}	1.08×10^{11}	4.75×10^{11}
2	UO_2 fuel pin diameter 5.5 mm/ 12.6%	30	3.08×10^{10}	1.18×10^{11}	4.98×10^{11}	2.77×10^{10}	1.05×10^{11}	4.47×10^{11}
		33	3.38×10^{10}	1.30×10^{11}	5.48×10^{11}	3.05×10^{10}	1.16×10^{11}	4.92×10^{11}
3	UO_2 fuel pin diameter 5.1 mm/ 12.3%	30	3.05×10^{10}	1.17×10^{11}	4.96×10^{11}	2.74×10^{10}	1.04×10^{11}	4.45×10^{11}
		33	3.35×10^{10}	1.28×10^{11}	5.46×10^{11}	3.02×10^{10}	1.14×10^{11}	4.90×10^{11}
4	UO_2 pin diameter5.5/ mm12.46%	30	2.95×10^{10}	1.12×10^{11}	4.82×10^{11}	2.71×10^{10}	1.03×10^{11}	4.36×10^{11}
		33	3.25×10^{10}	1.23×10^{11}	5.30×10^{11}	2.98×10^{10}	1.13×10^{11}	4.79×10^{11}

However at a power level of 33 kW, these flux levels match the values for HEU fuel. The fast and epithermal flux values at the irradiation sites and fission chambers also exhibit similar behaviour. The axial flux profiles for HEU and LEU fuel are shown in Figs 7.5—7.10. The height of the irradiation site is 19 cm, and the origin is assumed to be the bottom of the channel. It is obvious that the flux level drops along the axial distance of the core.

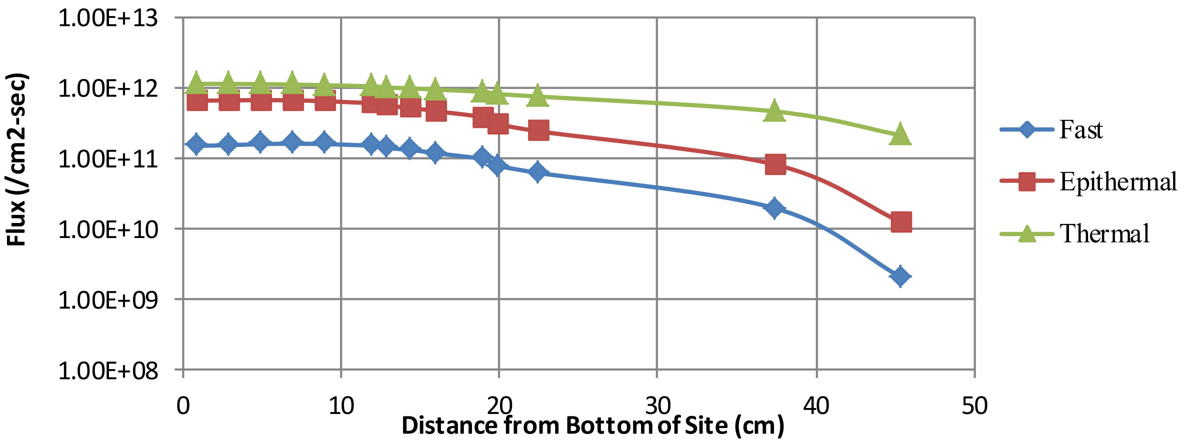

FIG. 7.5. Axial neutron flux profile at inner irradiation sites of PARR-2 (HEU fuel) (Courtesy of Pakistan Institute of Nuclear Science and Technology (PINSTECH), Pakistan).

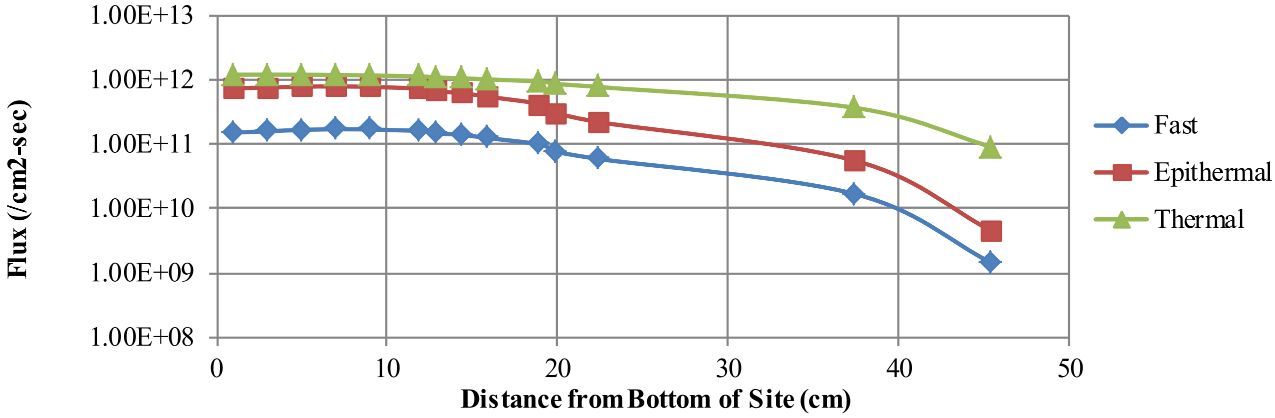

FIG. 7.6. Axial neutron flux profile at fission chambers of PARR-2 (HEU fuel) (Courtesy of Pakistan Institute of Nuclear Science and Technology (PINSTECH), Pakistan).

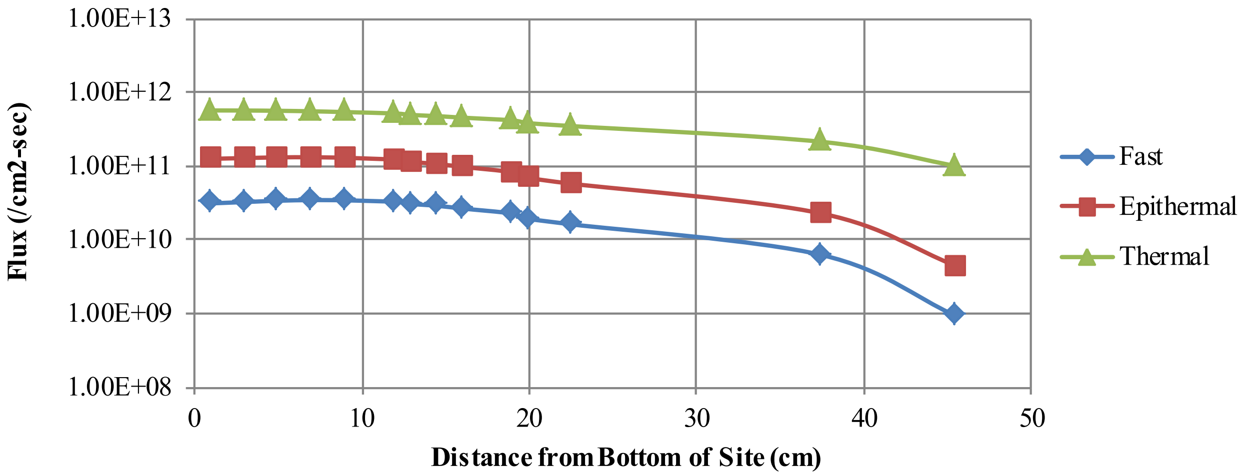

FIG. 7.7. Axial neutron flux profile at outer irradiation sites of PARR-2 (HEU fuel) (Courtesy of Pakistan Institute of Nuclear Science and Technology (PINSTECH), Pakistan).

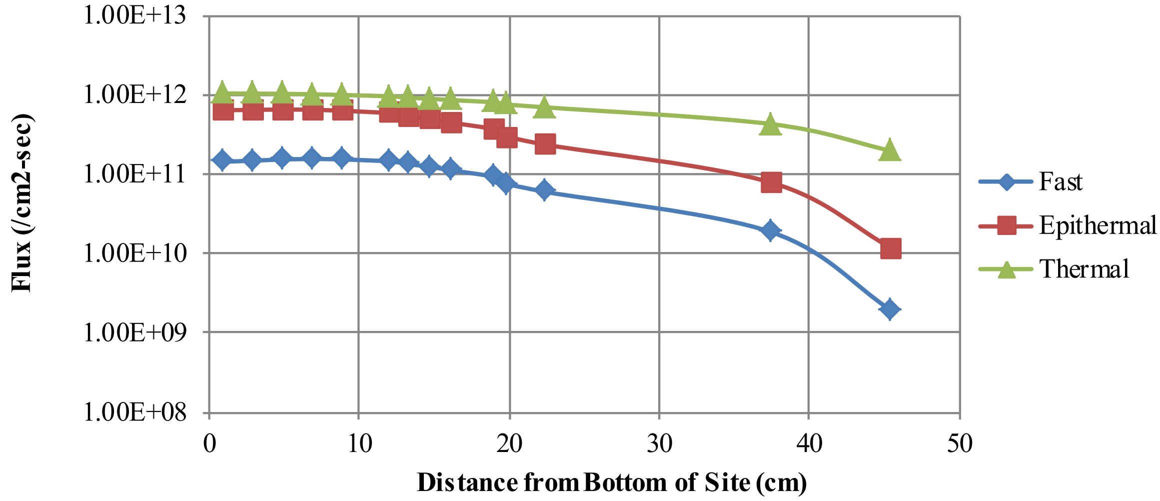

FIG. 7.8. Axial neutron flux profile at inner irradiation sites of PARR-2 (LEU fuel) (Courtesy of Pakistan Institute of Nuclear Science and Technology (PINSTECH), Pakistan).

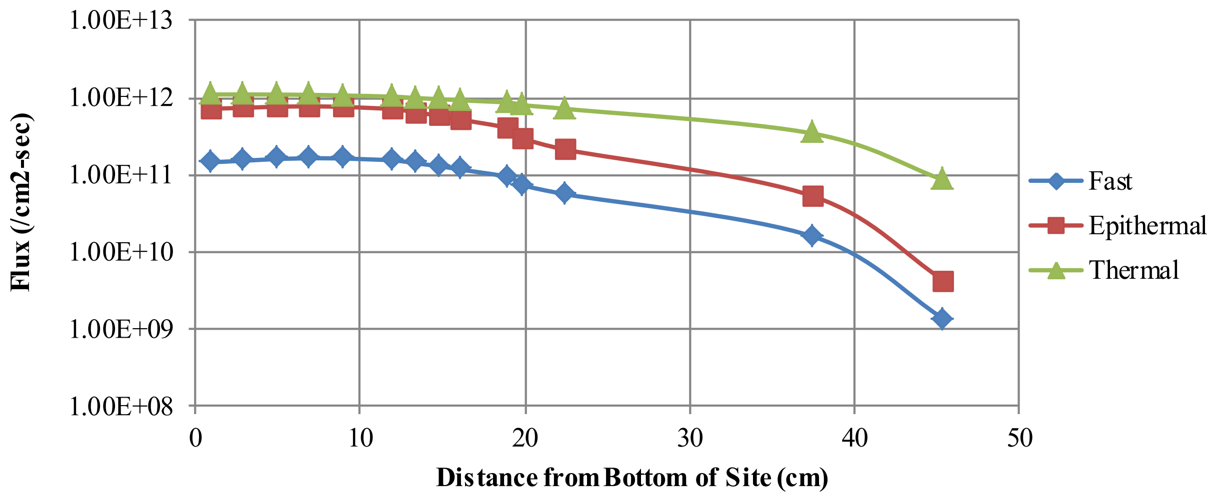

FIG. 7.9. Axial neutron flux profile at fission chamber of PARR-2 (LEU fuel) (Courtesy of Pakistan Institute of Nuclear Science and Technology (PINSTECH), Pakistan).

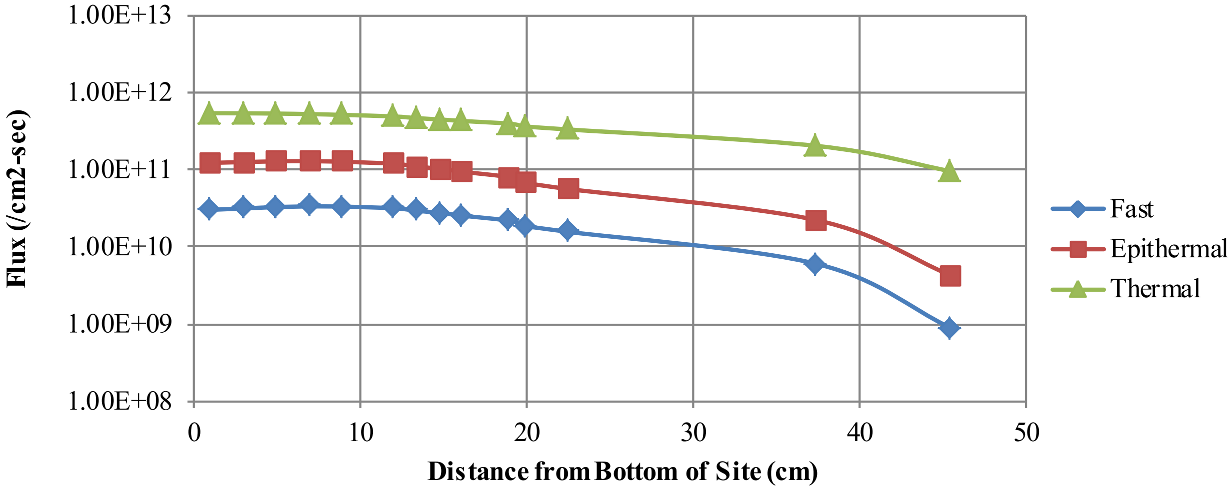

FIG. 7.10. Axial neutron flux profile at outer irradiation sites of PARR-2 (LEU fuel) (Courtesy of Pakistan Institute of Nuclear Science and Technology (PINSTECH), Pakistan).

Average values of reactivity coefficients are shown in Table 7.6. Due to increased content of ^{238}U in LEU fuel, the Doppler coefficient increases about ten times for LEU UO_2 fuel compared to HEU fuel. There is also some increment in the void coefficient, but the moderator temperature coefficient decreases for LEU fuel compared to HEU fuel. Peaking factors increase slightly for LEU fuel, as shown in Table 7.7. The reactivity worth of the top beryllium shim plate was also calculated and compared with quoted data in the Final SAR [7.2]. Comparison of these calculations in Fig. 7.11 indicates the HEU fuel reactivity worth of the top beryllium shim plate is higher than its value for LEU fuel.

TABLE 7.6. AVERAGE VALUES OF REACTIVITY COEFFICIENTS

Core	Fuel	Parameter	Temperature range (°C)	Average value
1	HEU (UAl_4–Al) 90.2 % enriched	Moderator temperature coefficient (pcm/°C)	20—100	–6.5291
		Doppler coefficient (pcm/°C)	20—400	–0.1397
		Void coefficient (pcm/%void)	20—100	–337.67
2	LEU (UO_2) pin diameter 5.5 mm 12.6 % enriched	Moderator temperature coefficient (pcm/°C)	20—100	–3.9659
		Doppler coefficient (pcm/°C)	20—400	–1.3951
		Void coefficient (pcm/%void)	20—100	–356.22
3	LEU (UO_2) pin diameter 5.1 mm 12.3 % enriched	Moderator temperature coefficient (pcm/°C)	20—100	–4.1985
		Doppler coefficient (pcm/°C)	20—400	–1.34239
		Void coefficient (pcm/%void)	20—100	–348.355
4	LEU (UO_2) pin diameter 5.5 mm 12.46% enriched	Moderator temperature coefficient (pcm/°C)	20—100	–3.86149
		Doppler coefficient (pcm/°C)	20—400	–1.39316
		Void coefficient (pcm/%void)	20—100	–344.014

TABLE 7.7. PEAKING FACTOR CALCULATIONS

Parameter	Core 1	Core 2	Core 3	Core 4
Max. power density (W/cm^3)	4.1159	4.16728	4.21557	4.66630
Average power density along hot channel (W/cm3)	3.6518	3.67685	3.70154	3.49493
Average power density of core (W/cm^3)	3.2505	3.25052	3.25052	3.24977
Axial peaking factor	1.1271	1.13338	1.13887	1.33516
Radial peaking factor	1.1234	1.13116	1.13875	1.07544
Total peaking	1.2662	1.28203	1.29689	1.43589

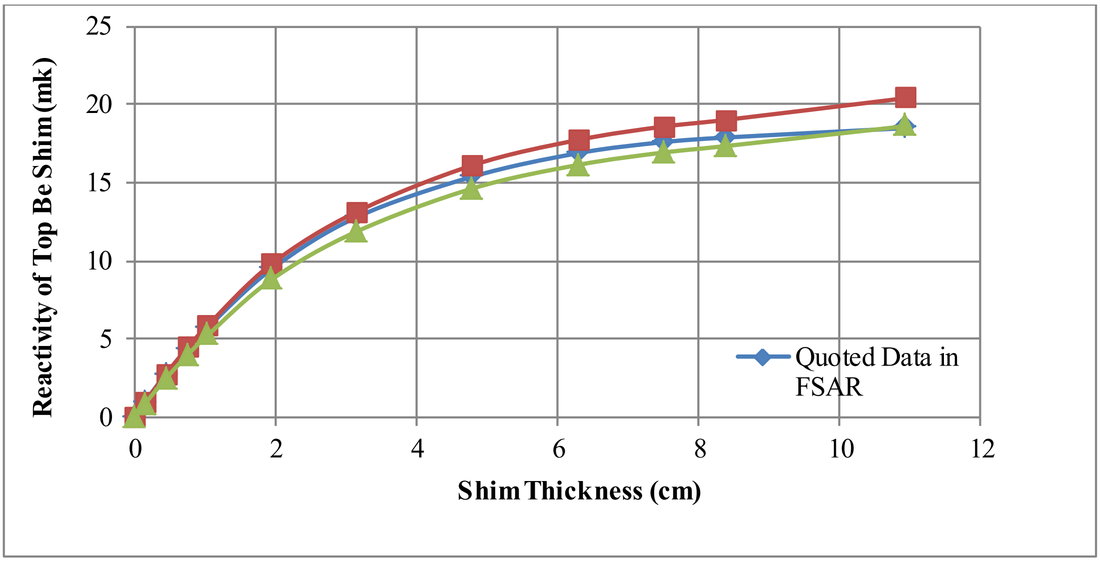

FIG. 7.11. Comparison of reactivity worth of top beryllium shim for HEU and LEU fuel of PARR-2 (Courtesy of Pakistan Institute of Nuclear Science and Technology (PINSTECH), Pakistan).

7.3. THERMAL-HYDRAULIC ANALYSIS

Computer code PARET is employed to implement steady state thermal-hydraulic and transient analyses [6.5]. With PARET, the core can be modelled in four regions. The code was originally developed for power reactors for the analysis of SPERT-III experiments, which was later modified to include a library of various parameters suitable to research reactors. PARET is basically a coupled neutronic–hydrodynamic heat transfer code employing point kinetics, one-dimensional hydrodynamics and one-dimensional heat transfer. The code supports a selection of heat transfer correlations.

7.3.1. Methodology

For the analysis, a two channel model is used in the PARET code. The first is the hottest plate in the core and its associated flow channel, and the second is the core average plate temperature and its associated flow channel. Axial power distribution is represented by 21 equidistant mesh points. It is assumed that about 90% of the total fission energy is deposited in fuel, about 4% is produced in the moderator, about 1% is produced in other reactor materials, and the remaining 5% is absorbed by neutrinos. The coolant inlet temperature is 20°C and the inlet pressure is 1.5 bar. Values for coolant mass flow rate were taken from the reported data [7.2]. For the HEU core, the melting points of both the UAl_4–Al fuel and aluminium cladding are about 650°C, whereas in the LEU cores, the values for the UO_2 fuel and Zircaloy-4 cladding are 2800°C and 1850°C, respectively. Reactivity feedback coefficients were computed in the neutronic analysis, and shown in Table 6.8. Values of prompt neutron lifetime and effective delayed neutron fraction for the HEU fuel were taken from the Final SAR [7.2], and for LEU fuel from the paper 'MNSR Transient Analyses and Thermal-Hydraulic Safety Margins for HEU and LEU Cores Using the RELAP5-3D Code' [7.8].

7.3.2. Results and discussion

7.3.2.1. HEU core

The axial power profile obtained from the neutronic analysis is given in Fig. 7.12. The computed axial temperature distribution in the hot and average channels is shown in Fig. 7.13. The results agree well with the reported data [7.2]. A maximum clad temperature of 55°C at a steady state power level of 30 kW was calculated. The average values of the heat transfer coefficient are 1274 W/m^{2}s and 1232 W/m^{2}s in the hot and average channels respectively. The calculated temperature difference across the core is 19.5°C, and the measured value is 20.5°C, which agrees reasonably well [7.2]. Maximum temperatures are also computed at various power levels. These results are shown graphically in Fig. 7.14.

During commissioning of PARR-2 with HEU fuel, power rising experiments and calculations were performed. Peak power was determined after insertion of a ramp reactivity of 4 mk, equal to the cold core excess reactivity. The intent of the work was to demonstrate the reactor's inherent safety. This has been simulated by PARET. Mass flow rate, which is a design characteristic, was taken from the Final SAR [7.2]. Computed results are shown in Tables 7.9 and 7.10. Calculations of the 4 mk transient analysis indicate a computed peak power of 78 kW for the existing HEU core, which matches reasonably well with the measured value of 87 kW [7.2]. The heat flux increases from 2.2 W/cm^2 at 30 kW to 5.8 W/cm^2 at 78 kW. These values of heat flux are well below the critical heat flux of 151 W/cm^2. Also the maximum cladding surface temperature in the existing HEU core remains 13.5°C below the water saturation temperature. Power and temperature histories for the existing HEU core are illustrated in Figures 7.15(a) and 7.15(b).

7.3.2.2. LEU core

Three potential LEU cores were considered:

— Core 2: enriched to 12.6% U^{235} and a fuel pin diameter of 5.5 mm;
— Core 3: enriched to 12.3% $U^{235}$and a fuel pin diameter of 5.1 mm;
— Core 4: enriched to 12.46% U^{235} and a fuel pin diameter of 5.5 mm, increased thickness of the control rod absorbing material and Zircaloy-4 as a control rod guide tube and grid plate material.

Power peaking factors computed through neutronic analysis are presented in Fig. 7.16. In order to achieve the same level of neutron flux, increasing the operating power level of LEU cores to 33 kW has been suggested. Axial temperature distributions of the fuel centre line, cladding and coolant in the hot channels of the three cores are illustrated in Figs 7.17 (a)—(c). Results show that at the increased steady state operating power level, the cladding temperature increases when compared with the existing HEU core, but would remain far below the temperature at which boiling occurs in the core. Fuel centre line temperatures are also very mild.

For core 2 with a fuel pin diameter of 5.5 mm, the values of the heat transfer coefficient are 1250 W/m^{2}s and 1209 W/m^{2}s in the hot and average channels respectively. The temperature difference across the core is 21.2°C. Peak fuel and clad surface temperatures are 69.8°C and 61.0°C respectively. Results of a 4 mk reactivity insertion transient analysis show that power peaks at 68.1 kW. An LEU core would attain a lower peak power due to the large Doppler coefficient compared to the HEU core. The maximum cladding surface temperature for core 2 is 88.6°C, less than 97.9°C for the HEU core. Both the temperature and power history in a 4 mk transient are shown in Figs 7.18 (a) and (b).

For core 3 with a fuel pin diameter of 5.1 mm, the values of heat transfer coefficient ranges are 1266 W/m^2s and 1221 W/m^2s for the hot and average channels respectively. The temperature difference across the core is 20.48°C. Peak fuel and cladding surface temperatures are 70.2°C and 61.4°C respectively. The power for a 4 mk reactivity insertion transient peaks at 70.27 kW. The maximum cladding surface temperature is 90.9°C. Both the temperature and power history in a 4 mk transient are shown in Figs 7.19 (a) and (b).

In a thermal-hydraulic and transient analysis of core 4, the temperature difference across the core is 22.6°C. Peak fuel and clad surface temperatures are 74.9°C and 60.1°C respectively. Results of a 4 mk reactivity insertion transient analysis show that power peaks at 66.2 kW. The LEU core 4 would attain a lower peak power due to the large Doppler coefficient compared to the HEU core. The maximum cladding surface temperature is 86.2°C, compared to 97.9°C for the HEU core. The decrease is due to a less pronounced power peak in the LEU core 4 with a higher Doppler coefficient of reactivity. Both the temperature and power history in a 4 mk transient are shown in Figs 7.20 (a) and (b).

TABLE 7.8. KINETIC PARAMETERS AND REACTIVITY FEEDBACK COEFFICIENTS

	Core 1 (existing HEU core)	Core 2 (proposed LEU core)	Core 3 (proposed LEU core)	Core 4 (proposed LEU core)
Prompt neutron generation time (μs)	57.00	47.00	50.50	47.00
Effective delayed neutron fraction (β_{eff})	0.00850	0.00845	0.00832	0.00845
Water temperature coefficient (%Δk/k/°C)	6.278×10^{-2}	3.966×10^{-3}	4.198×10^{-3}	4.276×10^{-3}
Void/density coefficient (%Δk/k /%void)	0.326	0.356	0.348	0.344
Doppler coefficient (%Δk/k/°C)	1.546×10^{-4}	1.395×10^{-3}	1.342×10^{-3}	1.395×10^{-3}

TABLE 7.9. RESULTS OF STEADY STATE THERMAL-HYDRAULIC ANALYSIS OF PARR-2

Parameter	Core 1 (existing HEU core)	Core 2 (proposed LEU core)	Core 3 (proposed LEU core)	Core 4 (proposed LEU core)
Fuel pin diameter (mm)	5.5	5.5	5.1	5.5
U^{235} enrichment (%)	90.2	12.6	12.3	12.46
Operating power (kW)	30	33	33	33
Power peaking factors				
Axial	1.1271	1.1333	1.1389	1.3352
Radial	1.1234	1.1311	1.1388	1.0754
Pressure at core inlet (kPa)	1.5	1.5	1.5	1.5
Saturation temperature in core (°C)	111.4	111.4	111.4	111.4
Steady state temperatures (°C)				
Coolant temperature rise across core	19.5	21.24	20.48	22.59
Peak clad surface temperature	54.97	61.01	61.37	60.06
Peak centreline temperature	55.20	69.82	70.22	74.94
Average heat flux (W/cm^2)	1.833	2.016	2.603	2.016
Peak heat flux (W/cm^2)	2.321	2.584	3.376	2.895
Critical heat flux (W/cm^2)	151.2	151.2	151.2	151.2
Margin to critical heat flux	65.1	58.5	44.8	52.2

TABLE 7.10. RESULTS OF 4 mk TRANSIENT ANALYSIS OF PARR-2

Parameter	Core 1 (existing HEU core)	Core 2 (proposed LEU core)	Core 3 (proposed LEU core)	Core 4 (proposed LEU core)
Fuel pin diameter (mm)	5.5	5.5	5.1	5.5
U^{235} enrichment (%)	90.2	12.6	12.3	12.46
Peak power (kW)	78.2	68.10	70.27	66.2
Peak temperatures (°C)				
Fuel centreline	98.5	106.74	110.17	116.4
Cladding surface	97.9	88.58	90.93	86.2

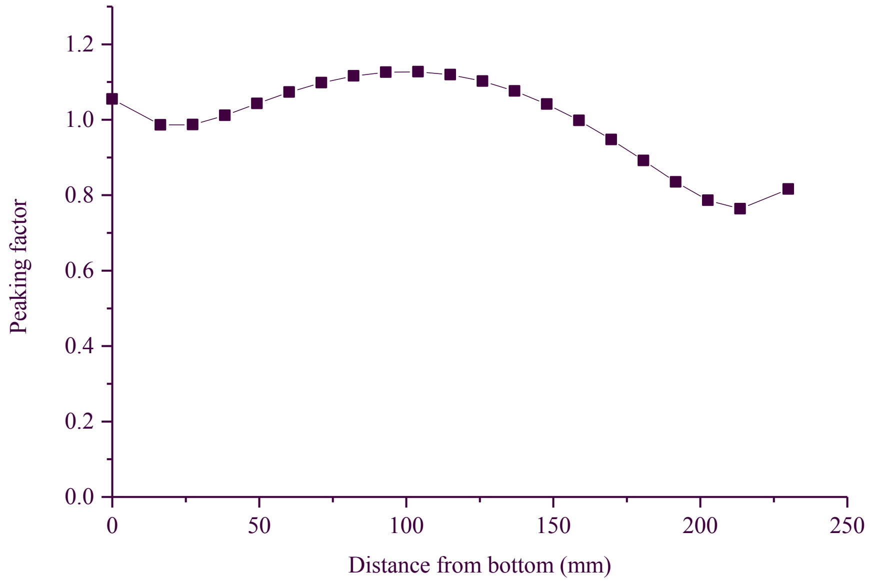

FIG. 7.12. Axial power profile in the HEU core (Reproduced from Ref. [6.3] with permission courtesy of Pakistan Institute of Nuclear Science and Technology (PINSTECH), Pakistan).

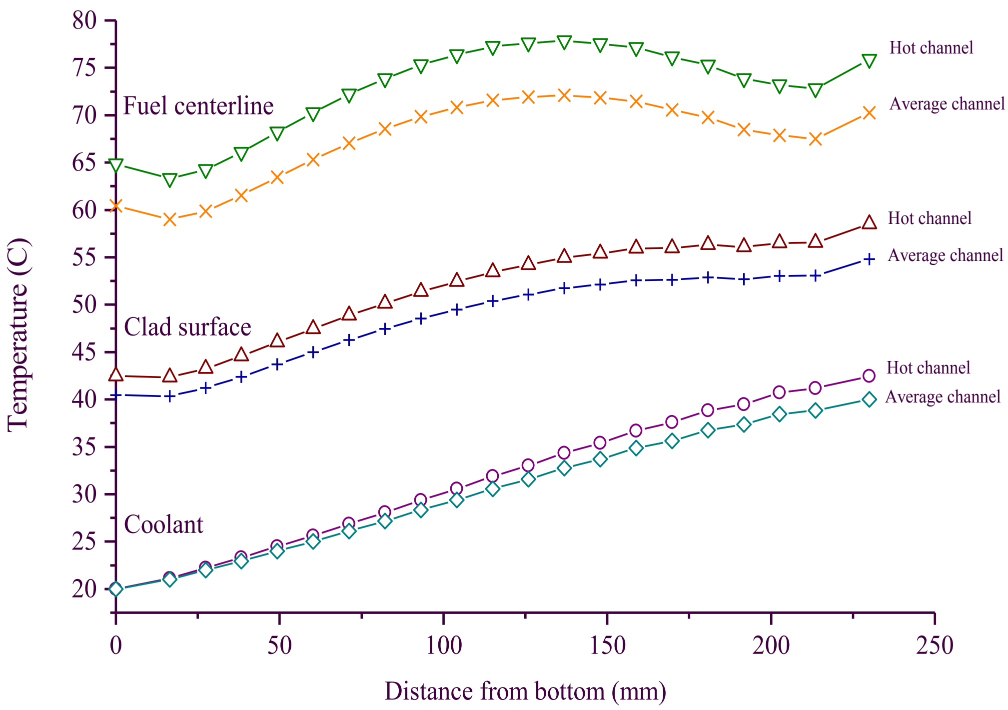

FIG. 7.13. Axial distribution of temperature in hot and average channels of HEU core at a steady state power level of 30 kW (Courtesy of Pakistan Institute of Nuclear Science and Technology (PINSTECH), Pakistan).

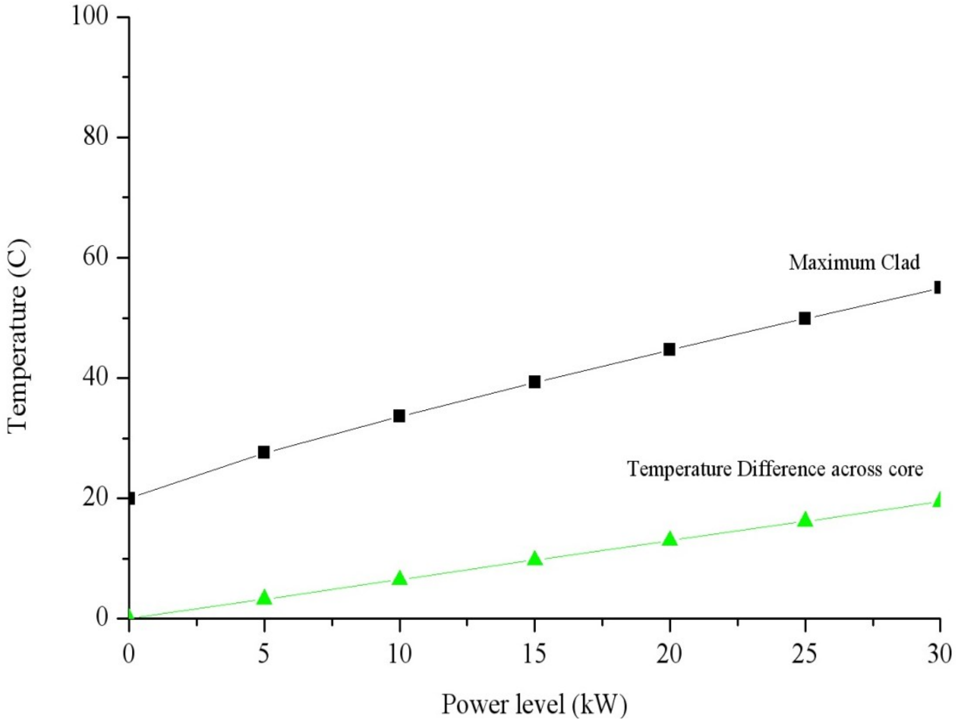

FIG. 7.14. Steady state temperatures as a function of power level in the HEU core (Reproduced from Ref. [7.3] with permission courtesy of Pakistan Institute of Nuclear Science and Technology (PINSTECH), Pakistan).

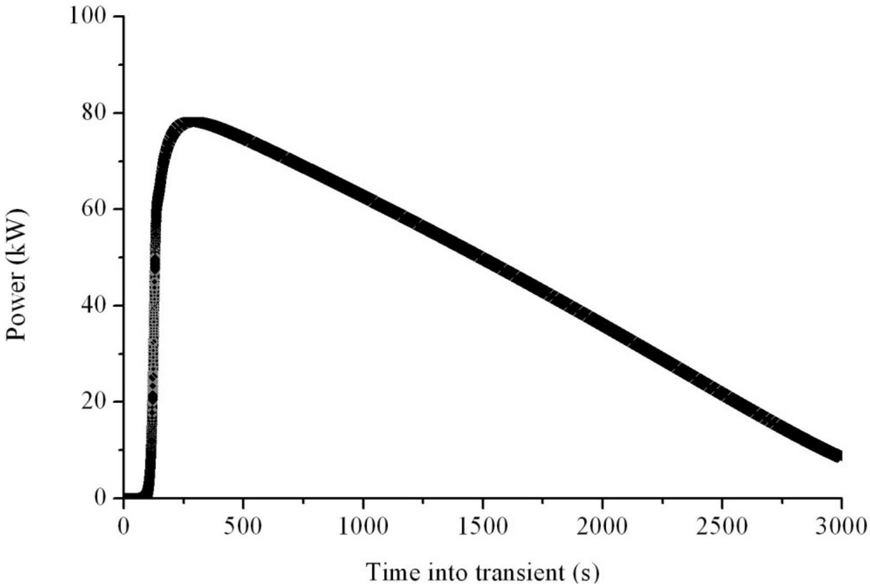

FIG. 7.15 (a). Power history in a transient from 4 mk ramp reactivity insertion in the HEU core (Reproduced from Ref. [7.3] with permission courtesy of Pakistan Institute of Nuclear Science and Technology (PINSTECH), Pakistan).

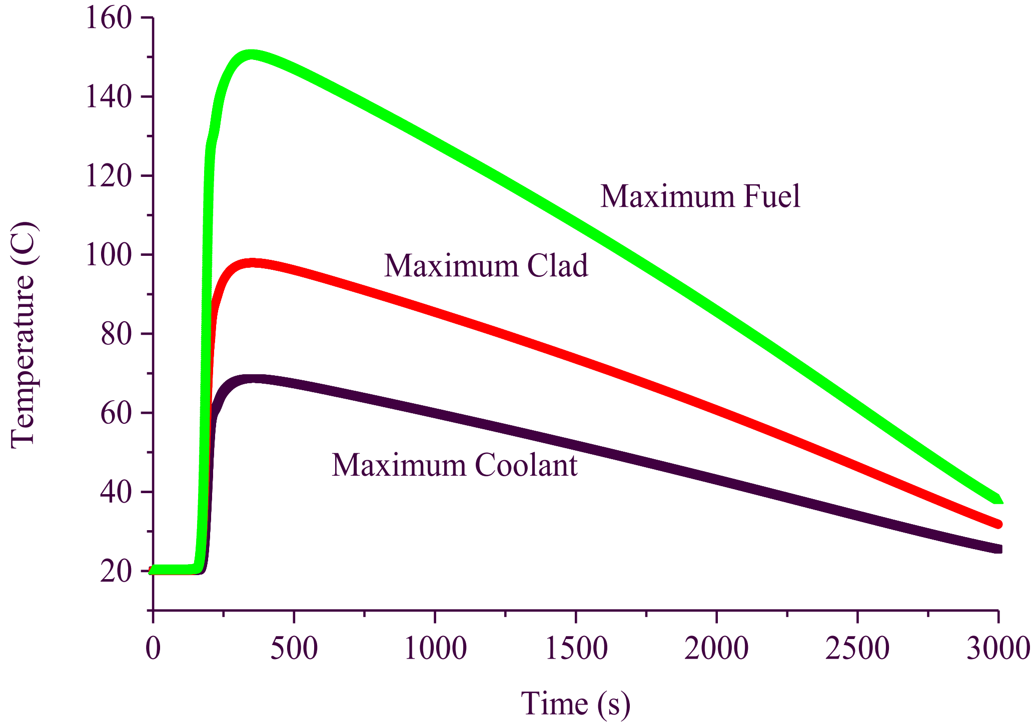

FIG. 7.15 (b). Temperature history in a transient from 4 mk ramp reactivity insertion in the HEU core (Reproduced from Ref. [7.3] with permission courtesy of Pakistan Institute of Nuclear Science and Technology (PINSTECH), Pakistan).

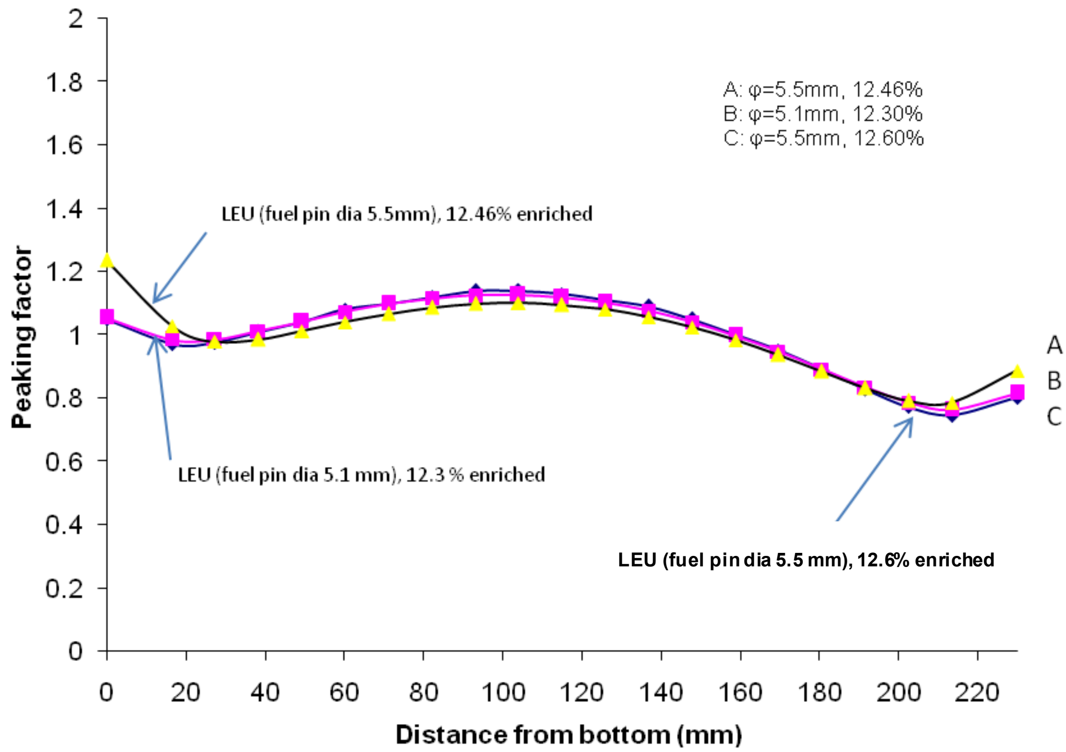

FIG. 7.16. Axial power density distribution in proposed LEU cores (Courtesy of Pakistan Institute of Nuclear Science and Technology (PINSTECH), Pakistan).

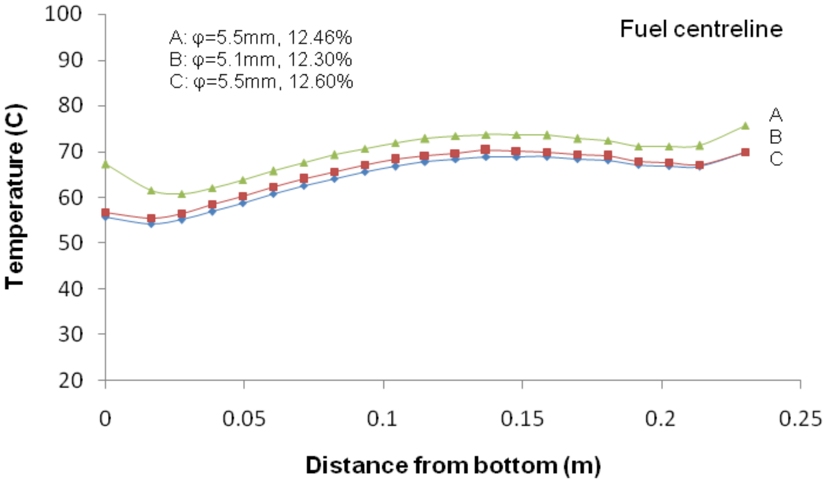

FIG. 7.17 (a). Axial distribution of fuel centre line temperature in the proposed LEU cores at a steady state power level of 33 kW (Courtesy of Pakistan Institute of Nuclear Science and Technology (PINSTECH), Pakistan).

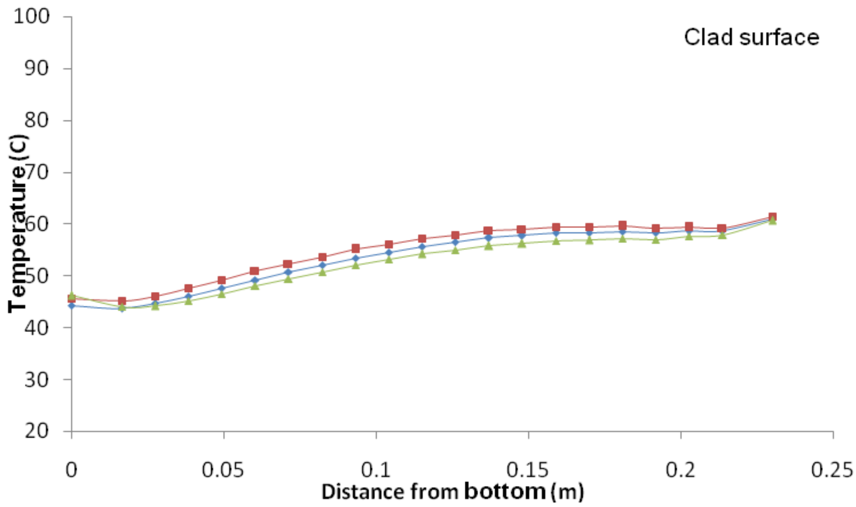

FIG. 7.17 (b). Axial distribution of clad temperature in the proposed LEU cores at a steady state power level of 33 kW (Courtesy of Pakistan Institute of Nuclear Science and Technology (PINSTECH), Pakistan).

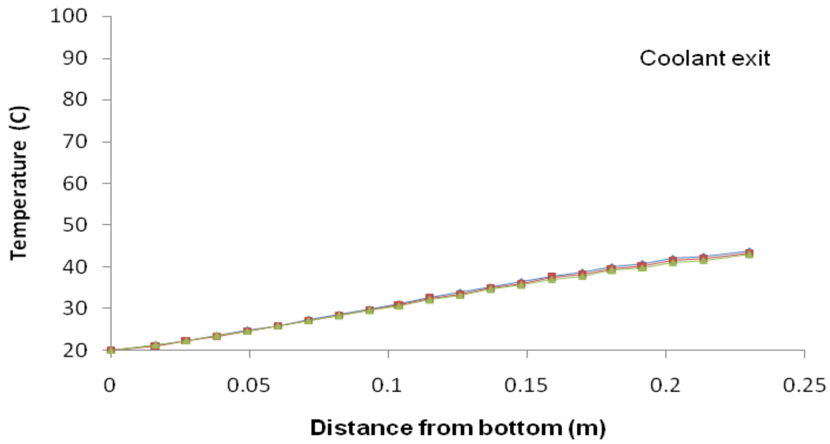

FIG. 7.17 (c). Axial distribution of coolant temperature in the proposed LEU cores at a steady state power level of 33 kW (Courtesy of Pakistan Institute of Nuclear Science and Technology (PINSTECH), Pakistan).

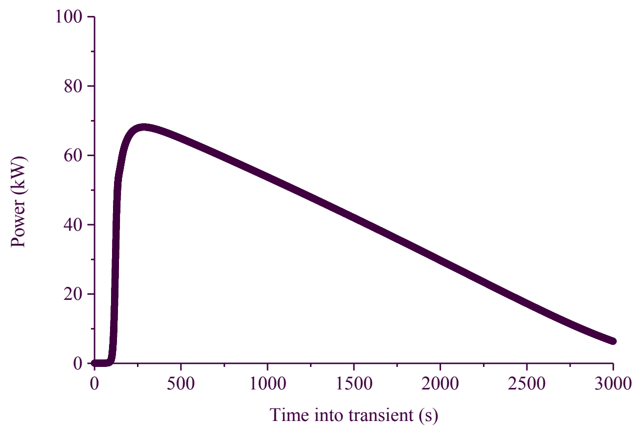

FIG. 7.18 (a). Power history in a transient from 4 mk ramp reactivity insertion in LEU core 2 (fuel pin diameter 5.5 mm and 12.6% enrichment) (Reproduced from Ref. [7.3] with permission courtesy of Pakistan Institute of Nuclear Science and Technology (PINSTECH), Pakistan).

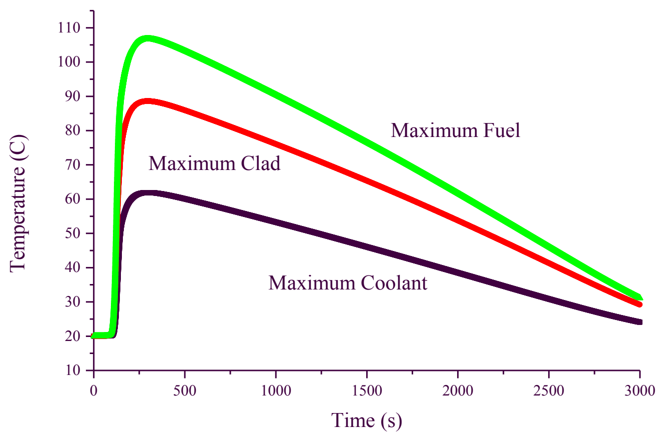

Fig. 7.18 (b). Temperature history in a transient from 4 mk ramp reactivity insertion in LEU core 2 (fuel pin diameter 5.5 mm and 12.6% enrichment) (Reproduced from Ref. [7.3] with permission courtesy of Pakistan Institute of Nuclear Science and Technology (PINSTECH), Pakistan).

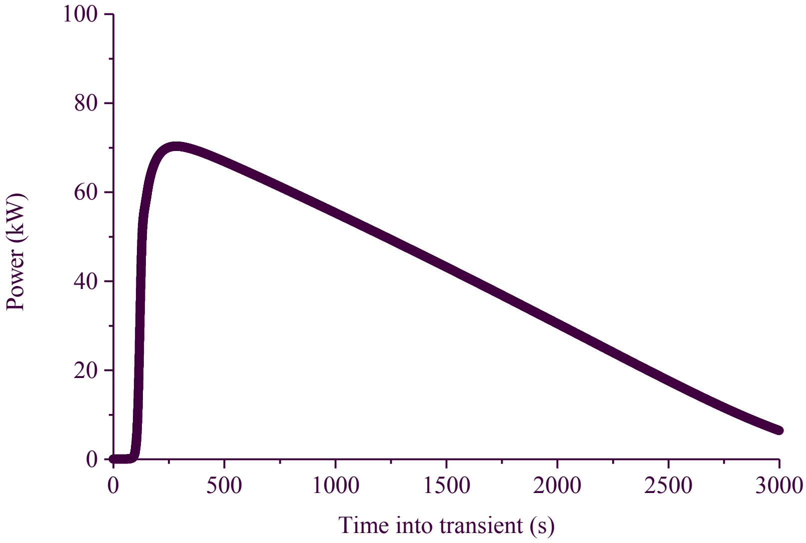

FIG. 7.19 (a). Power history in a transient from 4 mk ramp reactivity insertion in LEU core 3 (fuel pin diameter 5.1 mm and 12.3% enrichment) (Reproduced from Ref. [7.3] with permission courtesy of Pakistan Institute of Nuclear Science and Technology (PINSTECH), Pakistan).

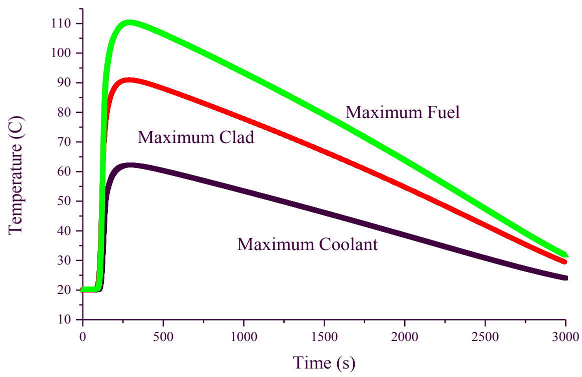

FIG. 7.19 (b). Temperature history in a transient from 4 mk ramp reactivity insertion in LEU core 3 (fuel pin diameter 5.1 mm and 12.3% enrichment) (Reproduced from Ref. [7.3] with permission courtesy of Pakistan Institute of Nuclear Science and Technology (PINSTECH), Pakistan).

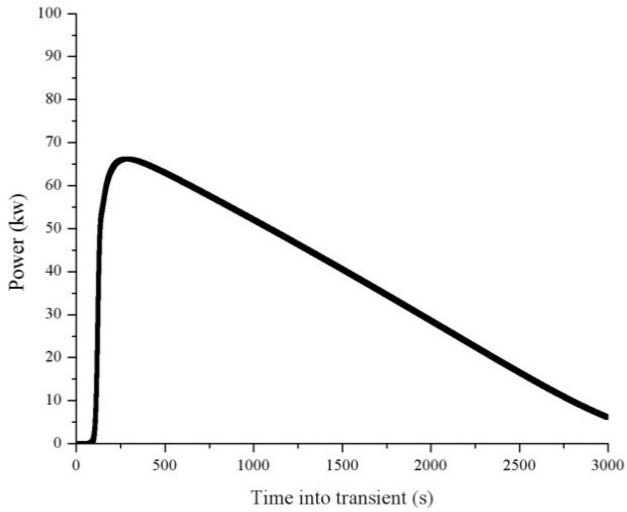

FIG. 7.20 (a). Power history in a transient from 4 mk ramp reactivity insertion in LEU core 4 (fuel pin diameter 5.5 mm and 12.46% enrichment) (Courtesy of Pakistan Institute of Nuclear Science and Technology (PINSTECH), Pakistan).

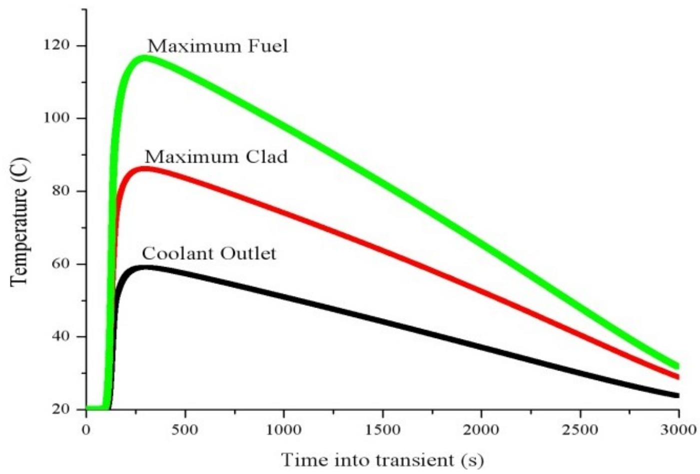

Fig. 7.20 (b). Temperature history in a transient from 4mk ramp reactivity insertion in LEU core 4 (fuel pin diameter 5.5 mm and 12.46% enrichment) (Courtesy of Pakistan Institute of Nuclear Science and Technology (PINSTECH), Pakistan).

7.4. RADIOLOGICAL CONSEQUENCE ANALYSIS

DBA and BDBA occurrences at PARR-2 were also analysed. Calculations were performed for the existing HEU-fuelled core and a prospective LEU-fuelled core. The composition of the existing HEU fuel is UAl_4–Al, while the prospective LEU fuel analysed was 12.46% enriched UO_2 fuel with zircaloy cladding (core 4). To calculate fission product inventory and the gamma ray spectrum in the core, burnup calculations are performed using ORIGEN2 code [7.9]. In the case of a DBA event, pit corrosion is assumed to occur in one fuel pin. As a result, gaseous fission products release through the pin hole, and ultimately these gases are dispersed in the atmosphere. Hotspot code is employed to model the dispersion of these gases in the atmosphere and perform dose calculations at different distances from the reactor. In the case of a BDBA event, it is assumed that pool water leaks and the reactor core is exposed to air. In this case the core does not melt. Gamma ray dose rate calculations are performed as a function of distance. Both DBA and BDBA events are described in detail in the following section.

7.4.1. **DBA**

7.4.1.1. Accident scenario

The following scenario was used for the DBA:

- The reactor is operating at 31 kW;
- The reactor has been operating for ten years at full power, 2.5 hours a day, five days a week;
- Pit corrosion of the cladding creates a hole in one fuel pin; and
- Gaseous fission products accumulate in the vessel top and are released to the environment without any retention through the operation of the gas purge system after six hours of reactor operation.

7.4.1.2. Assumptions

The following assumptions were made for the DBA:

- Continuous reactor operation occurs for the first 266 days;
- Reactor operation for 2.5 hours a day and 21.5 hours of decay time for five working days during the week is employed in ORIGEN2 for the last 10 weeks of reactor operation; and
- Dose rates are calculated at different distances and for different Pasquill stability classes.

7.4.1.3. Dose calculations

Fission product inventory was calculated using ORIGEN2. This is a versatile point depletion and decay computer code for use in simulating nuclear fuel cycles and calculating nuclide compositions. This code and its associated decay constants, cross-sections, and photon libraries were developed in the late 1960s for use in generic fuel cycle studies [7.9]. Noble gases are assumed to be released completely through the gas purge system, while 40% of iodine was considered to be released after retention in water [7.10].

The activity of the gaseous fission products after six hours of reactor operation and activity released to the atmosphere, allowing for 40% retention of iodine in water, is shown in Table 7.11. No significant difference in isotopic activity for HEU and LEU fuels at the same reactor power of 31 kW is observable.

When radioactive gases are released to the atmosphere, they are transported downwind and dispersed by a normal atmospheric mixing process. As a result, members of the local public are exposed. The dose received by an individual is due to inhalation of the radioactive material and the external dose due to beta and gamma radiation. The internal dose is calculated for thyroid, bone, kidney, muscle, etc., by grouping the radionuclides affecting these organs. The external dose due to beta and gamma radiation is calculated for all fission products released.

Hotspot version 2.06 is used to calculate the total effective dose equivalent (TEDE) and thyroid dose as a function of the distance from the release point. Hotspot is a hybrid of the well-established Gaussian plume model, widely used for initial emergency assessment or safety analysis planning. Meteorologists distinguish different states of the atmospheric surface layer as unstable, neutral, or stable. These categories refer to how a parcel of air reacts when displaced adiabatically in the vertical direction. Hotspot allows the selection of the atmospheric stability classification. Slightly unstable atmospheric conditions, Pasquill stability class C, in the east–northeast direction are observed frequently at the site. Radiation dose calculations are performed using the site specific meteorological data with an average wind speed of 2 m/s for ground level releases [7.10]. The breathing rate is taken to be 3.33×10^{-4} m^3/s for an average human being. Detailed dose calculations for TEDE and thyroid dose as a function of distance for Pasquill stability class C are presented in Table 7.12. The resulting maximum value of TEDE is 1.5 μSv, while the maximum value of the thyroid dose is 6.1 μSv.

In order to find the longest distance at which the maximum dose may occur, calculations are also performed for the other Pasquill stability classes. Fig. 7.21 shows the TEDE of an HEU MNSR core, while Fig. 7.22 shows the TEDE of an LEU MNSR core for all stability classes. No significant difference in TEDE profiles for HEU and LEU fuels is observable at the same operating power for both fuels. The longest distance is 500 m overall, while the maximum value of TEDE is 0.8 μSv. This value is obtained for stability class F. For all other stability classes, the maximum value of TEDE lies at a shorter distance.

TABLE 7.11. GASEOUS ACTIVITY OF THE CORE AND ACTIVITY RELEASED TO THE ATMOSPHERE

Nuclide	HEU core 1		LEU core 4	
	Core activity (Bq)	Activity released (Bq)	Core activity (Bq)	Activity released (Bq)
^{83m}Kr	9.8050×10^{11}	2.8503×10^{9}	9.7902×10^{11}	2.8460×10^{9}
^{85}Kr	1.2047×10^{11}	3.5021×10^{8}	1.1981×10^{11}	3.4827×10^{8}
^{85m}Kr	1.5984×10^{12}	4.6465×10^{9}	1.5888×10^{12}	4.6185×10^{9}
^{87}Kr	7.0337×10^{11}	2.0447×10^{9}	6.9856×10^{11}	2.0307×10^{9}
^{88}Kr	3.6989×10^{12}	1.0753×10^{10}	3.6730×10^{12}	1.0677×10^{10}
^{131m}Xe	3.6168×10^{10}	1.0514×10^{8}	3.6367×10^{10}	1.0572×10^{8}
^{133}Xe	5.1948×10^{12}	1.5101×10^{10}	5.1985×10^{12}	1.5112×10^{10}
^{133m}Xe	1.6491×10^{11}	4.7939×10^{8}	1.6509×10^{11}	4.7992×10^{8}
^{135}Xe	7.6812×10^{12}	2.2329×10^{10}	7.6886×10^{12}	2.2351×10^{10}
^{135m}Xe	1.2917×10^{12}	3.7549×10^{9}	1.2902×10^{12}	3.7506×10^{9}
^{138}Xe	1.3520×10^{6}	3.9302×10^{3}	1.3475×10^{6}	3.9173×10^{3}
^{128}I	6.7525×10^{4}	1.96×10^{2}	5.3761×10^{4}	6.2513×10^{1}
^{130}I	1.1292×10^{9}	3.28×10^{6}	9.2056×10^{8}	1.0704×10^{6}
^{131}I	2.3173×10^{12}	6.74×10^{9}	2.3280×10^{12}	2.7070×10^{9}
^{132}I	3.7925×10^{12}	1.10×10^{10}	3.8036×10^{12}	4.4228×10^{9}
^{133}I	7.7811×10^{12}	2.26×10^{10}	7.7848×10^{12}	9.0521×10^{9}
^{134}I	1.8385×10^{12}	5.34×10^{9}	1.8352×10^{12}	2.1340×10^{9}
^{135}I	8.0623×10^{12}	2.34×10^{10}	8.0549×10^{12}	9.3662×10^{9}

TABLE 7.12. TEDE OF PARR-2 CORE FOR DESIGN BASIS ACCIDENT (PASQUILL STABILITY CLASS C)

Distance from release (m)	HEU core/LEU core	
	TEDE (μSv)	Thyroid dose (μSv)
10	0	0.0
20	2.8×10^{-5}	1.1×10^{-4}
40	3.0×10^{-1}	1.2
80	1.5	6.1
100	1.5	5.9
200	6.7×10^{-1}	2.7
400	2.0×10^{-1}	7.9×10^{-1}
800	5.3×10^{-2}	2.1×10^{-1}
1000	4.3×10^{-2}	1.4×10^{-1}

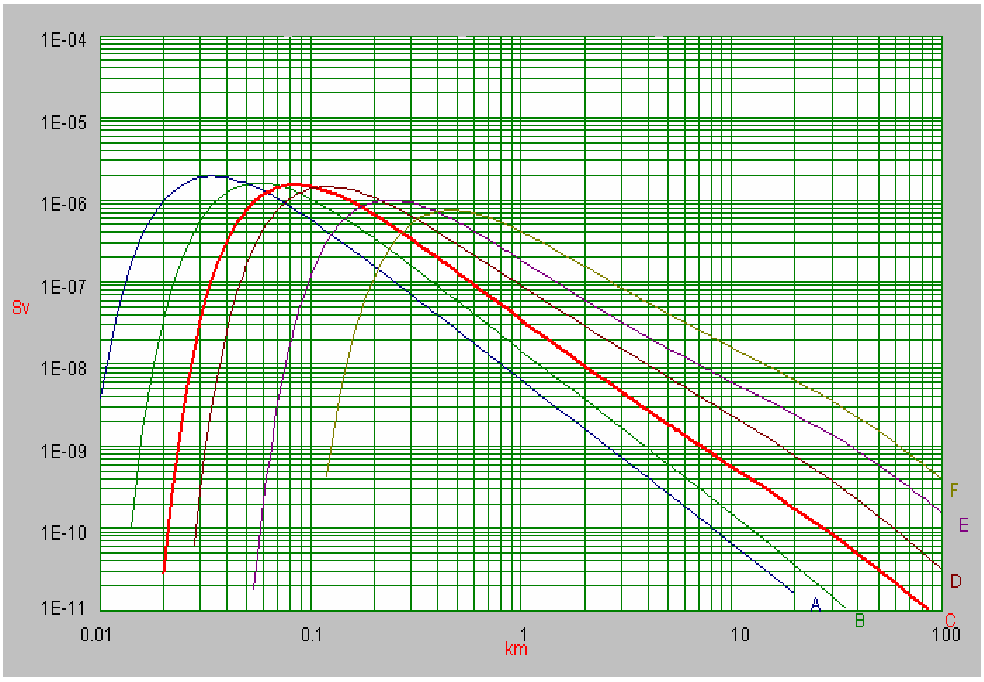

FIG. 7.21. TEDE profile for releases from a typical HEU MNSR core (Courtesy of Pakistan Institute of Nuclear Science and Technology (PINSTECH), Pakistan).

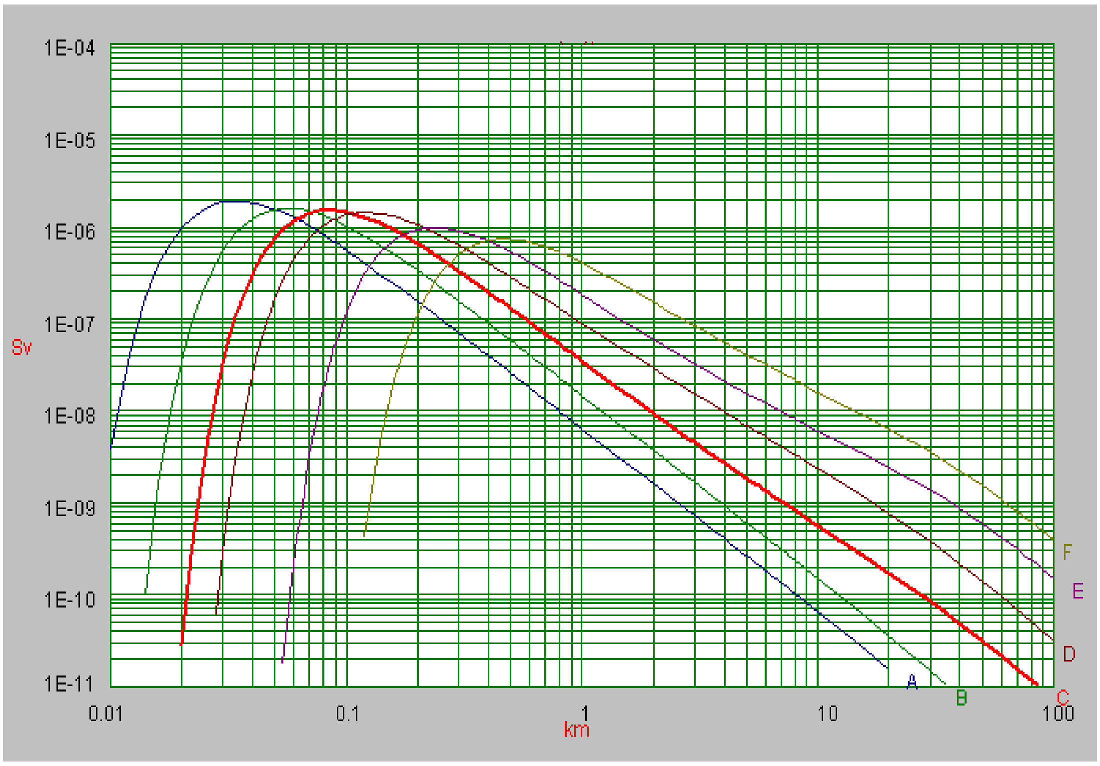

FIG. 7.22. TEDE profile for releases from a typical LEU MNSR core (Courtesy of Pakistan Institute of Nuclear Science and Technology (PINSTECH), Pakistan).

7.4.2. BDBA

7.4.2.1. Accident scenario

The following scenario was used for the BDBA:

— The reactor building collapses;
— Reactor vessel water and pool water leak at a rate of 4 m^3/h;
— The reactor core is exposed to air after 6 hours, but the core does not melt;
— The reactor was operating at 31 kW; and
— The reactor has been operating for ten years at full power, 2.5 hours a day, five days a week.

7.4.2.2. Assumptions

The following assumptions were made for the BDBA:

— Continuous reactor operation occurs for the first 266 days;
— Reactor operation for 2.5 hours a day and 21.5 hours of decay time for five working days during the week is employed in ORIGEN2 for the last 10 weeks of reactor operation; and
— Dose rates are calculated at different distances and for different Pasquill stability classes.

7.4.2.3. Dose calculations

ORIGEN2 code is used for the depletion calculations of PARR-2. By employing this code, a gamma ray photon spectrum of 18 energy groups was obtained. Gamma ray dose rate calculations are performed for a fully exposed core using Equation 7.1:

$$D = 0.0576\Phi_\gamma E\left(\frac{\mu_a}{\rho}\right) \tag{7.1}$$

where

D is the dose rate,
Φ_γ is the gamma flux,
E is the gamma energy and $\frac{\mu_a}{\rho}$ is the mass energy absorption coefficient.

Table 7.13 lists the gamma dose rate as a function of distance for both HEU and the proposed LEU cores for PARR-2. The dose rate is slightly higher for the LEU core. The gamma dose rate profile at different cooling times is shown in Fig. 7.23.

TABLE 7.13. GAMMA DOSE RATE OF THE PARR-2 CORE FOR BDBA

Distance from core (m)	Dose rate for HEU core (Sv/h)	Dose rate for LEU core (Sv/h)
5	1.865	1.972
6	1.295	1.369
7	0.951	1.006
8	0.728	0.770
9	0.575	0.609
10	0.466	0.493
20	0.116	0.123

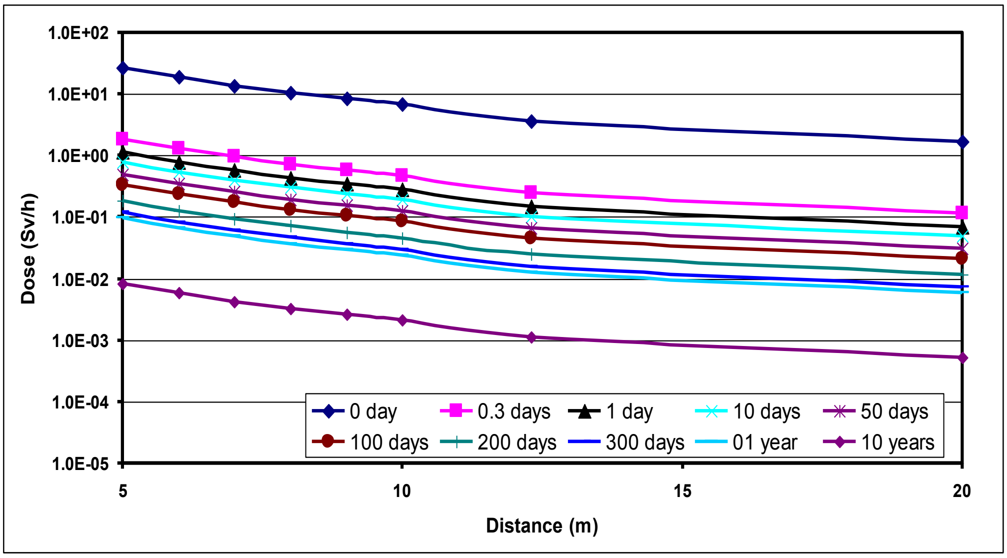

FIG. 7.23. Gamma dose rate of the PARR-2 HEU core at different cooling times (Courtesy of Pakistan Institute of Nuclear Science and Technology (PINSTECH), Pakistan).

7.4.2.4. Decay heat calculations

The gamma ray decay heat profile for both the HEU core and proposed LEU core of PARR-2 is shown in Fig. 7.24. Due to the same operating power and assumptions for operating history, the results for the HEU and LEU-fuelled cores overlap.

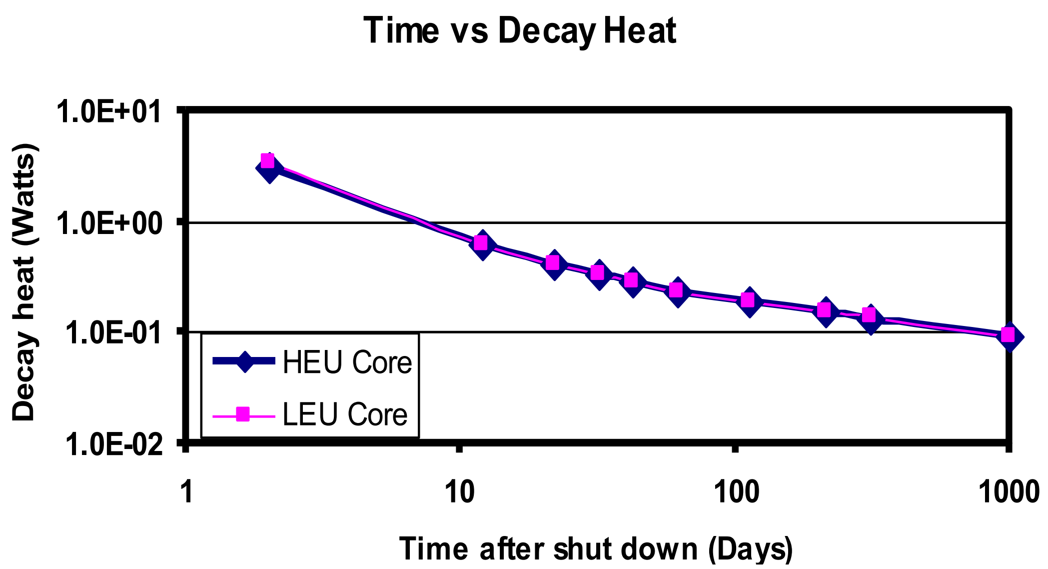

FIG. 7.24. Gamma ray decay heat of PARR-2 HEU and LEU cores at different cooling times (Courtesy of Pakistan Institute of Nuclear Science and Technology (PINSTECH), Pakistan).

7.5. CONCLUSION

The calculation methodology necessary for the conversion of an MNSR from HEU to LEU fuel is validated after analysis of the 90.2% enriched HEU core. Using the current HEU-fuelled core as an experimental model, analysis of the proposed UO_2 LEU core suggests that this is a suitable alternative fuel for PARR-2. However, the neutron flux at irradiation sites is slightly lower for LEU-fuelled reactor operation at 30 kW. Therefore, reactor power must be increased to a level of 33 kW to obtain the same thermal flux values as the existing HEU core. Using the same control rod for the LEU core that is in the current HEU core may result in lower values of shut-down margin and control rod worth. However, a slightly increased diameter of the control rod improves the shutdown margin to a value comparable to the corresponding value for the current HEU core. Changing the material of the control rod guide tube from aluminium to Zircaloy-4 results in a slight decrease in enrichment for the LEU fuel, despite the increase in diameter of the control rod absorbing material. With consideration of the core neutronic parameters, a UO_2 LEU-fuelled core with the following characteristics provides a suitable replica of the currently operating HEU core:

— Enrichment: 12.46%;
— Reactor power: 33 kW;
— Control rod absorber (cadmium) thickness: 4.5 mm;
— Guide tube and grid plate material: Zircaloy-4; and
— Cladding material of fuel pin: Zircaloy-4.

All other materials and structures are assumed to be the same as those in use in the current HEU core.

Analysis of the gaseous effluents from MNSRs as a result of accidental release indicates that the level of the dose is well below the criterion established by IAEA Safety Standards No. GSR Part 3. There is no significant difference between the dose values for HEU and prospective LEU fuels. Therefore, the existing HEU core and prospective LEU core of the MNSR are considered to be safe for the public, even in case of an accidental release of radioactive gases from the fuel.

REFERENCES TO SECTION 7

[7.1] MAHMOOD, T., PERVEZ, S., IQBAL, M., Neutronic analysis for core conversion (HEU–LEU) of Pakistan research reactor-2 (PARR-2), Annals of Nuclear Energy, 35/8, (2008), 1440-1446.

[7.2] QAZI, M.K., ISRAR, M., KARIM, A., Revised Final Safety Analysis Report (FSAR) on Pakistan Research Reactor-2, PINSTECH (1994).

[7.3] ISHTIAQ, H.B., PERVEZ, S., Safety analysis for core conversion (from HEU to LEU) of Pakistan research reactor-2 (PARR-2), Nuclear Engineering and Design, 240/1 (2010), 123-128.

[7.4] JONAH, S.A., LIAW, J.R., OLSON, A., MATOS, J.E., Criticality Calculations and Transient Analysis of the Nigeria MNSR (NIRR-1) for Conversion to LEU, RERTR Meeting, (2006).

[7.5] HALSALL, M. J., A Summary of WIMSD4 Input Options, AEEW-M 1327 (1980).

[7.6] FOWLER, T.B., VONDY, D.R., CUNNINGHAM, G.W., Nuclear Reactor Core Analyses Code CITATION, ORNL – TM – 2496 Rev. 2 (1971).

[7.7] OBENCHAIN, C.F., PARET – A Program for the Analysis of Reactor Transients, ACE Research and Development Report, IDO-17282 (1969).

[7.8] DUNN, F.E., THOMAS, J., LIAW, J., MATOS, J.E., MNSR Transient Analyses and Thermal Hydraulic Safety Margins for HEU and LEU Cores using the RELAP5-3D Code, RERTR Meeting, (2007).

[7.9] CROFF, A.G., A User's Manual for the ORIGEN Computer Code, OAK RIDGE National Laboratory, Oak Ridge (1980).

[7.10] RAZA, S.S., IQBAL, M., Atmospheric dispersion modeling for an accidental release from the Pakistan Research Reactor-1 (PARR-1), Ann. Nucl. Energy, 32, 1157-1166 (2005).

8. FEASIBILITY STUDY FOR CONVERTING THE SYRIAN MNSR CORE FROM HEU TO LEU FUEL

8.1. INTRODUCTION

The Syrian MNSR is a tank-in-pool type research reactor with HEU fuel enriched to 89.87% ^{235}U. Its core is formed from 347 fuel rods with a surrounding beryllium reflector of about 10 cm in thickness, as shown in Figures 8.1–8.3. The main characteristics of the MNSR, and the lattice positions of the fuel cage, including four tie rods and three dummy elements inserted into circles eight and ten respectively are described in Tables 8.1 and 8.2. A bottom reflector is supported on four supporting pieces made of aluminium locally known as 'the basement.'

The cold initial excess reactivity is approximately 4.00 mk, while the total β_{eff} is 8.08 [8.1]. The initial excess reactivity is therefore only about half the delayed neutron fraction in the reactor, and hence the reactor has a large margin for control.

The control of the reactor relies upon just one control rod in the centre of the core with an effective worth of about 7.00 mk, which ensures a shutdown margin of about 3.00 mk [8.1].

The actual operable time of the Syrian MNSR is about 2.5 hours at nominal power. The limitation of this time is due to the aforementioned small initial cold excess reactivity at reactor start-up. This reactivity is consumed during reactor operation by moderator temperature rise and xenon poisoning.

The reflector is a very important part of this reactor. If the reflector was not made of beryllium, it would not reach criticality. When both the side and bottom reflectors are substituted with water, the initial excess reactivity (IER) using this model is –174.04 mk [8.2]. The bottom reflector is responsible for only about 14% of this reactivity. The side reflector is by far more important than the bottom reflector.

The reactor is used mainly for NAA. The irradiation of samples in the reactor is achieved through ten vertical holes in the reactor, of which five, called internal irradiation sites (IIS), are located in the annulus beryllium reflector, with the other five, the external irradiation sites (EIS), located in the water surrounding the beryllium reflector. The internal holes are equipped with aluminium tubes, which are the irradiation tubes (IT) that host the samples during irradiation. Polyethelene tubes connect the ITs to the capsule ejector and control desk. The capsule transfer system is a rabbit type system consisting of a compressed air source, a transfer tube, a control desk and an irradiation tube.

Two rabbit systems are used to transfer the sample into and out of the reactor. MNSRs use HEU fuel, which brings 3.94 mk IER at reactor start-up when the fuel is fresh. The fuel is not highly consumed in the Syrian reactor; approximately 1% has been used since start-up in 1996.

The thermal neutron flux in these positions for both the IIS and EIS at rated power is about 1×10^{12} cm^{-2}s^{-1}, and 5×10^{11} cm^{-2}s^{-1}, respectively. These reactors have a good power to flux ratio. They also have a high ratio of thermal to fast flux, which is greater than four. The new LEU fuel is expected to keep these ratios as high as the HEU fuel. Since the nuclear properties of the HEU and LEU fuels differ, various safety issues should be examined and addressed.

FIG. 8.1. A schematic view of the core fuel rods (Courtesy of Atomic Energy Commission, Syrian Arab Republic).

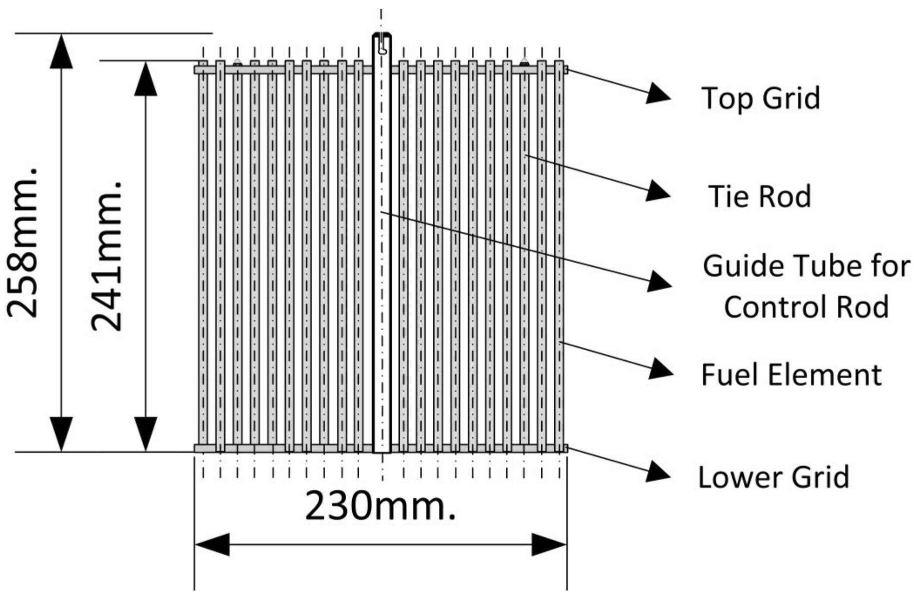

FIG. 8.2. A schematic longitudinal cross section of the reactor core (Courtesy of Atomic Energy Commission, Syrian Arab Republic).

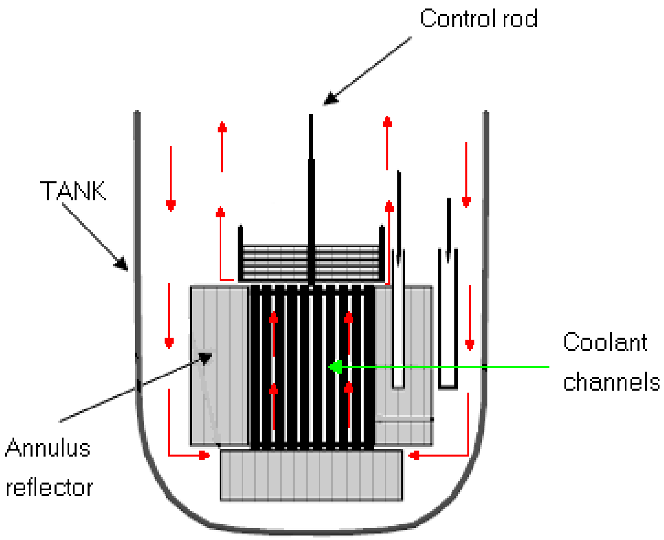

FIG. 8.3. A schematic representation of the lower part of the tank of the Syrian MNSR (Courtesy of Atomic Energy Commission, Syrian Arab Republic).

To achieve the goal of substituting the current HEU fuel with the proposed LEU fuel, both the HEU and LEU fuels were examined. The analysis included both neutronic and thermal-hydraulic aspects, in addition to a DBA and BDBA.

8.2. THE NEUTRONIC ANALYSIS

Neutronic calculations are executed using BMAC software [8.3], which uses WIMSD4 [8.4] as a cell code and CITATION [8.5] as a core calculation code. The generated cross-sections are then automatically transferred to CITATION code. Using BMAC software the parameters shown in Table 8.3 are found for the current MNSR HEU fuel.

The IER refers to the available reactivity at start-up and at full control rod withdrawal from the core. Flux values used in the calculation refer to four neutronic groups, whose upper energy limits are 10 MeV, 0.821 MeV, 5530 eV, and 0.625 eV. Since the results fit fairly well with experimental data, the software is used to calculate the new properties of these reactors, i.e. the case of LEU UO_2 fuel.

The physical properties of the UO_2 fuel used in the calculation are shown in Table 8.4 under conditions of 30°C external temperature, 28°C average moderator temperature and excess reactivity of 8.5078 mk. The table makes a comparison between the same physical properties for both the current and LEU UO_2 fuel, where the enrichment is reduced to 12.5% instead of approximately 90%. Since UO_2 fuel is used in power reactors, vast international experience is available for its use in research reactors. The behaviour of the fuel under irradiation is well known and requires no special precautions, especially at reduced burnup levels in MNSRs.

TABLE 8.1. MAIN PROPERTIES OF THE SYRIAN MNSR

Parameter	Description
Reactor type	Tank in pool
Rated thermal power	~30 kW
Fuel	UAl_4 dispersed in Al matrix
Fuel pin inner radius without cladding (mm)	4.3
Fuel pin outer radius without cladding (mm)	5.5
Fuel pin length (mm)	230
Cladding composition	Al
^{235}U percentage in the fuel pin	24.83
^{235}U enrichment	~90%
Uranium density in fuel pin	—
Core shape	Cylinder
Core diameter (cm)	23
Core height (cm)	23
Fuel element shape	Thin rod
Fuel elements number in the core	347
Reactor continuous operating time at rated power	≥2.5 hours
Refuelling period	≥10 years
Burnup	~1%
Control rod length (mm)	260
Absorber of the control rod	Cd
Total number of irradiation sites	10
Number of internal irradiation sites	5
Thermal neutron flux in outer irradiation sites	1×10^{11} cm^{-2}s^{-1} at rated power
Reactor cooling mode	Natural convection
Radial reflector thickness	10 cm

Reproduced from Ref. [8.1]

TABLE 8.2. LATTICE POSITIONS FOR THE FUEL CAGE OF THE SYRIAN MNSR

Circle number	Number of fuel rods	Circle diameter (mm)
1	6	21.9
2	12	43.8
3	19	65.7
4	26	87.6
5	32	109.5
6	39	131.4
7	45	153.3
8	52	175.2
9	58	197.1
10	65	219.0

Reproduced from Ref. [8.1]

TABLE 8.3. THE MAIN PARAMETERS OF THE SYRIAN MNSR CORE WITH HEU FUEL

Fuel properties	Value
IER with control rod fully withdrawn (mk)	3.9682
Thermal flux, IIS ($\times10^{12}$ cm^{-2}s^{-1})	0.995571
Deviation from reference flux (%)	—
Thermal flux, EIS ($\times10^{12}$ cm^{-2}s^{-}1)	0.490334
Deviation from reference flux (%)	—
Control rod worth (mk)	6.3629
Regulator worth(mk)	+1.1103
Flooding IIS worth (mk)	+2.9299
Flooding EIS worth (mk)	+0.9948
Normal shutdown margin (mk)	–2.3947
Effective shutdown margin (mk)	+0.4197
Enrichment (%)	89.87
Ratio of H to ^{235}U in core	201.4301
Ratio of H to U in core	181.2565
U^{235} load in the core (g)	994.6115
U load of one fuel rod (g)	3.189402
Number of dummy elements	3
Dummy element material	Al
Number of fuel rods	347
Clad material/thickness (mm)	Al/0.6

TABLE 8.4. SYRIAN MNSR CHARACTERISTICS WITH LEU FUEL

Reactor characteristics	UO_2, 13.10% enrichment
IER with control rod fully withdrawn (mk)	4.0456
Thermal flux, IIS ($\times 10^{12}$ $cm^{-2}s^{-1}$)	0.896232
Deviation from reference flux (%)	–9.978
Thermal flux, EIS ($\times 10^{12}$ $cm^{-2}s^{-}1$)	0.458209
Deviation from reference flux (%)	–6.552
Control rod worth (mk)	–5.1547
Regulator worth(mk)	1.0842
Flooding IIS worth (mk)	+2.9356
Flooding EIS worth (mk)	0.9492
Normal shutdown margin (mk)	–1.1091
Number of dummy elements	3
Dummy element material	Al
Number of fuel rods	347
Clad material/thickness (mm)	Al/0.6
Ratio of H to ^{235}U in core	141.2394
Ratio of H to U in core	18.70784
U^{235} load in the core (g)	1418.475
U load of one fuel rod (g)	31.20355

8.2.1. Results and discussion

Results for the current HEU fuel are shown in Table 8.3, while those for LEU are shown in Table 8.4. Neutron flux decreases at both the IIS and EIS by about 10%, which requires reactor power to be increased correspondingly by about 10% to 33 kW for the LEU fuel. The worth of the control rod also decreases when the LEU fuel is used. However, the shut-down margin will still be negative and acceptable.

8.3. THERMAL-HYDRAULIC ANALYSIS

This portion was achieved by the use of the program THYD [8.6] for the thermal and hydraulic aspects of the use of LEU fuel, while the BMAC package was used to evaluate the reactivity coefficients. The temperature coefficient was calculated for the MNSR coolant with HEU fuel in from 20°C to 98°C, to enable a detailed analysis of the transient. Tables 8.5—8.7 show the values of the resultant temperature and void coefficients.

TABLE 8.5. CALCULATED COOLANT TEMPERATURE COEFFICIENT FOR THE HEU SYRIAN MNSR (5.3 mm CLAD OD)

Temperature interval (°C)	20—30	30—40	40—50	50—60	60—70	70—80	80—90	90—98
Temperature coefficient (mk/°C)	–0.1200	–0.1321	–0.1567	–0.1806	–0.2217	–0.2082	–0.2730	–0.2484

TABLE 8.6. CALCULATED FUEL TEMPERATURE COEFFICIENT (DOPPLER) FOR THE HEU SYRIAN MNSR AS A FUNCTION OF TEMPERATURE

Temperature interval (°C)	10—15	15—20	20—25	25—30	30—35	35—40	40—45
Doppler coefficient (mk/°C)	0.0222	0.0240	–0.0261	–0.0008	–0.0234	0.0212	–0.0008
Temperature interval (°C)	45—50	50—55	55—60	60—65	65—70	70—75	75—80
Doppler coefficient (mk/°C)	–0.0472	0.0442	0.0002	-0.0184	0.0406	–0.0254	0.0238
Temperature interval (°C)	80—85	85—90	—	—	—	—	—
Doppler coefficient (mk/°C)	–0.0010	–0.0494	—	—	—	—	—

TABLE 8.7. CALCULATED VOID COEFFICIENTS FOR THE HEU AND LEU FUELS TO BE USED IN THE SYRIAN MNSR

Fuel type	UAl_4–Al	UO_2 13.10% (4.3 mm meat, 5.5 mm cladding outer diameter)	UO_2 12.60% (4.2 mm meat, 5.1 mm cladding outer diameter)
Void coefficient (mk/%void)	–3.53539	–4.01262	–3.96521

The behaviour of reactor power for the case of HEU fuel is shown in Fig. 8.4.

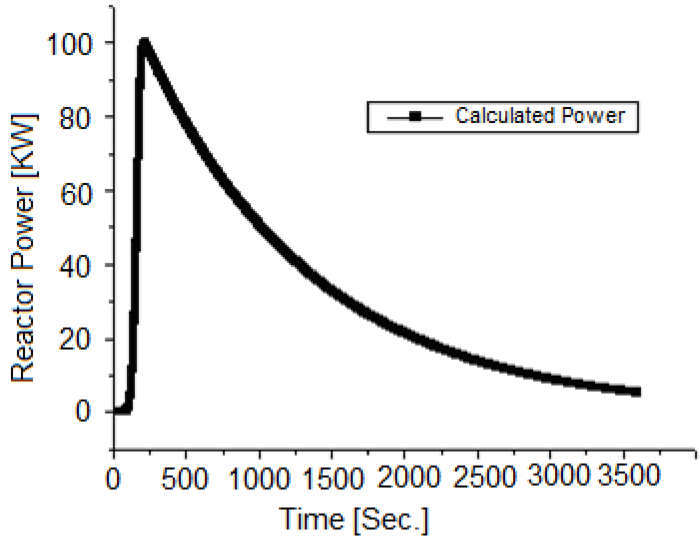

FIG. 8.4. Power behaviour during the insertion of a 3.6 mk reactivity step in the Syrian MNSR in the case of HEU fuel (Courtesy of Atomic Energy Commission, Syrian Arab Republic).

The power reaches a maximum of about 100 kW with the current HEU fuel, which is very near to the previously reported value of 99 kW [8.7]. The temperatures of the fuel, cladding and coolant are shown in Fig. 8.5.

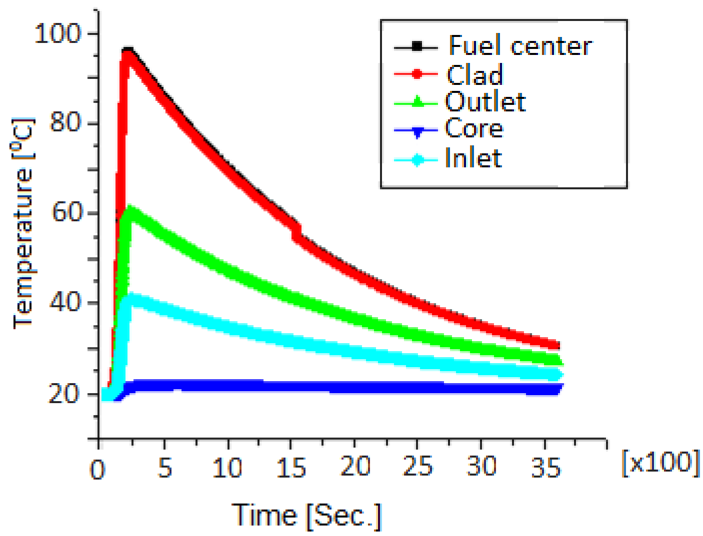

FIG. 8.5. Fuel centre, cladding and coolant inlet, outlet and core temperature behaviour during a 3.6 mk reactivity insertion in the Syrian MNSR with HEU fuel (time in seconds, and temperatures in °C) (Courtesy of Atomic Energy Commission, Syrian Arab Republic).

The temperatures are also in good agreement with the reported experimental values in the THYD literature [7.6]. The difference in temperature between the cladding and the centre of the fuel is negligible due to the good conductivity of the aluminium alloy and the dispersive fuel, so only one may be considered. The same parameters were calculated for the first proposed type of LEU fuel: UO_2 with 347 fuel rods, 4.3 mm meat and 5.5 mm pellet outer diameter. There are still three dummy elements made of aluminium alloy in the tenth fuel circle, and four aluminium tie rods in the eighth fuel circle, resulting in an IER of 4.4492 mk. The proposed LEU fuel matches the current HEU fuel in the dimensions of the meat and the cladding, but the required enrichment is about 13.1% for the same IER. The cladding material is now Zircaloy-4 alloy. Tables 8.8 and 8.9 list the temperature coefficients for the proposed LEU core.

TABLE 8.8. CALCULATED COOLANT TEMPERATURE COEFFICIENTS FOR THE PROPOSED LEU CORE (13.1 %, 4.3 MEAT OD) FOR SYRIAN MNSR

Temperature interval (°C)	20—30	30—40	40—50	50—60	60—70	70—80	80—90	90—98
Temperature coefficient (mk/°C)	–0.0491	–0.1433	–0.1015	–0.1942	–0.1665	–0.2274	–0.2398	–0.2309

TABLE 8.9. CALCULATED FUEL TEMPERATURE COEFFICIENTS FOR THE PROPOSED LEU CORE FOR SYRIAN MNSR

Temperature interval (°C)	20—30	30—40	40—50	50—60	60—70	70—80	80—90
Doppler coefficient (mk/°C)	–0.0155	–0.0070	–0.0023	–0.0502	–0.0056	–0.0240	–0.0076
Temperature interval (°C)	90—100	100—110	110—120	120—130	130—140	140—150	150—160
Doppler coefficient (mk/°C)	–0.0268	–0.0068	–0.0068	–0.0140	–0.0140	–0.0140	–0.0135
Temperature interval (°C)	160—170	170—180	180—190	190—200	—	—	—
Doppler coefficient (mk/°C)	–0.0135	–0.0135	–0.0135	–0.0135	—	—	—

The power excursion is shown in Fig. 8.6, while the behaviour of temperatures at the centre of the fuel, the cladding and the coolant are shown in Fig. 8.7. The power reaches a peak of 118.5 kW, compared to 100 kW for the HEU core, while the temperature at the centre of the LEU fuel does not exceed 117°C. The cladding outer surface temperature is approximately 105°C, which is below the saturation temperature of the coolant (113°C).

The difference between the temperatures of the cladding and the centre of the fuel is now observable because of the marked difference between the conductivities of the fuels and their cladding. The coolant outlet temperature is still in the range of 60°C to 65°C, and the average core coolant temperature is in the range of 40°C to 45°C. The new fuel appears to behave well in this type of reactor.

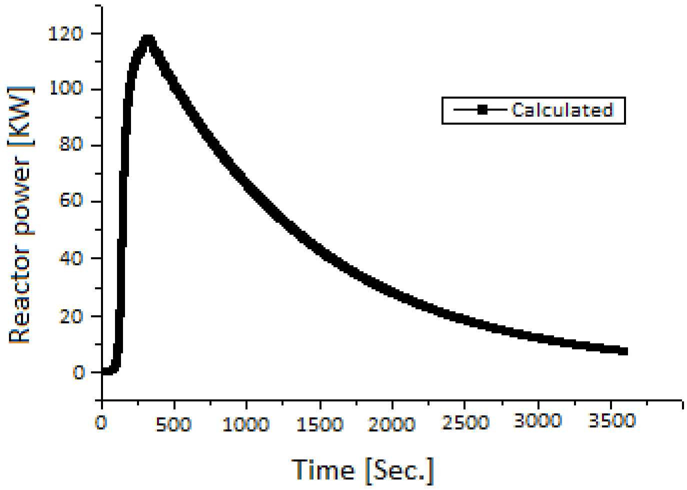

Fig. 8.6. Power behaviour during the insertion of a 3.6 mk reactivity step in the Syrian MNSR with LEU fuel (Courtesy of Atomic Energy Commission, Syrian Arab Republic).

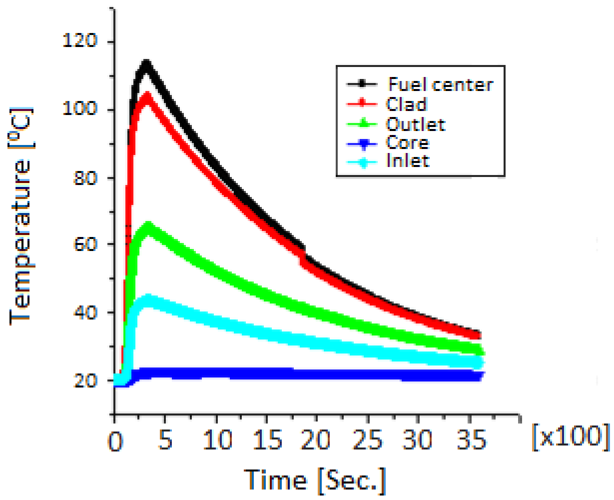

Fig. 8.7. Fuel centre, cladding and coolant inlet, outlet and core temperature behaviour during a 3.6 mk reactivity insertion in the Syrian MNSR with LEU fuel) (Courtesy of Atomic Energy Commission, Syrian Arab Republic).

8.4. CONCLUSION AND FUTURE ANALYSES

Analyses conducted to date have prepared a sufficient basis for a more comprehensive study of the conversion of the Syrian MNSR from HEU to LEU fuel, including the related licensing application. Upon a formal decision to conduct the conversion, DBA analyses, including dose calculations, and BDBA analyses, including dose calculations and decay heat calculations, will be performed.

REFERENCES TO SECTION 8

[8.1] CHINA INSTITUTE OF ATOMIC ENERGY, Safety Analysis Report (SAR) for the Syrian Miniature Neutron Source Reactor, CIAE, Beijing (1993).

[8.2] ALBARHOUM, M., Automation of the Modeling and Some Neutronic Calculations of the Syrian Miniature Neutron Source Reactor, Annals of Nuclear Energy 35 9 (2008) 1760–63.

[8.3] ALBARHOUM, M., Optimization of the Reflector Design of the Syrian MNSR, Progress in Nuclear Energy 51 6–7 (2009) 676–679.

[8.4] ASKEW, J.R., FAYER, F.J., KEMSHELL, P.B., A General Description of Lattice Code WIMSD, Journal of the British Nuclear Energy Society (1966).

[8.5] FOWLER, T.B., VONDY, D.R., CUNNINGHAM, G.W., Nuclear Reactor Core Analysis Code: CITATION, ORNL-TM-2496 Rev. 2, Oak Ridge National Laboratory, Oak Ridge (1971).

[8.6] ALBARHOUM, M., MOHAMMED, S., A Thermal Hydraulic Code (THYD) for the Miniature Neutron Source Reactor Thermal-Hydraulic Transients, Progress in Nuclear Energy 51 3 (2009) 470–473.

[8.7] HAINOUN, A., ALISSA, S., Full-Scale Modeling of the MNSR Reactor to Simulate Normal Operation, Transients and Reactivity Insertion Accidents under Natural Circulation Conditions Using the Thermal Hydraulic Code ATHLET, Nuclear Engineering and Design 235 (2005) 33–52.

APPENDIX I

GEOMETRY DATA FOR THE GENERIC MNSR MCNP MODELS

TABLE I.1. LATTICE POSITIONS FOR THE FUEL CAGE

Circle no.	Lattice no.	Circle diameter (mm)	Rod pitch (mm)
0	1	0.00	0.00
1	6	21.90	11.47
2	12	43.80	11.47
3	19	67.70	10.86
4	26	87.60	10.98
5	32	109.60	10.78
6	39	131.40	10.58
7	45	153.30	10.70
8	52	175.20	10.58
9	58	197.10	10.68
10	65	219.00	10.58

TABLE I.2. DIMENSIONS OF BERYLLIUM REFLECTOR AND SHIM TRAY, mm

Be reflector (side)	Outer diameter	435.00
	Inner diameter	231.00
	Height	238.15
Be plate (bottom)	Thickness	50.00
	Diameter	290.00
Shim tray	Inner radius	123.00
	Outer radius	130.00
	Height	109.50
Be shims (top)	Diameter	243.00
	Thickness and number	1.50 (10) 3.00 (20) 6.00 (8) 12.00 (8)
	Total thickness	109.50

TABLE I.3. DIMENSIONS OF CONTROL ROD AND ADJUSTER RODS, cm

		HEU	LEU
Control rod geometry	Radius of Cd	0.195	0.225
	Radius of Cd+cladding	0.25	0.275
	Length	26.6	26.6
Control rod guide tube	Inner radius	0.45	0.445
	Outer radius	0.595	0.595
	Length	42.2	42.2
Cadmium regulators	Number	4	4
	Radius of central Al rod	1.7	1.7/0.9*
	Inner radius of Cd	1.7	1.7/0.9
	Outer radius of Cd	1.8	1.8/1.0
	Inner radius of SS clad**	1.8	1.8/1.5
	Outer radius of SS clad**	2.0	2.0/1.7
	Length	37.3	37.3
Cadmium regulators guide tube	Inner radius	2.10	
	Outer radius	2.45	
	Length	540	

* Cadmium regulators (adjuster rods) have different designs in the NIRR-1 and GHARR-1 to match the measured reactivity worths in these HEU cores
**SS clad = stainless steel cladding

TABLE I.4. DIMENSIONS OF IRRADIATION CHANNELS, cm

Inner channels	Number/size	5/S
	Inner radius (small)	1.1
	Outer radius (small)	1.25
	Length	528.5
Outer channels	Number/size	2/L+3/S (same as inner channels)
	Inner radius (large)	1.7
	Outer radius (large)	1.85
	Height	540
Slant tube	Number	1
	Inner radius	2.405
	Outer radius	2.755
Fission chambers	Number	2
	Inner radius	0.5
	Outer radius	0.65

TABLE I.5. DIMENSIONS OF REACTOR VESSEL AND POOL, cm

Reactor vessel	Inner radius	30.0
	Outer radius	30.95
	Height	560
Reactor pool	Inner radius	135
	Outer radius	138
	Height	650

TABLE I.6. DIMENSIONS OF FUEL CAGE, cm

		HEU	LEU
Fuel cage	Max outer diameter (grid plates)	23.1	23.1
	Total height (fuel and end plugs)	24.8	24.8
CR guide tube	Inner radius	0.45	0.445
	Outer radius	0.595	0.595
	Length	42.2	42.2

APPENDIX II

MATERIAL COMPOSITIONS OF THE GENERIC HEU AND LEU CORES

All compositions of materials and their impurities used for the generic HEU and LEU core models are defined and presented in this section.

II.1 COMPOSITIONS OF HEU UAl ALLOY FUEL

The specifications for the HEU fuel uranium content are shown in wt% in Table II.1, with the impurity content in ppm shown in Table II–2. The design density of UAl alloy is 3.456 g/cm^3. A fuel loading of 2.88 g ^{235}U per pin was used. The ^{235}U enrichment is 90.0 wt%, with 1.0 wt% of ^{234}U and 0.0 wt% of ^{236}U in the uranium. The wt% of uranium in the UAl alloy fuel meat is 27.7%. The UAl alloy fuel meat compositions and impurities as shown in Tables II.2 and II.3 were specified explicitly in wt% in the MCNP model.

TABLE II.1. DESIGN SPECIFICATIONS FOR URANIUM ISOTOPES, wt% URANIUM

Material	^{235}U	^{238}U	^{234}U	^{236}U	Total
wt%	90.0	9.0	1.0	0.0	100.0

TABLE II.2. DESIGN SPECIFICATIONS FOR MAXIMUM ALLOWED CONTENT OF IMPURITY IN UAl ALLOY FUEL MEAT; μg IMPURITY/g UAl ALLOY (EQUIVALENTLY, ppm)

Material	Al	C	Ca	Mg	Be	Cr	Li
ppm	10	650	20	10	0.05	240	8
Material	Fe	Ni	N	Gd	B	Cd	Total
ppm	725	450	20	0.25	2.8	1	2137.1

TABLE II.3. UAL ALLOY FUEL MEAT COMPOSITION AND IMPURITIES USED IN THE MCNP MODEL

Material	^{235}U	^{238}U	^{234}U	^{236}U	Al	B	Cd
wt%	24.8814	2.4881	0.2765	0.0	72.1405	0.00028	0.0001
Material	Gd	C	Ca	Mg	Be	Cr	Li
wt%	0.000025	0.065	0.002	0.001	0.000005	0.024	0.0008
Material	Fe	Ni	N				
wt%	0.0725	0.045	0.002				

II.2 COMPOSITION OF ALUMINIUM ALLOY AL-303-1

Al-303-1 was used in HEU fuel cladding, four tie rods, and five dummy fuel rods. The chemical composition data of the Al-303-1 was based on NIRR-1 Table 5.4 in the 2005 FSAR [II.1], but revised values were used for the generic HEU core. The composition and impurities are shown in Table II.4 as wt% which was used explicitly in the MCNP model. The aluminium alloy Al-303-1 has a density of 2.7 g/cm^3.

TABLE II.4. COMPOSITION OF AL-303-1 IN THE MCNP MODEL

Material	Al	Fe	Si	Cu	Zn	Mn	Mg	Ti	B
wt%	97.75	1.20	1.0	0.005	0.003	0.003	0.005	0.005	1.0×10^{-4}

II.3 COMPOSITION OF ALUMINIUM ALLOY LT-21

Aluminium alloy LT-21 is used for the reactor vessel, lower core support, slant tube, shim tray, irradiation channel tubes, fission chambers, radial support structure, and adjuster rod guide tubes. The composition and impurities are shown in Table II.5 as wt% which was used explicitly in the MCNP model. The aluminium alloy LT-21 has a density of 2.7 g/cm^3.

TABLE II.5. COMPOSITION OF ALUMINIUM ALLOY LT-21 IN THE MCNP MODEL

Material	Al	Si	Mg	Fe	Ni	Cu	Mn	Ti	Cd	B
wt%	98.1648	0.9	0.675	0.2	0.03	0.01	0.01	0.01	0.0001	0.0001

II.4 COMPOSITION OF STAINLESS STEEL

Stainless steel (SS-304) is used as the cladding material for cadmium in the control rod and the four reactivity adjuster rods. The composition employed in the MCNP model is provided in Table II.6 in wt%. No impurity information is provided. Each element is represented explicitly in the MCNP model. The density of stainless steel is 7.8 g/cm^3.

TABLE II.6. COMPOSITION OF STAINLESS STEEL (SS-304) IN THE MCNP MODEL

Material	Fe	Cr	Ni	Mn	S	C	P	Si
wt%	70.845	18	8	2	1	0.08	0.045	0.03

II.5 COMPOSITION OF BERYLLIUM

The reflector is composed of beryllium metal, with the impurities shown in Table II.7 that were specified in the GHARR-1 SAR [II.2]. Each element is represented explicitly as wt% in the MCNP model as shown in Table II.8. The impurities are provided in ppm in Table II.8. Note that the beryllium contains 2.5 wt% beryllium oxide. Beryllium metal has a density of 1.85 g/cm^3 and BeO has a density of 3.0 g/cm^3. The density of this two-component mixture is given by:

$$\frac{1}{\rho} = \left(\frac{1}{\left(\frac{w}{o} \times \frac{Be}{\rho_{Be}}\right)} + \frac{1}{\left(\frac{w}{o} \times \frac{BeO}{\rho_{BeO}}\right)} \right) \tag{II.1}$$

Calculation gives a theoretical density of 1.8679 g/cm^3 for the mixture. However, since no information is available on the as-built density of beryllium used in MNSRs, the density of the mixture was set to 1.85 g/cm^3, or 99% of theoretical density, in the MCNP model.

TABLE II.7. IMPURITIES IN THE BERYLLIUM REFLECTOR [II.2]

Material	Fe	Si	Eu	Cu	Mg	Ni	Co	Sm	Mn
ppm	4000	800	0.1	200	1000	100	10	0.5	20

Material	B	Li	Dy	Al	Cd	Zn	Cr	N	Gd
ppm	2	1	1	3000	0.5	150	200	200	0.1

Material	BeO	Pb	Ag
ppm	25000	30	15

TABLE II.8. COMPOSITION OF THE BERYLLIUM REFLECTOR IN THE MCNP MODEL

Material	Fe	Si	Eu	Cu	Mg	Ni	Co	Sm	Mn
wt%	0.4	0.08	1×10^{-5}	0.02	0.1	0.01	0.001	5×10^{-5}	0.002

Material	B	Li	Dy	Al	Cd	Zn	Cr	N	Gd
wt%	0.0002	0.0001	0.0001	0.3	5×10^{-5}	0.015	0.02	0.02	0.00001

Material	O	Pb	Ag	Be
wt%	1.6	0.003	0.0015	97.42708

II.6 COMPOSITION OF TOP GRID PLATE AND WATER FOR HEU GENERIC CORE

The honeycomb shaped top grid plate was assumed to be a mixture of 20% aluminium alloy (LT-21) and 80% water. The composition employed in the MCNP model is provided in Table II.9. The density of the top grid plate is 1.34 g/cm^3 ($0.2 \times 2.7 + 0.8 \times 0.99825 = 1.3386$).

TABLE II.9. COMPOSITION OF TOP GRID PLATE IN THE MCNP MODEL

Material	Al	Si	Mg	Fe	Ni	Cu
wt%	39.5589	0.3627	0.272	0.0806	0.0121	0.004

Material	Mn	Ti	Cd	B	H	O
wt%	0.004	0.004	0.00004	0.00004	6.6335	53.0678

II.7 COMPOSITION OF WATER AS COOLANT AND MODERATOR

The composition of water employed in the MCNP model is provided in Table II.10. The density of water at 20°C is 0.99825 g/cm^3.

TABLE II.10. COMPOSITION OF WATER IN THE MCNP MODEL

Material	H	O
wt%	11.1898	88.8102

II.8 COMPOSITION OF ZIRCALOY-4 FOR THE LEU GENERIC CORE

For the generic LEU core, the fuel pin cladding, control rod guide tube, upper and lower grid plates, dummy rods, and tie rods are composed of Zircaloy-4 with a design density of 6.5 g/cm^3. The primary constituents, taken from Ref. [II.1], are provided in Table II.11. The impurities, also from Ref. [II.1], are shown in Table II.12.

TABLE II.11. DESIGN SPECIFICATIONS FOR ZIRCALOY-4

Material	Zr	Fe	Cr	Sn
wt%	97.93	0.24	0.13	1.7

TABLE II–12. DESIGN SPECIFICATIONS FOR MAXIMUM ALLOWED IMPURITY LEVELS IN ZIRCALOY-4

Material	Al	B	Cu	Mg	Cl	Cd	Co	U	Ni
wt%	0.0075	0.00005	0.005	0.002	0.01	0.00005	0.002	0.00035	0.007

Material	Si	Ti	Mn	Mo	Pb	V	W	Hf
wt%	0.012	0.005	0.005	0.005	0.013	0.005	0.01	0.01

The primary constituents were modelled explicitly in MCNP, and the impurities were included in the form of their natural boron equivalents. The impurity content, atomic weight, thermal absorption cross section, and natural boron equivalent are provided in Table II–13, and the final composition is given in Table II.14.

Two special Zircaloy-4 compositions were generated for the generic LEU core model. First, the fuel pin cladding includes a homogenized pellet-cladding gap with 6% helium and 94% Zircaloy-4 by volume. Therefore, the fuel element OD is 5.5 mm, the fuel pellet OD is 4.3 mm, and the cladding and helium gap are homogenized. The second special composition is for the upper grid plate, which is 80% water and 20% Zircaloy-4 by volume.

TABLE II.13. IMPURITIES IN ZIRCALOY-4

Element	Content (ppm)	Atomic weight (g/mol)	σ_a (b)	Natural boron equivalent (ppm)
Al	75	26.98154	0.23	0.009
B	0.5	10.811	761	0.500
Cu	50	63.546	3.8	0.042
Mg	20	24.305	0.066	0.001
Cl	100	35.4527	33.5	1.342
Cd	0.5	112.411	2520	0.159
Co	20	58.9332	37.2	0.179
U	3.5	238.0289	7.57	0.002
Ni	70	58.9332	4.5	0.076
Si	120	28.0855	0.168	0.010
Ti	50	47.867	6.1	0.091
Mn	50	54.93805	13.3	0.172
Mo	50	95.94	2.5	0.019
Pb	130	207.2	0.171	0.002
V	50	50.9415	5	0.070
W	100	183.84	18.2	0.141
Hf	100	178.49	104	0.828
Total (ppm B)				3.642
^{10}B (ppm)				0.671
^{11}B (ppm)				2.971

TABLE II.14. COMPOSITION OF ZIRCALOY-4 IN THE MCNP MODEL

Material	Zr	Fe	Cr	Sn	^{10}B	^{11}B
wt%	97.93	0.24	0.13	1.7	6.713×10^{-5}	2.971×10^{-4}

II.9. UO2 FUEL URANIUM ISOTOPES AND IMPURITIES FOR GENERIC LEU CORE

The specifications [II.3] for the UO_2 LEU uranium content are shown in Table II.15, with the impurity content in Table II.16. The ^{235}U enrichment is 12.5 wt%, with a maximum of 0.2 wt% of ^{234}U and a maximum of 0.25 wt% of ^{236}U in the uranium. The UO_2 LEU fuel compositions and impurities as shown in Table II.17 were specified explicitly in wt% in the MCNP model. The design density of UO_2 is 10.6 g/cm^3.

TABLE II.15. DESIGN SPECIFICATIONS FOR URANIUM ISOTOPES

Material	^{235}U	^{238}U	^{234}U	^{236}U
wt%	12.5	87.05	0.2	0.25

TABLE II.16. DESIGN SPECIFICATIONS FOR MAXIMUM ALLOWED CONTENT OF IMPURITY IN UO2, μg impurity/g UO2 (EQUIVALENTLY, ppm)

Material	Al	C	Ca	Mg	Cl	Cr	Co	F	H
ppm	250	100	100	100	25	250	100	15	1.3

Material	Fe	Ni	N	Si	Th	Total
ppm	500	250	75	500	10	2276.3

TABLE II.17. UO_2 FUEL COMPOSITION AND IMPURITIES IN THE MCNP MODEL

Material	^{235}U	^{238}U	^{234}U	^{236}U	^{16}O
wt%	10.992	76.546	0.176	0.220	11.839

Material	Al	C	Ca	Mg	Cl	Cr	Co	F	H
wt%	0.025	0.01	0.01	0.01	0.0025	0.025	0.01	0.0015	0.00013

Material	Fe	Ni	N	Si	Th	Total
wt%	0.05	0.025	0.0075	0.05	0.001	100.00[1]

[1] The UO_2 fuel composition and impurities are normalized to 100 wt% with a bulk UO_2 density of 10.6 g/cm^3.

The honeycomb shaped top grid plate was assumed to be a mixture of 20% Zircaloy-4 and 80% water. The composition employed in the MCNP model is provided in Table II.18. The density of the top grid plate is 2.099 g/cm3 ($0.2 \times 6.5 + 0.8 \times 0.99825 = 2.0986$).

TABLE II.18. COMPOSITION OF TOP GRID PLATE IN THE MCNP LEU MODEL

Material	Zr	Fe	Cr	Sn	^{10}B	^{11}B	H	O
wt%	60.72	0.15	0.08	1.05	4.16×10^{-7}	1.84×10^{-6}	4.25	33.74

The reactivity worth change due to different homogenized compositions of top grid plate and water is shown in Table II.19. Two additional volume mixture ratios are presented here to see the reactivity effect of different homogenization assumptions to bind the envelope. The reactivity changes due to the change of volume ratios are relatively small.

TABLE II.19. REACTIVITY EFFECT OF HOMOGENIZED COMPOSITIONS OF TOP GRID PLATE IN THE MCNP MODELS

Water	Al or Zircaloy-4	Homogenized top grid density, g/m^3		Generic core reactivity change, mk	
Vol.%	Vol.%	HEU	LEU	Vol.%	Vol.%
80	20	1.33654	2.09654	—	—
60	40	1.67740	3.19740	–0.05±0.08	0.03±0.08
40	60	2.01827	4.29827	–0.24±0.08	0.10±0.08

REFERENCES TO APPENDIX II

[II.1] NIGERIA RESEARCH REACTOR-1, Final Safety Analysis Report, Centre for Energy Research and Training, Energy Commission of Nigeria, Ahmadu Bello University, Zaria, CERT/NIRR-1/001, (2005).

[II.2] AKAHO, E.H.K., MAAKUU, B.T., ANIM-SAMPONG, S., EMI-REYNOLDS, G., et al., Ghana Research Reactor -1, Final Safety Analysis Report, GAEA-NNRI-RT-90, (2003).

[II.3] INTERNATIONAL ATOMIC ENERGY AGENCY, Summary Report on 2nd RCM on MNSR Conversions, IAEA, Vienna, (2008).

APPENDIX III

EVALUATION OF INITIATING EVENTS

For LEU conversion, only those results that would change as a result of changing the core from HEU to LEU fuel need to be addressed.

TABLE III.1.

Yes	No	Initiating event description	What needs to be done
√		**Insertion of excess reactivity of 3.77 mk** When a total excess reactivity of 3.77 mk is released, the peak power reached 101 kW. The corresponding maximum outlet temperature was ~60°C and the maximum temperature difference was 35.47°C corresponding to maximum radiation at the top of reactor vessel as 173 µSv/hr. This clearly demonstrates that the safety margin of the reactor is relatively large even if the total cold excess reactivity is released.	Calculations need to be done to compare results for the HEU and LEU cores.
√		**Reactivity insertion accident** During an MNSR operation, the maximum excess reactivity is attained by total withdrawal of the control rod. For a new core, this will be about 4 mk. The transient analysis code RELAP5 was used to calculate the transient response for ramp and step reactivity insertions. The code has combined thermal-hydraulic and neutronics models, which describe the phenomena.	Calculations of step and ramp insertions need to be done to compare results for the HEU and LEU cores.
	√	**Loss of electrical power** During start up or at steady state, the control rod is in the core or fully withdrawn. A loss of electrical power during any of these states will cause the electromechanical clutch on the control rod to disengage, resulting in a reactor scram. If for some reason the reactor does not scram and the control rod is fully withdrawn, the resulting power increase will be as described in Section 16.4.1 of Ref. [III.1]. Under both conditions no adverse consequences are expected.	No calculations need to be done because the results are bounded by the results in Chapter 1, Section 16.4.1 of Ref. [III.1].
	√	**Control system failure** The control and protection system has been designed using fail-safe principles. If however, failure occurs which does not result in reactor shut-down, the limiting consequence is total withdrawal of the control rod.	No calculations need to be done because the results are bounded by the results in another section.

TABLE III.1 (cont.)

Yes	No	Initiating event description	What needs to be done
		Loss of reactor coolant accident The initial conditions that are assumed in this analysis are that the reactor is operating at its nominal power of 31 kW, the total reactor coolant volume is about 1.5 m^3 and the water inventory of the reactor pool is about 30 m^3. The accident analysis is for two cases:	
	√	1. Rupture of reactor vessel or failure of seal between upper and lower sections of vessel: During normal reactor operation the container is not under internal pressure; therefore any leak in the lower to upper section joint could cause only a small exchange of reactor and pool water. There would be no reduction in the height of water over the core and consequently there will be no loss of shielding and no loss of cooling.	No calculations are needed. The conclusion will be the same for both the HEU and LEU cores.
		2. Loss of coolant due to rupture of purification system main pipe: During this accident, the operators will notice the accident from both the low level alarm signal and the γ-radiation monitoring system. However, even if the operator does not notice the accident, the lowest position of the purification inlet pipe is still 0.5 m higher than the elevation of the top of the core; therefore the core would still be shielded by 0.5 m of water. The consequence of the accident is less severe compared with that of a maximum hypothetical accident discussed in Chapter 1, Section 16.4.6 of Ref. [III.1] which considers the uncovering of the core. The effective dose the public would receive would be negligible and the reactor could be safely operated after the fault is corrected.	No calculations were done in the SAR for the HEU core. The zircaloy cladding of the LEU fuel pins will melt at a much higher temperature than the aluminium cladding of the HEU fuel pins.
√		**Loss of pool water shielding** The initial conditions that can be assumed are that the reactor is operating at full power of 31 kW, the reactor vessel is 1.5 m^3, and the wall of the pool is a 400 mm thick reinforced concrete structure. The volume of the pool water is 30 m^3, in addition the underground water level beneath the site is lower than the elevation of the core. The accident results from a major earth movement that causes a crack in the bottom of the pool. The pool water will drain below the level of the core. Simultaneous loss of reactor vessel water is not credible because the container is designed and constructed to give support to its contents while suspended within an empty pool. Loss of both line and auxiliary electrical power is assumed. The control rod is assumed to stall at its balance point.	Doses at the top of the reactor and in the reactor building will be larger in the LEU core because the LEU core has a higher power level and a longer lifetime.
	√	**Flooding accident** All the materials used for fabricating the fuel element and the beryllium reflectors exhibit excellent corrosion resistance in highly purified deionized water. However, in case the reactor is flooded or the underground water penetrates into the pool or the reactor vessel, it would cause the reactor and pool water quality to be degraded and this will accelerate the rate of corrosion. This would be detected during the periodic monitoring for pH and conductivity of the vessel and pool water. Therefore, leakage of ground water into the reactor pool could be corrected before having a serious effect on corrosion. However, assuming that the problem was not corrected, fuel cladding will fail and the fission products will be dispersed into the reactor vessel. Consequently, this will lead to possible contamination of the environment. For the reasons stated above, the reactor is sited where flooding is not possible. The base elevation of the site is sufficiently high. During the construction of the reinforced concrete for the pool, water was encountered. However, French drains (structural remedy) were made specially to drain any water collection. In addition the steel liner was also checked against leakage.	The same results that are described in the SAR for the HEU core also apply to the LEU core. No new calculations are needed. In fact, the zircaloy cladding of the LEU fuel pins will be much more corrosion resistant than the aluminium cladding of the current HEU fuel. However, it needs to be noted that zircaloy hydriding is a serious issue in power reactors since it limits the service life of zircaloy components [III.2]. The operating environment in MNSR reactors is much more moderate than in power reactors and zircaloy hydriding is not expected to be a safety issue or limit the lifetime of the LEU fuel rods.

TABLE III.1 (cont.)

Yes	No	Initiating event description	What needs to be done
	√	**Air crash accident** The probability of direct hit of a crashed aircraft on the reactor is very small since the core of the reactor is located five meters under the ground. In the event of direct aircraft crash on the building, the multi-barrier building structure is expected to isolate the reactor core from the crash. The multi-barrier structure includes: — The steel roof structure; — Steel reinforced concrete roof structure; — Steel rail for hoist crane; — Reactor pool cover; and — Reactor tank cover.	No changes are expected for the LEU core because the results do not depend on the enrichment of the uranium or design of the reactor core.
	√	**Seismic accident** The vessel is an important barrier against the release of fission products. To ensure its safety and reliability during any earthquake, the design of the vessel has taken into consideration an earthquake load. Two types of earthquakes stipulated by US Atomic Energy Commission (USAEC) were adopted for the design, namely safe shutdown earthquake (SSE) and operation base earthquake (OBE). The SSE usually takes the intensity one grade higher than that recorded in local history, while the maximum ground acceleration of OBE considered is not smaller than half that of SSE. The assumptions made for the design are as follows: The ground acceleration of SSE is 0.2 g, which is equivalent to intensity of grade 8. The maximum ground acceleration of OBE was fixed at 0.1 g. The design spectrum stipulated in Regulatory Guide 1.60 of the USAEC was selected as the spectrum for this reactor [III.3], and the damping coefficient is 2%. The analysis was carried out using the code SAP-5. The design and construction of the reactor vessel and its support system were based on the above specifications and will therefore tolerate an earthquake with intensity 8. It is also expected from the analysis that the core assembly inside the vessel will remain intact. It may be noted that the reactor is located in an area of extremely low seismicity.	No changes are expected for the LEU core because the results do not depend on the enrichment of the uranium or design of the reactor core.
√		**DBA** There is no accident that could cause a significant release of fission products from the core either from melting or failure in the clad. For the purpose of analysis, it is assumed that pit corrosion of the clad has created clad failure in one or more fuel elements, such that a hole or holes in the clad totalling 0.5 cm can exist. It has to be recognized that the control of reactor water quality is such that clad failures are not expected. In addition, monitoring of the reactor vessel water will be performed periodically and this is expected to permit the discovery of clad failures well before they reach this size.	Doses resulting from the DBA will be larger in the LEU core because the LEU core has a higher power level and a longer lifetime.
√		**BDBA** The BDBA is sometimes called the maximum hypothetical accident. The BDBA is not expected to occur and is therefore not analysed. It is described for purposes of emergency planning only, as it is always an accident that is more severe than the DBA. The accident is considered with the following assumptions: — The reactor building collapses; — Reactor vessel water and pool water leak at a rate of 4 m^3/hr; — The reactor core is exposed to air after 6 hours; — The HEU reactor was operating at 30 kW, and the LEU reactor at 34 kW; — The reactor has been operating for 10 years at full power 2.5 hours a day, 5 days a week. Under these conditions, the reactor core would be cooled by natural circulation of air and by thermal radiation. The core would not melt, and any exposure will be in the form of external exposure due to the unshielded core.	Doses resulting from the BBDA will be larger in the LEU core because the LEU core has a higher power level and a longer lifetime.

TABLE III.1 (cont.)

Yes	No	Initiating event description	What needs to be done
		Auxiliary systems:	
	√	**Failure of a water level monitor** A float switch is used to monitor the water level in the reactor vessel and pool. If these sensors fail, the net effect will either be loss of coolant or flooding which has been addressed in sections 16.4.4, 16.4.5 and 16.4.10 of Ref. [III.1]. The dose rate above the pool will increase and an alarm will signal in the control room, notifying the operator to investigate. After a period of several weeks the water level will fall, to the bottom of the intake pipe of the water treatment plant. The operator then observes that the treatment plant is pumping air rather than water and takes corrective action. The consequences of the failure of water level monitor do not pose any serious hazard to persons working in the control room and other rooms around the reactor.	No changes are expected for the LEU core.
	√	**Failure to operate the reactor gas purge system** If the operator does not operate the gas purge system as required by the weekly maintenance schedule, then hydrogen would collect in the gas space at the top of the vessel for a period of 14 days instead of the usual seven. The expected level of hydrogen is less than the explosive concentration for H (>4%). Consequently a single failure to operate the gas purge system is no hazard to the reactor.	No changes are expected for the LEU core.
	√	**Concurrent reactor water purification system operation and reactor operation** In case the purification system was operated at the same time as the reactor, then the short lived radionuclides, which normally decay in the reactor container, would accumulate on the deionizer column. The dose rate in the vicinity of the deionizer column would increase and this will be indicated on the display on the control console. This would alert the operator who would take the appropriate action. The radiation field would be expected to decay to normal within two days after turning off the deionizer.	No changes are expected for the LEU core.

TABLE III.1 (cont.)

Yes	No	Initiating event description	What needs to be done
		Irradiation systems:	
√		**Inadvertent reactivity increase due to a rabbit tube filled with water** Based on experiments performed in the zero power testing of the reactor, filling the five inner tubes with water would create 1.95 mk (i.e.: 5 × 0.39 mk) of reactivity.	The change in reactivity due to filling the five inner tubes with water need to be evaluated for the HEU and LEU cores.
	√	**Explosion of irradiated sample** The experiment conducted with a PY2510 thermometer, in-pile thermometer, placed in the bottom of the inner irradiation tube, showed that the temperature there was 54°C. At this temperature, explosion of the sample cannot occur in the reactor.	This temperature must be measured after start-up of the LEU core. The result is expected to be the same as for the HEU core and no additional analysis is required.
√		**Core replacement accident** The fuel assembly must be removed and a new assembly installed for a number of reasons. Two of these reasons are: 1. When the maximum BURNUP of the reactor fuel is achieved, the top Be reflector is at its maximum thickness of 10.95 cm, the central control rod is almost withdrawn to its upper end, and the reactor can no longer operate at its rated power for 2–2.5 hours. 2. Conversion of the core from HEU to LEU fuel.	This accident needs to be reanalysed because of the differences between the HEU and LEU cores.
	√	**Human error** Human error during control operation cannot lead to serious consequences because of the inherent safety features of the reactor. There is nothing about human error which other aspects of this analysis have not covered. Human errors in critical activities such as adding Be reflector shim plates, spent core removal and fresh core installation have been considered as part of the analysis. The chances of human error will be greatly reduced through training of staff.	These statements apply equally well to the LEU core. No changes are needed in the conversion analysis.

III.1. SUMMARY

The reactor operates at a low power level with inherent safety features, and is not at risk of core melting. Therefore, it presents a low risk to the environment. Even if the core was uncovered due to collapse of the building, the maximum possible effective dose that may be received by members of the public is much less than 0.05 Sv. Therefore, the reactor will not cause any harm to staff, public or the environment.

REFERENCES TO APPNEDIX III

[III.1] NIGERIA RESEARCH REACTOR-1, Final Safety Analysis Report, Centre for Energy Research and Training, Energy Commission of Nigeria, Ahmadu Bello University, Zaria, CERT/NIRR-1/001, August 2005, Chapter 16.

[III.2] Z. ZHAO, M. BLAT-YRIEIX, J.-P.MORNIROLI, A. LEGRIS, L. THUINET, Y. KIHN, A. AMBARD, and L. LEGRAS, Characterization of Zirconium Hydrides and Phase Field Approach to a Mesoscopic-Scale Modeling of Their Precipitation, Journal of ASTM International, Vol. 5, No. 3 (2008).

[III.3] UNITED STATES ATOMIC ENERGY COMMISSION, Design Response Spectra for Seismic Design of Nuclear Power Plants, Regulatory Guide 1.6, Rev. 1, USAEC, Germantown (December 1973).

APPENDIX IV

REACTIVITY CHANGES FOR REMOVAL OF HEU CORE AND INSTALLATION OF LEU CORE

In the procedure to remove the HEU core of Table IV.1 all steps are followed in the prescribed sequence. Scenario 1 is a failure to insert the five strings of four cadmium rabbits. Scenario 2 is a failure to insert four of the five strings of four Cd rabbits. Scenario 3 is a failure to insert three of the five strings of four cadmium rabbits.

TABLE IV.1. REMOVAL OF HEU CORE

		Procedure		Scenario 1		Scenario 2		Scenario 3	
		Reactivity worth mk	Net excess mk	Reactivity worth mk	Net excess mk	Reactivity worth mk	Net excess mk	Reactivity worth mk	Net excess mk
Starting conditions									
Excess reactivity of core with Al shim tray in place with no Be shims		4.00	4.00	4.00	4.00	4.00	4.00	4.00	4.00
Control rod fully inserted		–7.00	–3.00	–7.00	–3.00	–7.00	–3.00	–7.00	–3.00
HEU core removal steps									
1	Remove the organic glass cover of the reactor pool	0.00	-3.00	0.00	–3.00	0.00	–3.00	0.00	–3.00
2	Put neutron and γ detectors into the slant tubes outside the vessel for monitoring changes of neutron and γ doses	0.00	–3.00	0.00	–3.00	0.00	–3.00	0.00	–3.00
3	Put strings of 4 Cd rabbits into each of the 5 inner irradiation tubes (each string worth -2.48 mk in the NIRR-1 MNSR; total worth is -12.4 mk) [IV.1].	–12.40	–15.40	0.00	–3.00	–2.48	–5.48	–4.96	–7.96
4	Place the transfer cask to be used for removing the HEU core into the pool.	0.00	–15.40	0.00	–3.00	0.00	-5.48	0.00	–7.96
5	Remove the control rod and its drive mechanism.	7.00	–8.40	7.00	4.00	7.00	1.52	7.00	–0.96
6	Take the Al shim tray and all top Be shims out of the reactor vessel (reactivity worth from Section 1.5, Table 9)[1] [IV.1].	1.61	–6.79	1.61	5.61	1.61	3.13	1.61	0.65
7	Take out the HEU core and put it into the transfer cask using the special tool. [2]	—	—	—	—	—	—	—	—
8	Cover the transfer cask and take it out of the reactor pool.	—	—	—	—	—	—	—	—

[1] This is the maximum reactivity if the core were to fall back into the Be reflector.
[2] A core with an excess reactivity of 4.0 mk will become subcritical by about 167 mk (k_{eff} = 0.85714±0.00006) when it is removed from the Be reflector.

To install the LEU core described in Table IV.2, all steps are followed in the prescribed sequence. Scenario 1 is the removal of the five strings of cadmium rabbits immediately after the LEU core is installed. Scenario 2 is the removal of four of five strings of the cadmium rabbits immediately after the LEU core is installed. Scenario 3 is the removal of three of five strings of the cadmium rabbits immediately after the LEU core is installed.

TABLE IV.2. INSTALLATION OF LEU CORE

		Procedure		Scenario 1		Scenario 2		Scenario 3	
		Reactivity worth mk	Net excess mk	Reactivity worth mk	Net excess mk	Reactivity worth mk	Net excess mk	Reactivity worth mk	Net excess mk
	LEU CORE INSTALLATION STEPS								
	Starting conditions								
	Fully inserted strings of 4 Cd rabbits in each of the 5 inner irradiation tubes (reactivity worth from NIRR-1).	—	−12.40	—	−12.40	—	−12.40	—	−12.40
	Four fully inserted adjuster rods in the LEU core (reactivity worth from Section 1.7, Table 16).	−1.66	−14.06	−1.66	−14.06	−1.66	−14.06	−1.66	−14.06
	Begin LEU core installation								
1	Put the LEU core into the vessel and install it in the Be reflector using the handling tool (Reactivity worth from Section 1.7, Table 16).	6.34	−7.72	6.34	−7.72	6.34	−7.72	6.34	−7.72
2	Put the aluminium shim tray without beryllium shims on top of the LEU core using the handling tool (Reactivity worth from Section 1.7, Table 16).	−1.36	−9.08	—	—	—	—	—	—
3	Insert the new design LEU central control rod and its drive mechanism.	−7.00	−16.08	—	—	—	—	—	—
4	Remove cadmium rabbit strings from each of the 5 inner irradiation tubes (string of 4 Cd rabbits, each worth +2.48 mk; total worth is12.4 mk)	12.40	−3.68	12.40	4.68	9.92	2.20	7.44	−0.28
5	Remove neutron and γ detectors for monitoring changes of neutron and γ doses from the slant tubes outside the vessel	0.00	−3.68	—	—	—	—	—	—

TABLE IV.2. INSTALLATION OF LEU CORE (cont.)

		Procedure		Scenario 1		Scenario 2		Scenario 3	
		Reactivity worth	Net excess	Reactivity worth	Net excess	Reactivity worth	Net excess	Reactivity worth	Net excess
		mk	mk	mk	mk	mk	mk	mk	mk
6	Replace the organic glass cover of the reactor pool.	0.00	−3.68	—	—	—	—	—	—
7	Start up MNSR with LEU fuel; adjust net excess reactivity to less than 4 mk	—	—	—	—	—	—	—	—
	Starting condition of LEU core								
	Excess reactivity of core with Al shim tray in place and no Be shims	<4.00	<4.00	—	—	—	—	—	—
	New design LEU central control rod fully inserted	−7.00	~ −3.00	—	—	—	—	—	—

REFERENCE TO APPENDIX IV

[IV.1] JONAH, S., NIRR-1 of Nigeria, private communication, February 2012.

ACRONYMS AND ABBREVIATIONS

ANL	Argonne National Laboratory
BDBA	beyond design basis accident
CERT	Centre for Energy Research and Training (Nigeria)
CHF	critical heat flux
CIAE	China Institute of Atomic Energy
CRP	coordinated research project
DBA	design basis accident
DNB	departure from nucleate boiling
DNBR	departure from nucleate boiling ratio
EIS	external irradiation sites
FIR	flow instability power ratio
FP	fission products
FPED	full power equivalent days
FSAR	final safety analysis report
GHARR-1	Ghana Research Reactor-1
HCF	hot channel factors
HEU	high enriched uranium
ID	inner diameter
IER	initial excess reactivity
IIS	internal irradiation sites
IT	irradiation tube
LEU	low enriched uranium
LWR	light water reactor
MCNP	Monte Carlo N-Particle Transport Code System
MNSR	miniature neutron source reactor
NAA	neutron activation analysis
NIRR-1	Nigeria Research Reactor-1
NNRI	National Nuclear Research Institute (Ghana)
NSTRI	Nuclear Science and Technology Research Institute (Islamic Republic of Iran)
OBE	operation base earthquake
OD	outer diameter
ONB	onset of nucleate boiling
ONBR	onset of nucleate boiling ratio
OSV	onset of significant voiding
PARR-2	Pakistan Research Reactor-2
PINSTECH	Pakistan Institute of Nuclear Science and Technology
SAR	safety analysis report
SSE	safe shutdown earthquake
TEDE	total effective dose equivalent

CONTRIBUTORS TO DRAFTING AND REVIEW

Abrefah, R.G.	National Nuclear Research Institute, Accra, Ghana
Adelfang, P.	International Atomic Energy Agency
Akaho, E.H.K.	National Nuclear Research Institute, Accra, Ghana
Albarhoum, M.	Atomic Energy Commission, Damascus, Syrian Arab Republic
Ames, C.	International Atomic Energy Agency
Ampomah-Amoako, E.	National Nuclear Research Institute, Accra, Ghana
Arshi, S.S.	Nuclear Science and Technology Research Institute, Tehran, Islamic Republic of Iran
Birikorang, S.A.	National Nuclear Research Institute, Accra, Ghana
Bokhari, I. H.	Pakistan Institute of Nuclear Science and Technology, Islamabad, Pakistan
Dix, J.	International Atomic Energy Agency
Du, K.	China Institute of Atomic Energy, Beijing, China
Dunn, F.E.	Argonne National Laboratory, Argonne, Illinois, USA
Hanlon, T.	International Atomic Energy Agency
Ibrahim, Y.V.	Centre for Energy Research and Training, Zaria, Nigeria
Iqbal, M.	Pakistan Institute of Nuclear Science and Technology, Islamabad, Pakistan
Jonah, S.A.	Centre for Energy Research and Training, Zaria, Nigeria
Khalafi, S.	Nuclear Science and Technology Research Institute, Tehran, Islamic Republic of Iran
Kalimullah, M.	Argonne National Laboratory, Argonne, Illinois, USA
Li, Y.	China Institute of Atomic Energy, Beijing, China
Liaw, J.R.	Argonne National Laboratory, Argonne, Illinois, USA
Mahmood, T.	Pakistan Institute of Nuclear Science and Technology, Islamabad, Pakistan
Matos, J.E.	Argonne National Laboratory, Argonne, Illinois, USA
Mirvakili, S.M.	Nuclear Science and Technology Research Institute, Tehran, Islamic Republic of Iran
Nyarko, B.J.B.	National Nuclear Research Institute, Accra, Ghana
Odoi, H.C.	National Nuclear Research Institute, Accra, Ghana
Peld, N.D.	International Atomic Energy Agency
Xia, P.	China Institute of Atomic Energy, Beijing, China
Sogbadji, R.B.M.	National Nuclear Research Institute, Accra, Ghana
Sollychin, R.	International Atomic Energy Agency
Voronov, M.	International Atomic Energy Agency

ORDERING LOCALLY

In the following countries, IAEA priced publications may be purchased from the sources listed below or from major local booksellers.

Orders for unpriced publications should be made directly to the IAEA. The contact details are given at the end of this list.

CANADA

Renouf Publishing Co. Ltd

22-1010 Polytek Street, Ottawa, ON K1J 9J1, CANADA

Telephone: +1 613 745 2665 • Fax: +1 643 745 7660

Email: order@renoufbooks.com • Web site: www.renoufbooks.com

Bernan / Rowman & Littlefield

15200 NBN Way, Blue Ridge Summit, PA 17214, USA

Tel: +1 800 462 6420 • Fax: +1 800 338 4550

Email: orders@rowman.com Web site: www.rowman.com/bernan

CZECH REPUBLIC

Suweco CZ, s.r.o.

Sestupná 153/11, 162 00 Prague 6, CZECH REPUBLIC

Telephone: +420 242 459 205 • Fax: +420 284 821 646

Email: nakup@suweco.cz • Web site: www.suweco.cz

FRANCE

Form-Edit

5 rue Janssen, PO Box 25, 75921 Paris CEDEX, FRANCE

Telephone: +33 1 42 01 49 49 • Fax: +33 1 42 01 90 90

Email: formedit@formedit.fr • Web site: www.form-edit.com

GERMANY

Goethe Buchhandlung Teubig GmbH

Schweitzer Fachinformationen

Willstätterstrasse 15, 40549 Düsseldorf, GERMANY

Telephone: +49 (0) 211 49 874 015 • Fax: +49 (0) 211 49 874 28

Email: kundenbetreuung.goethe@schweitzer-online.de • Web site: www.goethebuch.de

INDIA

Allied Publishers

1st Floor, Dubash House, 15, J.N. Heredi Marg, Ballard Estate, Mumbai 400001, INDIA

Telephone: +91 22 4212 6930/31/69 • Fax: +91 22 2261 7928

Email: alliedpl@vsnl.com • Web site: www.alliedpublishers.com

Bookwell

3/79 Nirankari, Delhi 110009, INDIA

Telephone: +91 11 2760 1283/4536

Email: bkwell@nde.vsnl.net.in • Web site: www.bookwellindia.com

ITALY

Libreria Scientifica "AEIOU"

Via Vincenzo Maria Coronelli 6, 20146 Milan, ITALY
Telephone: +39 02 48 95 45 52 • Fax: +39 02 48 95 45 48
Email: info@libreriaaeiou.eu • Web site: www.libreriaaeiou.eu

JAPAN

Maruzen-Yushodo Co., Ltd

10-10 Yotsuyasakamachi, Shinjuku-ku, Tokyo 160-0002, JAPAN
Telephone: +81 3 4335 9312 • Fax: +81 3 4335 9364
Email: bookimport@maruzen.co.jp • Web site: www.maruzen.co.jp

RUSSIAN FEDERATION

Scientific and Engineering Centre for Nuclear and Radiation Safety

107140, Moscow, Malaya Krasnoselskaya st. 2/8, bld. 5, RUSSIAN FEDERATION
Telephone: +7 499 264 00 03 • Fax: +7 499 264 28 59
Email: secnrs@secnrs.ru • Web site: www.secnrs.ru

UNITED STATES OF AMERICA

Bernan / Rowman & Littlefield

15200 NBN Way, Blue Ridge Summit, PA 17214, USA
Tel: +1 800 462 6420 • Fax: +1 800 338 4550
Email: orders@rowman.com • Web site: www.rowman.com/bernan

Renouf Publishing Co. Ltd

812 Proctor Avenue, Ogdensburg, NY 13669-2205, USA
Telephone: +1 888 551 7470 • Fax: +1 888 551 7471
Email: orders@renoufbooks.com • Web site: www.renoufbooks.com

Orders for both priced and unpriced publications may be addressed directly to:

Marketing and Sales Unit
International Atomic Energy Agency
Vienna International Centre, PO Box 100, 1400 Vienna, Austria
Telephone: +43 1 2600 22529 or 22530 • Fax: +43 1 2600 29302 or +43 1 26007 22529
Email: sales.publications@iaea.org • Web site: www.iaea.org/books

18-03511

International Atomic Energy Agency
Vienna
ISBN 978–92–0–101818–2
ISSN 1011–4289